UNIVERSITY OF GLASGOW

STUDIES OF THE THERMAL STABILITY AND DEGRADATION MECHANISMS OF TEREPHTHALATE POLYESTERS AND TELECHELIC POLY(METHYL METHACRYLATES)

BY

MAHMOUD BOUNEKHEL BSc

A THESIS SUBMITTED IN PART FULFILLMENT
OF THE REQUIREMENTS FOR THE DEGREE OF
DOCTOR OF PHILOSOPHY

FACULTY OF SCIENCE
DEPARTMENT OF CHEMISTRY

JUNE 1990

ProQuest LLC.
789 East Eisenhower Parkway
P.O. Box 1346
Ann Arbor, MI 48106 – 1346

ACKNOWLEDGEMENTS

I would like to express my sincere gratitude to Dr Ian C. McNeill, my supervisor, for the guidance, encouragement and patience provided during the course of this work.

Many thanks are also extended to all the members of the academic staff who may contributed in someways. Particularly to J.Gorman and G.McCulloch for their technical assistance and to my friends and colleagues in the Macromolecular Chemistry Group .

I would also like to thank all the members of my family for their support and patience during my academic life.

Finally, the Algerian Ministry of Higher Education is also acknowledged for the award of the research scholarship and the financial support.

CONTENTS PAGE N^{o}

CHAPTER SIX THERMAL DEGRADATION OF POLYARYLATES

SUMMARY

The preparation of polymers of improved stability requires an understanding of the relationship between structure and mechanism of decomposition. In this project, this relationship is explored for several classes of polymer.

The main degradation techniques which have been used, described in Chapter 2, are thermogravimetry (TG), thermal volatilisation analysis (TVA) and differential thermal analysis (DTA). Degradation products have been separated and analysed using subambient TVA, and GC-MS, IR and MS spectroscopy.

The preparation and spectroscopic analysis of poly(alkylene terephthalates), poly(ether-esters), polyarylates and α,ω-bifunctional poly(methyl methacrylate) described in Chapter 3.

In Chapters 4 and 5,studies of the thermal degradation of poly(alkylene terephthalates) and poly(ether-esters) made by melt polymerisation of terephthaloyl chloride with aliphatic diols and poly(ethylene glycols) (Mw 200, 1000) are reported. In order to achieve a detailed analysis of the degradation products, both temperature programmed and isothermal experiments were performed on these polymers. From the results obtained, the general mechanism of decomposition has been established.

In Chapter 6, a similar investigation of nine different polyarylates, including fire retardant polyarylates, made by interfacial polycondensation from aromatic diols and terephthaloyl chloride is reported and the effects of fire retardant incorporated to the backbone of polymer are discussed. It is clear there are many close similarities in mechanism, especially in the sense that similar radicals are usually involved.

In Chapter 7, the results of a comprehensive study of the thermal degradation of four different α,ω-bifunctional poly(methyl methacrylates) made by the anionic route are analysed and the general mechanism of decomposition has been proposed. The effect of the functional end groups on the thermal stability and mechanistic behaviour are discussed.

CHAPTER ONE

INTRODUCTION

1.1 POLYESTERS

Polyesters are heterochain macromolecules, which take their name from the ester group in the repeating units of the polymer chain, made by the condensation or self esterification of ω–hydroxy carboxylic acids, ring opening polymerisation of ω–lactones or the reactions of dicarboxylic acids or their derivatives with diols . Their structures can be represented in the following general formulae :

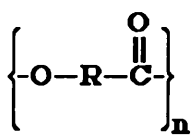

and

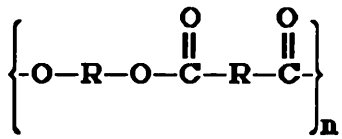

The polyesters in this study have the latter type of structure.

Polyesters are used in many industrial applications as fibres and resins, because of their wide range of mechanical, electrical and optical properties, which may be controlled by incorporation of flexible chain sections such as $-(CH_2)_m-$, $-(CH_2CH_2O)_m-$ or rigid groupings such as aromatic rings .

One of the materials now known as polyesters was first made as early as 1833 when Gay-Lussac and Pelouze made a polyester from lactic acid. However, the first commercially significant product was made from glycerol

and phthalic acid and led later to the development of alkyd resin. In the late 1920s, an extensive study undertaken by Carothers, in which he prepared low molecular weight aliphatic polyesters, laid the foundations of step-polymerisation chemistry and established relationships between molecular structure, molecular weight and polymer properties [1]. These polymers did not attract great commercial interest, however, because of their low melting points. The discovery of poly(ethylene terephthalate) and poly(butylene terephthalate), by Whinfield and Dickson in the 1940s [2,3] led to a rapid growth in applications as fibres and films because of their high heat distortion temperature, high rigidity and toughness, good mechanical properties, excellent surface appearance, low moisture absorption, good electrical insulation properties, solvent resistance and dimension stability [4].

On the other hand, polyesters based on aromatic dicarboxylic acids (or their derivatives) with diphenols (polyarylates), are considered as a class of new engineering polymers. This type of polymer was first prepared in the late 1950s [5,6], but commercial development was only introduced in 1970, using a polyarylate derived from p-hydroxy benzoic acid. This has a highly crystalline structure which remains unchanged up to 330 ^{o}C and exhibits a higher thermal stability than PET and PBT.

Through the variation in the backbone molecular structure and modification by copolymerisation, linear polyesters can be produced with a wide range of properties and uses.

1.2 TELECHELIC POLYMERS

Telechelic polymers are those with reactive groups at the chain ends. For the preparation of these telechelic polymers, various polymerisation routes can be employed (e.g: ring opening, radical, anionic, group transfer,

cationic, step growth) and polymer chain scission may also be used [7]. The concept of prepolymers was already established in 1947 by Byer [8]. Thirteen years later Bamford et.al.[9] synthesised the first telechelic polymer from styrene and demonstrated the functionality by coupling reactions to produce a new material with different properties. Since then, such polymers have become increasingly important for practical use, e.g, as a prepolymer for block copolymer formation or as crosslinking agents.

Telechelic polymers have great industrial interest, since they are the basis of liquid polymer technology, whereby the polymer can be cast and injection molded. The liquid telechelic polymer can be linked into a desired network by a multifunctional agents, which offers processing advantages and excellent properties. Also they were relevant to the development of thermoplastic elastomers consisting of triblock or multiblock copolymers[7,10].

The telechelic polymers studied in this investigation are based on methyl methacrylate monomer and were prepared by the anionic route. The desired telechelic polymer (α,ω-bifunctional PMMA) can be formed via the termination of living propagating species in the anionic polymerisation of the monomer.

1.3 GENERAL ASPECTS OF POLYMER DEGRADATION

Changes in polymeric materials due to degradation have been known from the beginning of history. The rotting of wood and cloth, the deterioration of meat and the burning of wood are all examples of irreversible changes which have been caused by chemical bond scission reactions in the backbone of the macromolecules, within the environment to which they have been exposed during their life cycle [11-13].

In various types of degradation environment (e.g : thermal, mechanical, photochemical, radiation chemical, biological and chemical), the properties of every polymer are affected by those chemical reactions involved in the degradation mechanism.

1.4 THERMAL DEGRADATION OF POLYMERS

Studies of the thermal behaviour of polymers, particularly their thermal degradation, are of prime importance in relation to processing and applications.

In the polymer field, thermal degradation refers to the changes occurring in the polymer at elevated temperatures. These changes involve rupture of bonds in the main or side chains, as evidenced by a diminution of the chain size and the evolution of low molecular weight products [13]. The subject has received a great deal of attention by a number of investigators over the last forty years.

Various thermal methods of analysis have been used to study polymer degradation reactions continuously, usually involving direct measurement of weight loss by thermogravimetry (TG) or of the evolution of volatile degradation products e.g, by thermal volatilisation analysis (TVA), which is a particularly versatile form of evolved gas analysis. These techniques will be discussed in detail in the next chapter.

1.5 CLASSIFICATION OF DEGRADATION REACTIONS

Thermal degradation reactions may be divided into two general categories, namely, depolymerisation and side group scission reactions.

1.5.1 DEPOLYMERISATION

There are two types of depolymerisation reactions. Depolymerisation by the unzipping of the main chain backbone may proceed to give monomer. This process is mostly encounted with polymers produced from 1:1-disubstituted alkenes and certain cyclic monomers. Reverse polymerisation (depropagation) to yield 100 % monomer is observed in the case of PMMA and poly(α-methyl styrene). On the other hand, in cases where the polymer structure and radical reactivity favour transfer, hydrogen abstraction occurs at various points along the polymer chain leading to dimer, trimer, etc. (intramolecular transfer) and reduction of molecular weight following intermolecular transfer.

In heterochain polymers such as poly(ethylene terephthalate) a further type of depolymerisation involves an ester exchange reaction to form short chain fragments with carboxylic acid and vinyl ester end groups as shown below:

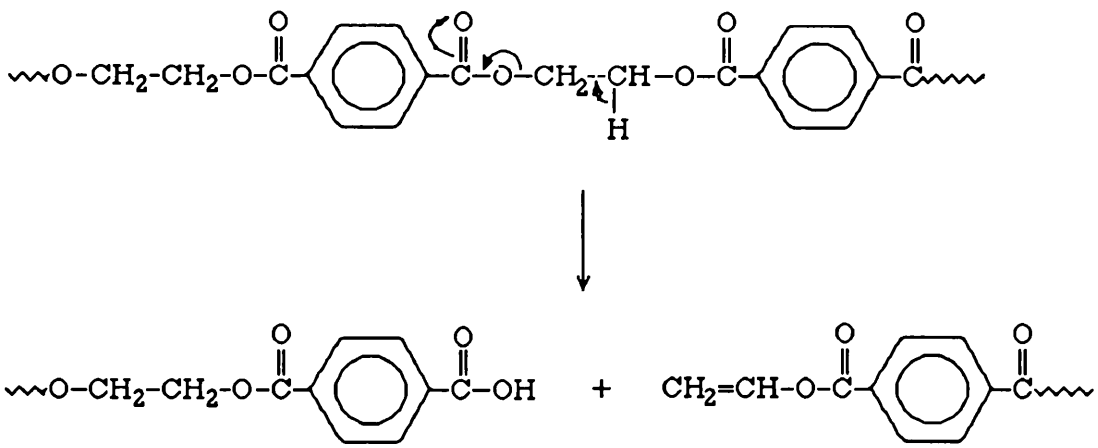

Scheme 1.1: Initial decomposition of poly(ethylene terephthalate).

When depolymerisation occurs, the products have chemical composition closely similar to that of the original polymer.

1.5.2 SIDE GROUP REACTIONS

Degradation may also be associated with side groups attached to the polymer chain, involving two types of reaction.

a) Elimination of part or all of the side groups to liberate low boiling point volatile products may occur. Thus, poly(t-butyl methacrylate) (P t-BMA) [14] or poly(vinyl chloride) (PVC) [15,16] decompose to produce isobutene and hydrogen chloride, respectively (Scheme 1.2).

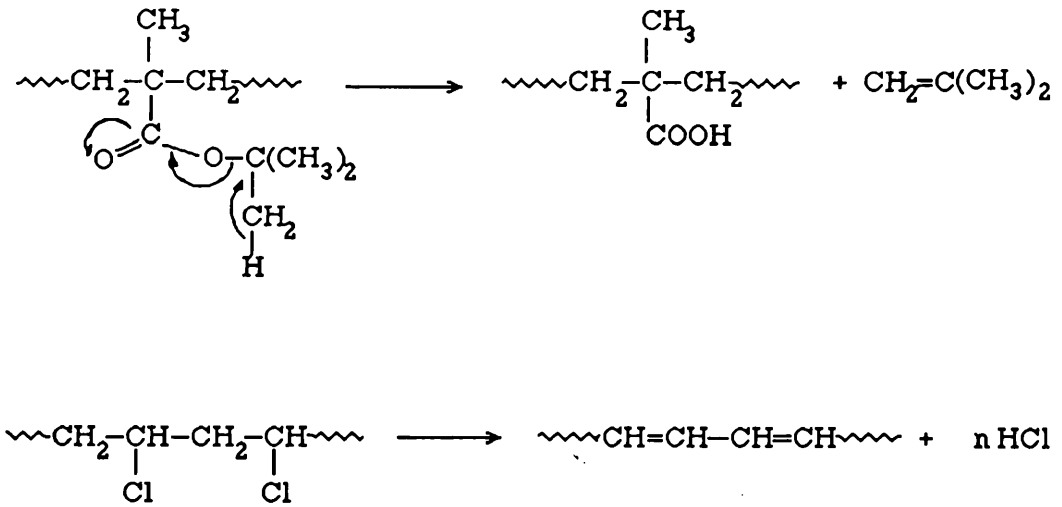

Scheme 1.2: Elimination reactions in P t-BMA and PVC.

b) Cyclisation: This process involves reaction between neighbouring side groups with or without loss of a small molecule as shown in Scheme 1.3. Polymers containing nitrile groups, as in the case of polyacrylonitrile and poly(methacrylonitrile) [17], undergo cyclisation by

rearrangement to form six-membered rings containing nitrogen. In other cases such as poly(methacrylic acid) (PMAA) [14,18], however, neighbouring side groups undergo dehydration to yield six-membered cyclic anhydride rings along the polymer chain.

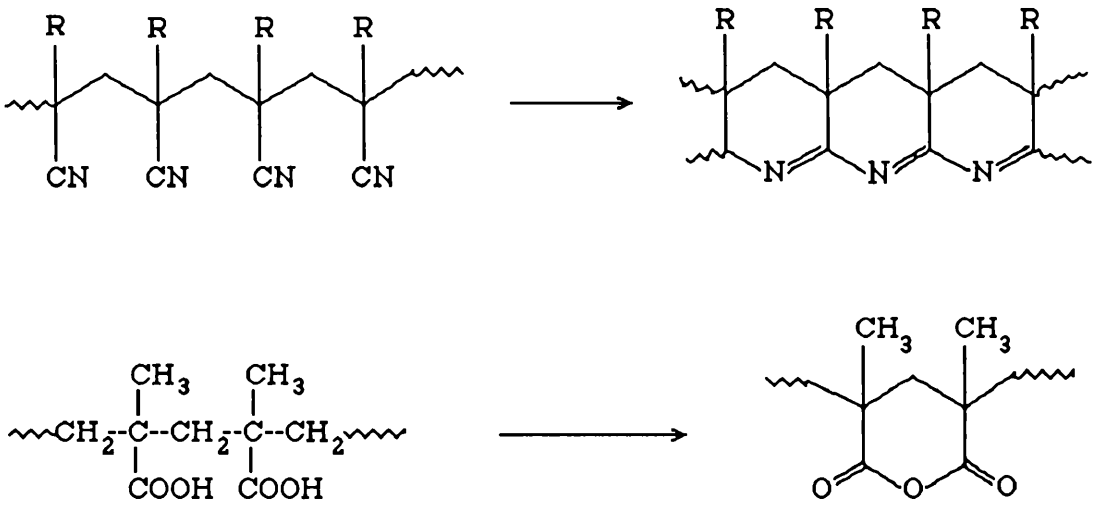

Where R = H and CH_3

Scheme 1.3: Cyclisation reaction in PAN, PMAN and PMAA.

In the case of most side group reactions, the volatile products and partially degraded polymer residue will differ considerably in composition from the original polymer.

1.6 EFFECT OF STRUCTURE ON DEGRADATION AND STABILITY

The degradation of polymers is usually accompanied by the scission of the backbone links and the evolution of volatile products. Crosslinking of chains promoted by heating, however, can increase the stability of the polymer by the formation of a rigid infusible network.

Linear carbon-carbon chains as in vinyl polymers are not very stable

and the most stable polymers of this type tend to decompose thermally around 350 °C. The presence of tertiary hydrogen atoms is often a source of weakness in the polymer. The stability is improved by replacing hydrogen by fluorine atoms as in polytetrafluoroethylene. However, polymers with linear chains of carbon atoms, in general, are not heat-resistant.

On the other hand, some polymers containing aromatic rings and heteroatoms in the backbone have been found to have outstanding thermal stability. These include some polyamides and polyesters. For example, fully aromatic polyamides and polyesters are known which are completely stable up to 500 °C, as in poly(p-benzamide) [19], poly(p-phenylene terephthalamide) [20] and poly(4-hydroxy–benzoic acid) [21]. The incorporation of a metal into organic molecules is a further method of achieving a combination of characteristic polymer behaviour and high thermal stability, as in the case of poly(acrylic acid) salts.

1.7 FIRE RETARDANT POLYMERS

Synthetic polymeric materials are increasingly used in textiles, the car industry, construction and furnishing of homes, offices and public buildings. These polymers are frequently flammable organic compounds. This is now a critical factor which determines their potential uses. The fire hazard associated with the flammability and fatalities in fire incidents are often not the result of burning. Instead, victims are poisoned by toxic gases or suffocated by smoke which limits visibility, thereby making escape more difficult. The smoke resulting from synthetic plastics is often more dense and the fumes more poisonous than from natural materials such as cellulose.

In order to achieve optimum fire retardant properties in a polymer, it is necessary to have quantitative measurement of flammability, which depends on the ignition, rate of flame spread and duration of burning after ignition[12].

During the "burning" of polymers it is the volatile products of thermal degradation which burn rather than the polymer itself. The combustion of these materials provides the energy required to sustain the supply of fuel and so keep the system burning as shown in Scheme 1.4 [22].

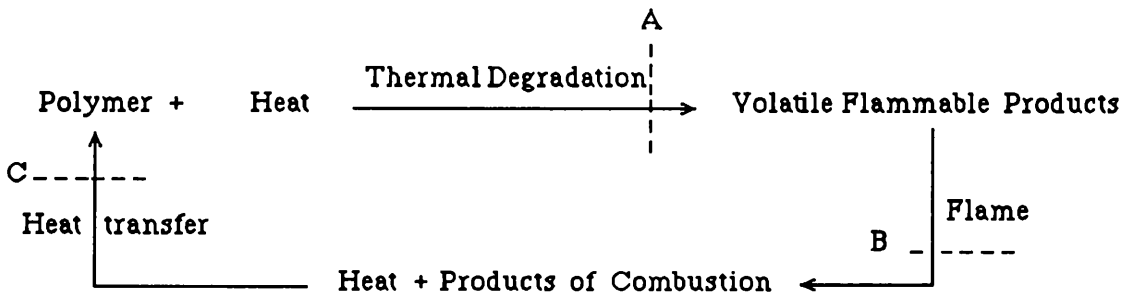

Scheme 1.4: Outline of burning processes for organic polymers.

A fire retarded polymer is usually achieved by interfering with at least one of the stages at points A, B and C. The following changes may be involved:

1) Modification of the thermal degradation process.

2) Quenching the flame .

3) Reduction of the supply of heat from the flame back to the decomposing products.

The incorporation of a fire retardant into a polymeric material can be achieved by two approaches, using additives or reactives. The former are mixed with the polymer to be protected during processing, while the reactives are already part of the polymer structure incorporated during

polymerisation. Reactive fire retardant polymers have an advantage over additive type, since they exhibit bound antioxidation. On the other hand, they may have a bigger effect on the chemical stability of the polymer.

Six common elements are associated with the incorporation of fire retardant properties in a polymeric material are boron, aluminum, phosphorus, antimony, chlorine and bromine. Phosphorus is strongly associated with changes of thermal degradation process, antimony, chlorine and bromine with flame quenching and the remaining elements with inhibition of heat flow [12]. Many fire retardants, however, have effects both on condensed phase reactions and in flame quenching or char formation.

1.8 AIM OF PRESENT WORK

Polyesters form an important group of polymers, with major application as fibres and resins. They have therefore attracted much industrial interest.

The work seeks first to establish the relationship between structure and stability for a group of polymers of the polyester type and to elucidate decomposition mechanisms. A further objective is to explore the effect on polymer properties, particularly thermal stability and mechanism of decomposition, of introducing fire retardant structures into the backbone of the polymer.

A new type of polymers with α,ω-bifunctional end groups (telechelic polymers), based on methyl methacrylate, were synthesised and examined thermally. These typesof polymers are potentially useful as intermediates for the preparation of new copolymers with desired properties.

****

CHAPTER TWO

THERMAL AND ANALYTICAL TECHNIQUES

2.1 INTRODUCTION

An understanding of the long chain nature of polymers led to an appreciation of the unique properties that might be obtained in polymeric materials. This encouraged a rapid growth of polymer production. In order to limit or if possible to prevent the degradation of polymers, various methods have been employed. Great improvements may be achieved by the synthesis of new materials with desired properties. The development of more sophisticated equipment allows the physical properties and thermal stability of polymers to be assessed more easily.

The methods of characterisation of polymers can be classified into two main categories, namely, thermal and analytical techniques.

In this chapter, a full description is given of the experimental methods employed in the present work. Particular emphasis is given to the thermal volatilisation analysis (TVA) technique which has been used extensively through out the work.

2.2 THERMAL ANALYSIS

2.2.1 THERMAL VOLATILISATION ANALYSIS (TVA)

Thermal volatilisation analysis (TVA) is a versatile thermoanalytical technique developed in this department by McNeill el. al [23-28]. A polymer sample is heated to elevated temperatures under continuous high vacuum conditions and the small pressure developed during the degradation processes can be measured and recorded by means of a Pirani gauge as a function of time or temperature. The recorded pressure is a measure of rate of volatilisation of products.

The basic principle of a TVA system is illustrated schematically in Figure 2.1, in which a Pirani gauge has been placed between the heated sample and the cold trap (-196 ^{o}C).

A modification to the apparatus involves an additional cold trap at some temperature higher than -196 ^{o}C, placed between the heated sample and Pirani gauge as shown in Figure 2.2. The Pirani will now respond only to the products which are sufficiently volatile and able to pass through the first trap. This form of TVA is known as differential condensation TVA.

By running a series of experiments each with different first trap temperature, much information about the volatility of degradation products can be provided from comparison of the several TVA traces.

In further development of the TVA system, the line is subdivided into parallel lines all opened simultaneously. The current form of apparatus employed in this laboratory is depicted in Figure 2.3, in which four parallel lines each have initial cold trap and a main trap (-196 ^{o}C). The initial trap temperature differs from one line to another and 0, -45, -75 and -100 ^{o}C have been found convenient for polymer degradation. A further Pirani gauge

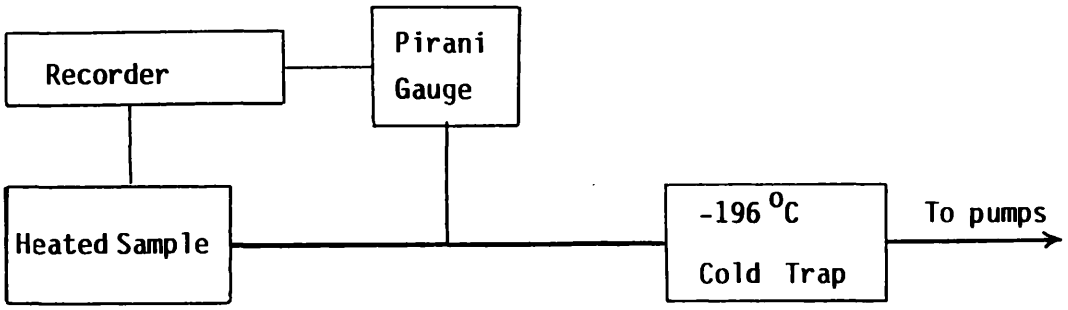

Figure 2.1: Schematic diagram of basic TVA system.

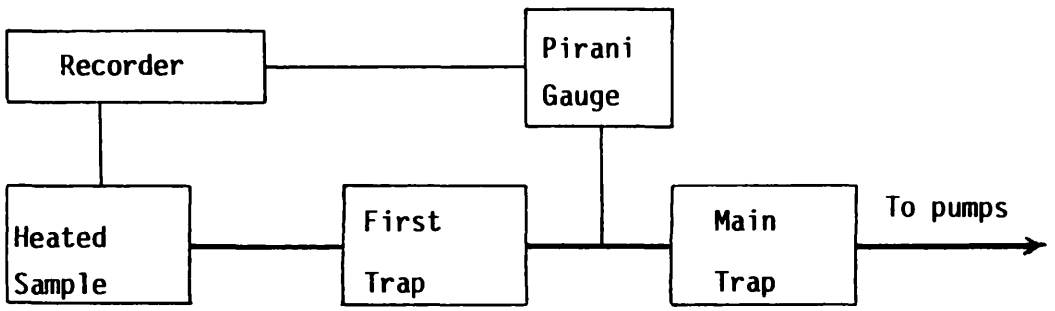

Figure 2.2: Single line differential condensation TVA system.

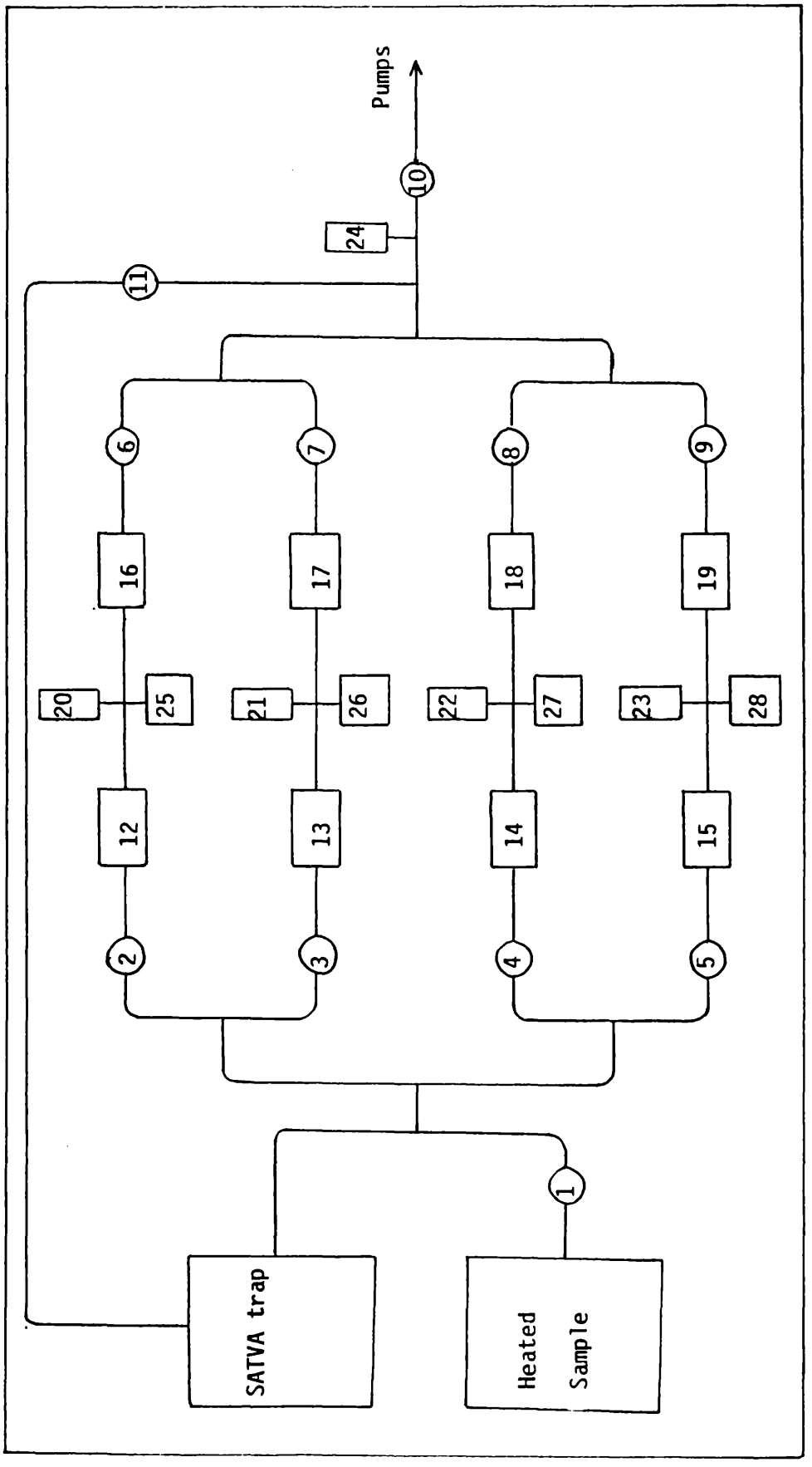

Figure 2.3: Four parallel line differential condensation TVA system. 1-11, Stopcocks:; 12-15, Initial cold traps (0, -45, -75 and -100 ^{o}C); 16-19, Main traps (-196 ^{o}C); 20-24, Pirani gauge heads and 25-28, Take off collection points.

is attached to the TVA system beyond the main cold traps to detect the permanent gases passing through the initial and -196 ^{o}C traps.

A polymer sample, commonly in the form of a powder or thin film, is contained in the degradation tube which is inserted into a Perkin-Elmer F-11 gas chromatography oven, modified to heat the degradation tube to a maximum temperature of approximately 500 ^{o}C as shown in Figure 2.4 and equipped with a linear temperature programmer. The oven can be operated isothermally or with linear increase of temperature in the range of 1 to 40 ^{o}C/min. Oven temperature is recorded as a millivolt output along with that of the Pirani gauges, using a Leeds-Northerup " Speedomax W " 12 point strip chart recorder. Due to a temperature differential across the degradation tube base, sample temperature is lower than the oven temperature, except for isothermal heating when the tube and oven reach thermal equilibrium. It is convenient to calibrate these temperatures by means of a second thermocouple inserted directly through the socket 1 of FIgure 2.4 until it contacts the base of degradation tube. The system is then evacuated and the blank tube heated to 500 ^{o}C as in a normal TVA experiment. The corresponding temperatures for both oven and sample are simultaneously recorded as shown in Figure 2.5.

The pumping system consists of an Edwards Speedivac EO1 mercury diffusion pump, backed by an Edwards Speedivac ED100 rotary pump. Using the system, an initial pressure of 10^{-5} mbar is obtainable. Edwards G5C-2 Pirani gauge heads with Pirani model 11 or 14 control units are employed to measure pressures.

Since the outputs of Pirani gauges attached to the vacuum line show minor variation, it is essential to get completely coincident traces for the same pressure. First, a circuit depicted in Figure 2.6 was adjusted to achieve coincidence for the Pirani responses. The line was set up as for a

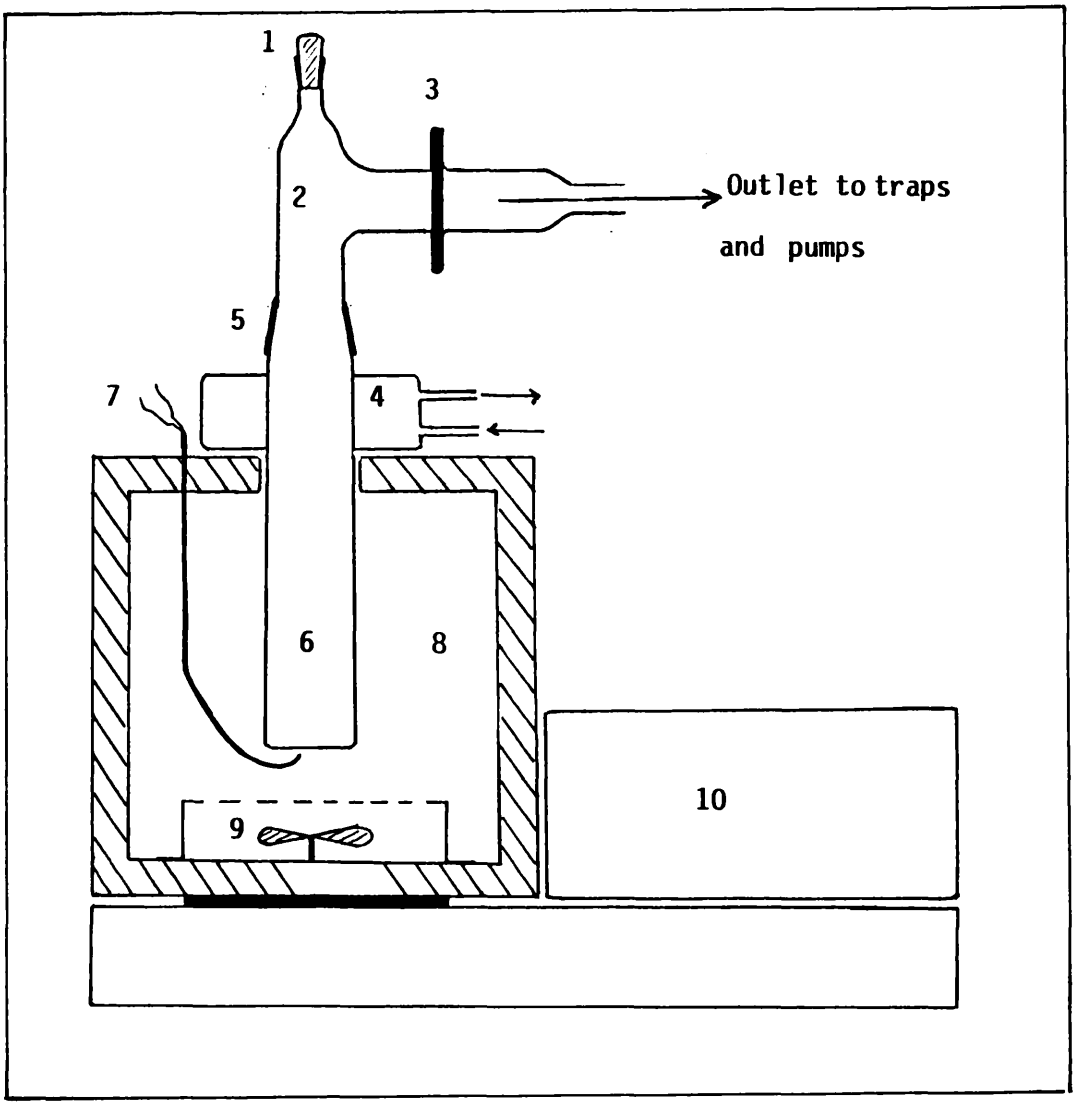

Figure 2.4: Heated sample assembly. **1**, B 14 stopper; **2**, removal lid joint; **3**, flange joint; **4**, cold water cooling jacket; **5**, B 39/40 ground glass socket; **6**, degradation tube; **7**, chromel-alumel thermocouple; **8**,, oven; **9**, fan; **10**, programming module.

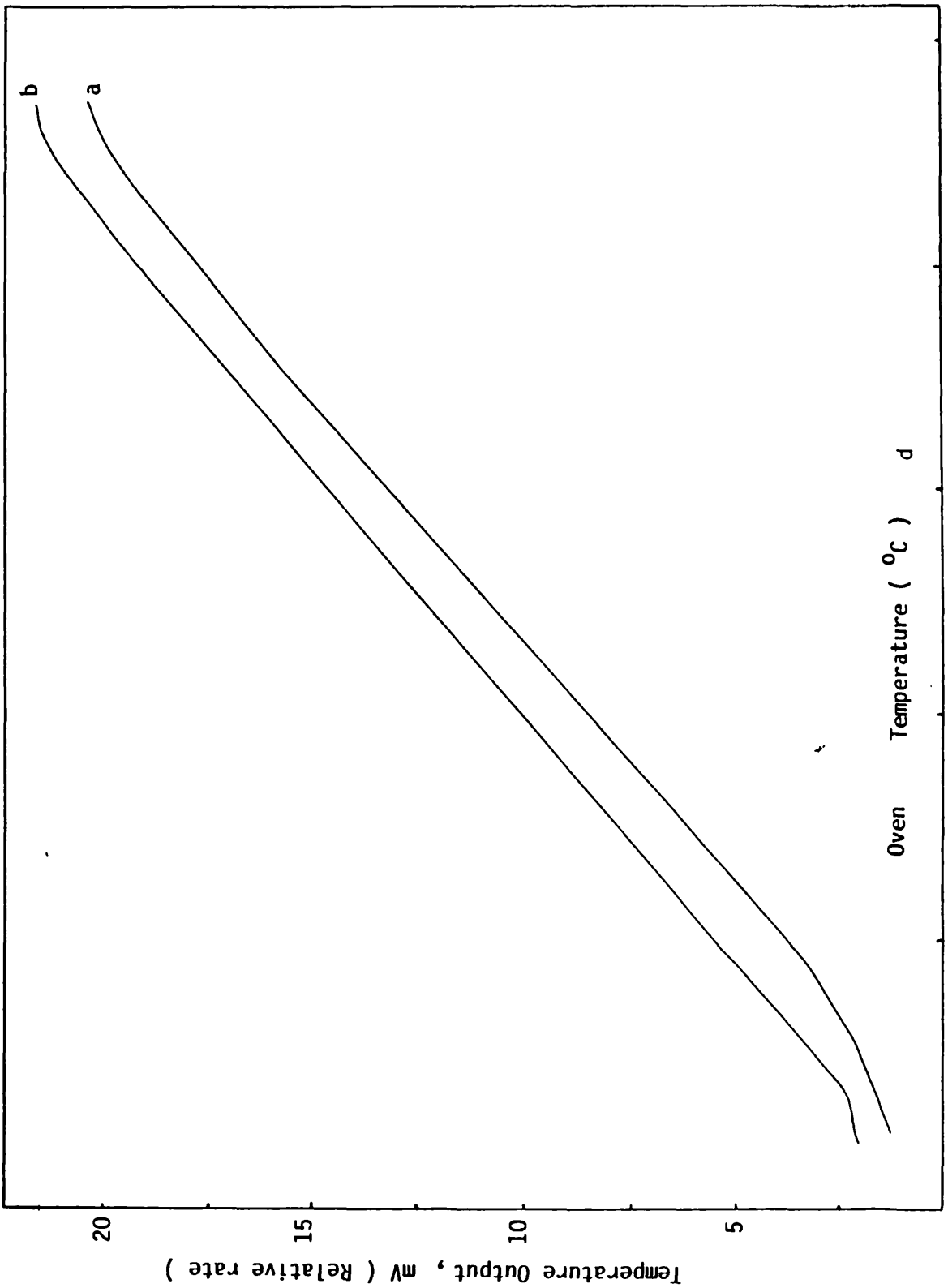

Figure 2.5: Tube temperature calibration chart. **a** (Sample temperature) and **b** (Oven temperature).

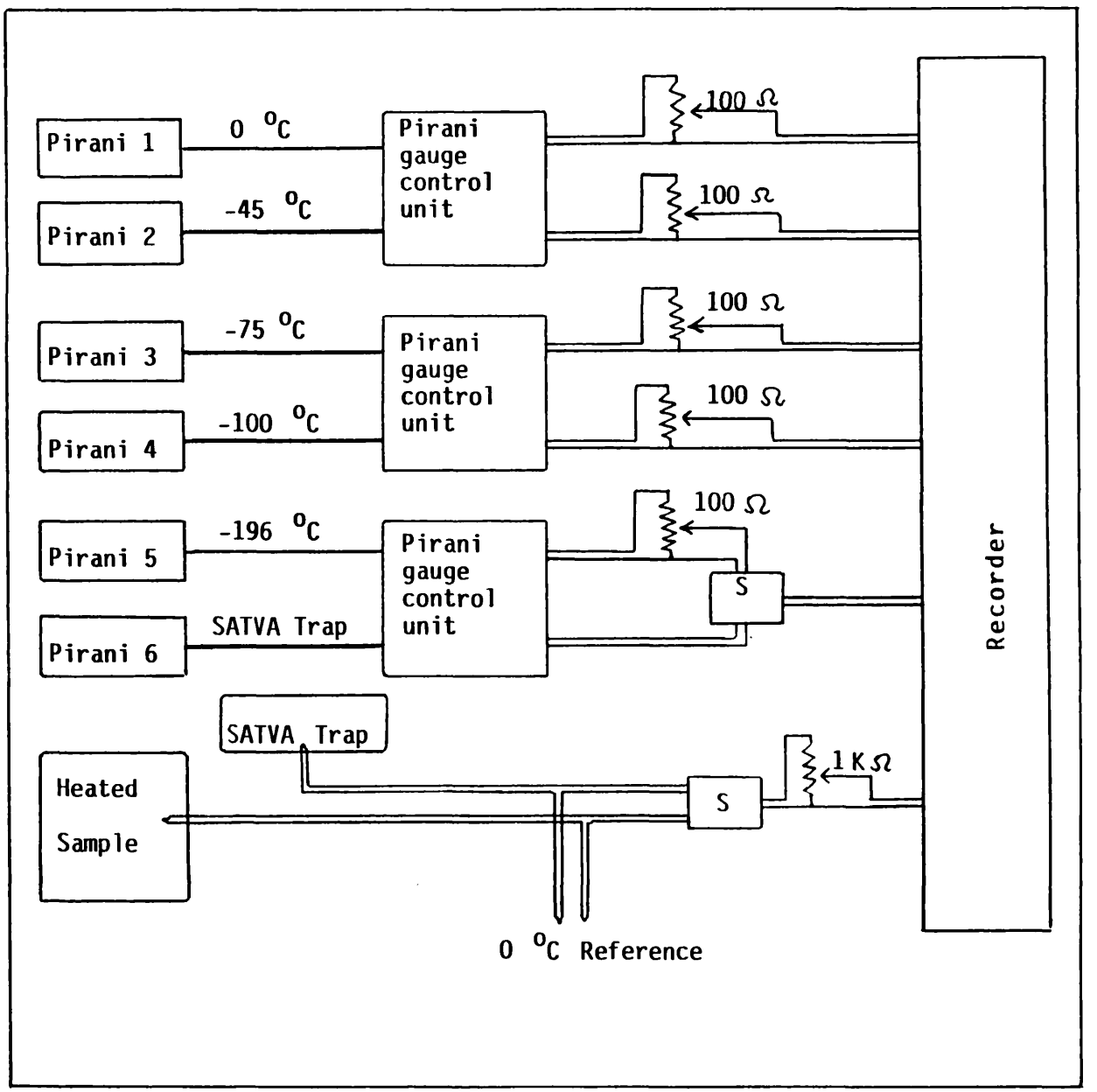

Figure 2.6: Circuit for adjustment of coincidence of Pirani gauges and temperature outputs in TVA system. S = switches.

normal TVA experiment and the Pirani gauges were adjusted to zero when a vacustat gauge indicated optimum high vacuum ($10^{-5} - 10^{-6}$ mm Hg). The line was then isolated from the pumps, dry nitrogen was introduced and the apparatus was pumped down until half of full scale output and isolated from the pumps. When a steady pressure recorded, the outputs of the five Pirani gauges were brought into coincidence by means of the 100 Ω variable resistances. The system was then pumped down in stages and the coincidence was checked at each stage. A further check was made by degrading potassium permanganate which evolves only oxygen as volatile gases at -196 °C under TVA conditions. With this sample, all five TVA traces should be coincident.

In the TVA traces obtained in this thesis, the standard designations used for traces corresponding to 0, -45, -75, -100 and -196 °C cold traps are as follows:

————	0 °C (and colder traps if coincidence)	
— • — • —	-45 °C	"
— ••— ••—	-75 °C	"
.....	-100 °C	"
— — — —	-196 °C	"

2.2.1.1 Degradation Products Analysis

Once the degradation of polymer sample has been completed, a great of information may be obtained about the nature of degradation products. Subsequently, these products are divided into four main fractions in accordance with their volatility.

1) **Residue:** The involatile material remaining at degradation temperature.

2) **Cold ring fraction:** Products volatile at degradation temperature but not at ambient temperature. This fraction usually accumulates on the upper part of the inner wall of the degradation tube.

3) **Condensable volatile products:** Products which escape from the hot zone during the degradation process and condense at the initial or the main cold traps. This is the fraction recorded by TVA together with -196 ^{o}C cold trap trace.

4) **Non-condensable gases:** The permanent volatile gases at -196 ^{o}C. These gases can be studied by means of degradation in a closed system, followed by collection in a gas cell using Toepler apparatus and analysis.

2.2.1.2 Subambient TVA (SATVA)

The degradation products released in TVA which are volatile at ambient temperature and condensable at -196 ^{o}C can be separated if their volatility differs sufficiently. The SATVA technique developed independently by McNeill et. al.[29] and Ackerman and McGill [30-32] may be employed to fractionate these products.

Figure 2.7 illustrates diagrammatically the basic principle of a TVA system which can be used, after degradation, for separation of products by SATVA, using Pirani 2 to monitor distillation. The degradation products released from the heated sample are condensed at the trap A (-196 ^{o}C) under continuous high vacuum. Pirani 1 measures the evolution of volatile products whilst Pirani 2 records only the permanent gases at -196 ^{o}C which pass through trap A.

The layout of the recently improved trap A which is connected directly into the TVA system, is shown in detail in Figure 2.8. This trap commonly is known as the subambient TVA trap. The sample tube, containing the volatile

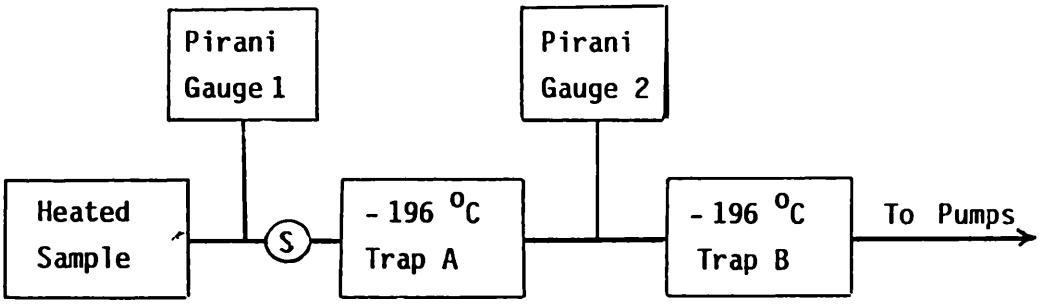

Figure 2.7: Principal features of a SATVA system.

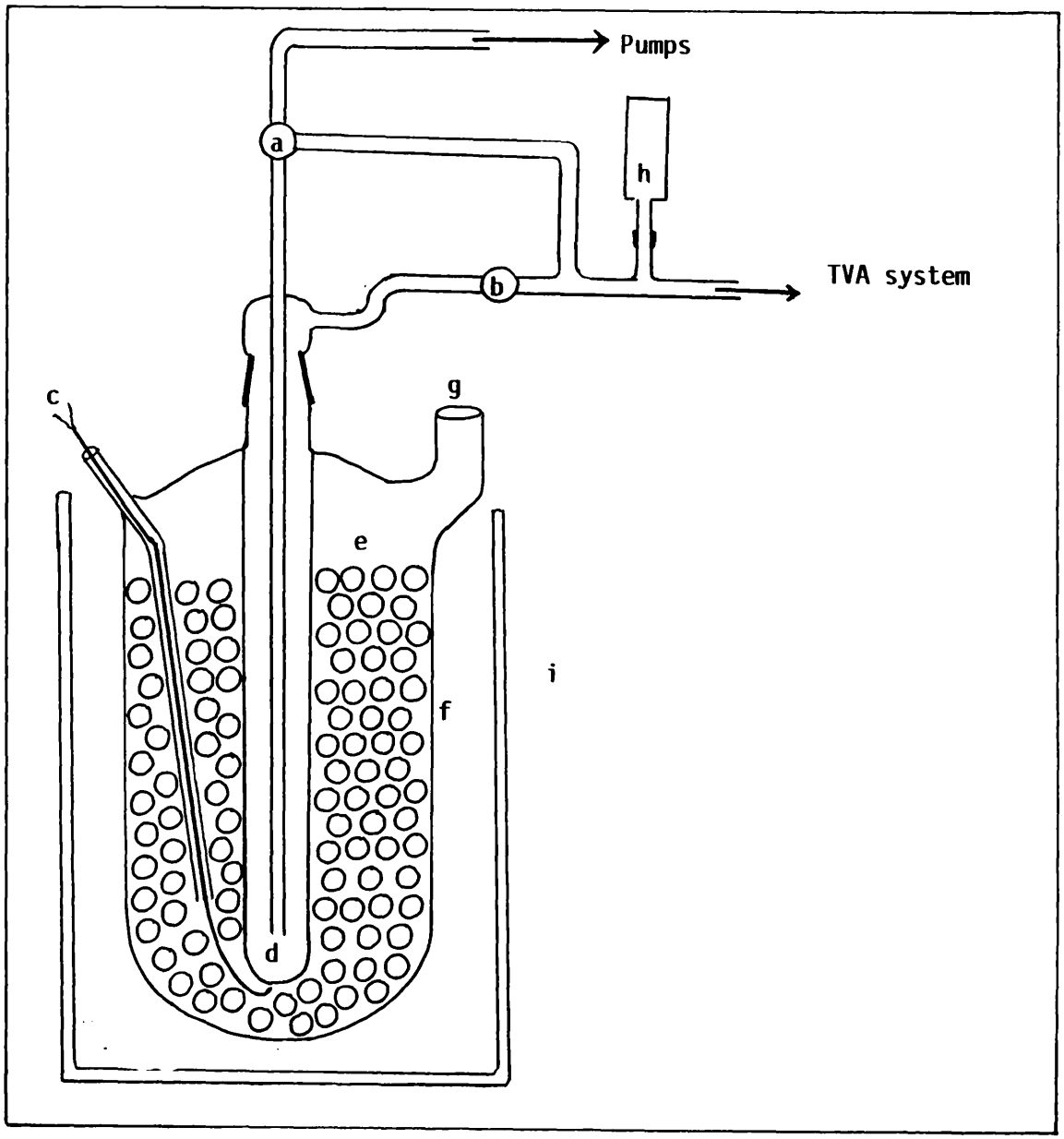

Figure 2.8: Arrangement of SATVA trap . e **a**, three way stopcock; **b**, stopcock ; **c**, thermocouple ; **d**, sample tube ; **e**, glass beads ; **f**, pyrex glass jacket ; **g**, filler port ; **h**, Pirani gauge head ; **i** , dewar vessel with liquid N_2 .

degradation products, is surrounded by a pyrex glass jacket containing glass beads at -196 ^{o}C, cooled in liquid nitrogen. The glass beads inserted into the jacket via the filler port were used to secure slow warming up which facilitates the separation of products. A thermocouple records the sample tube temperature. Trap B is also surrounded with liquid nitrogen.

Once all the degradation products have been transferred to the SATVA trap, the stopcock placed between the heated sample and trap A is closed. The SATVA trap is then allowed to warm up to ambient temperature by removing the liquid nitrogen. Each of the degradation products will distil into trap B over a temperature range dependent on the volatility of the corresponding material and their distillation being measured by Pirani 2. The change in pressure and temperature associated with evolution of degradation products from trap A into trap B are recorded simultaneously as a function of time.

The separation of degradation products is achieved by linking the SATVA trap directly to the 4-line TVA apparatus as shown earlier in Figure 2.3. Stopcock (b) is closed and three way stopcock (a) of Figure 2.8 is opened to the TVA system. Initially, stopcocks 3, 4 and 5 of Figure 2.3 are closed and so any material escaping from the SATVA trap will pass through the first line and condense at the -196 ^{o}C cold trap. When the peak corresponding to the material evolved has reached a minimum, stopcock 3 opened and stopcock 2 is closed. The isolated fraction in the first line is collected in a gas cell attached at a take off collection point for spectroscopic analysis, whilst the second peak fraction is distilled in line 2. Similarly, further peak fractions may be distilled in lines 3 and 4. Figures 2.9 and 2.10 show diagrams of the gas cell and cold finger used during the collection of separated condensable volatile product fractions, respectively.

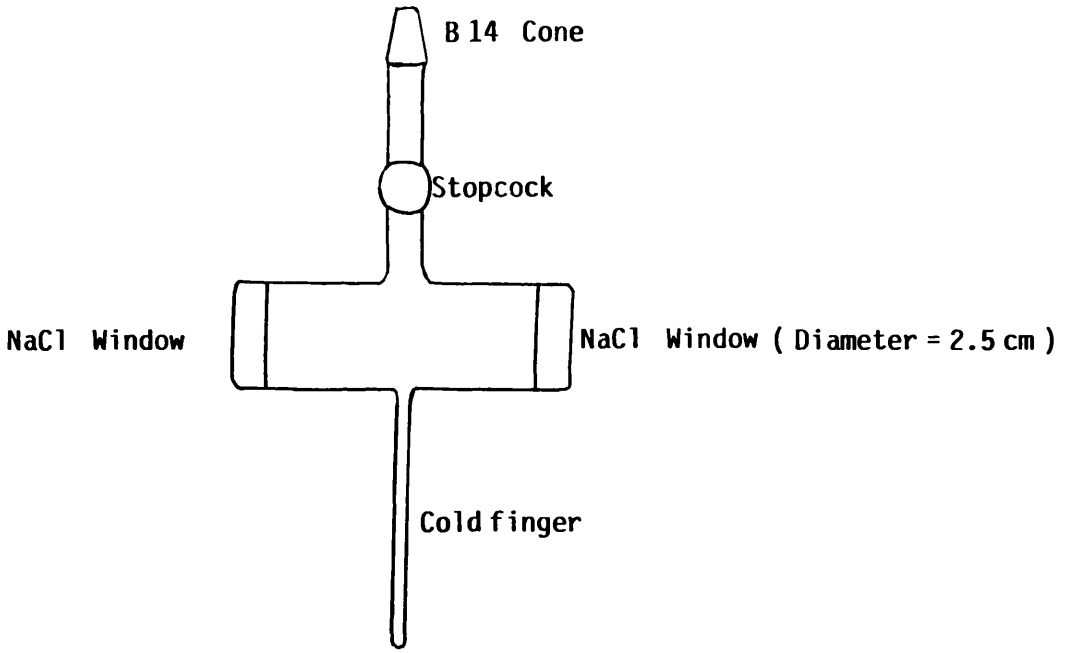

Figure 2.9: Gas cell for IR analysis .

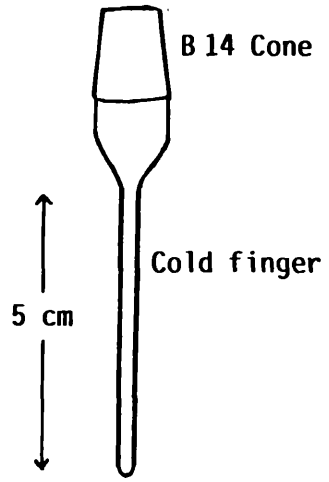

Figure 2.10: Cold finger for the collection of liquid fraction of degradation products .

2.2.2 THERMOGRAVIMETRY (TG)

Thermogravimetry (TG) is an important technique which allows a polymer sample to be raised from ambient temperature to 1000 ^{o}C while weight loss is recorded directly as a function of temperature or time under either dynamic nitrogen or vacuum conditions. The stability of a polymer can be assessed and the extent of weight loss at each stage of breakdown can be determined quantitatively.

Sometimes the TG curves do not clearly distinguish overlapping processes. These are more readily evident using differential thermogravimetry (DTG) which records the derivative of the weight loss curve.

A Dupont 990 Thermal Analyser was used to obtain TG and DTG curves simultaneously. Degradation was carried out under dynamic inert atmosphere (N_2, 80 ml/min) from ambient temperature to 600 ^{o}C at a heating rate of 10 ^{o}C/min. Isothermal degradation was employed at appropriate temperatures for 100 min. Samples in the form of powder were of the order 3-5 mg.

2.2.3 DIFFERENTIAL THERMAL ANALYSIS (DTA)

When a polymer undergoes a change in its physical state (melting point, glass transition temperature) or undergoes chemical reaction (cyclisation, dehydration, degradation), DTA detects the change from the temperature difference between sample and inert reference, during programmed heating. These changes may result in heat absorption (endothermic) or heat evolution (exothermic). Conventionally, these changes will be recorded by downwards or upwards deflection, respectively, in the DTA curve.

A Dupont 451 Thermal Analyser was employed to measure the differential temperature between sample and inert reference as the same temperature is raised. The DTA traces were obtained in an inert N_2 flow of 60 ml/min from ambient temperature to 500 ^{o}C at heating rate of 10 ^{o}C/min.

2.2.4 DIFFERENTIAL SCANNING CALORIMETRY (DSC)

DSC is a technique similar to DTA depending on detection of heat absorption or evolution, but it records quantity of heat to maintain sample and inert reference at the same temperature during any physical or chemical change as the polymer temperature is increased.

2.2.5 TOEPLER LINE

This technique allows the collection and subsequently identification of non-condensable gases at -196 ^{o}C which cannot be trapped under TVA conditions. The layout of Toepler line is illustrated in Figure 2.11.

In experiments to collect and characterise the permanent gases at-196 ^{o}C released from polymer degradation using the Toepler line, degradations were performed in sealable tubes similar to that shown in Figure 2.11. The sample was inserted into the base of tube 4 which was then connected to a vacuum line via cone 1. While the tube was being continuously evacuated (10^{-5} mbar), the constriction was carefully sealed. The tube 4 was clamped horizontally into a furnace whilst tube 3 was surrounded by liquid nitrogen, and heating was carried out as in normal TVA. When the degradation had been completed, the sealed tube was removed and a small magnetic bar was inserted carefully through cone 2 which was attached to a Toepler line at socket 8 of Figure 2.11 while the tube 3 still surrounded with liquid nitrogen (-196 ^{o}C).

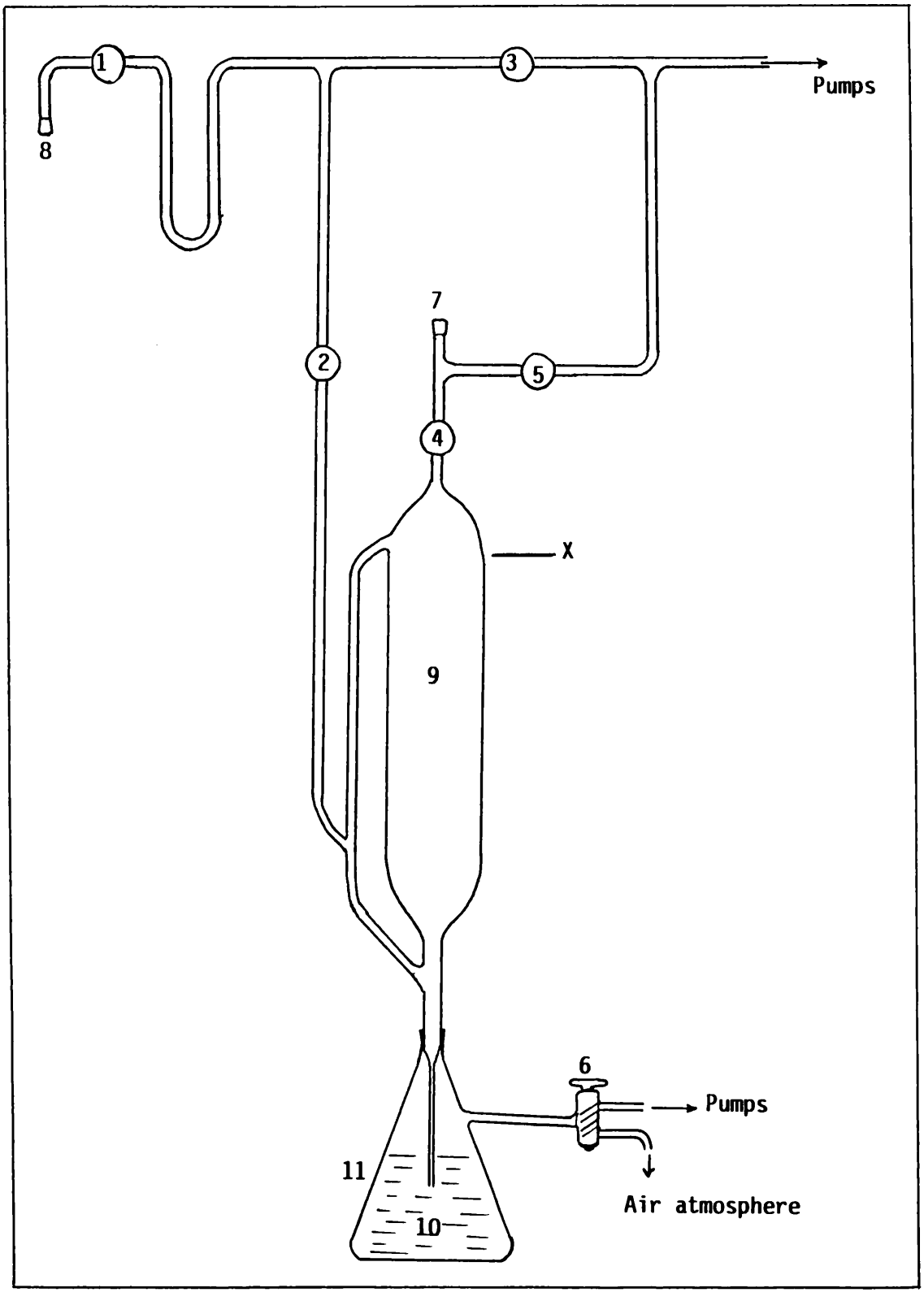

Figure 2.11: Layout of Toepler apparatus . **1-5**, stopcocks ; **6**, two way stopcock ; **7**, take off collection point (gas cell) ; **8**, B 14 socket ; **9**, reservoir ; **10**, mercury ; **11**, conical flask

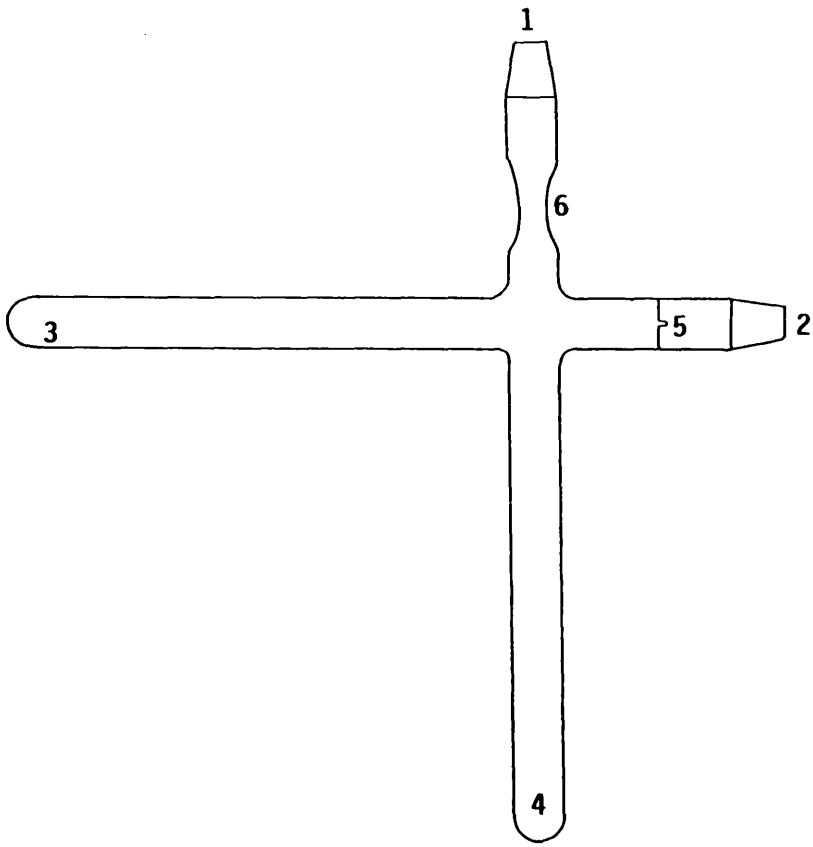

Figure 2.12: Sealable tube . **1** and **2**, B 14 cone ; **3** and **4** , sample tube ; **5**, break-seal ; **6** constriction .

At take off collection point 8 in the Toepler line, a gas cell was connected and the system was evacuated by opening all stopcocks to the vacuum pumps. Once a high vacuum (10^{-5} mbar) had been obtained, stopcocks 3 and 5 were closed, isolating the Toepler apparatus from the pumping system. The break-seal was then broken by the magnetic bar releasing the non-condensable gases into the system.

Compression of the non-condensable gases into the gas cell was carried out as follows. Stopcock 2 was closed and the two way stopcock was opened to the atmosphere,which caused the mercury in the conical flask to be pushed up into reservoir and as the mercury level rose higher the gases were compressed into the gas cell. When the mercury level reached X of reservoir level, the two way tap was closed and stopcock 4 was then closed. By opening the two way stopcock to the pumps, the mercury level fell down to its original level. The isolated gases were thus collected for spectroscopic analysis by closing the stopcock of the gas cell.

2.3 ANALYTICAL TECHNIQUES

Studies in polymer degradation have made extensive use of analytical techniques which can be subdivided into three classes, namely, determination of molecular weight, spectroscopy and chromatography.

The molecular weight can be measured using several methods (e.g. viscometry, osmometry, light scattering and gel permeation chromatography). The spectroscopic methods include ultraviolet, infrared, raman, emission, nuclear magnetic resonance, mass and electron spin resonance spectroscopy. Finally, various types of chromatography may be employed for the separation, identification and quantitative analysis of products released from the degradation of polymeric materials.

The most widely applied chromatographic techniques are gas liquid chromatography (GLC) and thin layer chromatography (TLC). In addition to these, GPC can be used to fractionate a polymer sample according to molecular size. The combination of these methods can provide a great deal of information about a polymer.

2.3.1 INFRARED SPECTROSCOPY

Infrared spectra were recorded either on a Perkin Elmer 257 grating spectrophotometer, Perkin Elmer 983 with PE 3600 data system or Philips PU 9800 FT-IR instrument.

Samples were examined in the form of a solid KBr disc, a thin film cast on a salt plate from a solution in an appropriate solvent, or in the gas phase, as appropriate. Gas cells equipped with 25 mm NaCl windows (Figure 2.9) were used to obtain the ir spectra of those products released from the polymer degradation with an appreciable vapour pressure at ambient temperature. The identification of degradation products from their ir spectra was performed by a comparison with spectra of authentic samples [33-35].

2.3.2 MICROANALYSIS

Elemental analysis for carbon, hydrogen, chlorine and bromine was carried out using a Carlo Erba Elemental Analyzer 1106. They were flash combusted to CO_2 and H_2O which were separated and measured quantitatively using gas liquid chromatography. The halogen X_2 (Cl_2 and Br_2) were measured by titration of X^-.

2.3.3 MASS SPECTROMETRY

A modified low resolution Kratos MS 12 mass spectrometer with a Micromass DS 55 data handling system and a high resolution Kratos DS 9025 mass spectrometer with a Micromass DS 90 data handling system. These were used to assist identification of degradation products. Moreover, when possible, a Micromass QX-200 quadropole mass spectrometer attached directly to the TVA apparatus between the main trap and pumps was employed. The products of degradation volatile at ambient temperature, with molecular weight less than 200, can be analysed. The non-condensable gases at -196 ^{o}C could also be bled into the mass spectrometer during the degradation process.

2.3.4 ^{13}C CROSS POLARISATION MAGIC ANGLE SPINNING NUCLEAR MAGNETIC RESONANCE SPECTROSCOPY (CP MAS-NMR)

In a solid the dipole-dipole interaction, usually averaged out by molecular tumbling in solution, is dominant leading to line widths usually of a few kilohertz. In order to overcome this and get reasonable high resolution spectra, a combination of magic angle spinning (MAS) and high power proton decoupling was used.

The ^{13}C CP MAS-NMR spectra (UDIRL, Durham) were recorded following a cross polarisation C-H preparation sequence which permits us to get better signal to noise ratio at any given time. On the other hand, a C-O carbon, cross-polarises differently to a C-H, so even though a sample may contain one of each they may not give signals of equal intensity. The spectra can be interpreted in the same way as solution state spectra. All the

spectra are referenced to TMS. Each plot is presented with standard spectrum and two edited spectra. The Non-Quaternary Suppression (NQS) spectrum shows only peaks from quaternary carbons. The Quaternary Suppression (QS) spectrum is just the difference between the NQS and the standard spectrum and shows signals only from non-quaternary carbons.

2.3.5 GAS CHROMATOGRAPHY – MASS SPECTROMETRY (GC-MS)

Volatile liquid products from the degradation of a polymer sample cannot be fully separated by means of SATVA, because of the small quantities and the fact that some of the products are of similar volatility. A better separation was achieved using a Perkin Elmer Sigma 3 Chromatograph interfaced to a Kratos MS 30 mass spectrometer with DS 90 data handling system. This was operated with columns and conditions as illustrated in Table 2.1.

Column	BP -10	DB - 5
Column packing	14 % Cyanopropyl-dimethyl siloxane	5 % Phenyl silicone
Polarity	Slightly polar	Polar
Length (mm)	25	15
Inside diameter (mm)	0.33	0.25
Film thickness (μ m)	0.5	1
Gas carrier	He	He

Table 2.1: Columns used for the separation of liquid degradation products.

CHAPTER THREE

EXPERIMENTAL

3.1 TEREPHTHALATE POLYESTERS

3.1.1 PURIFICATION OF MONOMERS

a.Terephthaloyl chloride, supplied by Aldrich Chemical Co Ltd, was purified by recrystallisation three times from n-hexane, dried and stored in a desiccator until further use.

b.Dimethyl terephthalate (DMT), resorcinol and hydroquinone were supplied by Koch-Light Laboratories Ltd. Decamethylene glycol (DMG), catechol, tetrabromocatechol (TBC), 4.4'-isopropylidene *bis*- (2.6-dibromo phenol) (IPBP), 4.4'-isopropylidene *bis*- (2.6-dichlorophenol) (IPCP), 4.4'-isopropylidene *bis*- [2-(2.6-dibromo phenoxy)-ethanol] (IPBPE) and p.p'-biphenol (BP) were supplied by Aldrich Chemical Co. Ltd. Poly (ethylene glycol) 200 (PEG200) was supplied by Poly Sciences Inc. and ethylene glycol (EG), butylene glycol (BG) and poly ethylene glycol 1000 (PEG1000) by BDH Ltd. EG, BG and PEG200 were distilled, the first and last 5 % being discarded. The distillate was shaken with activated anhydrous alumina and allowed to stand for 24 hours, followed by filtration and then stored in a desiccator until required. PEG1000 was dissolved in anhydrous ether / methanol (10:1) to effect complete solution and recrystallised three times at -10 ^{o}C. DMG, DMT, catechol, resorcinol, hydroquinone, TBC, BP, BPA, IPBPE, IPBP and IPCP were each purified by recrystallisation from absolute alcohol.

3.1.2 SYNTHESIS OF TEREPHTHALATE POLYESTERS

The methods followed to synthesise terephthalate polyesters were melt and interfacial pol condensation processes, in which terephthaloyl chloride was reacted with one of the diols (aliphatic, aromatic) as illustrated in the following equation.

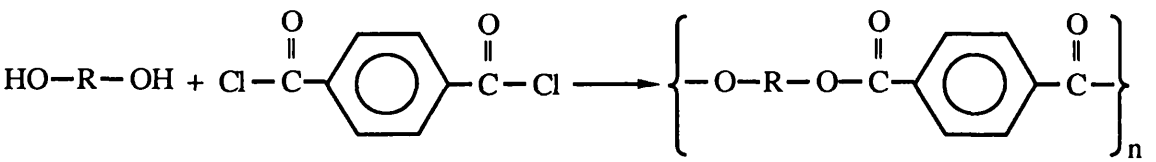

Where R was varied to give different polymer types as follows :

1.Poly(alkylene terephthalates) R = $(-CH_2)_m-$

where

m=2	poly(ethylene terephthalate)	PET
m=4	poly(butylene terephthalate)	PBT
m=10	poly(decamethylene terephthalate)	PDMT

2.Polyarylates

a. Fully aromatic polyarylates

where:

R = 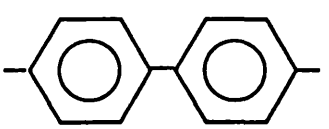

poly(p.p'-biphenylene terephthalate) PA1

R = 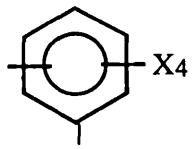

X=H	1) para : poly (1,4-phenylene terephthalate)	PA2
	2) meta : poly (1,3-phenylene terephthalate)	PA3
	3)ortho : poly (1,2-phenylene terephthalate)	PA4
X=Br, ortho:	poly (tetrabromo-1,2-phenylene terephthalate)	Br-PA4

b. Aliphatic / aromatic polyarylates

where :

R = 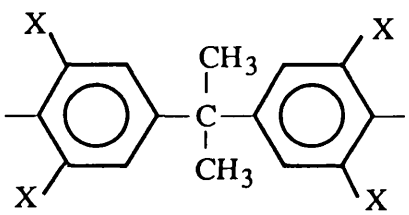

X=H	poly (*bis*-phenol A – terephthalate)	PA5
X=Cl	poly (tetrachloro *bis*-phenol A – terephthalate)	Cl-PA5
X=Br	poly (tetrabromo *bis*-phenol A – terephthalate)	Br-PA5

R = 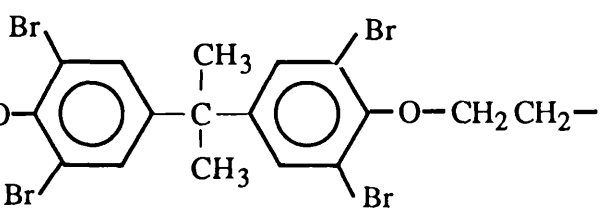

Br-PA6

3. Poly ether-ester

where R= -- $(CH_2-CH_2-O)_m$-- PPEGT

3.1.2.1. Melt Polycondensation

The following polymers were prepared by melt polycondensation: PET, PBT, PDMT, PA4, Br-PA6 and PPEGT. Except in the case of PET, the polymerisation was carried out as discribed by Flory and Leutner [36]. In a three necked round-bottomed flask fitted with nitrogen inlet, the diol (0.1 mol) was added to terephthaloyl chloride (0.1 mol) under a slow stream of nitrogen. The mixture was heated for 40-60 min. at 80-85 ^{o}C to drive off most of the hydrogen chloride. The temperature was then slowly increased over 3 hours to 240-260 ^{o}C, after which the pressure was reduced to 0.9 mbr over 20 min. and the polymerisation continued for a further 30 min. Poly (ethylene terephthalate), however, was prepared from dimethyl terephthalate and ethylene glycol in the presence of calcium acetate and antimony trioxide as catalysts[2,3]. Table 3.1 summarises the polymerisation conditions for the above polymers.

3.1.2.2. Interfacial Polycondensation

The remaining polymers were synthesised by interfacial polycondensation [6,37]. The polymerisation was carried out in a three-necked round-bottomed flask (500 ml), equipped with a mechanical stirrer, in which a solution of one of the aromatic diols (0.1 mol) and sodium hydroxide (0.2 mol) in water (250 ml) was first prepared. A second solution containing terephthaloyl chloride (0.1 mol) in methylene chloride (100 ml) was prepared. A detergent solution consisting of sodium lauryl sulphate

Polymeristion Conditions

Polymer	Temperature / °C	Time / min.	Atmosphere
PET	197	120	Nitrogen
	222	30	"
	255-260	60	"
	270	30	Vacuum
PBT	80-85	60	Nitrogen
	180	100	"
	240	30	"
	180	120	Vacuum
PDMT	85-90	35	Nitrogen
	155	30	"
	218	30	"
	255-60	150	"
PPEGT	85	35	"
	155	40	"
	220	25	"
	270	180	"
PA4	100	40	"
	150	30	"
	200	30	"
	240	20	"
	240	150	Vacuum
Br-PA6	85	60	Nitrogen
	120	30	"
	160	30	"
	225	40	"
	260	60	"

Table 3.7: Polymerisation conditions for terephthalate polyesters synthesised by melt polycondensation.

(1.5 g) in water (15 ml) was added to the diol solution under slow stirring. The acid chloride solution was then introduced as rapidly as possible during vigorous stirring which was continued for a further 5-10 min. The polymer was precipitated in acetone, filtered and washed several times with distilled water to remove detergent and salt. The purified polymer was dried in a vacuum oven at 40 ^{o}C for 24 hours.

3.1.3 CARACTERISATION OF TEREPHTHALATE POLYESTERS

The characterisation of terephthalate polyesters was carried out by means of microanalysis, infrared and solid state ^{13}C CP MAS-NMR spectroscopy.

3.1.3.1 Microanalysis:

Percentages of carbon, hydrogen, chlorine and bromine were determined and the analytical results are summarised in Tables 3.2 and 3.3

3.1.3.2 Infrared Spectroscopy:

The ir spectra for the terephthalate polyesters, shown in Figures 3.1-3.9,were obtained in the solid state using the KBr disc technique and the main characteristic bands are listed in Tables 3.4 and 3.5.

3.1.3.3 ^{13}C MAS-NMR Spectroscopy :

The ^{13}C cross polarisation magic angle spining nuclear magnetic resonance spectra for each of the solid polyarylates, are shown in Figures 3.10-3.18 and their respective ^{13}C nmr chemical shifts are listed in Tables 3.6 and 3.7. These assignments were made according to the ^{13}C nmr

Polymer code N°		C %		H %	
		Calculated	Found	Calculated	Foound
Poly alkylene terephthalates	PET	62.5	61.67	4.16	4.26
	PBT	65.45	64.95	5.45	5.28
	PDMT	71.05	71.37	7.88	8.64
Poly ether-ester	PPEGT1	59.24	58.56	6.17	6.65
	PPEGT2	55.21	54.99	8.25	9.70

Table 3.2 : Elemental analysis for poly(alkylene terephthalates) and poly(ether-ester).

Polymer		C %		H %		Cl %		Br %	
		Calculated	Found	Calculated	Found	Calculated	Found	Calculated	Found
Polyarylates	PA1	74.57	75.94	3.67	3.79	—	—	—	—
	PA2	70.00	70.10	3.33	3.21	—	—	—	—
	PA3	70.00	67.73	3.33	3.33	—	—	—	—
	PA4	70.00	69.86	3.33	3.27	—	—	—	—
	PA5	77.09	77.89	5.03	5.17	—	—	—	—
Halogenated Polyarylates	Br-PA4	30.21	31.08	0.72	0.31	—	—	57.55	57.46
	Cl-PA5	55.64	54.61	2.82	2.44	28.62	27.58	—	—
	Br-PA5	40.94	41.13	2.07	1.30	—	—	47.47	47.42
	Br-PA6	42.56	42.66	2.88	2.89	—	—	41.99	45.22

Table 3.3 : Elemental analysis for polyarylates and halogenated polyarylates.

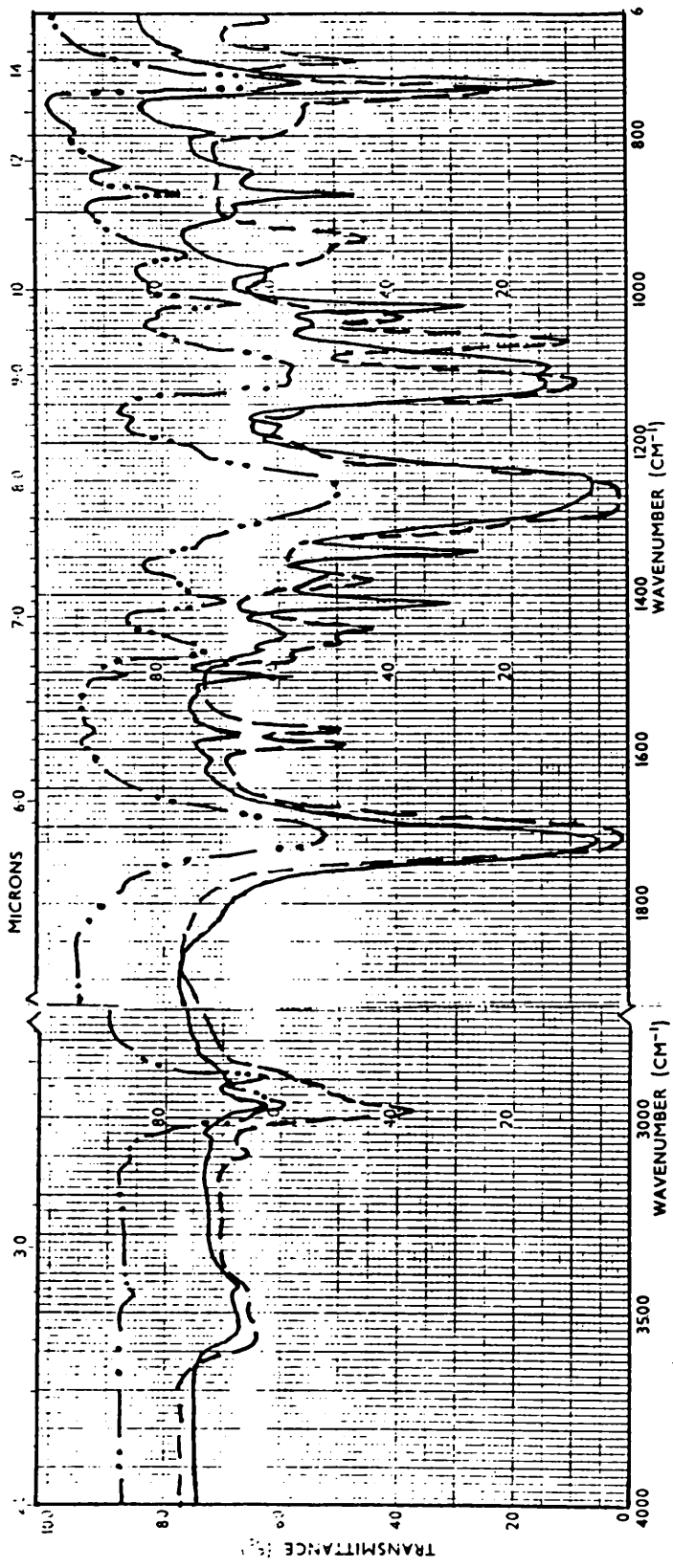

Figure 3.1: Infrared spectra of poly(alkylene terephthalates). PET (——), PBT (– – –) and PDMT (—··—).

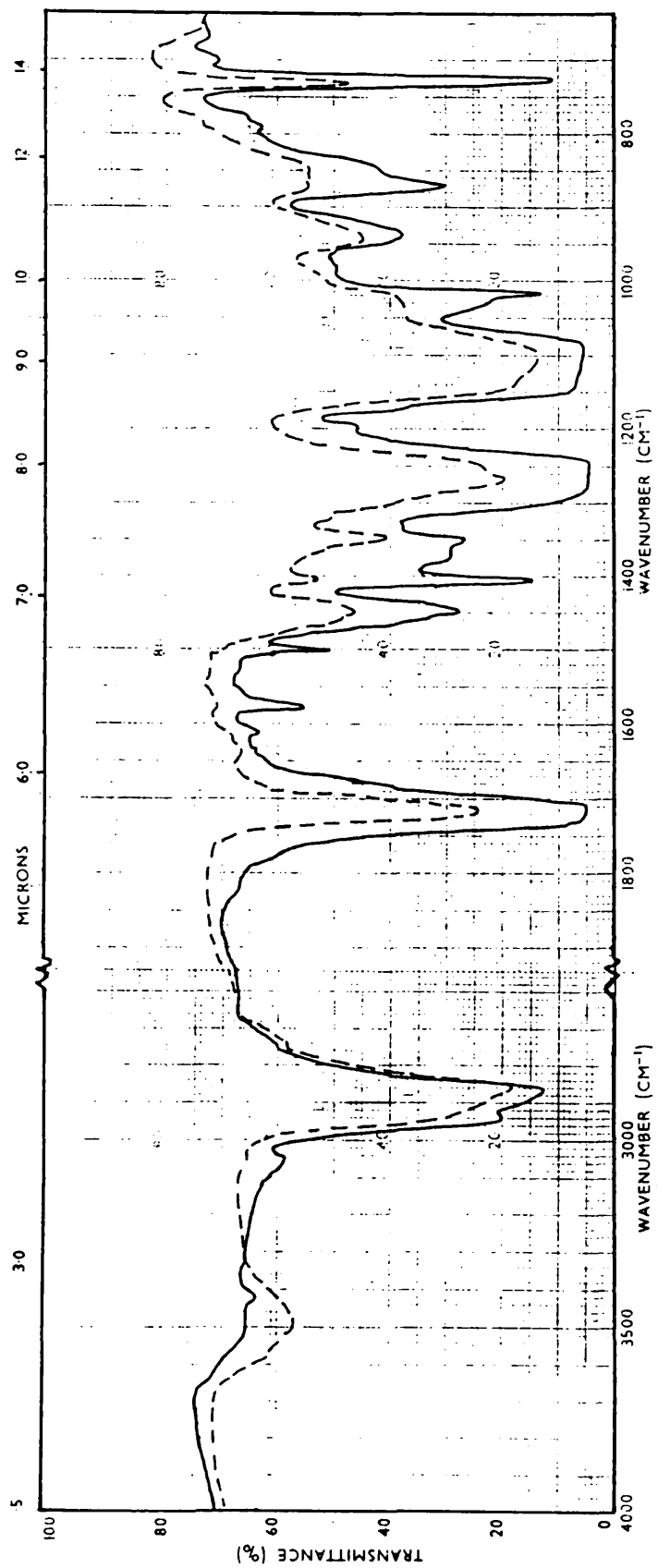

Figure 3.2: Infrared spectra of poly(ether esters) . PEGT1 (———) and PEGT2 (— — —) .

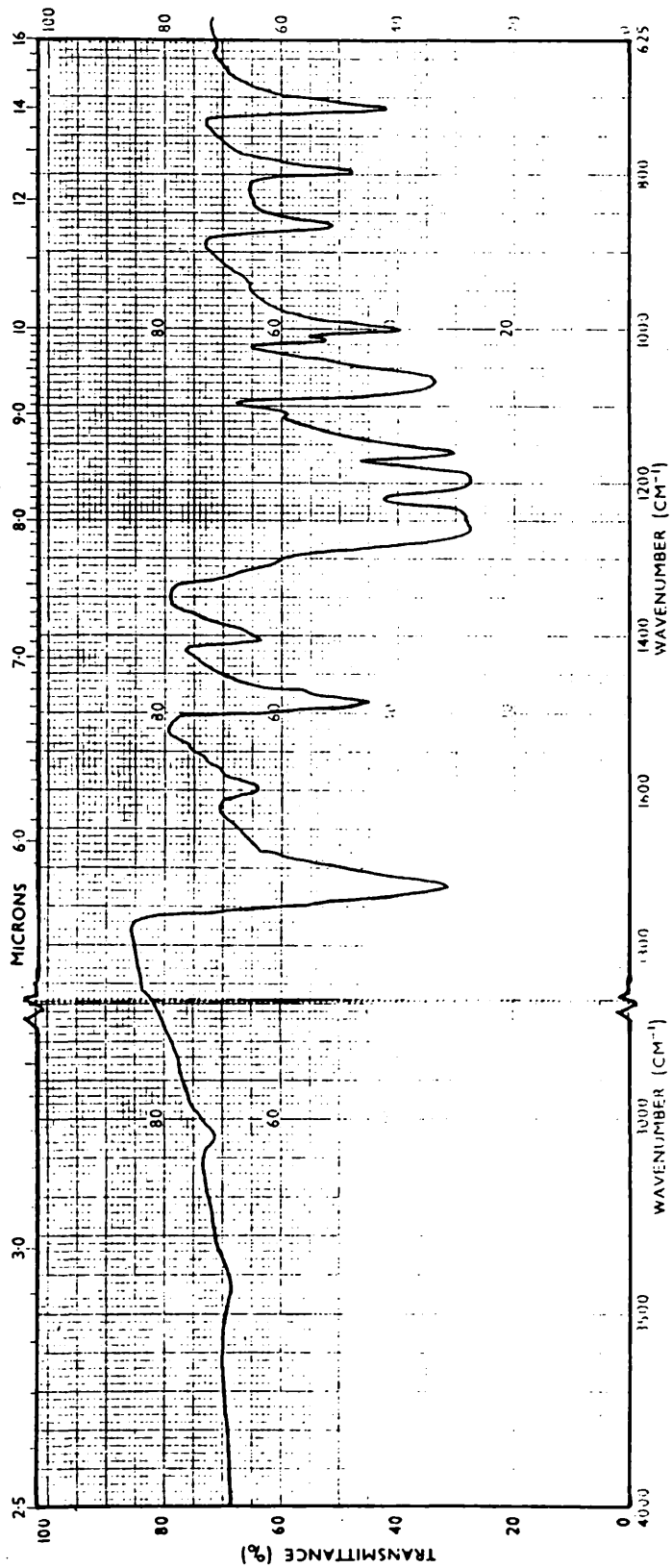

Figure 3.3: Infrared spectrum of poly(biphenylene terephthalate) (PA1) .

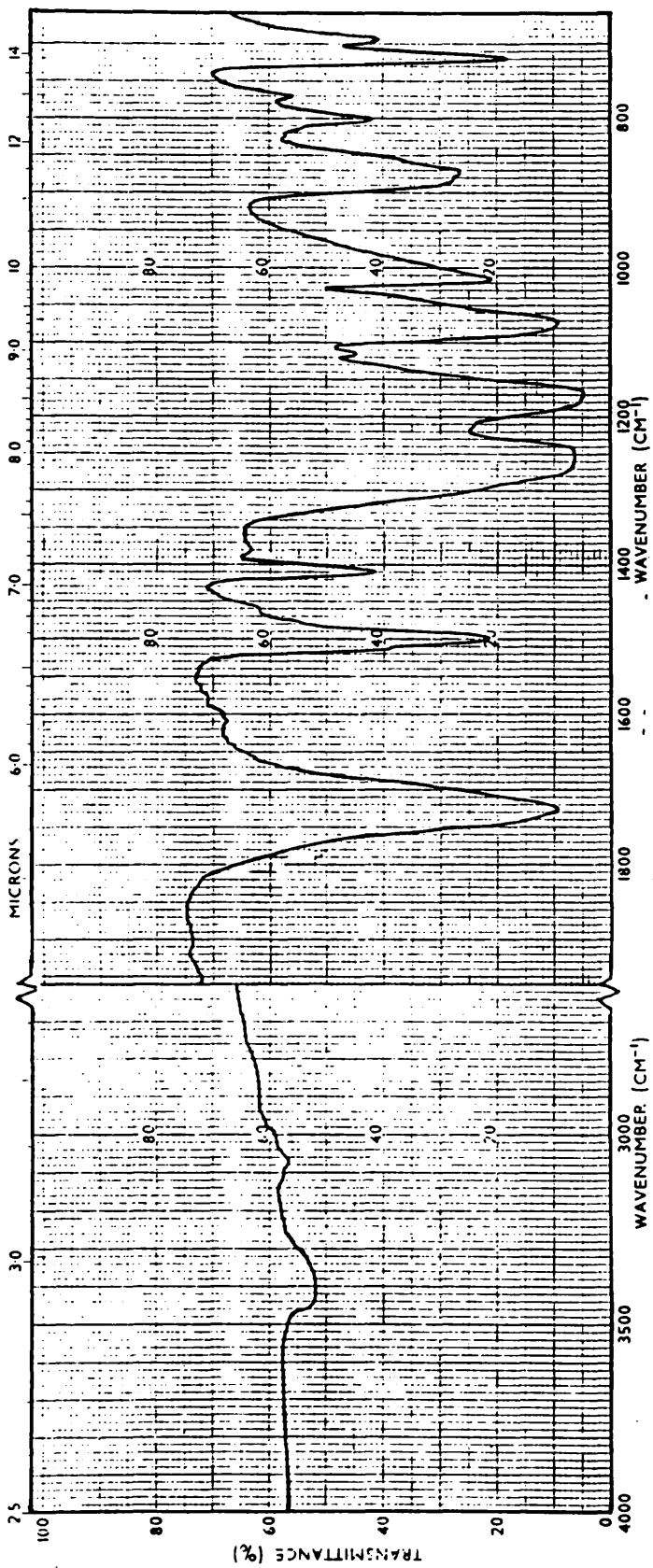

Figure 3.4: Infrared spectrum of poly(1,4 phenylene terephthalate) (PA2)

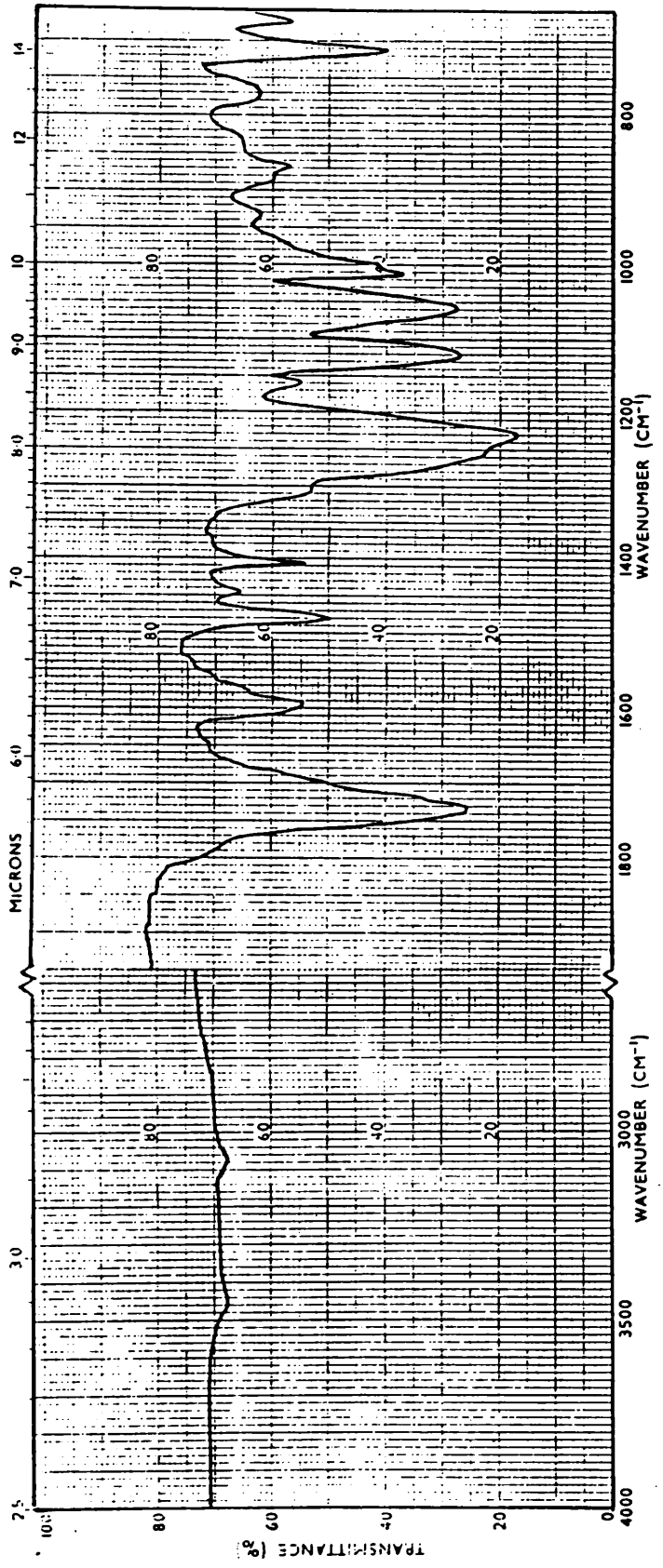

Figure 3.5: Infrared spectrum of poly(1,3 phenylene terephthalate) (PA3)

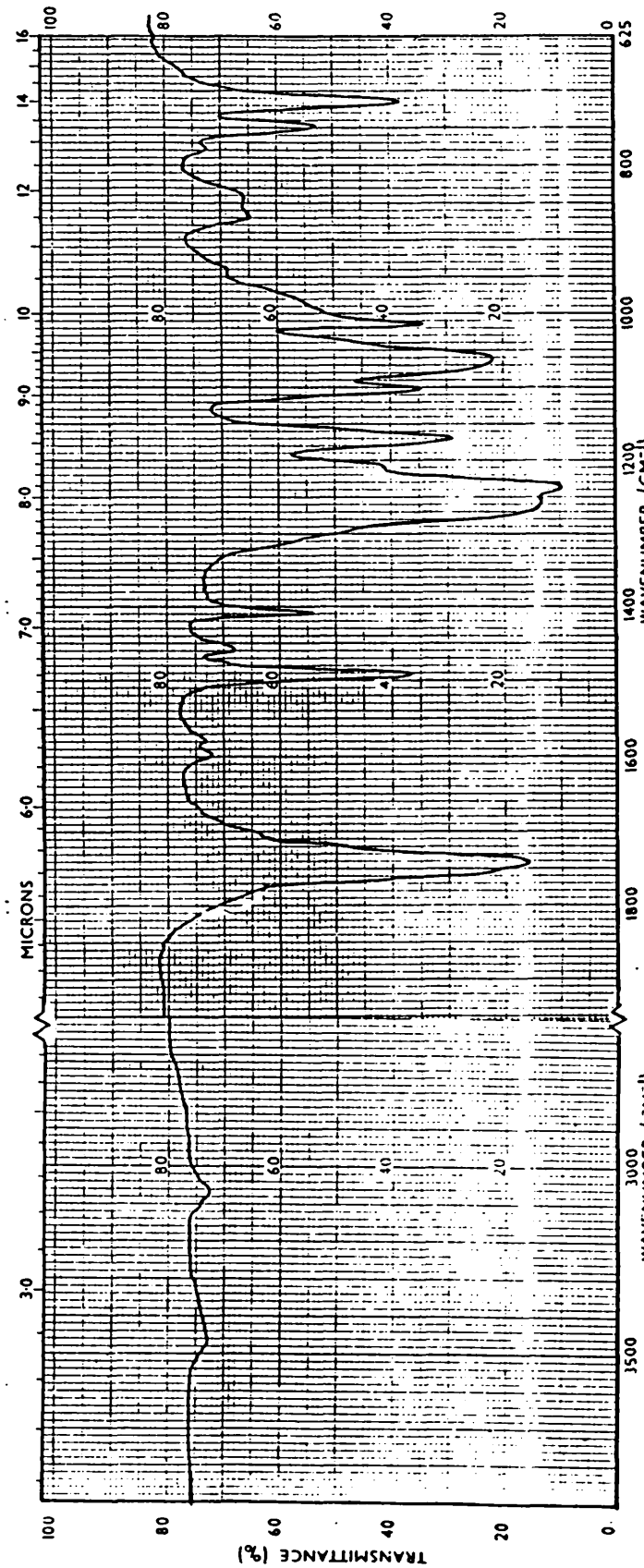

Figure 3.6: Infrared spectrum of poly(1,2-phenylene terephthalate) (PA4) .

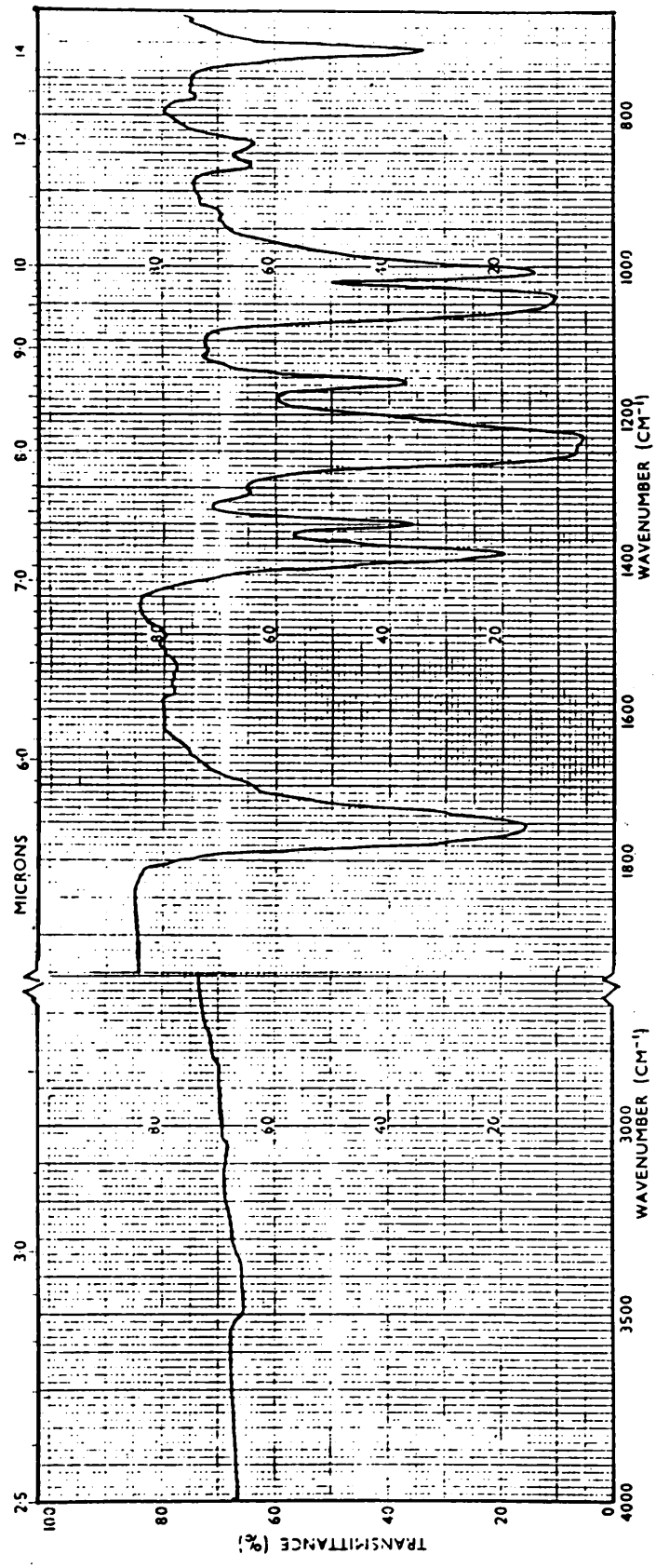

Figure 3.7: Infrared spectrum of poly(tetrabromo 1,2 phenylene terephthalte) (Br PA4)

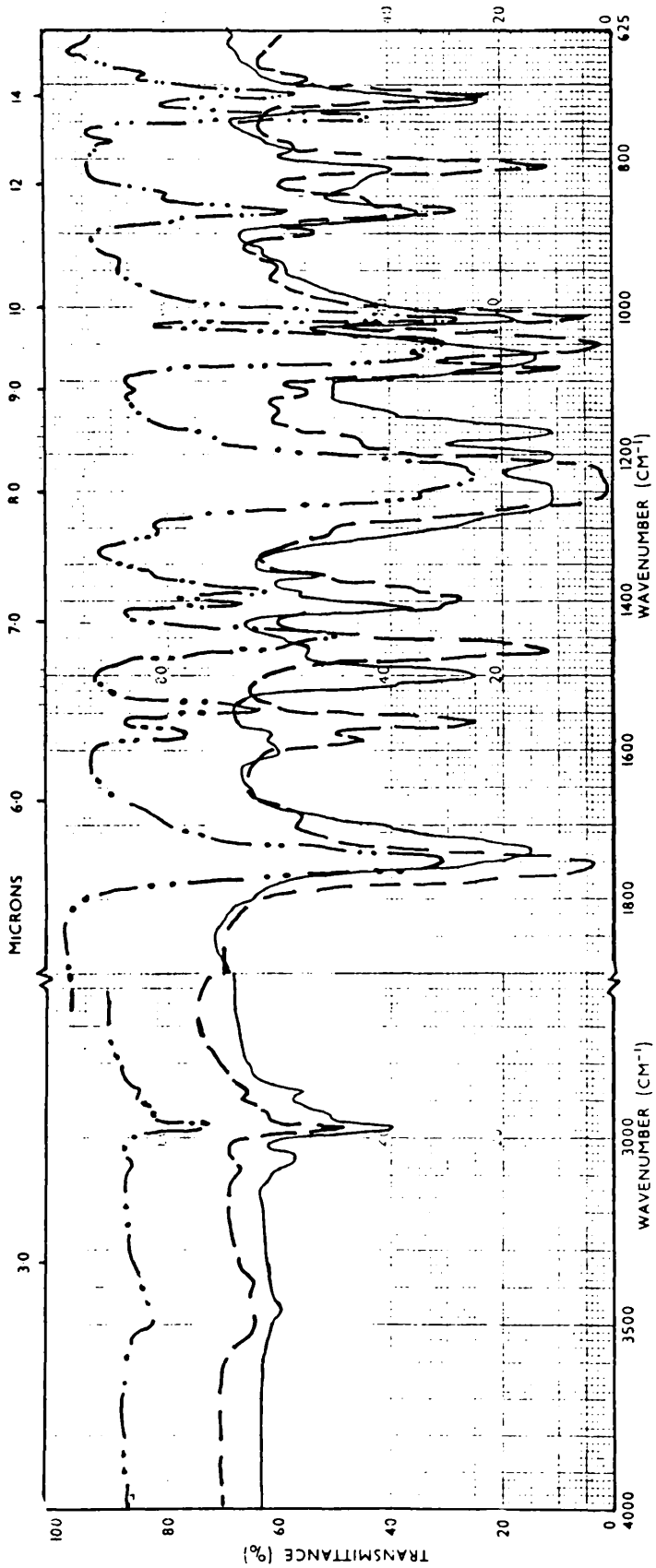

Figure 3.8: Infrared spectra of poly(bisphenol A terephthalates).

PA5 (——) , Cl-PA5 (– – –) and Br-PA5 (—·—) .

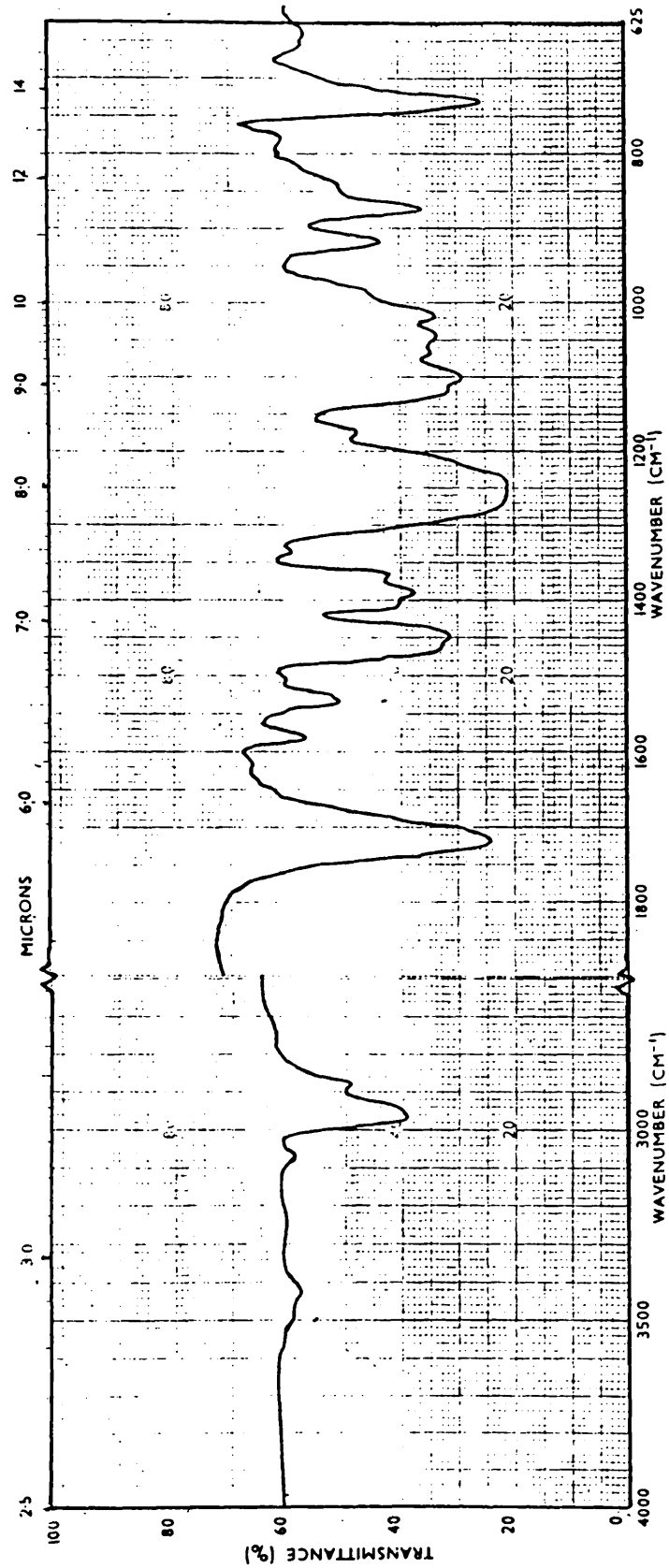

Figure 3.9: Infrared spectrum of Br-PA6.

Absorption bonds (cm^{-1})				Assignment
Poly (alkylene terephthalates)			Poly ether-ester	
PET	PBT	PDMT	PPEGT	
3040	3040	3050	3040	υ C-H in aromatic ring
2960 2905	2960 2900	2960 2920 2870	2940 2870 2850	υ C-H in aliphatic chain
1720	1715	1710	1715	υ -CO- in ester group
1240-1290 1100	1230-1280 1100	1220-1260 1100	1240-1290 1080-1150	υ C-O-C overlapping of several vibrations in ester group linkage
1020	1015	1020	1020	β C-H in aromatic ring
870, 729	870, 729	870, 840,725	940,870,725	γ C-H in p-disubstitution aromatic ring

Table 3.4 : Assignment of IR absorptions in Figures 3.1 and 3.2.

N.B : υ = stertching , β = in-plane bending , δ = antisymmetric deformation and γ = out-of plane bending .

Absorption bands (c m-1)									Assignment
Polyarylates					Halogenated polyarylates				
PA1	PA2	PA3	PA4	PA5	Br-PA4	Cl-PA5	Br-PA5	Br-PA6	
3050	3070	3070	3060	3050	3060	3080	3070	3070	υ C-H in aromatic ring
—	—	—	—	2960 2920	—	2985 2895	2970 2870	2970 2880	υ C-H in aliphatic chain
1725	1725	1735	1740	1750	1750	1750	1750	1720	υ -CO- in ester group
1600	1600	1590	1595	1600	1600	1590	1585	1585	υ C=C in aromatic ring
1485 1405	1495 1410	1495 1410	1490 1410	1500 1410	1390 1350	1470 1395	1450 1400	1450 1390	δ C-H in aromatic ring
1230-60 1160 1070	1240-70 1170 1070	1220-80 1120 1060	1235-60 1170 1070	1240-60 1140 1070	1220-60 1155 1040	1210-60 1080 1050	1210-60 1065 1050	1220-85 1100 1040	υ C-O-C overlapping of several vibrations in ester group linkage
1000	1015	1015	1015	1010	1010	1010	1015	1020	β C-H in aromatic ring
870 795 720	870 800 720	870 770 715	870 750 715	870 815 725	870 840 710	870 810 725	870 740 710	870 730	γ C-H in disubstitution in aromatic ring

Table 3.5 : Assignment of IR absorptionsin Figures (3.3 - 3.9)

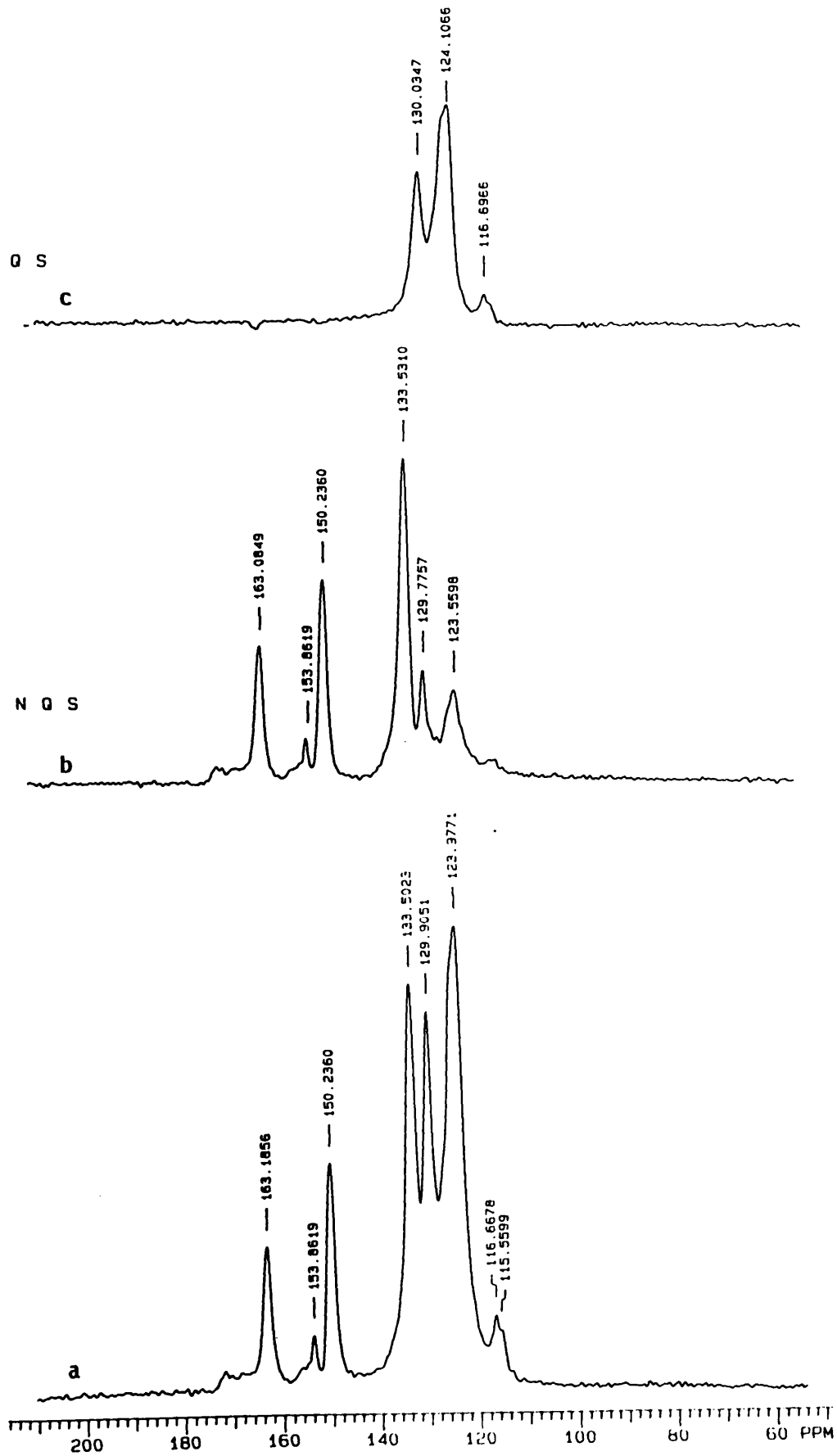

Figure 3.10: ^{13}C CP MAS-NMR spectra of solid PA1 .

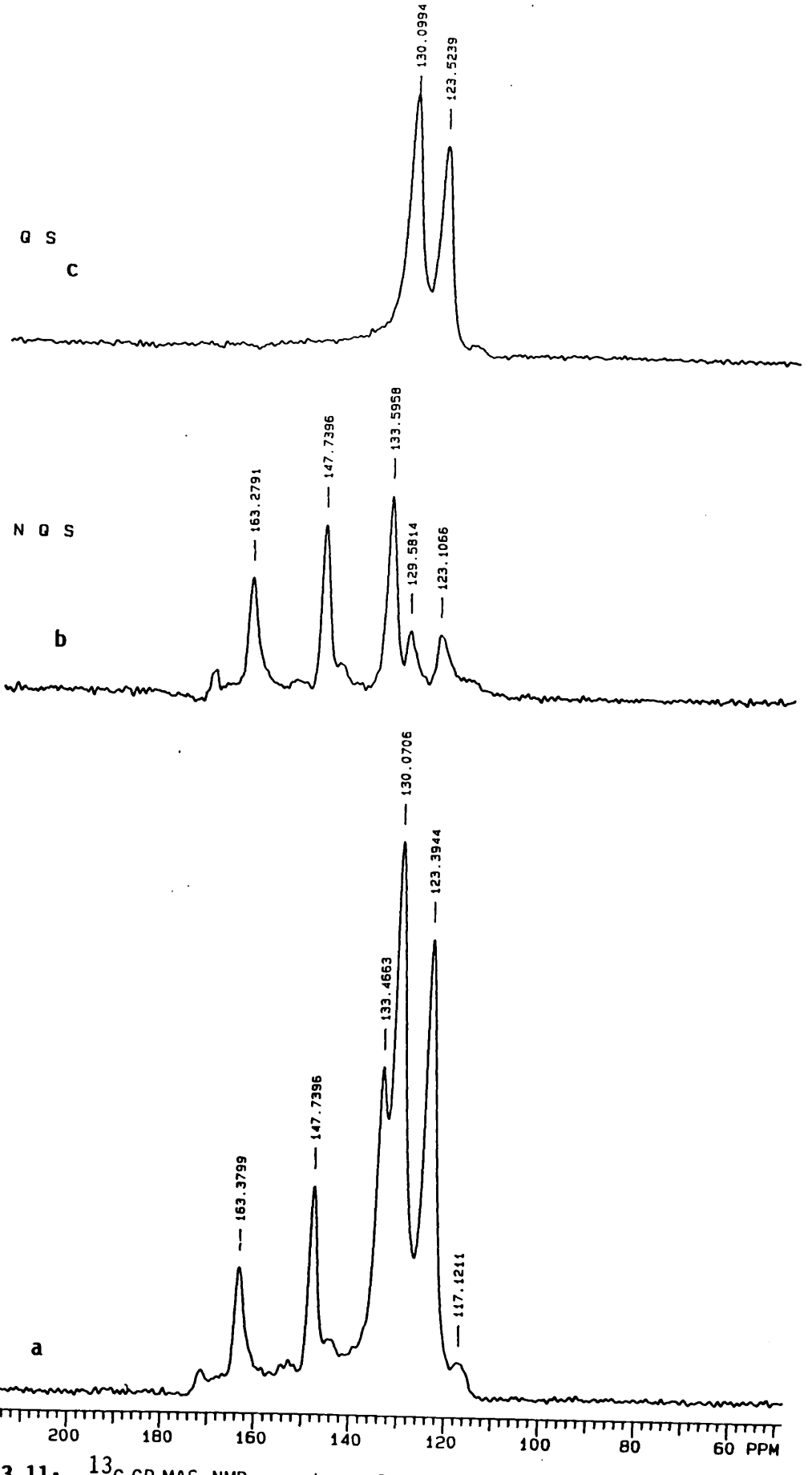

Figure 3.11: ^{13}C CP MAS-NMR spectra of solid PA2 .

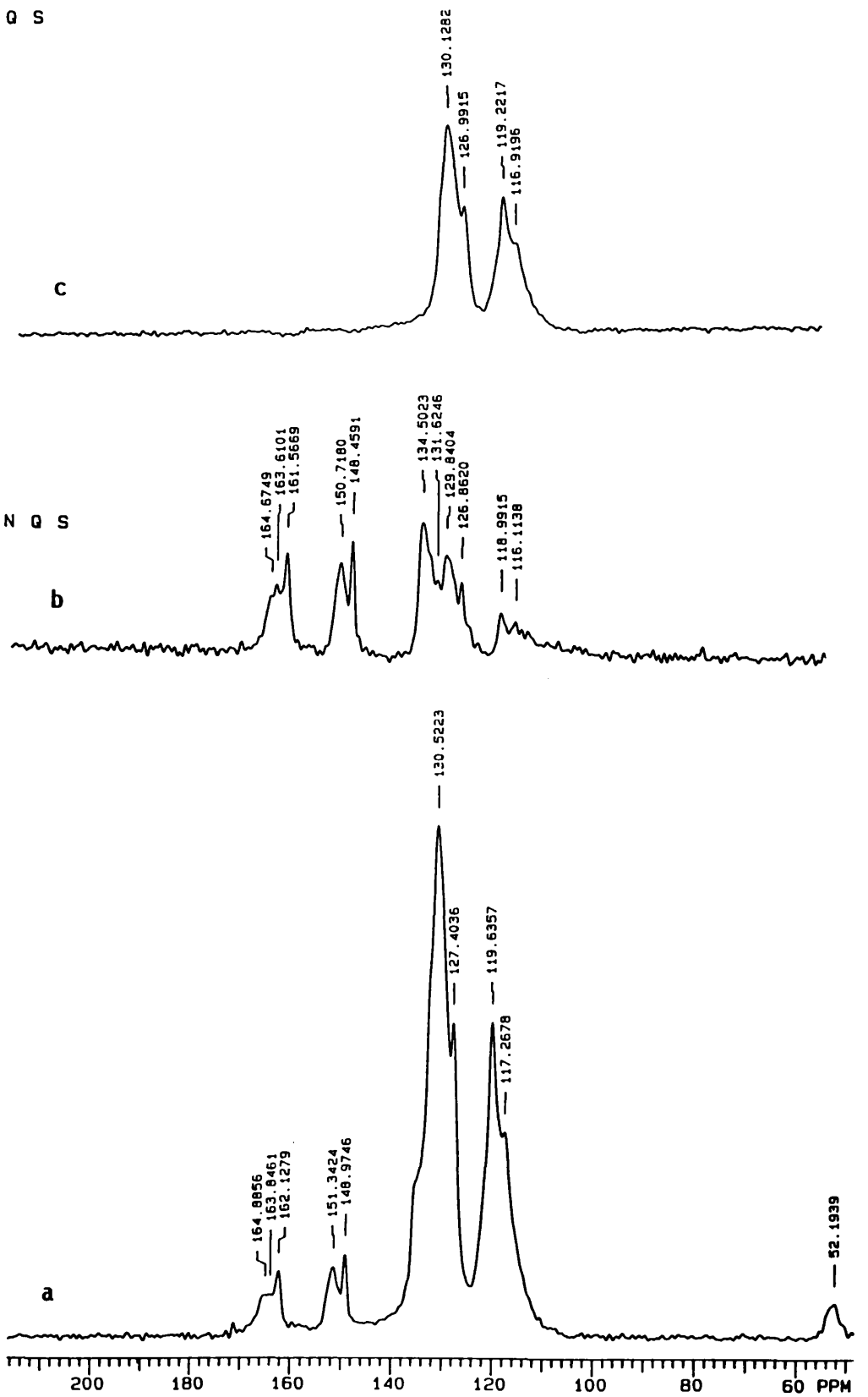

Figure 3.12: ^{13}C CP MAS-NMR spectra of solid PA3 .

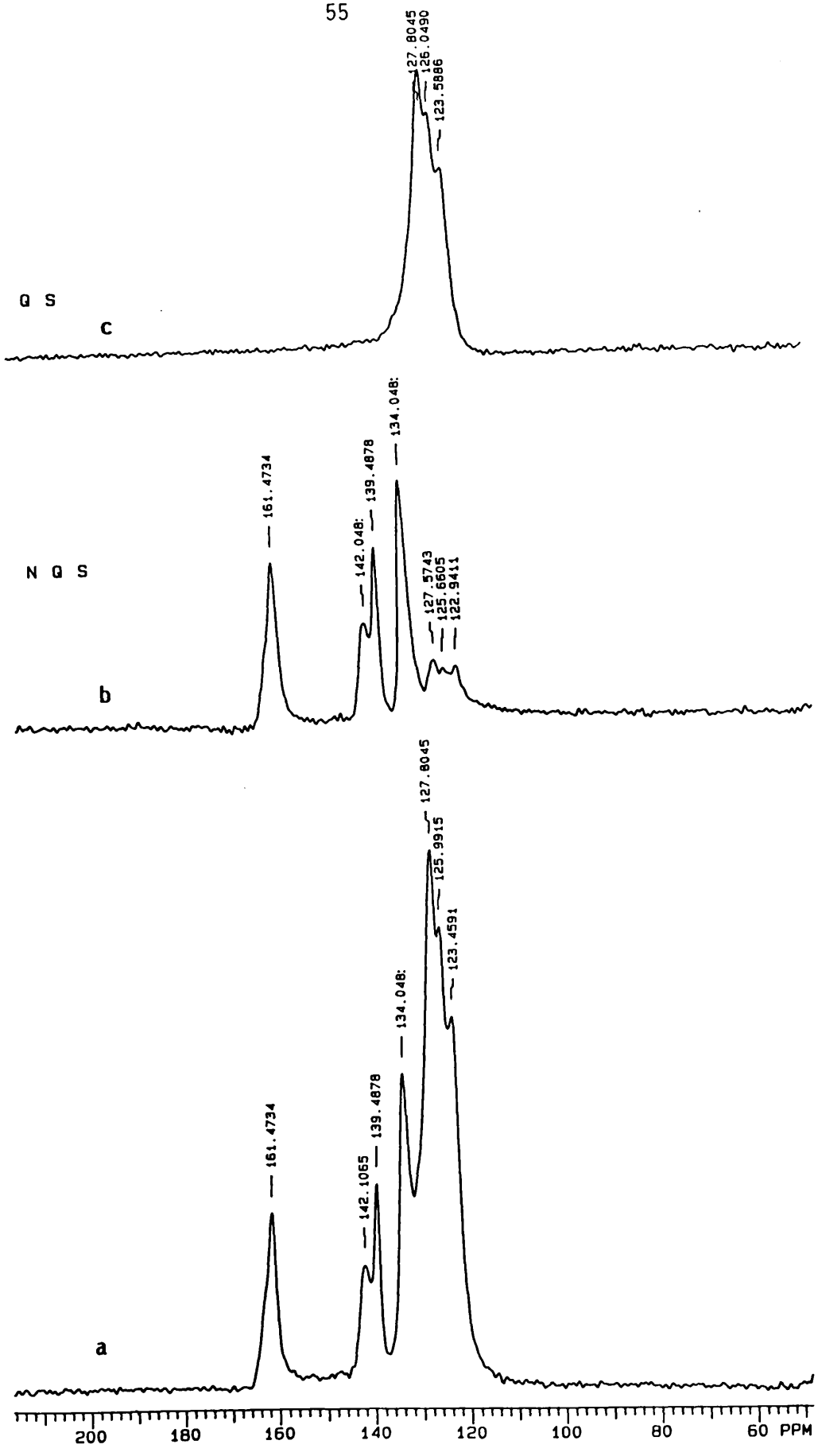

Figure 3.13: ^{13}C CP MAS-NMR spectra solid PA4 .

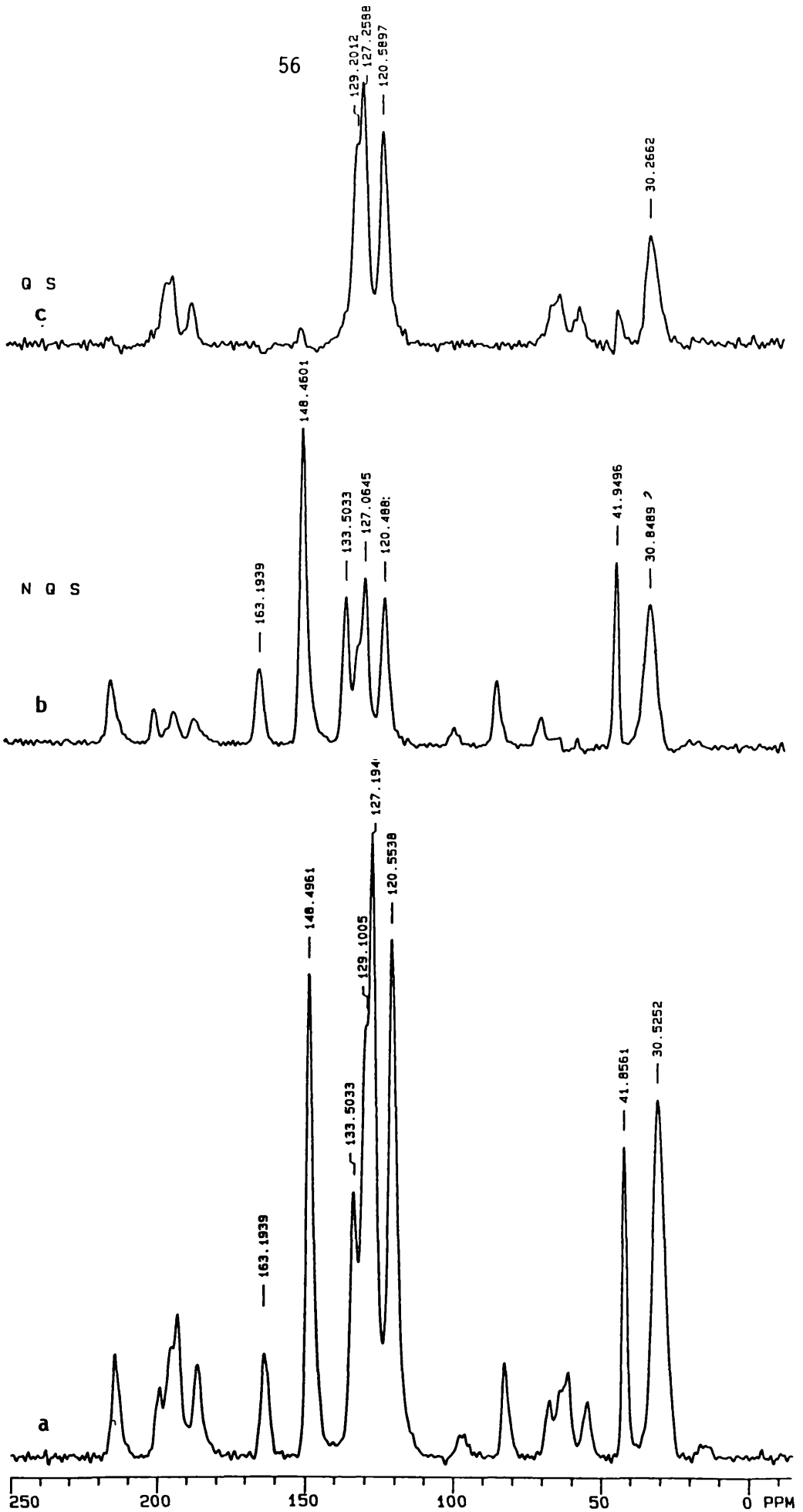

Figure 3.14: ^{13}C CP MAS-NMR spectra of solid PA5 .

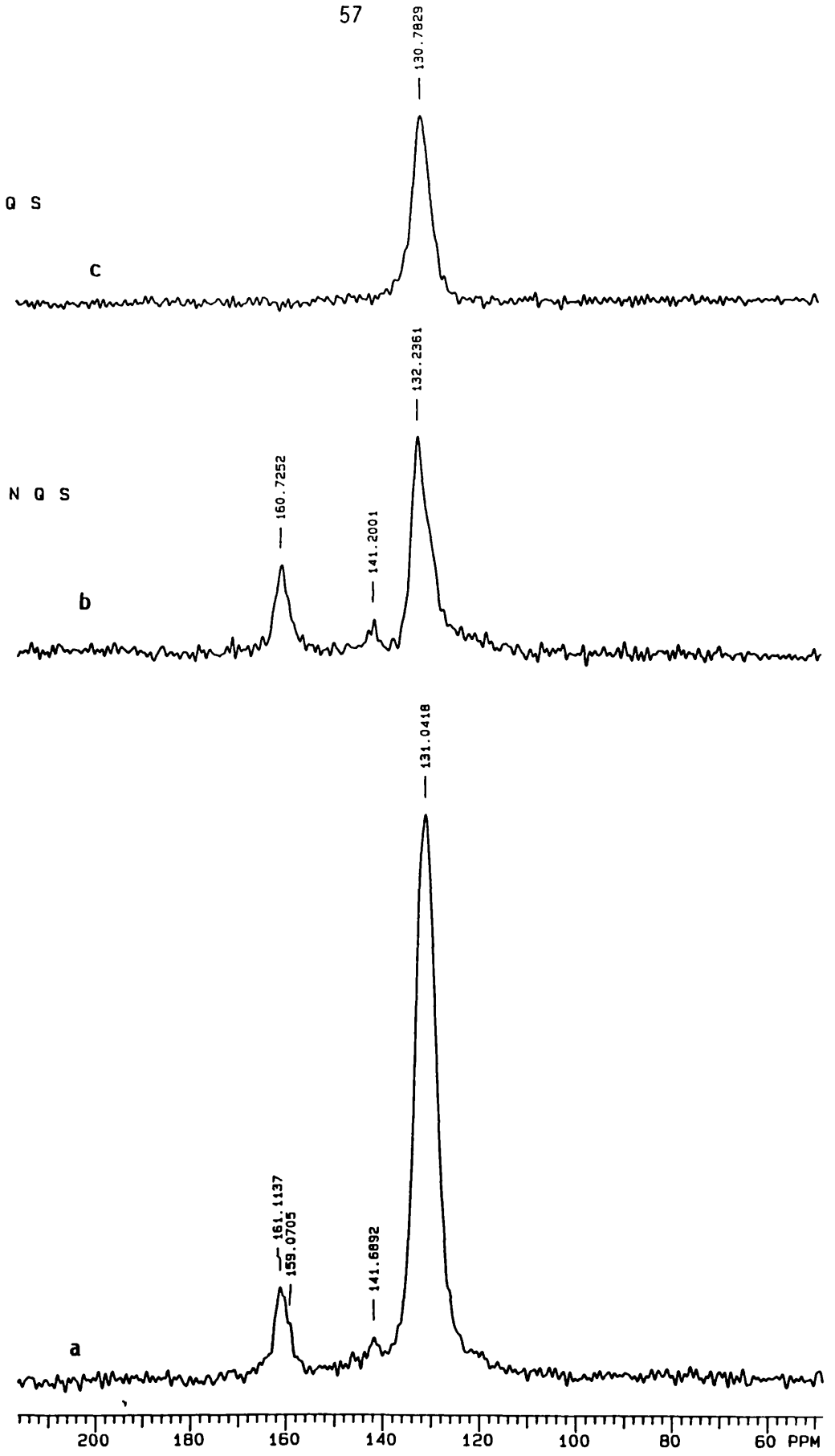

Figure 3.15: ^{13}C CP MAS -NMR spectra of solid Br-PA4 .

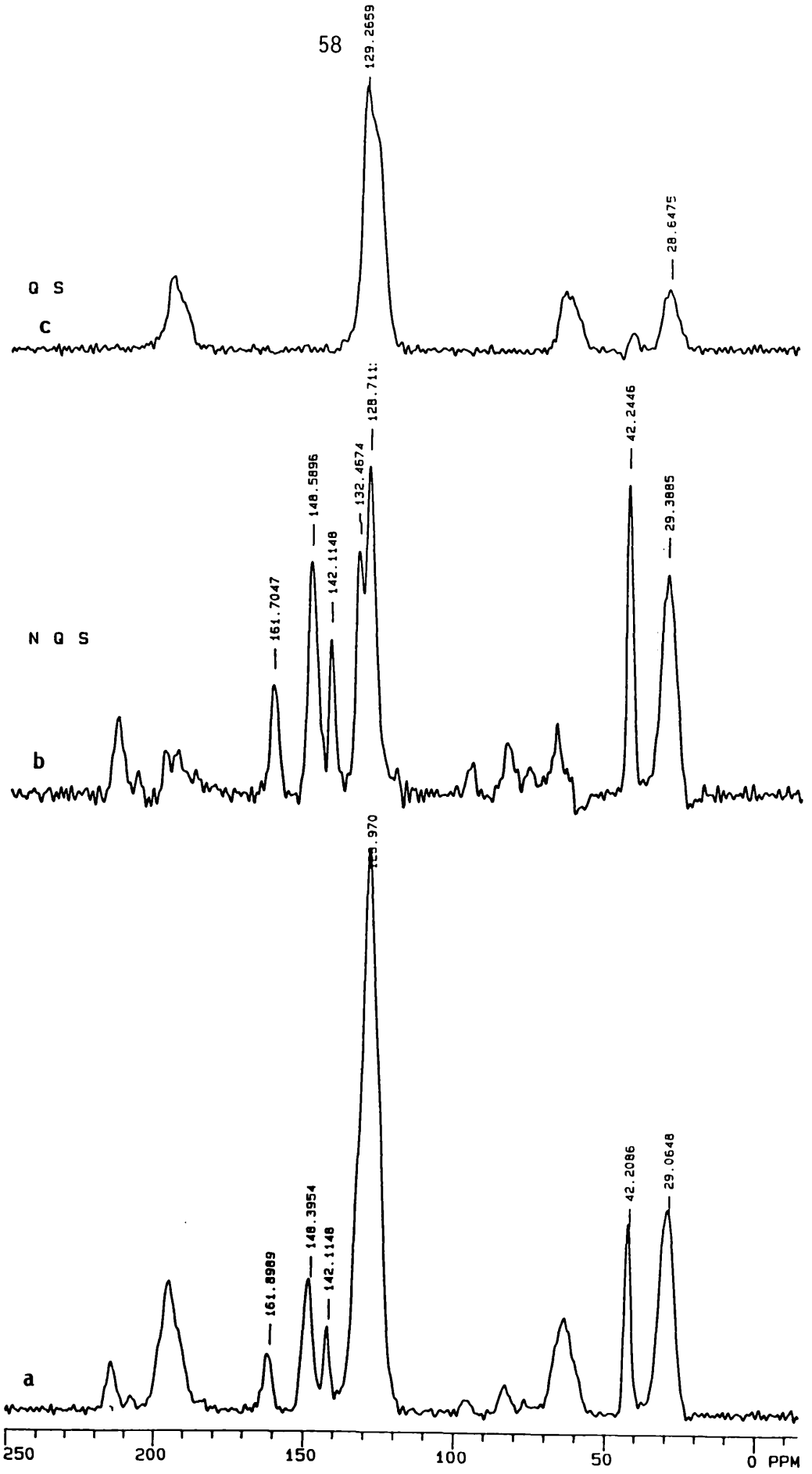

Figure 3.16: ^{13}C CP MAS-NMR spectra of solid Cl-PA5 .

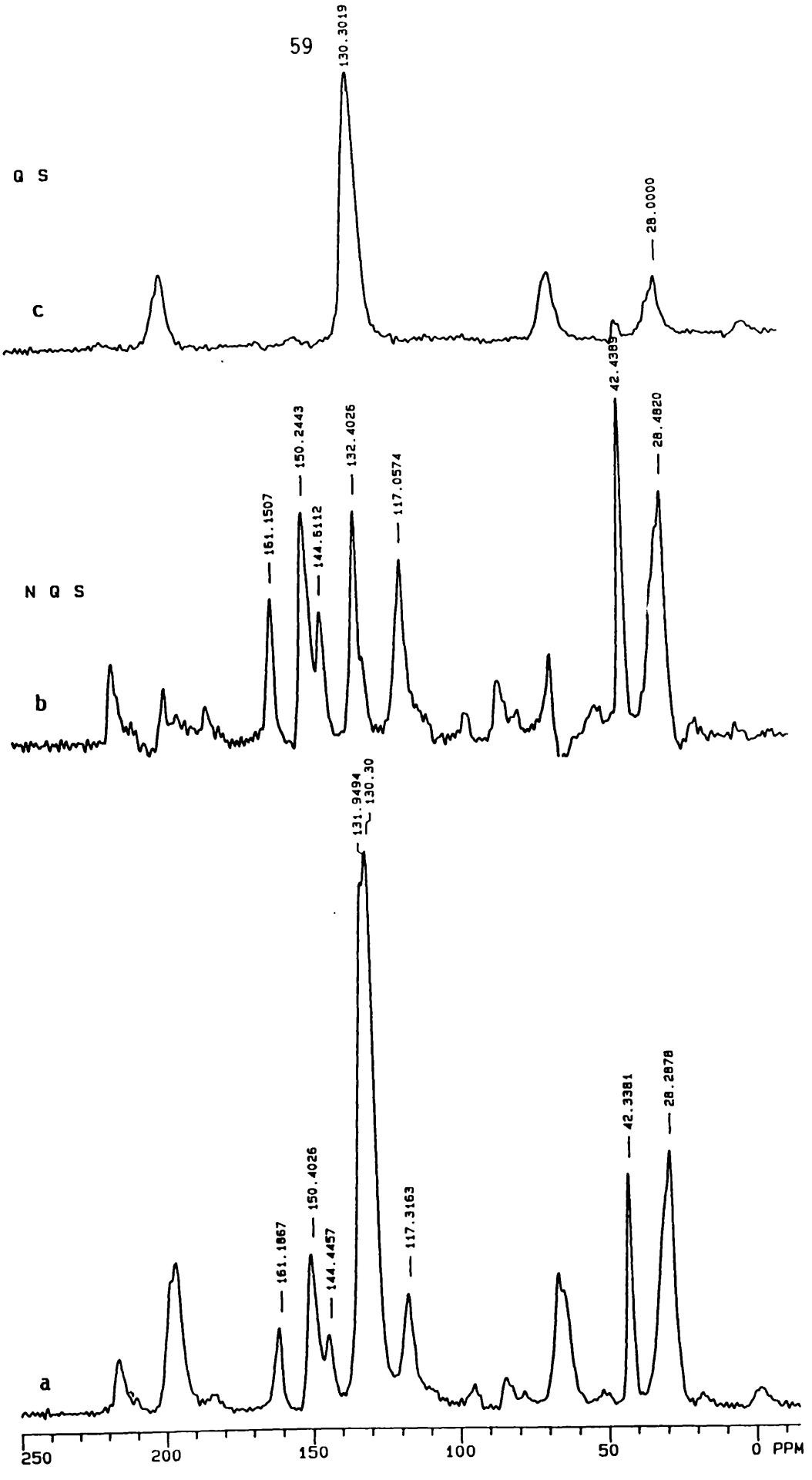

Figure 3.17: ^{13}C CP MAS-NMR spectra of solid Br-PA5 .

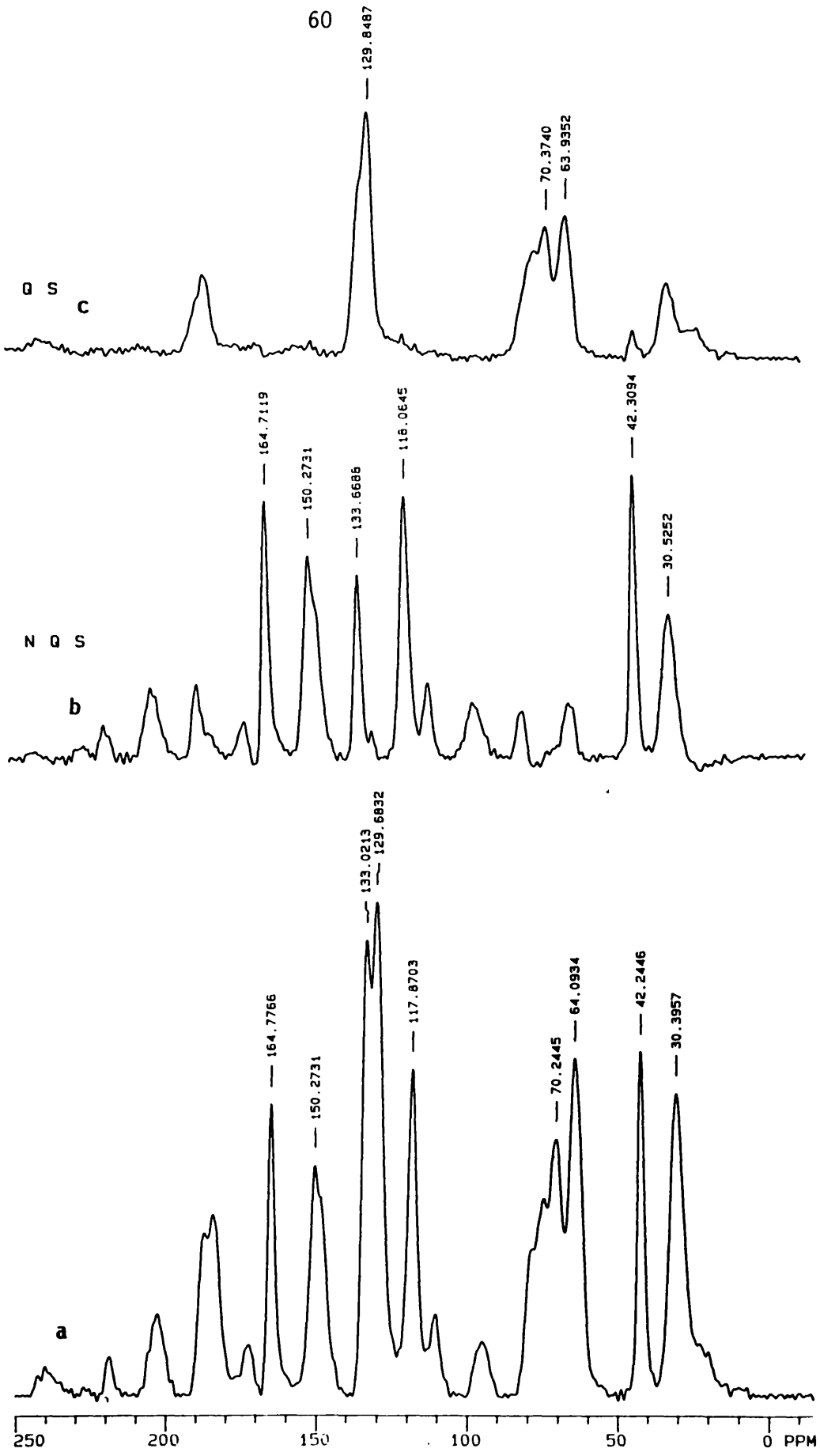

Figure 3.18: ^{13}C CP MAS-NMR spectra of solid Br-PA6 .

Polymer	PA1	PA2	PA3	PA4	Br-PA4
Y	2	1	1	1	1
Position	para	para	metha	ortho	ortho
X	H	H	H	H	Br
C -1,4	133.53	133.60	134.50	134.05	132.
C -2,3,5,6	130.03	130.10	130.13	127.80	130.78
C=O	163.08	163.28	161.57	161.47	160.73
C -1'	150.23	147.74	148.46	142.05	141.20
C -2'	116.7	123.52	119.22	123.59	132.24
C -3'	124.11	123.52	126.99	126..05	132.24
C -4'	129.77	147.74	119.22	126.05	132.24
C -5'	124.11	123.52	150.72	123.59	132.24
C -6'	116.7	123.52	116.92	139.49	141.20

Table 3.6 : The assignment of the chemical shifts in the ^{13}C CPMAS-NMR spectra for fully aromatic polyarylates.

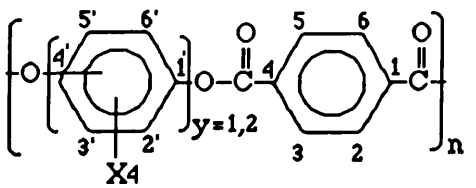

Polymer	PA5	Cl-PA5	Br-PA5	Br-PA6
X	H	Cl	Br	Br
C -1,4	133.50	132.46	132.40	133.66
C -2,3,5,6	129.5	129.26	130.30	129.84
C=O	163.19	161.70	161.15	164.71
C -1'	148.46	148.58	150.25	150.27
C -2',6'	120.58	142.11	144.61	___
C -3',5'	127.25	___	132	133
C -4'	27.25	128.71	117.06	118.06
C -α'	41.95	42.24	42.44	42.31
C -β'	30.27	28.65	28.00	30.53
C -α	___	___	___	63.94
C -β	___	___	___	70.37

Table 3.7 : The assignment of the chemical shifts in the ^{13}C CPMAS-NMR spectra for aliphatic / aromatic polyarylates.

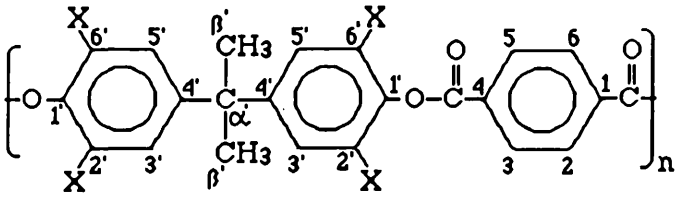

X-PA5 where (X= H, Cl, Br)

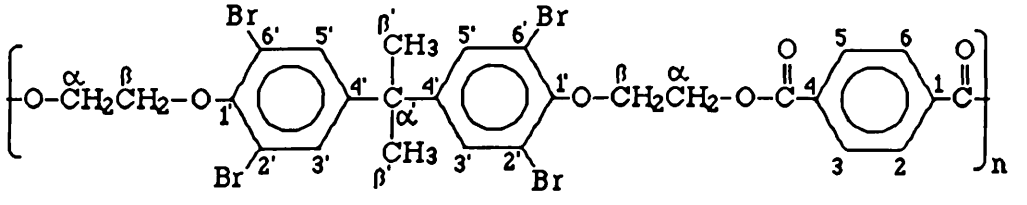

Br-PA6

chemical shifts in solution of the various structural elements present in the backbone of the chain [38]. However, to obtain the spectra shown in Figures 3.14 and 3.16-3.18 some spining side bands appeared, which are not peak picked. Furthermore, in the NQS spectra the mobile carbon signals such as the methyl and methylene groups are not suppressed. Finally, in some spectra signals arising from different carbons were undistinguishable, though they are not magnetically equivalent.

The specta for each polymer are presented as follow: (**a**) standard spectrum, (**b**) non- qua ternary spectrum and (**c**) quaternary spectrum.

3.2 α,ω– BIFUNCTIONAL POLY(METHYL METHACRYLATE)

3.2.1 PURIFICATION OF STARTING MATERIAL

a. Methyl methacrylate (MMA) (Aldrich Chemical Co Ltd), was dried over calcium hydride for a week and freshly distilled four times under vacuum before use.

b. Naphthalene was recrystallised three times from dry methanol, dried in a vacuum oven at 30 ^{o}C for 24 hours and stored in a desiccator until required.

c. Tetrahydrofuran (THF) was purified by distillation under dynamic nitrogen atmosphere. It was refluxed with cuprous chloride (600 ml / 1 g) over night, followed by distillation over potassium hydroxide. The distilled THF was then transferred to a three-necked round-bottomed flask A1 connected to another flask A2 as shown in Figure 3.19 and refluxed with benzophenone (3 g) and sodium metal (2 g) under dynamic nitrogen

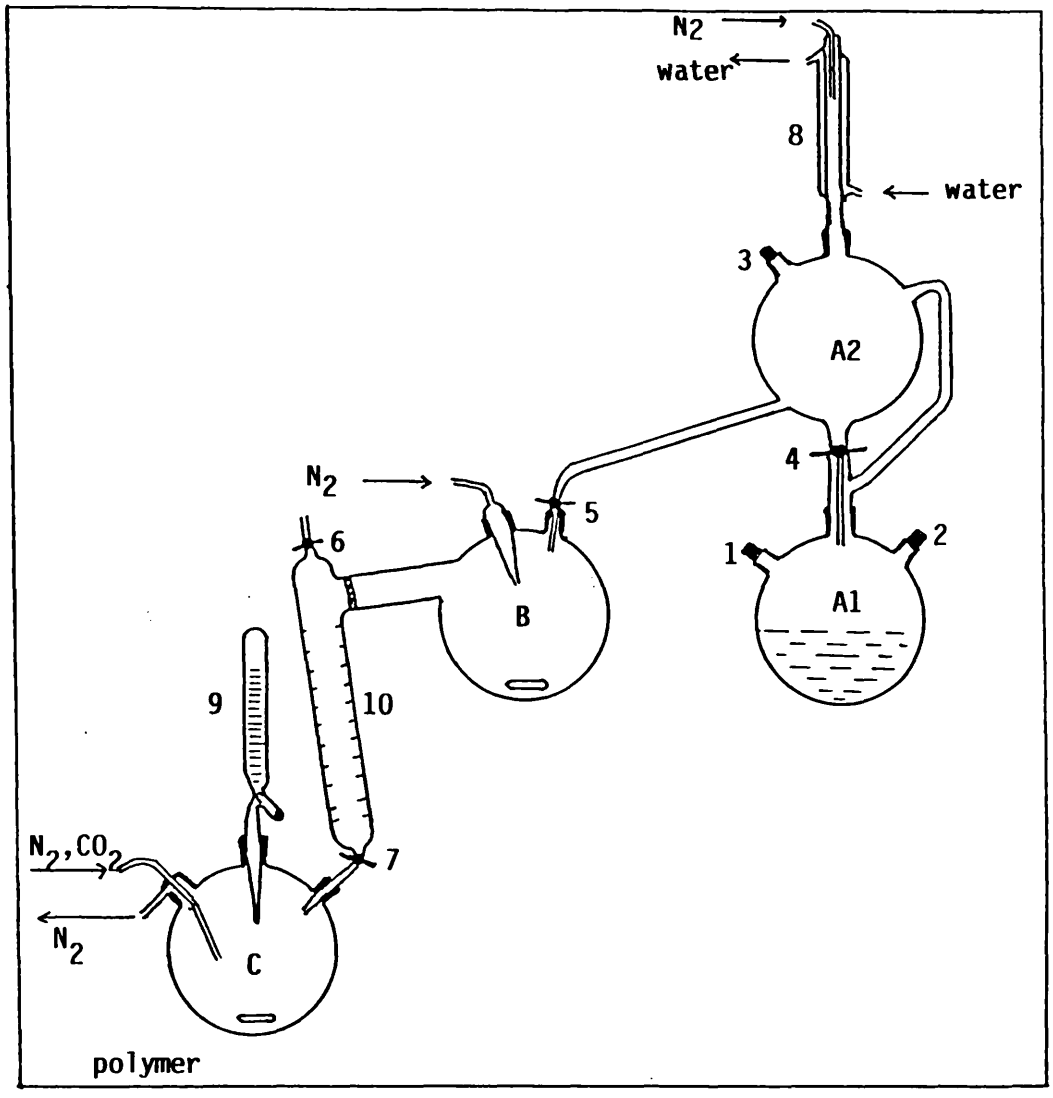

Figure 3.19: Apparatus used for the preparation of telechelic PMMA . A1 , A2 , B, and C = 1000 ml around bottomed flasks ; 1,2,and 3 = stoppers ; 4,5,6 and 7 = stopcocks ; 8 = condenser ; 9 = dropping vessel containing methyl methacrylate ; 10 = measuring cylinder ; .

atmosphere in order to destroy peroxides. When the colour became dark blue, the stopcock was closed and the THF was distilled into flask A2.

3.2.2 PREPARARION OF SODIUM NAPHTHALENIDE INITIATOR

Sodium metal (1 g) and naphthalene (3 g) were introduced into flask B under nitrogen atmosphere. The distilled THF in flask A2 was directly added into B and once the addition was complete, the flask B was disconnected from the A1/A2 assembly. After 20 min., a greenish colour developed in the initiator solution, which was stirred for 5 hours at room temperature. The dark green solution was then transferred into the three necked round-bottomed flask C (1000 ml) connected to a vessel containing fresh MMA (22 ml) and a capillary tube through which, nitrogen gas was passed.

3.2.3 POLYMERISATION

The initiator solution was cooled to -80 ^{o}C in a methylene chloride/ liquid nitrogen bath over 15 min., followed by the addition of MMA over 20 min. under continuous stirring. The living polymer (red colour)was killed by passing a slow stream of dry carbon dioxide through the nitrogen inlet.

During the termination process, some of the living polymer was terminated with hydrogen (PMMA-H).This precipitated on addition of the solution to methanol. Although PMMA-H may be precipitated in methanol, the sodium carboxylate terminated polymer, PMMA-COONa, remains soluble. This was precipitated in petroleum ether (b. 40-60 ^{o}C), after removal of most of the methanol by evaporation at 30 ^{o}C. The PMMA-COONa was filtered and dried under vacuum at room temperature for 24 hours.

PMMA was also made with sodium ethoxy end structure, PMMA-CH_2CH_2-ONa. In this case, the living polymer was terminated by the addition of ethylene oxide. Carboxyl and alcohol terminated polymers, PMMA-COOH and PMMA-CH_2CH_2-OH, were prepared by the addition of acidified methanol (MeOH / HCl) to PMMA-COONa and PMMA-CH_2CH_2-ONa, respectively.

Equations 2-6 describe the mechanism by which α,ω-bifunctional poly methyl methacrylate was synthesised.

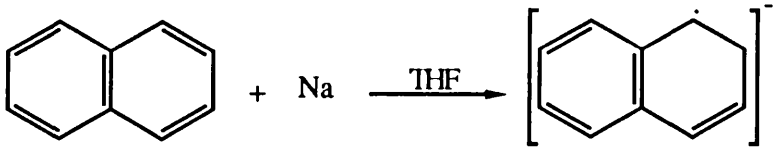

Eq.2

Initiator (greenish)

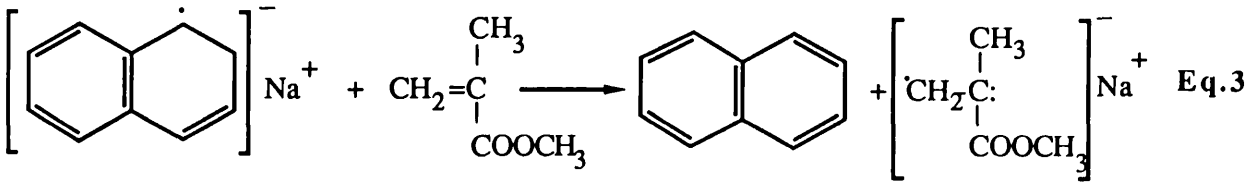

Eq.3

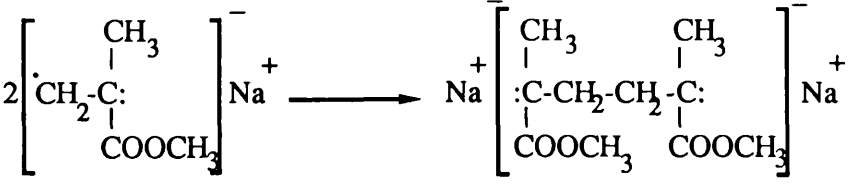

Eq.4

Dianion (red)

The dianion formed is capable of propagating a chain of MMA units.

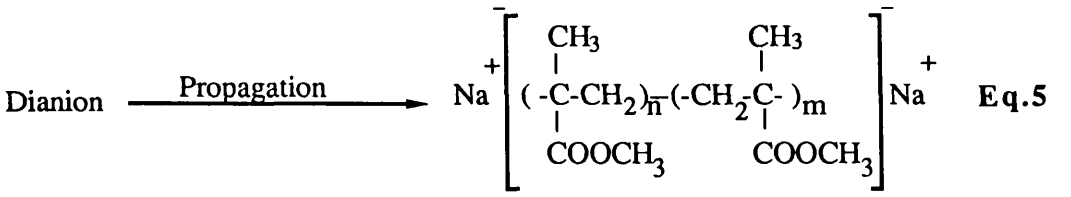

Living polymer

The polymerisation was terminated by a suitable additive such as acid (for H terminal), carbon dioxide or ethylene oxide, giving the overall chain structure.

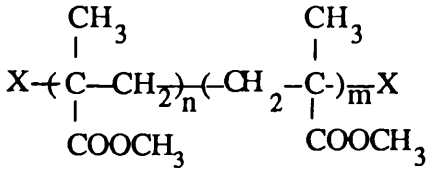

where: X= -H, -COONa, -COOH, -CH_2CH_2-ONa and -CH_2CH_2-OH

The resulting terminal structures (both chain ends) are therefore as shown below:

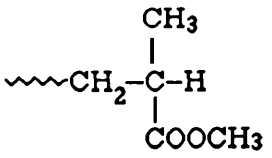

PMMA–H

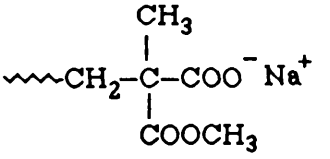

PMMA–COONa

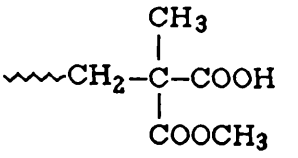

PMMA–COOH

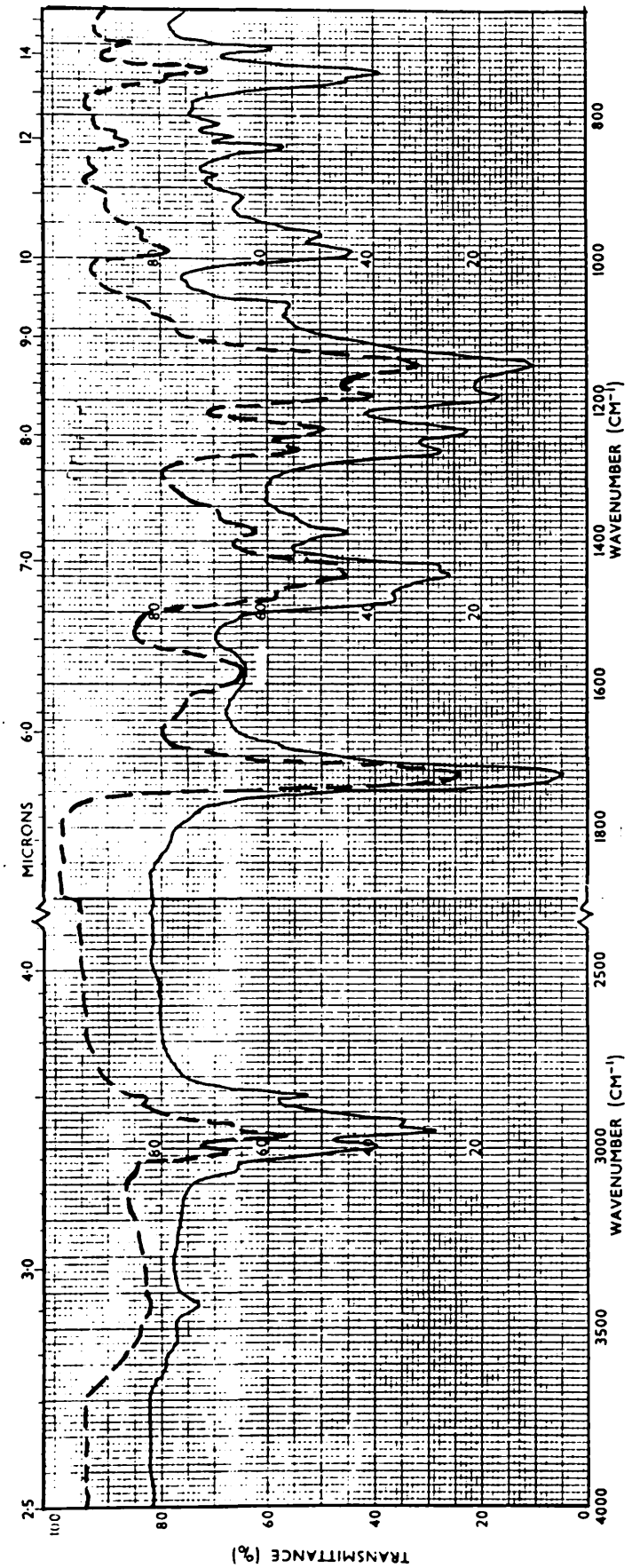

Figure 3.20: Infrared spectra of PMMA-COONa (- - -) and PMMA-CH_2CH_2ONa (——).

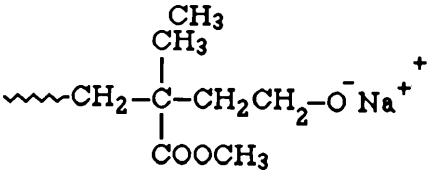

PMMA $-CH_2CH_2ONa$

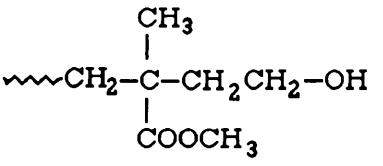

PMMA$-CH_2CH_2OH$

3.2.4 CHARACTERISATION OF α.ω–BIFUNCTIONAL PMMA

3.2.4.1. Infrared Spectroscopy:

The ir spectra for α.ω–bifunctional PMMA, obtained in the solid state as KBr disc, shown in Figure 3.20, exhibited characteristic bands of PMMA with new bands corresponding to the functional terminator for the polymer, such as 1560-1565 cm^{-1} attributed to the carboxylate ion absorption band (-CO-O^-) or a weak band at 1570-1585 cm^{-1} due to terminal ethoxy ion, (-CH_2CH_2-O^-) .

3.2.4.2. Molecular Weight Determination

Gel permeation chromatography (PSCC, Shawbury) was used to determine the molecular weight and distribution for α,ω-bifunctional PMMA using tetrahydrofuran (THF) as solvent. The data are listed in Table3.8.

	PMMA-COONa	PMMA-CH_2CH_2-ONa
Molecular Weight (Mw)	8730	22700
Average Molecular Weight (Mn)	4876	11700
Distribution Mw/Mn	1.677	1.936

Table 3.8: The molecular weight and distribution for α,ω-bifunctional PMMA.

CHAPTER FOUR

THERMAL DEGRADATION OF POLY(ALKYLENE TEREPHTHALATES)

4.1 INTRODUCTION

The thermal degradation behaviour of some poly (alkylene terephthalates) has previously been investigated by several workers [39-42], who studied degradation products, rate of decomposition, activation energies and the mechanism of decomposition. Smith el. al.[43], showed that poly (alkylene terephthalates) with structure as shown in Scheme 4.1 and (m=2-4) melt above 220 ^{o}C with solubility temperatures of approximately 150 ^{o}C in diphenyl ether. However, the higher homologs (m>4) have much lower melting points (less than 160 ^{o}C) and are much more soluble. It has been reported [44-47], that poly(ethylene terephthalate) (PET) and poly(butylene terephthalate) (PBT) contain traces of low molecular weight oligomers which consist mainly of cyclic n-mers. Salvatore et. al.[48] and Lüderwald [49] studied the degradation by direct pyrolysis-mass spectrometry. and reported that poly (alkylene terephthalates) are preferentially degraded by cleavage of the ester bond. Furthermore, Adams[50] and Lüderwald and Urrutia [51], suggested that bond scission occurs with transfer of a hydrogen to yield a hydroxyl end group and a radical that would be unstable (Scheme 4.1).

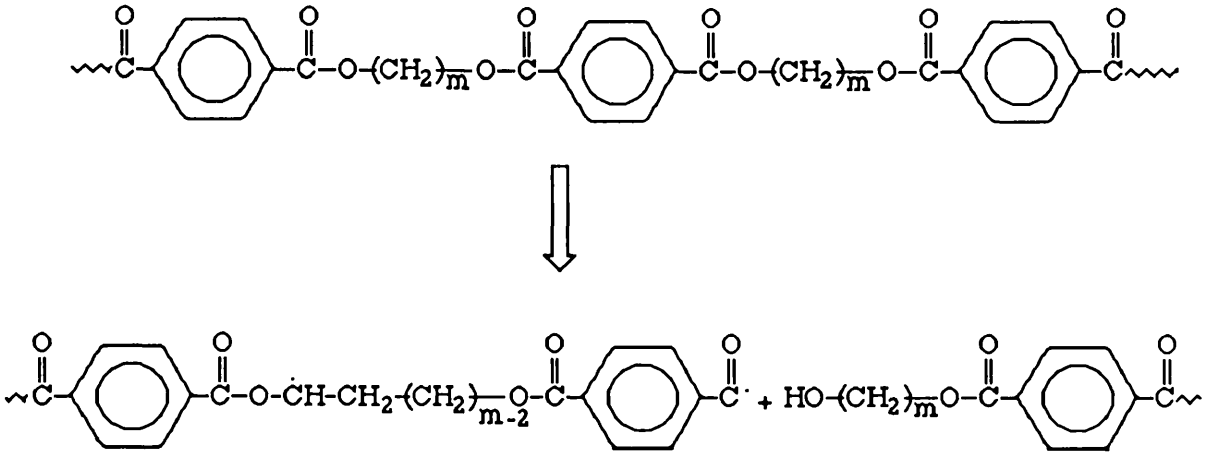

Scheme 4.1

A third thermal process involves decarboxylation to produce various products.

Several workers have concluded that an intramolecular exchange reaction predominates in the primary thermal degradation processes of PET and PBT causing the formation of short chain fragments with carboxylic acid and unsaturated ester end groups [39-42,48,49].

For example, in the case of PET, Goodings [41] reported that terephthalic acid, acetaldehyde and carbon monoxide are the major volatile products, together with anhydride groups, benzoic acid, acetophenone, vinyl benzoate, ketones, water, methane, ethylene and acetylene as minor products. Moreover, various vinyl esters were reported [52]. Yoda et. al.[53], who investigated the gelation in PET by heating at 263-300 ^{o}C, showed that under nitrogen flow crosslinking occurs to a negligible extent. For degradation in air, however, chain scission and crosslinking occur.

On the other hand, it has been proposed [39] that thermal degradation of PBT proceeds by a pathway involving two major reactions. After the initial scission by intramolecular exchange,it is suggested that an ionic

decomposition process with an activation energy of 27.9 Kcal.mol^{-1}, occurring at vinyl ends, leads to THF. At higher temperature, a concerted ester pyrolysis reaction yields butadiene as illustrated in Scheme 4.2.

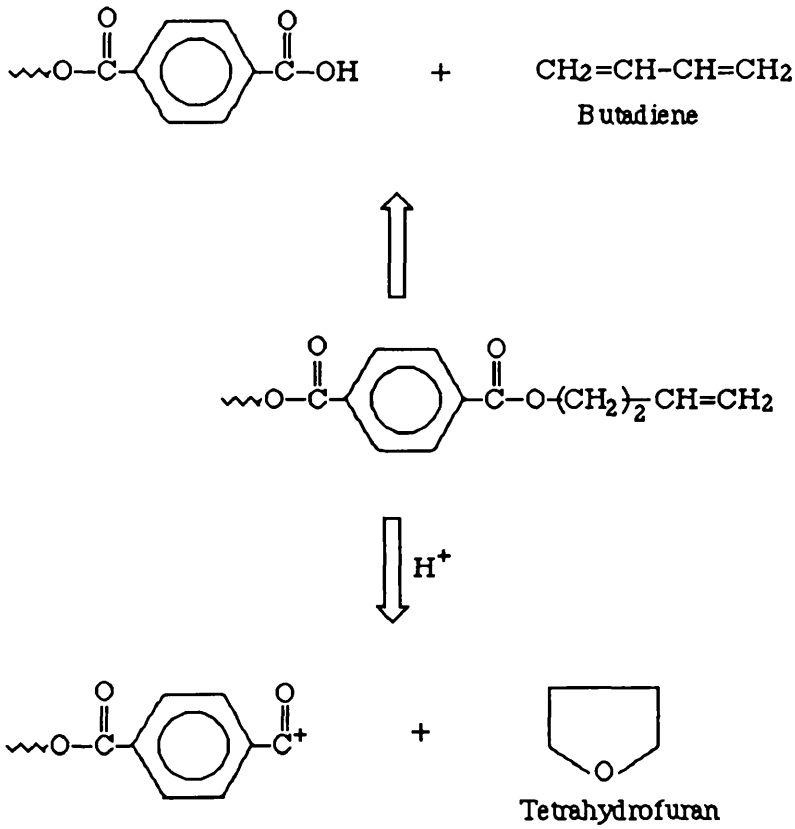

Scheme 4.2

In addition, carbon dioxide, carbon monoxide, benzoic acid, terephthalic acid and mono-3-butenyl terephthalate are formed. Toluene,

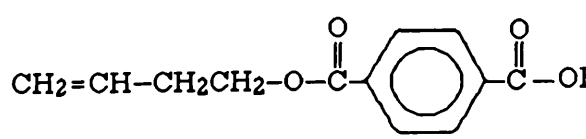

Mono-3-butenyl terephthalate

phenol and benzene are present as minor components. However, Passalaiqua et. al.[40], who studied the thermal degradation of PBT at 240-280 °C by the measurement of intrinsic viscosity, carboxyl end groups and weight loss, proposed that butadiene is evolved while carboxyl end groups increase, before the formation of THF.

In the case of poly (decamethylene terephthalate) (PDMT), there has apparently been no report of the identification of degradation products and no mechanism of decomposition has been proposed.

In order to get better insight into the structural changes in the thermal degradation of these polymers and to ascertain the effect of variation of the diol component in the backbone structure on their stability and the mechanism of decomposition, the thermal degradation of three different poly(alkylene terephthalates) has been studied using programmed and isothermal heating conditions using thermal volatilisation analysis (TVA) under vacuum and also TG and DTG in nitrogen atmosphere. The product fractions in the TVA experiments (i.e non-condensable and condensable gases, volatile liquids, cold ring fraction and residue) were analysed by means of the IR, MS, and GC-MS techniques. The stability of the poly(alkylene terephthalates) has been examined and their general mechanisms of decomposition have been established.

4.2 THERMAL ANALYSIS

4.2.1 THERMOGRAVIMETRY (TG)

The TG curves for poly(alkylene terephthalates) recorded under dynamic nitrogen with a heating rate of 10 °C/min., are shown in Figure 4.1.

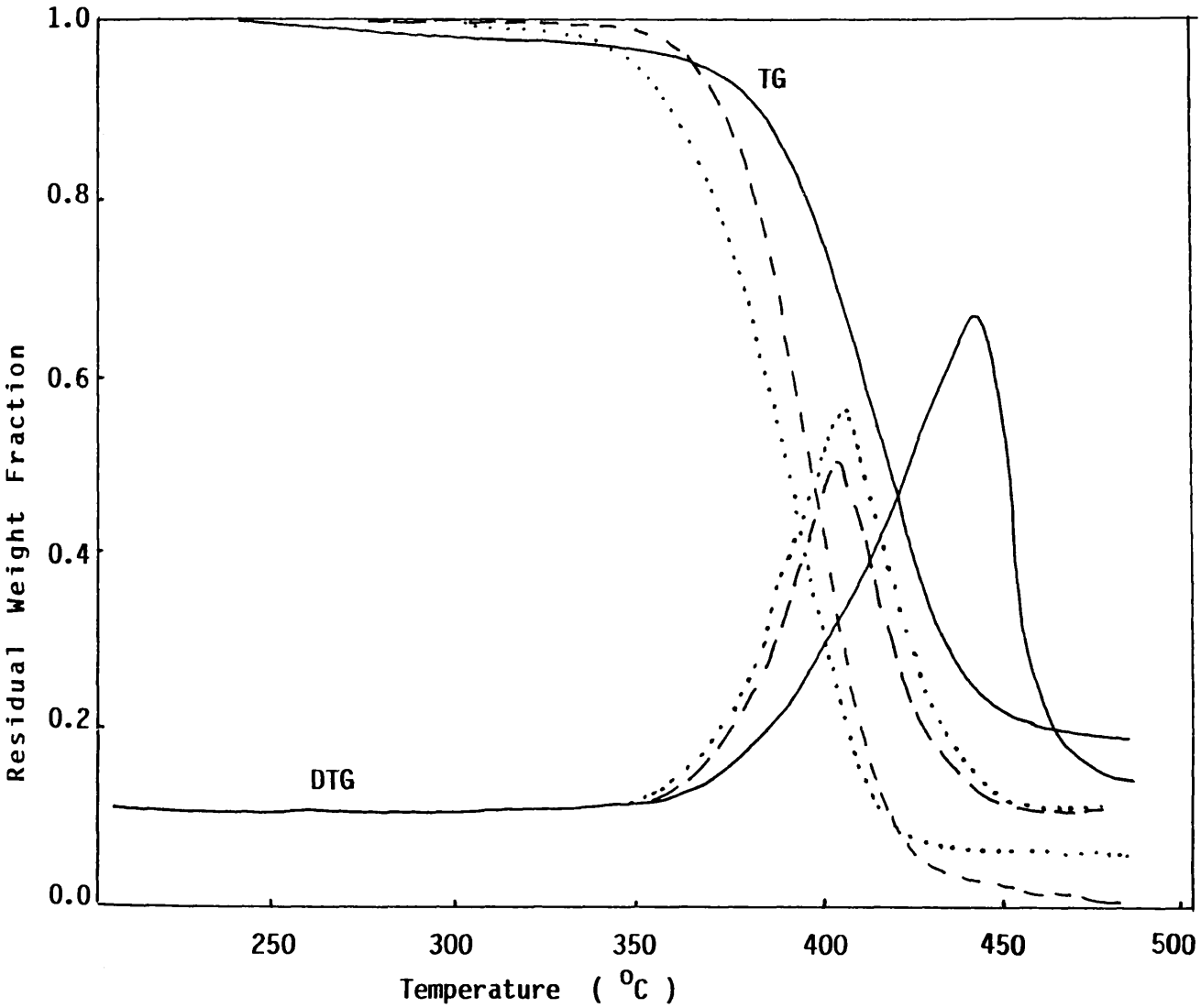

Figure 4.1: Thermogravimetric traces for PET (———), PBT (.....) and PDMT (- - - - -). Heating rate, 10 °C / min ; under nitrogen atmosphere .

For each polymer, a single stage decomposition process occurs during thermal degradation, in which the onset is above 300 ^{o}C, the maximum rate of weight loss is in the range of 400-445 ^{o}C and there is a negligible residue at 500 ^{o}C.

4.2.2 THERMAL VOLATILISATION ANALYSIS (TVA)

The TVA curves for poly(alkylene terephthalates) are illustrated in Figures 4.2 and 4.3, showing that the evolution of volatile products is a one stage process in the range 300-462 ^{o}C, reaching maximum rate of decomposition around 400-440 ^{o}C, which is in general agreement with the TG and DTG data.

The TVA traces for the Pirani gauges following 0, -45, -75, -100 and -196 ^{o}C cold traps are separated, indicating the presence of various volatile substances of different volatility including non-condensable gases. It is also clearly evident that the proportion of volatile products decreases in the order

PET > PBT > PDMT

Quantitative measurements of weight of residue, cold ring fraction and volatile products at ambient temperature and the main data from TVA, TG and DTG are summarised in Table 4.1. The differences in the onset temperatures for PET, PBT and PDMT degradation indicated by TVA and TG may be due to the fact that TVA does not record evolution of CRF, which is, however, detected by weight loss in TG.

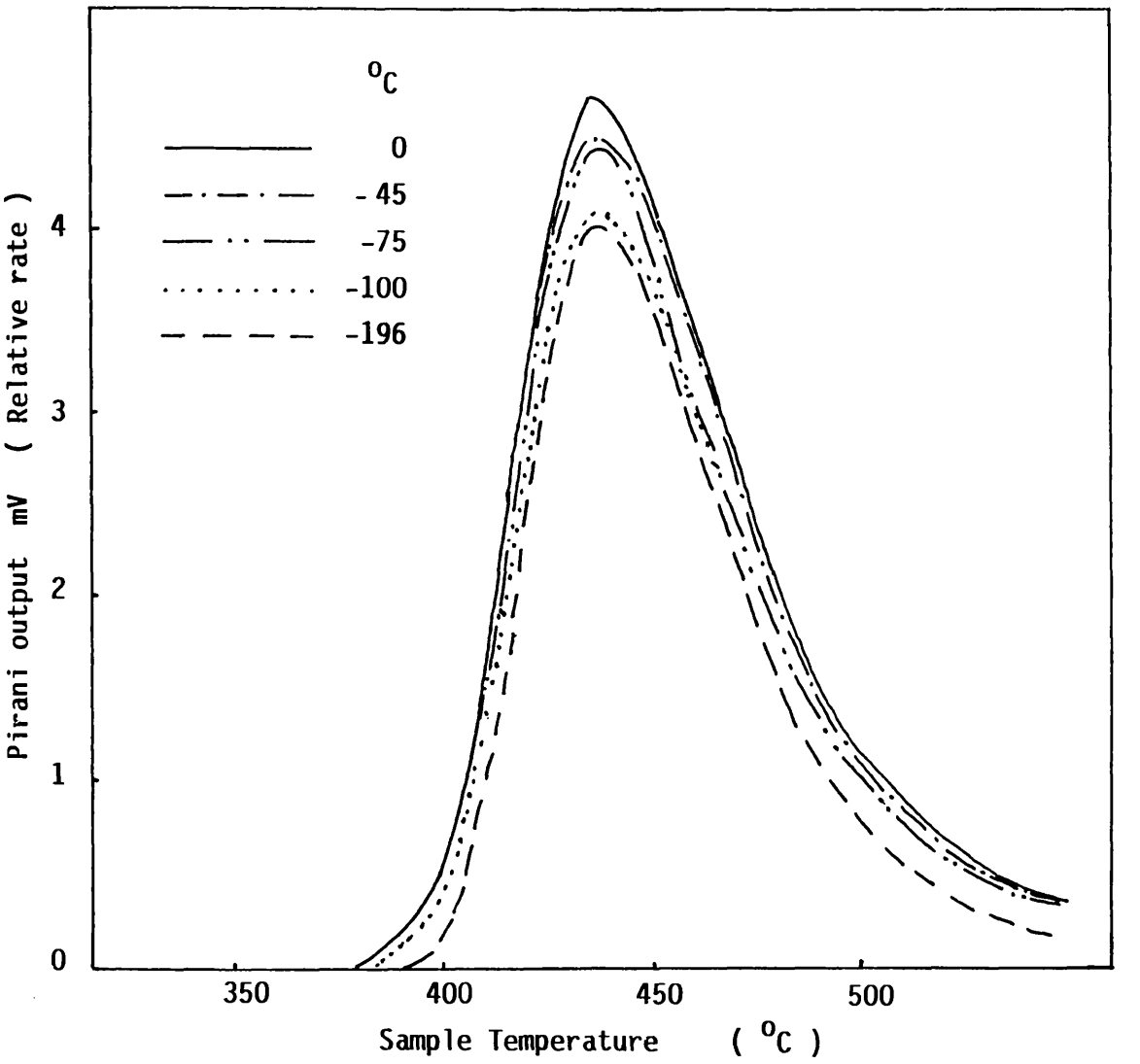

Figure 4.2: TVA traces for poly(ethylene terephthalate) degradation under vacuum . Heating rate 10 ^{o}C/min .

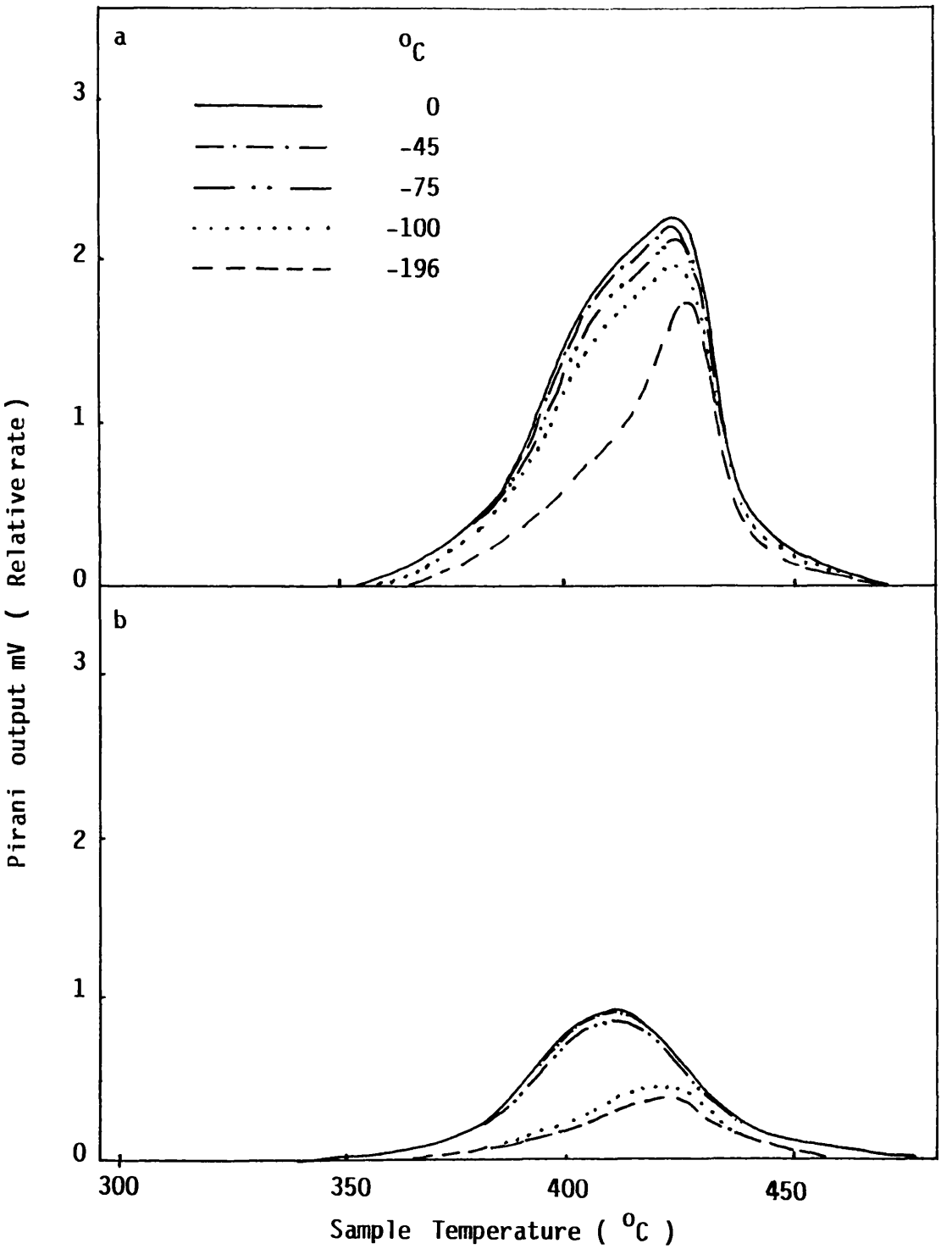

Figure 4.3: TVA traces for a) poly(butylene terephthalate) and b) poly(decamethylene terephthalate) degradation under vacuum . Heating rate 10 ^{o}C/min .

Polymer Code		PET	PBT	PDMT
T V A	T onset / °C	378	355	343
	T max / °C	438	420	403
	Residual fraction[a] wt %	5.2	5.2	1.2
	Cold ring fraction wt %	82.1	83.1	87.1
	Volatile products wt %	12.7	11.7	11.6
T G & D T G	T onset / °C	260	300	324
	T max / °C	445	405	404
	Residual fraction[a] wt %	19	6	1

a: Residual fraction at 500 °C

Table 4.1 : TVA, TG and DTG data for poly(alkylene terephthalates) decomposition.

4.3 CHARACTERISATION OF DEGRADATION PRODUCTS

The degradation products were separated into four main fractions in accordance with their different volatilities. The substances from each fraction were separated and analysed by means of IR spectroscopy, mass spectrometry and GC-MS as reported in Table 4.2. The non-condensable gases detected in the degradation of each of the poly(alkylene terephthalates) were collected in a closed system to facilitate spectroscopic analysis. Carbon monoxide was revealed in all cases and methane in PET only.

4.3.1 POLY(ETHYLENE TEREPHTHALATE) (PET)

4.3.1.1 Condensable volatile products

The sub-ambient TVA separation for condensable volatile products illustrated in Figure 4.4, shows three distinct fractions, which were separately collected in a gas cell or cold finger as gas or liquid, respectively, for further spectroscopic analysis. The first fraction is due to carbon dioxide as a major component, together with traces of ethylene and ketene. Acetaldehyde was identified as the product responsible for the second SATVA fraction. The material giving the last fraction was collected as a liquid and subjected to GC-MS investigation, in which products were separated and identified under the conditions described in Chapter Two. The gas chromatogram of the total liquid fraction products from the PET degradation and their assignments are shown in Figure 4.5. Vinyl benzoate and benzaldehyde were found as major components, together with traces of dioxane, toluene and divinyl benzoate.

		Products			Methods of Analysis
Polyester Code		PET	PBT	PDMT	
Non-condesable		Carbon monoxide, methane	Carbon monoxide	Carbon monoxide	IR & MS
Condensable Volatile	Gases	Carbon dioxide, ethylene, ketene and acetaldehyde	Carbon dioxide, butadiene	Carbon dioxide	IR & MS
	Liquids	Benzene, 1,4-dioxane,toluene, benzaldehyde, vinyl benzoate and di-vinyl terephthalate	THF, benzene, di-hydrofuran, 1,5-hexadiene, benzaldehyde 4-vinyl cyclohexene, butanol-1, 1,4-butane diol and 1-butene-3-ol	1,9-Decadiene decamethylene glycol and 1-decene-9-ol	IR & MS & GC-MS
Cold Ring Fraction		Benzoic acid, terephthaldehydic acid, terephthalic acid, cyclic trimer, mono-vinyl terephthalate, dimethyl terephthalate, V(m=2) mono-2-hydroxyethyl terephthalate and short chain fragments with anhydride group.	Benzoic acid, terephthaldehydic acid, terephthalic acid, cyclic dimer, mono-3-butenyl terephthalate mono-4-hydroxybutyl terephthalate III (m, n= 4,1) and short chain fragments with anhydride group .	Benzoic acid, terephthaldehydic terephthalic acid, 9-decenyl-terephthalate, III(m,n=10,1) mono-10-hydroxydecyl-terephthalate and short chain fragments with anhydride group.	IR & MS

Table 4.2: Identification of degradation products by IR, MS and GC-MS.

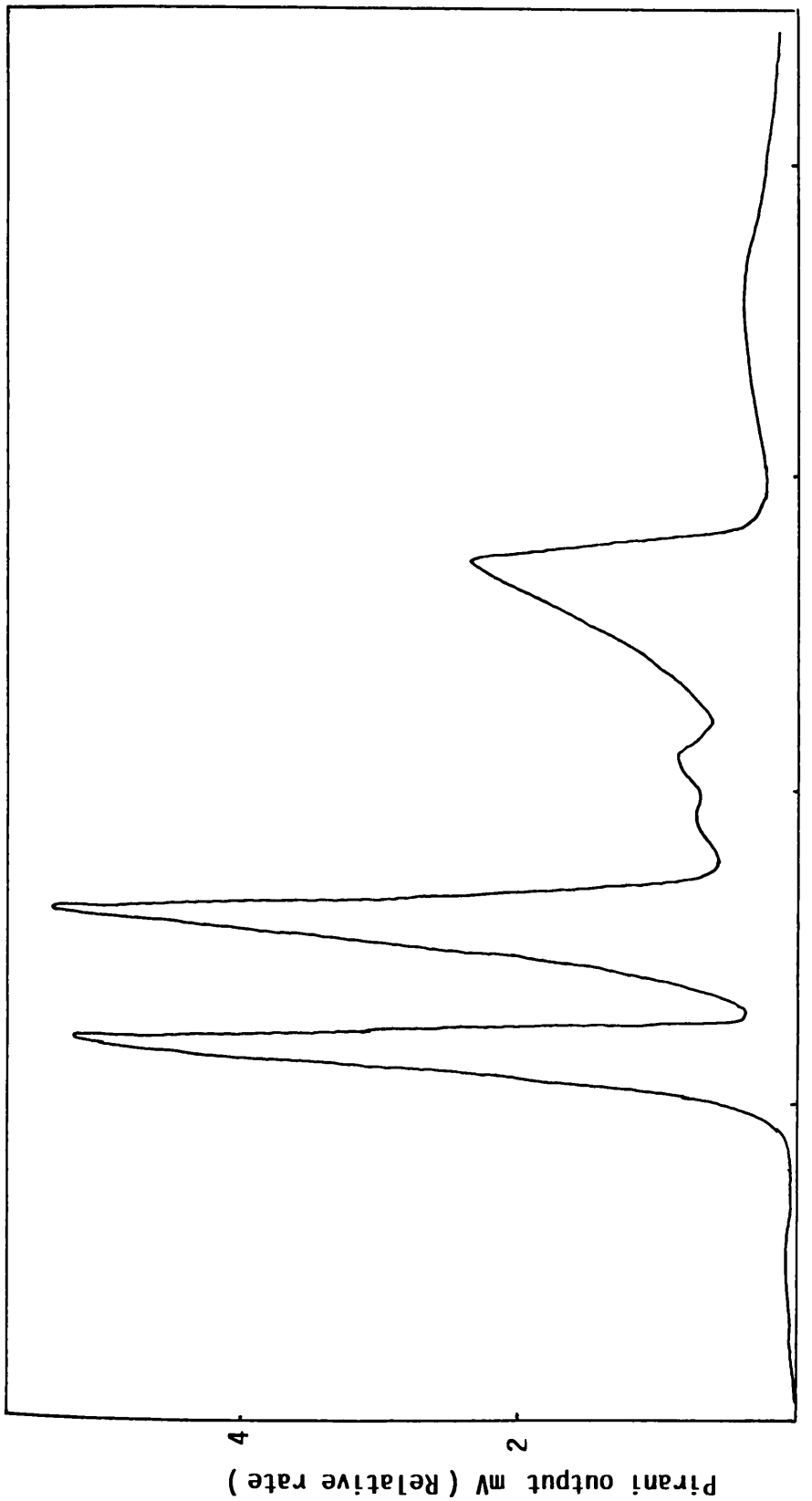

Figure 4.4: Subambient TVA trace for warm up from -196 ^{o}C to ambient temperature of condensable volatile products from degradation of poly(ethylene terephthalate) to 500 ^{o}C.

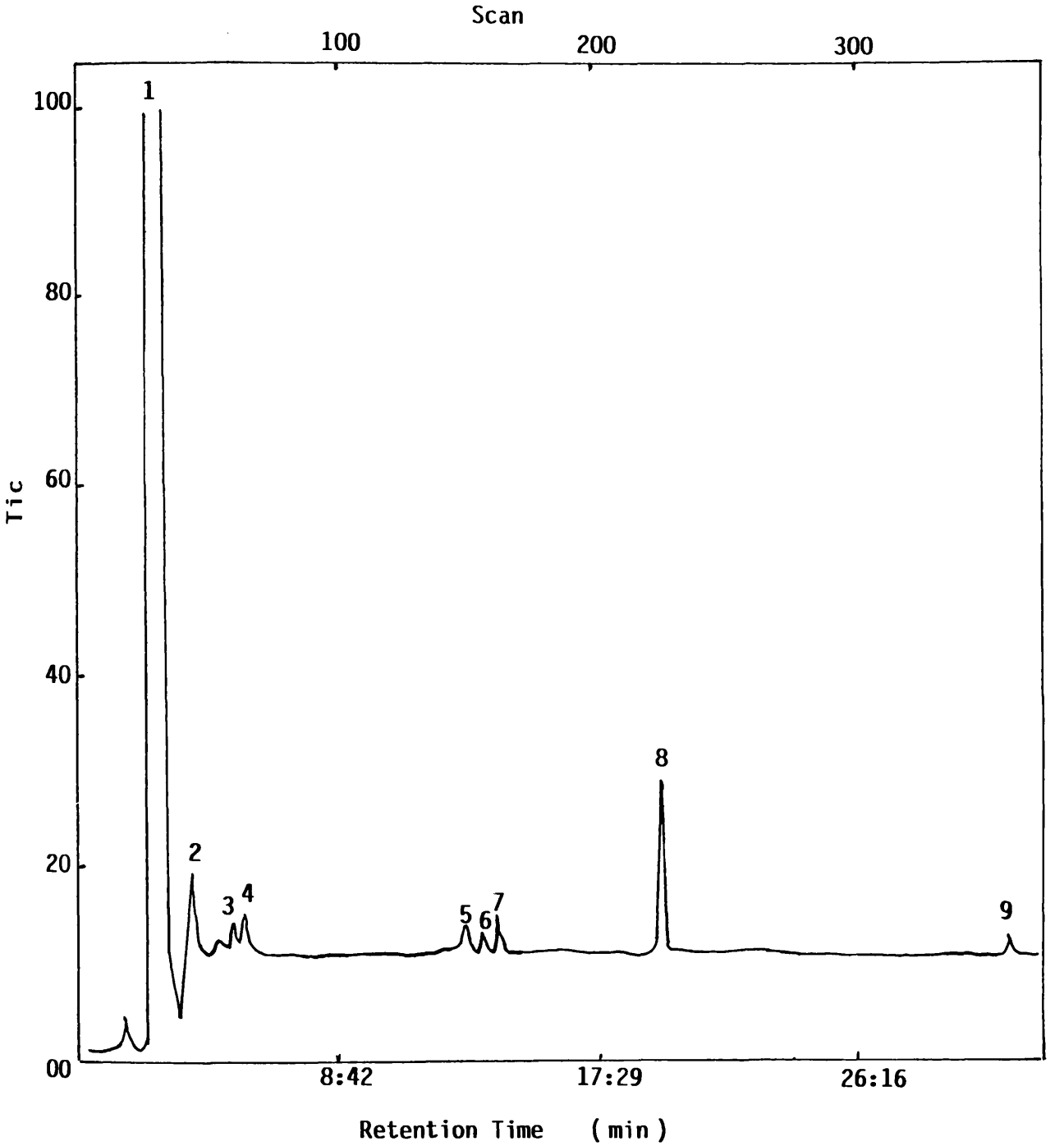

Figure 4.5: Gas chromatogram for the liquid fraction in SATVA separation of products from the degradation of PET to 500 ^{o}C .

Assignments: **1**, THF (solvent); **2**, dioxane ,**3**, toluene; **4**,unidentified **5**, benzaldehyde; **6** and **7**, unidentified; **8**, vinyl benzoate ; **9**, divinyl terephthalate .

4.3.1.2 Cold ring fraction

Some volatile material condensed on the inner wall of the cooled upper part of the TVA tube as CRF, giving two bands which were removed separately for further analysis. The ir spectrum for the upper CRF consists of frequency bands which are characteristic of terephthalic acid and short chain fragments terminated by (-CH=CH_2) or (-COOH) end groups. However, the mass spectrum, recorded at 220 °C, exhibits many peaks corresponding to different molecular ions, as reported in Table 4.3.

Product	m / e	Intensity %
Benzoic acid	122	3
Terephthaldehydic acid	150	10.1
Terephthalic acid	166	38
Hydroxyethyl methyl terephthalate ester	225	6.7
Short chain fragment V (m=2)	341 (M-OH)	13.9

M-OH = Molecular weight minus OH

Table 4.3: Material present in the CRF from the degradation of PET under programmed heating to 500 °C.

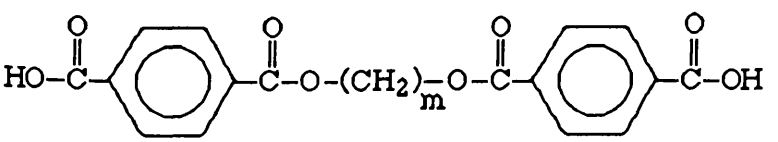

V (m=2)

In the case of the lower CRF, the ir spectrum shows bands characteristic of the original polymer and a new band at 1790 cm^{-1}, corresponding to the stretching vibration of the anhydride group, showing that the lower CRF is a short chain fragment containing the anhydride group (-CO-O-CO-).

4.3.2 POLY(BUTYLENE TEREPHTHALATE) (PBT)

4.3.2.1 Condensable volatile products

The condensable volatile products were fractionated by SATVA. The SATVA curve illustrated in Figure 4.6, indicates four main peaks. The first two were shown by ir spectroscopy to be due to carbon dioxide and 1.3-butadiene, respectively. Peaks 3 and 4 products were collected as a liquid fraction and characterised by means of IR, MS and GC-MS analysis. The GC chromatogram in Figure 4.7 exhibits 12 peaks. Tetrahydrofuran and 4-vinyl cyclohexene were major components, and the minor products included traces of benzene, 3-butene-1-ol, benzaldehyde, dihydrofuran, butanol and 1.4-butane diol.

4.3.2.2 Cold ring fraction

Two bands were observed as CRF. The upper part (white solid) was collected for spectroscopic analysis, its ir spectrum showed strong bands at 2660 and 2530 cm^{-1} and a broad band at 3360-2400 cm^{-1}, due to the carboxylic acid group. The mass spectrometric investigation was carried out at different probe temperatures. At 200 ^{o}C, the mass spectrum shows peaks corresponding to the molecular ions of mono-4-hydroxybutyl terephthalate, 3-butenyl terephthalate and terephthaldehydic acid. However,

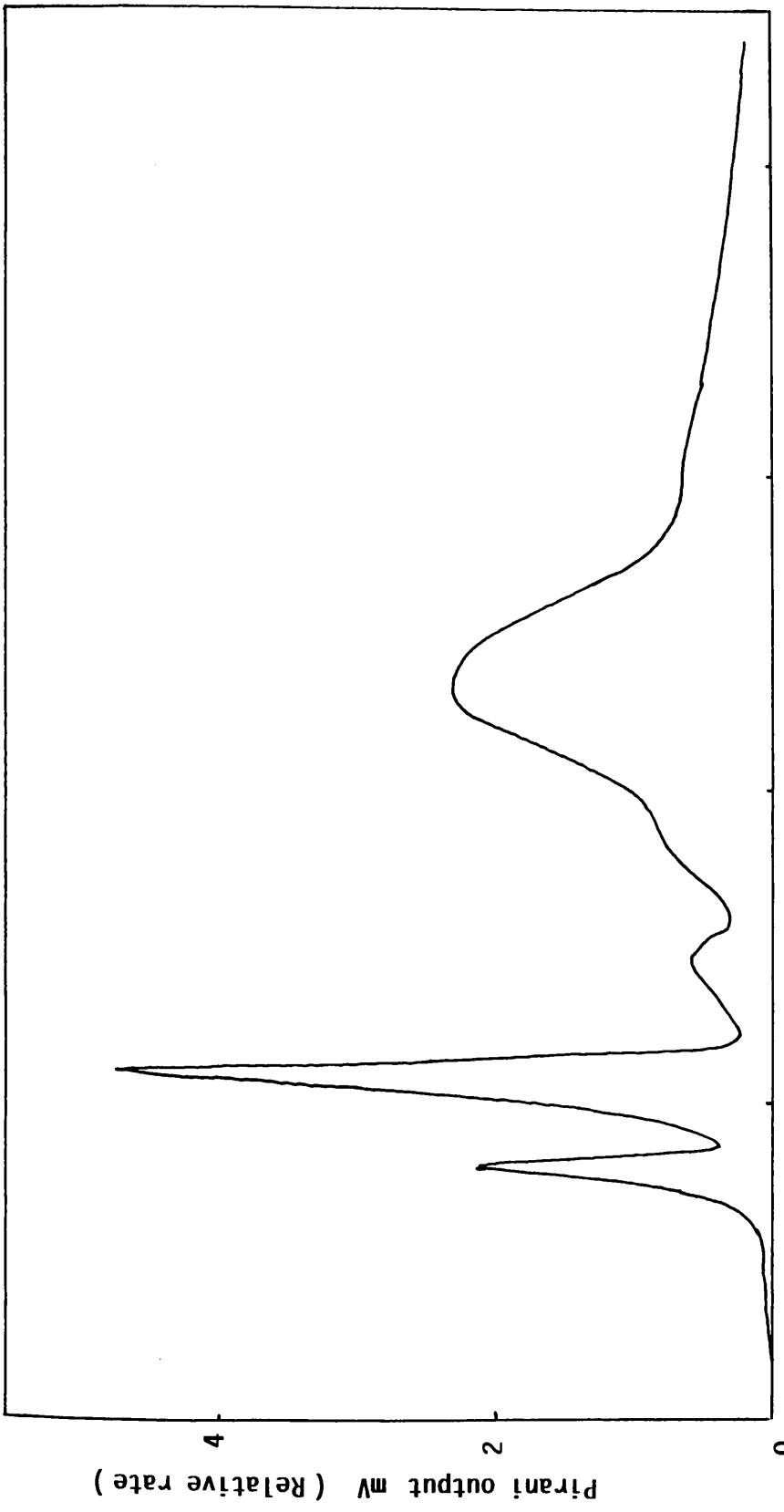

Figure 4.6: Subambient TVA trace for warm up from -196 ^{o}C to ambient temperature of condensable volatile products from degradation of poly(butylene terephthalate) to 500 ^{o}C.

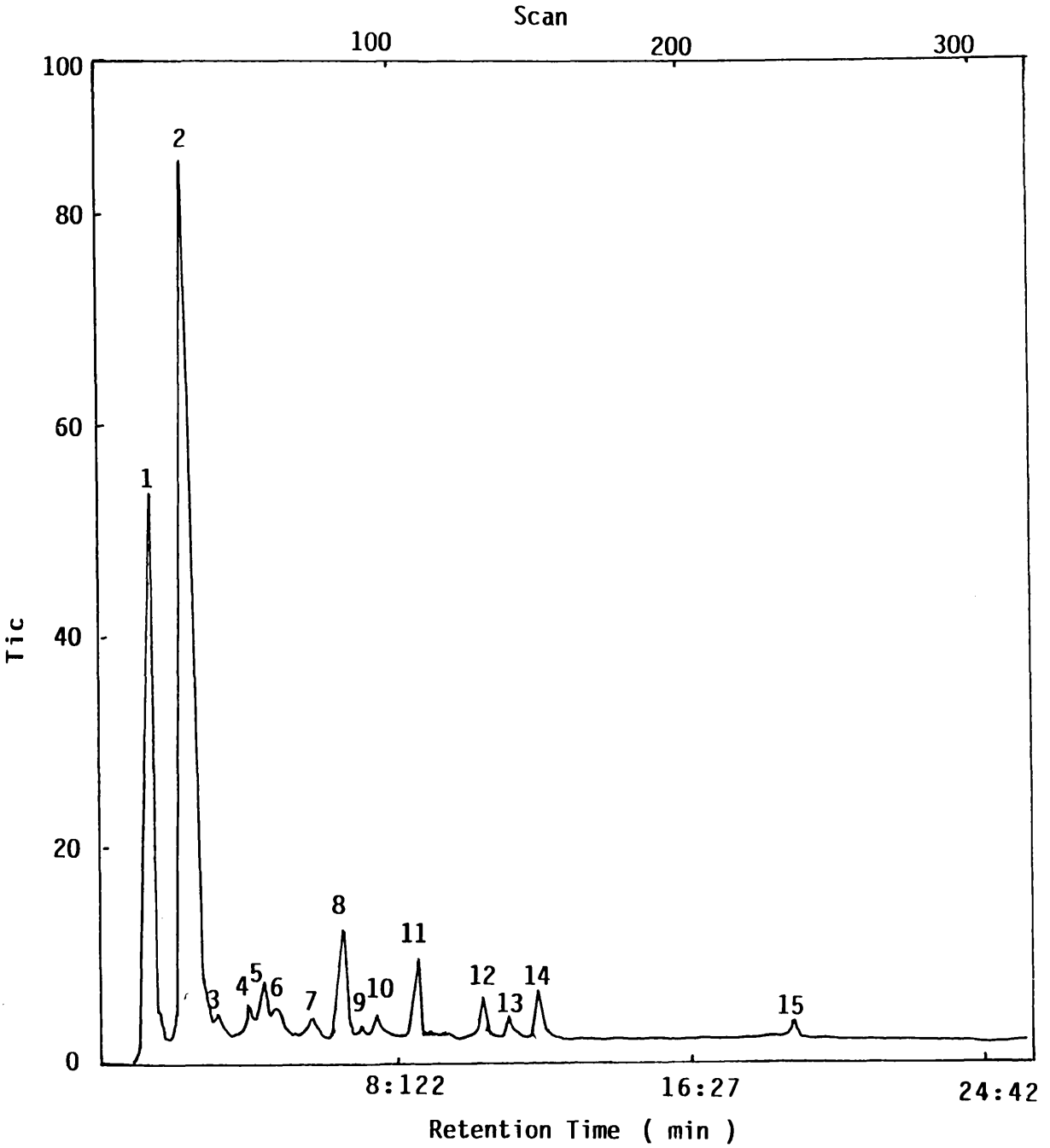

Figure 4.7: Gas chromatogram for the liquid fraction in SATVA separation of products from the degradation of PBT to 500 ^{o}C .

Assignments: **1**, Methanol(solvent); **2**, THF; **3**, benzene ; **4**, dihydrofuran; **5**, toluene ; **6**, 1,5-hexadiene ;**7**, unidentified; **8**, 4-vinyl cyclohexene; **9** and **10** , unidentified; **11**, 1,4-butane diol ; **12** , unidentified; **13** , benzaldehyde ; **14** and **15** , unidentified .

at higher temperatures, new fragment patterns developed corresponding to a cyclic dimer, terephthalic acid and a short chain fragment with carboxyl end group. Table 4.4 summarises the products present in the upper part of the CRF and their intensity.

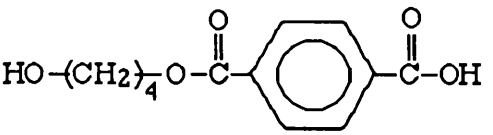

Mono-4-hydroxybutyl terephthalate

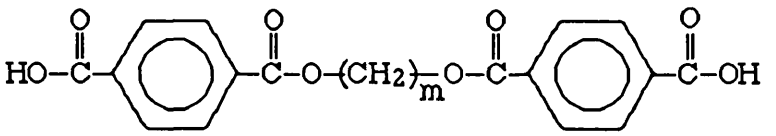

V (m=4)

Product	m / e	Intensity %	
		200 °C	220 °C
Benzoic acid	122	--	4.3
Terephthaldehydic acid	150	7	--
Terephthalic acid	166	--	20.3
Mono -3 -butenyl terephthalate	203 (M-OH)	32.2	--
4 -Hydroxybutyl terephthalate	239	3.1	--
Short chain fragment V (m=4)	369 (M-OH)	--	17
Cyclic dimer	440	--	0.3

M-OH = Molecular weight minus OH

Table 4.4: Material present in the CRF from the degradation of PBT under programmed heating to 500 °C

The lower CRF (yellowish) gave an ir spectrum showing a new band at 1790 cm^{-1} due to the anhydride group and the remaining bands were similar to those present in the spectrum of the original polymer (PBT), indicating that the lower CRF consists of short chain fragments including anhydride groups.

4.3.3 POLY(DECAMETHYLENE TEREPHTHALATE) (PDMT)

4.3.3.1 Condensable volatile products

The SATVA curve in Figure 4.8 shows two distinct peaks. The first is due to carbon dioxide, whereas 1.9-decadiene was identified by ir as the main component at the second peak. In addition, GC-MS investigation indicated the presence of 1.9-decadiene together with traces of decamethylene glycol and 1-decene-9-ol as shown in Figure 4.9.

4.3.3.2 Cold ring fraction

Two bands deposited in the upper part of TVA tube as CRF were removed separately for spectroscopic analysis. The ir spectrum of the upper part of the CRF resembles that of the polymer, but shows new bands corresponding to the carboxylic acid group. However, the mass spectrum exhibits many peaks attributed to the molecular ions of terephthalic acid and mono-9-decenyl terephthalate.

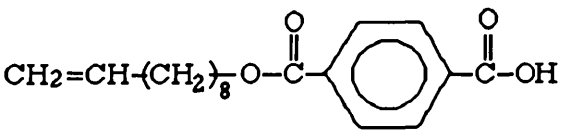

Mono-9-decenyl terephthalate

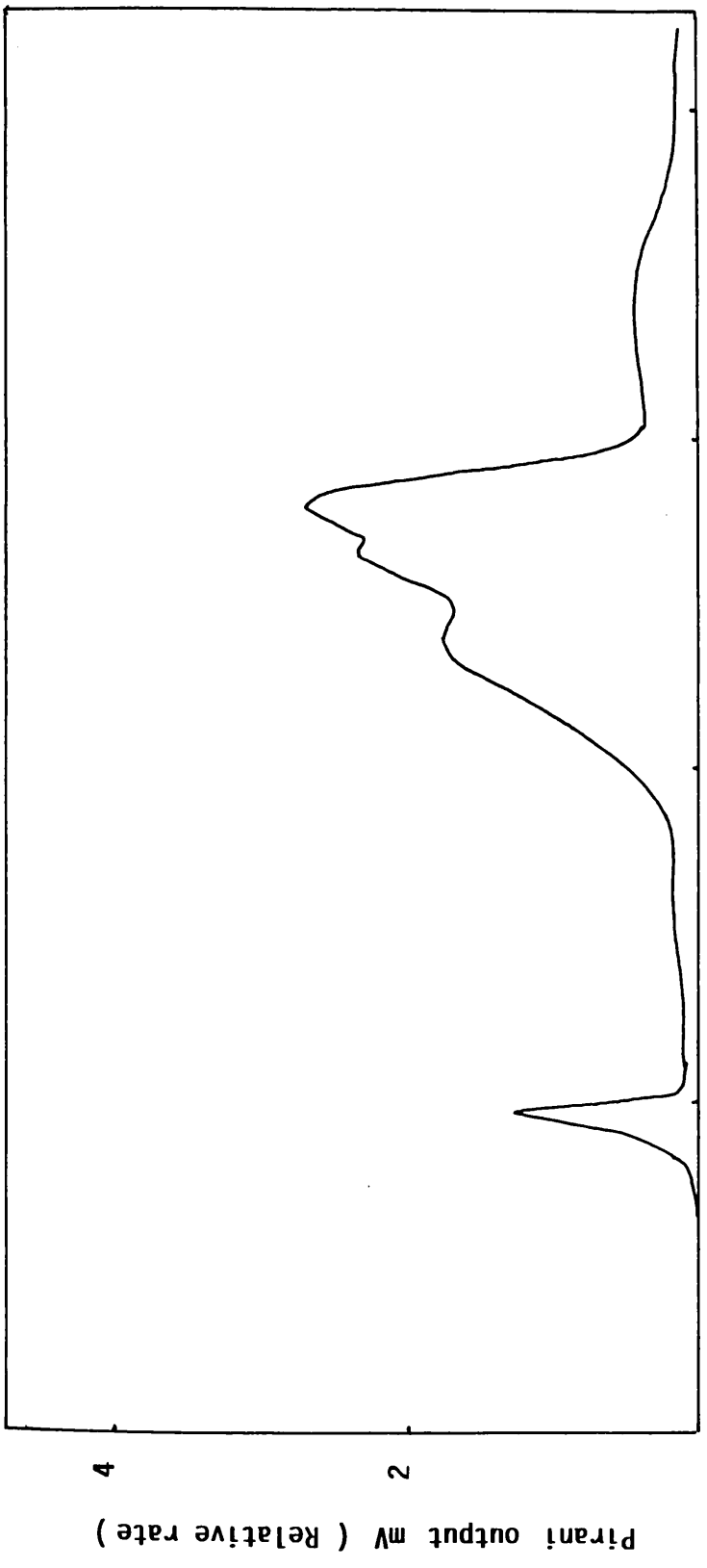

Figure 4.8: Subambient TVA trace for warm up from -196 ^{o}C to ambient temperature of condensable volatile products from degradation of poly(decamethylene terephthalate) to 500 ^{o}C .

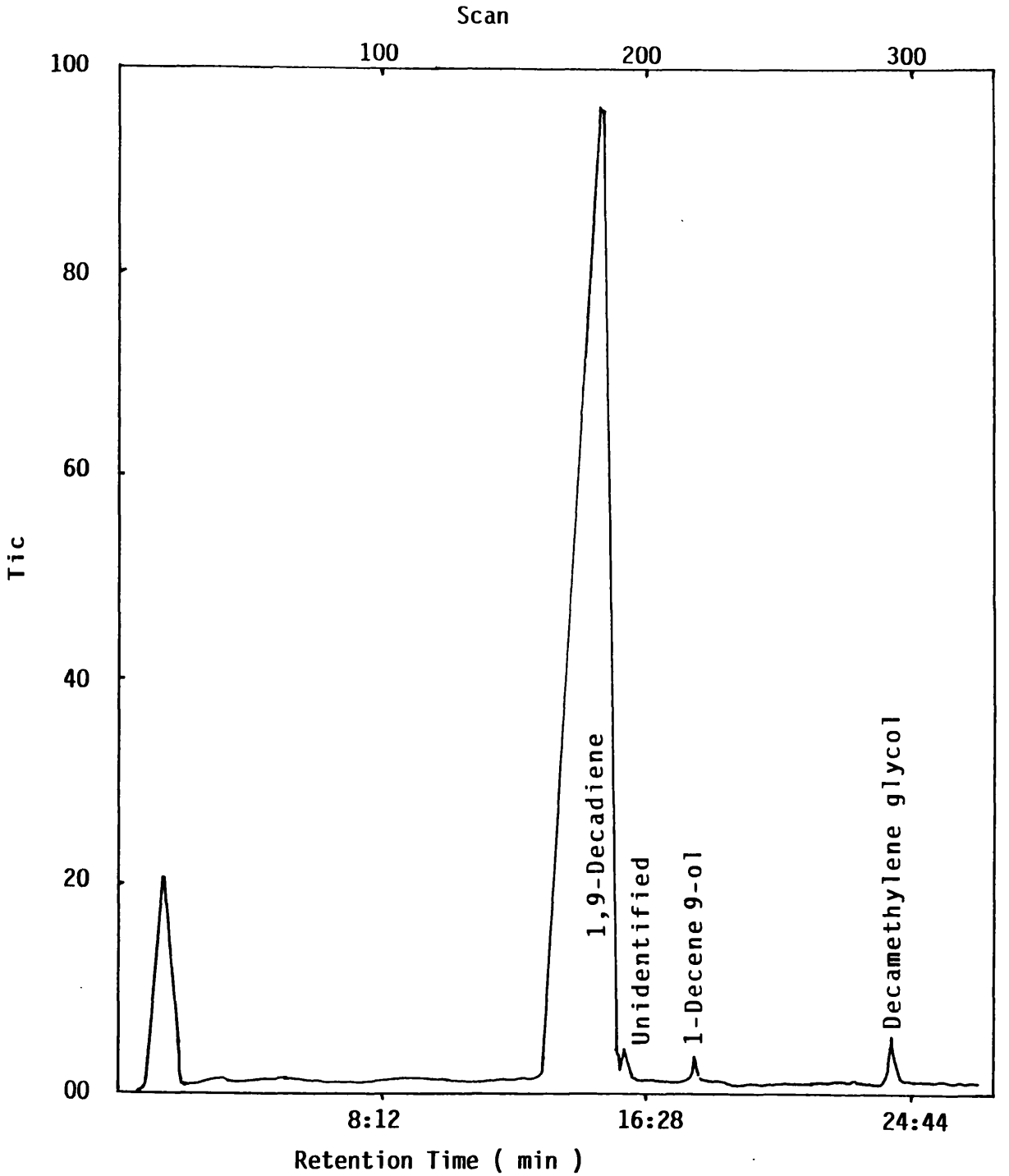

Figure 4.9: Gas chromatogram for the liquid fraction in SATVA separation of products from the degradation of PDMT to 500 ^{o}C .

In the case of the lower CRF, the ir spectrum showed a new band at 1790 cm^{-1} due to the anhydride group. However, the remaining bands are similar to the original spectrum of PDMT, indicating that the lower CRF consists of short chain fragments with anhydride groups within the chain.

4.4 ISOTHERMAL DEGRADATION OF POLY(ALKYLENE TEREPHTHALATES)

Isothermal degradation was carried out at various temperatures under vacuum, in order to get a better insight into the structural changes in the polymer during thermal degradation processes.

4.4.1 POLY(ETHYLENE TEREPHTHALATE)

4.4.1.1 Cold ring fraction

A sample of PET (200 mg) was heated isothermally at 300, 365, 385 and 405 ^{o}C for 100 min. at each temperature, successively. The CRF was collected at each temperature for quantitative measurements and spectroscopic analysis

The ir and mass spectra for the CRF at 300 ^{o}C indicate the presence of a cyclic trimer [44]. At the higher temperature of 365 ^{o}C, more CRF was formed and the ir spectrum shows bands corresponding to the carboxylic acid group (2660, 2540 and 1685 cm^{-1}) and vinyl ester end group (1640 cm^{-1}). These bonds indicate the presence of terephthalic acid and short chain fragments with vinyl ester or carboxylic acid end groups. However, the production of a short chain fragment containing anhydride groups was observed at 385 ^{o}C. In addition the mass spectra for the CRF at 300, 365,

385 and 405 °C show many abundant peaks corresponding to various molecular ions, which are summarised in Table 4.5.

The quantitative measurements of the main fractions (i.e volatile products, cold ring fraction and residue) after successive isothermal degradation of PET at different temperatures are listed in Table 4.6 .

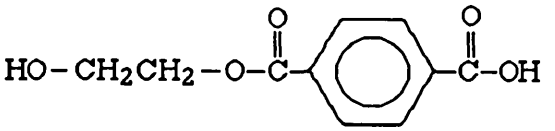

Mono-2-hydroxyethyl terephthalate

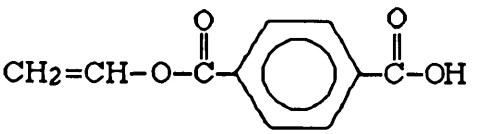

Mono-vinyl terephthalate

4.4.1.2 Production of volatile products

PET was degraded isothermally at 300, 365, 385 and 405 °C for 100 min at each temperature successively and the condensable volatile degradation products were separated by SATVA.

Acetaldehyde was observed at 365, 385 and 405 °C as the major component. Carbon dioxide was present in traces at 365 °C and the amount increased at higher temperatures. The evolution of non-condensable gases was observed at temperature over 365 °C.

Product	m / e	Relative abundance %				
		300 °C	365 °C		385 °C	405 °C
			A	B		
Benzoic acid	122	--	--	1.2	2.2	2.2
Terephthaldehydic acid	150	--	9.3	8.7	9.5	9.9
Terephthalic acid	166	--	--	1.1	2.3	4.6
Mono-2-hydroxyethyl terephthalate	193 (M-OH)	--	--	17.4	24.1	15.6
Dimethyl terephthalate	194	--	48.4	--	--	--
Short chain fragment V (m =2)	341 (M-OH)	--	--	9.1	1.9	2.4
Short chain fragment containing anhydride group	534	--	--	13.9	18.8	15.9
Mono-vinyl terphthalate	175 (M-OH)	--	--	3.4	7.5	5.2
Cyclic trimer	533	51.8	--	31.7	6	7.8

Table 4.5: Material present in the CRF from isothermal degradation of PET at different temperatures shown for 100 min under vacuum.

Temperature / °C	300	365	385	405	Total
Residual fraction wt %	92.1	82.7	66.5	18.1	18.1
Cold ring fraction wt %	5.3	8.5	11.5	38.4	63.7
Volatile products wt %	2.6	0.9	4.7	10	18.2

Table 4.6: Quantitative data for the main degradation products fractions from isothermal degradation of PET for 100 min at each temperature shown.

4.4.2 POLY(BUTYLENE TEREPHTHALATE)

4.4.2.1 Cold ring fraction

A sample of PBT (200 mg) was heated isothermally at 305, 343 and 390 °C for 100 min. at each temperature, successively. A white solid material was observed at 305 °C as CRF, the ir spectrum of which showed bands characteristic of terephthalic acid as the major product with a weak band at 1710 cm^{-1} corresponding to the stretching vibration of the ester group. However, the mass spectrum for the CRF at 305 °C showed many intense peaks attributed to the molecular ions of various compounds, as shown in Table 4.7.

The quantitative data for the main fractions after successive periods of isothermal degradation at 305, 343 and 390 °C are presented in Table4.8.

4.4.2.2 Production of volatile products

SATVA curves for the condensable volatile products of isothermal degradation of PBT at 305, 343 and 390 °C were obtained. It was found that 1.3-butadiene and carbon dioxide began to be formed at 305°C and significant amounts were evolved at higher temperatures. However, tetrahydrofuran started to be produced at about 340 °C.

4.4.3 POLY(DECAMETHYLENE TEREPHTHALATE)

A sample of PDMT (235 mg) was degraded isothermally at 301, 345 and 375 °C for 100 min at each temperature, successively.

Product	m / e	Intensity %		
		305 °C	343 °C	390 °C
Benzoic acid	122	3.8	3	2.5
Terephthaldehydic acid	150	12	10.7	10.4
Terephthalic acid	166	18.9	2.7	3.1
Mono -3 -butenyl terephthalate	203 (M-OH)	5.6	38	21.9
Mono - 4 -hydroxybutyl terephthalate	239	3.8	0.9	--
Short chain fragment V (m = 4)	369 (M-OH)	13	26.5	14
Cyclic dimer	440	0.3	0.3	--

Table 4.7: Material present in the CRF from isothermal degradation of PBT at different temperatures shown for 100 min under vacuum.

Temperature / °C	305	343	390	Total
Residual fraction wt %	97.9	42.2	0.6	0.6
Cold ring fraction wt %	1.8	53.2	40.1	95.1
Volatile products wt %	0.4	2.5	1.4	4 .3

Table 4.8: Quantitative data for the main degradation products fractions from isothermal degradation of PBT for 100 min at each temperature shown.

4.4.3.1 Cold ring fraction

The CRF at 301 and 345 °C consists mainly of terephthalic acid and short chain fragments with unsaturated ester [-CO-O-$(CH_2)_8$-CH=CH_2] or carboxylic acid (-COOH) end groups. However, the ir spectrum of the CRF at 375 °C indicates the formation of short chain fragments including anhydride groups (-CO-O-OC-). The various products are listed in Table 4.9.

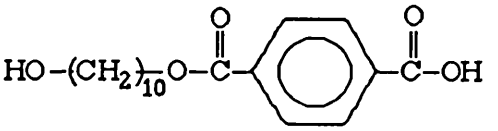

Mono-10-hydroxydecyl terephthalate

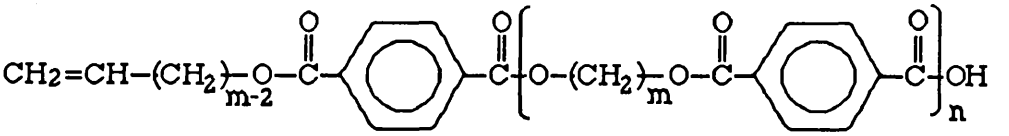

III (m,n=10, 1)

Quantitative measurements of the main fractions at 301, 345 and 375 °C in the isothermal degradation of the PDMT are shown in Table 4.10.

4.5 DETERMINATION OF ACTIVATION ENERGY

Isothermal TG traces were recorded at different temperatures under dynamic nitrogen flow (80 ml/min), and the curves for percentage volatilisation (W_t / W_o %) versus time are shown in Figures 4.10, 4.13 and 4.16, where W_t is the weight loss after time t and W_o is the original weight of polymer sample. By plotting ln (W_t / W_o %) versus time as shown

Product	m / e	Intensity %		
		301 °C	343 °C	375 °C
Benzoic acid	122	7.9	4.6	5
Terephthaldehydic acid	150	10	8.8	9.4
Terephthalic acid	166	4	66.1	13
Mono -9-decenyl terephthalate	287 (M-OH)	4.4	1.1	2
Mono -10 -hydroxydecyl terephthalate	323	2.2	--	--
Short chain fragment III (m, n = 10, 1)	592	0.5	--	--

Table 4.9: Material present in the CRF from isothermal degradation of PDMT at different temperatures shown for 100 min under vacuum.

Temperature / °C	301	345	375	Total
Residual fraction wt %	97.9	71.3	4	4
Cold ring fraction wt %	1.7	24.9	65.4	92
Volatile products wt %	0.4	1.7	1.9	4

Table 4.10: Quantitative data for the main degradation fractions from isothermal degradation of PDMT for 100 min at each temperature shown.

in Figures 4.11, 4.14 and 4.17, the rate constants at the various degradation temperatures were calculated and used to determine the apparent activation energy for the initial decomposition of each of the poly(alkylene terephthalates).

The activation energy was calculated by applying the Arrhenius equation:

$$\ln k = \ln A - \frac{E_a}{R.T}$$

Where: k rate constant of volatilisation

R gas constant (1.9872 cal / ^{o}k.mol)

T temperature in ^{o}K

E_a activation energy

By plotting ln k versus 1/T a straight line was obtained for all polymers with a slope of $-E_a/R$ as shown in Figures 4.12, 4.15 and 4.18.

The values of activation energy for poly(alkylene terephthalates) are listed in Table 4.11.

Polymer Code	PET	PBT	PDMT
Activation Energy (K cal. / mol)	52.1	50.6	33.6

Table 4.11: Activation energy for the isothermal degradation of poly(alkylene terephthalates) under vacuum.

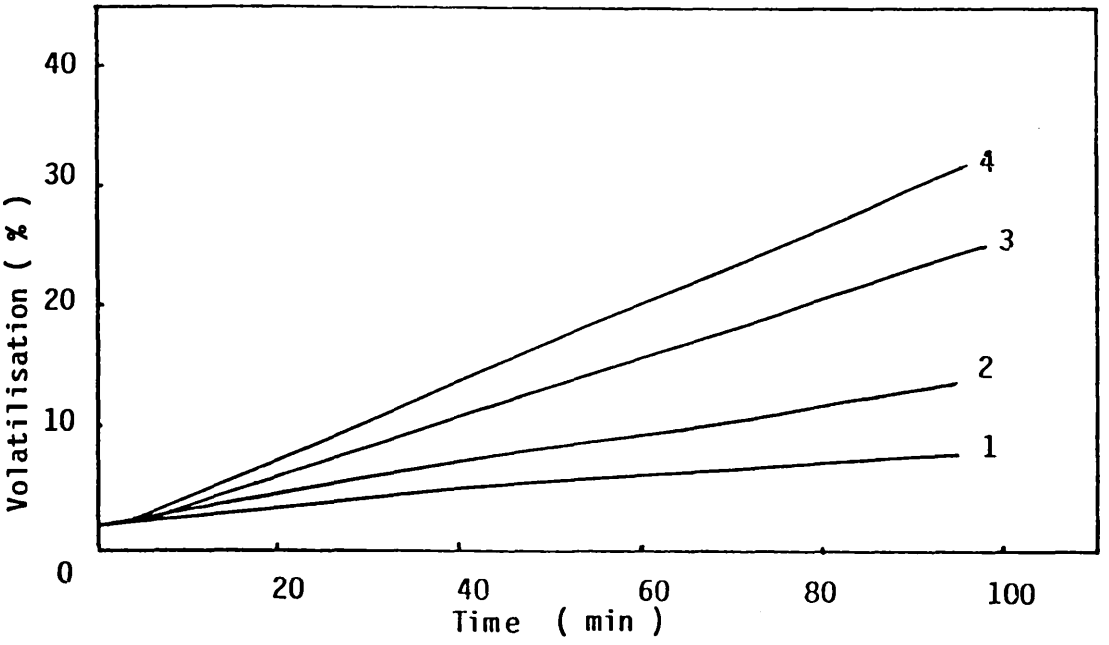

Figure 4.10: Dependence of volatilisation on time and temperatures during isothermal degradation of PET under vacuum . 1,325 ; 2,333 ; 3,345 and 4,355 ^{o}C .

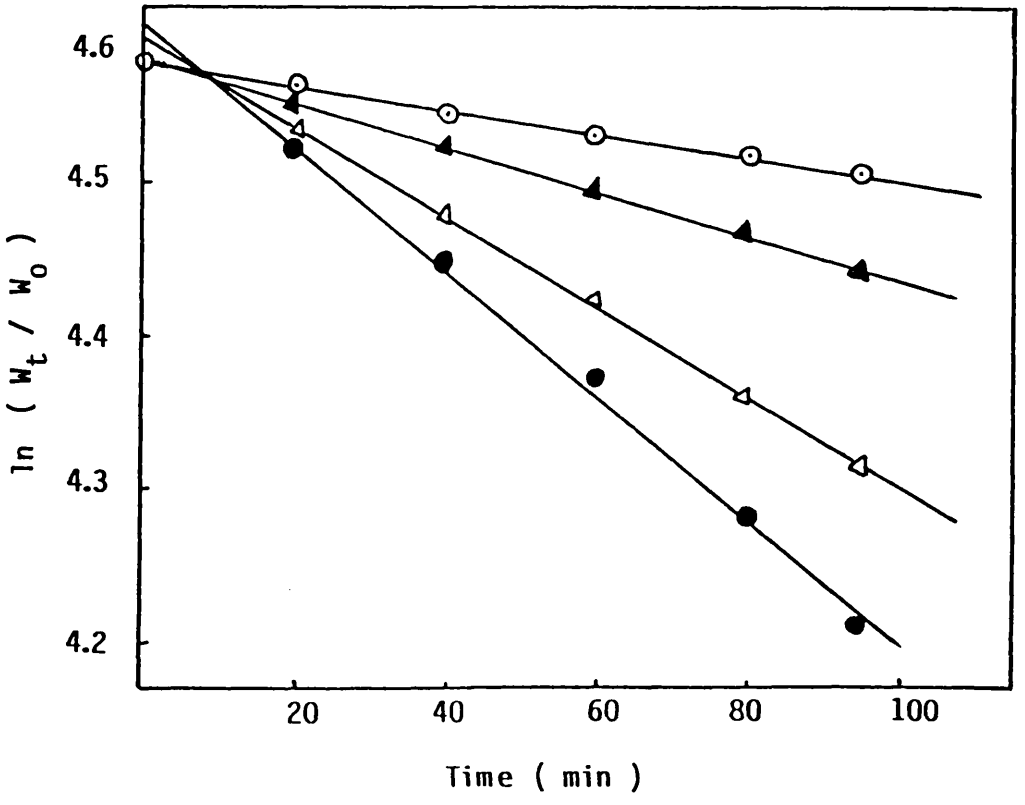

Figure 4.11: Plot of ln (W_t / W_o) versus time for PET at temperatures ⊙ , 325 ^{o}C; ▲ , 333 ^{o}C; △ , 345 ^{o}C; ● , 355 ^{o}C .

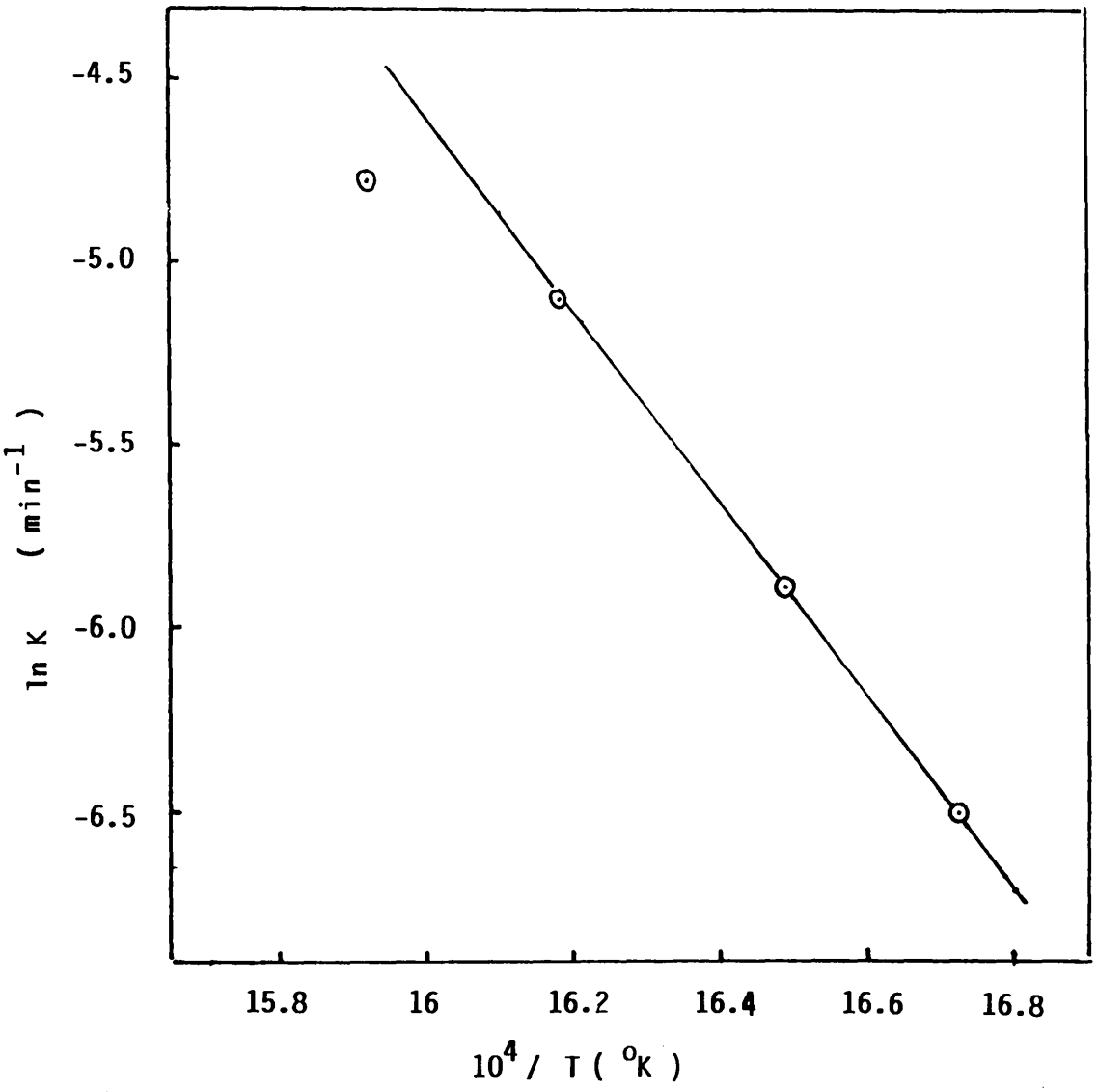

Figure 4.12: Arrhenius plot for poly(ethylene terephthalate) (PET) degradation .

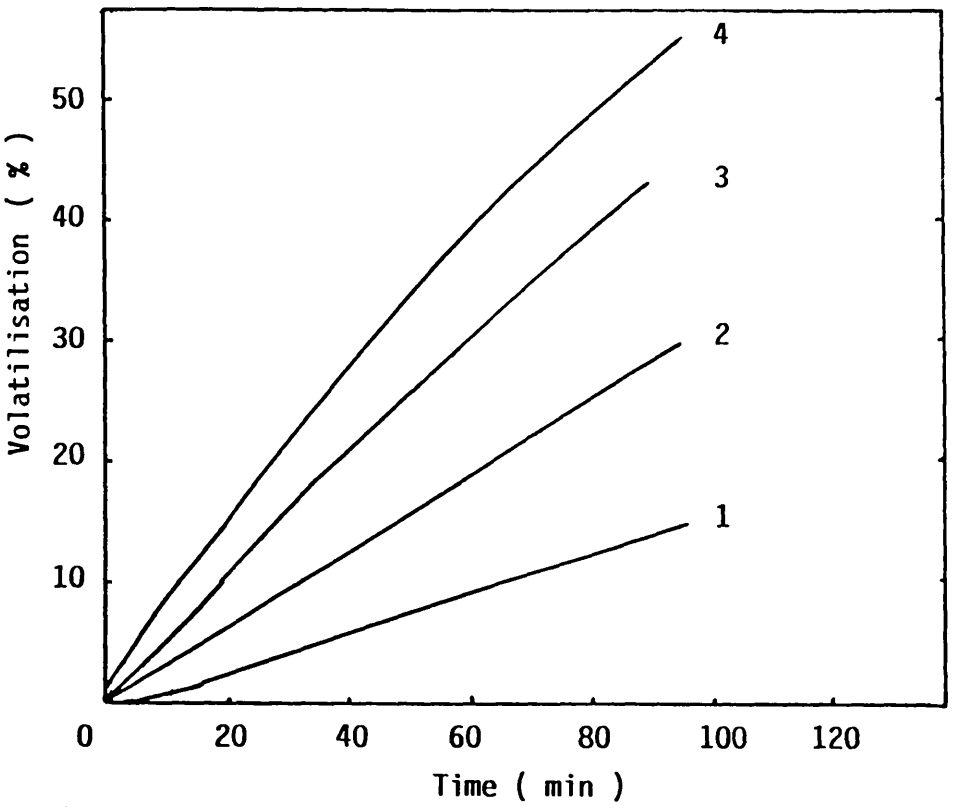

Figure 4.13: Dependence of volatilisation on time and temperatures during isothermal degradation of PBT under vacuum . 1, 300 ^{o}C ; 2, 310 ^{o}C 3, 315 ^{o}C ; 4, 320 ^{o}C .

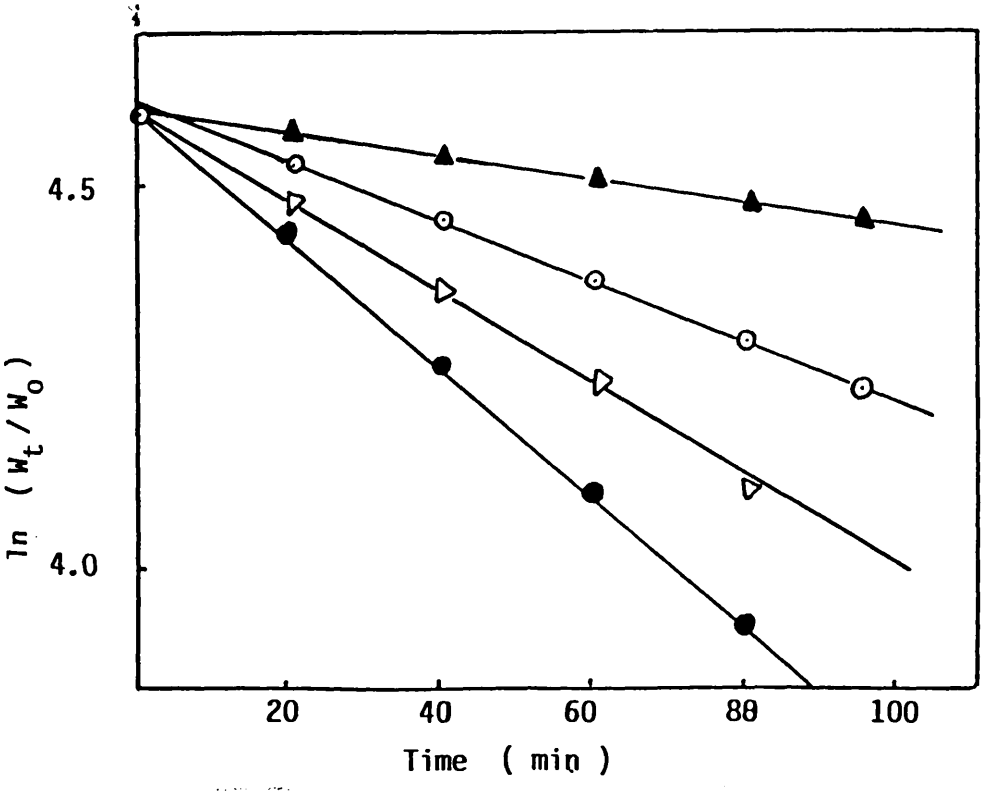

Figure 4.14: Plot of ln (W_t / W_o) versus time for PBT at temperatures ▲, 300 ^{o}C; ⊙ , 310 ^{o}C; △ , 315 ^{o}C; ● , 320 ^{o}C .

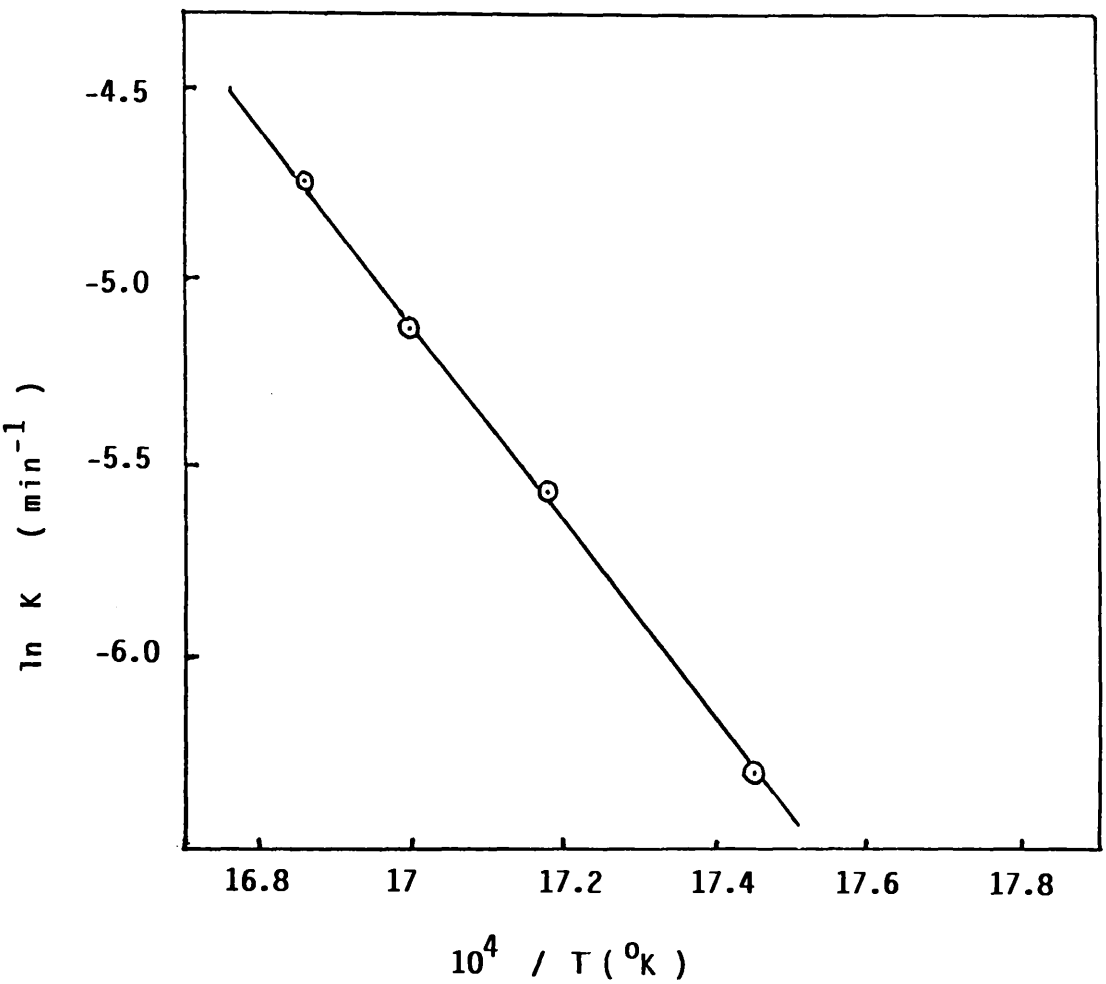

Figure 4.15: Arrhenius plot for poly(butylene terephthalate) (PBT) degradation .

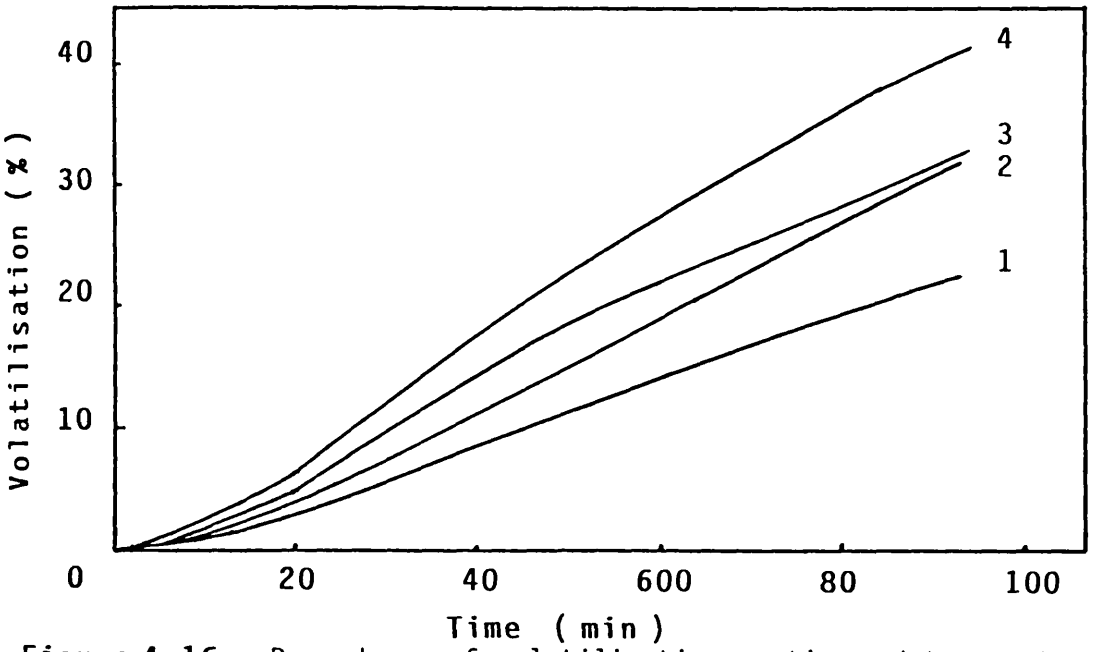

Figure 4.16: Dependence of volatilisation on time and temperatures during isothermal degradation of PDMT under vacuum. 1 , 310 ^{o}C ; 2, 315 ^{o}C ; 3 , 320 ^{o}C ; 4 , 325 ^{o}C .

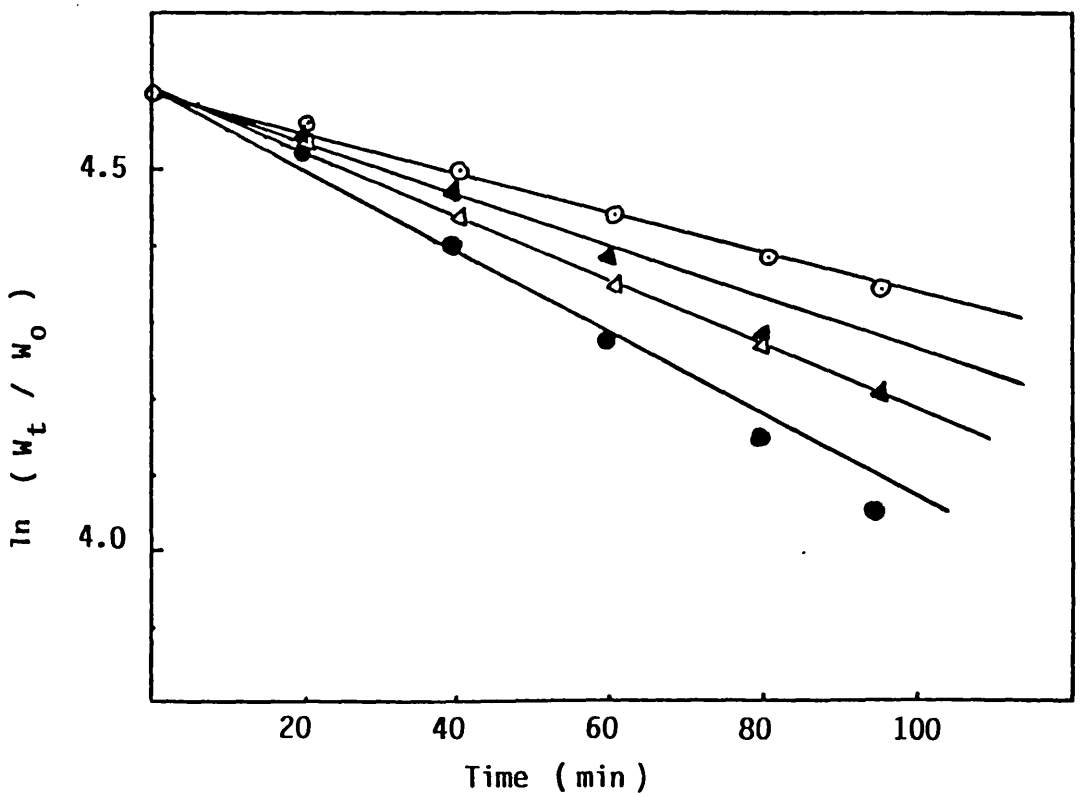

Figure 4.17: Plot of ln (W_t / W_o) versus time for PDMT at temperatures ⊙ , 310 ^{o}C; ▲, 315 ^{o}C; △, 320 ^{o}C; ● , 325 ^{o}C .

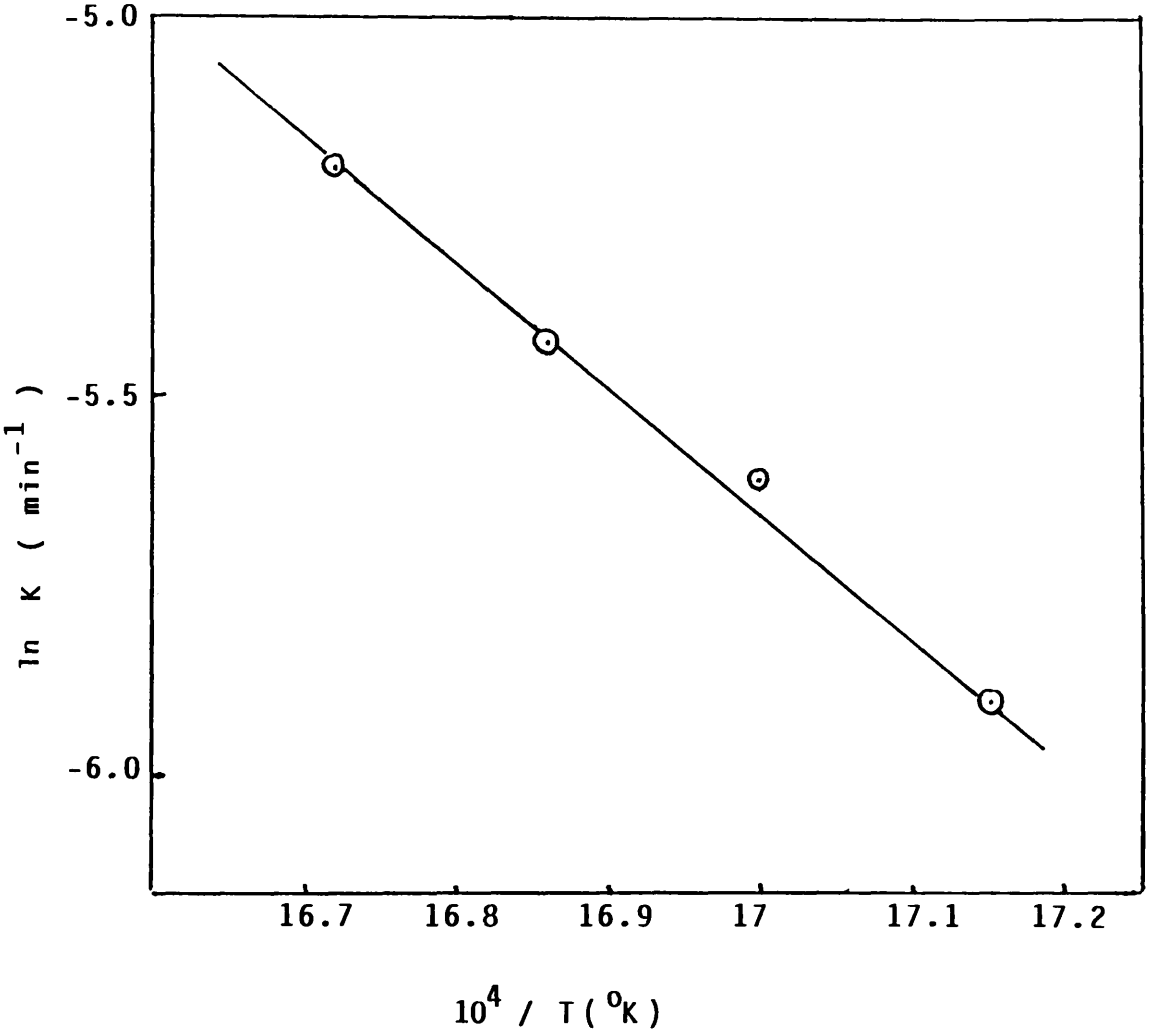

Figure 4.18: Arrhenius plot for poly(decamethylene terephthalate) (PDMT) degradation .

4.6 MECHANISM OF DECOMPOSITION

On the basis of the information obtained by identification of most of the degradation products, it is proposed that the initial decomposition reaction for poly(alkylene terephthalates) may involve chain scission at the (C-O) bond leading to short chain fragments I and II terminated by carboxylic acid and unsaturated ester groups respectively [39-42,46] as shown in Scheme 4.3.

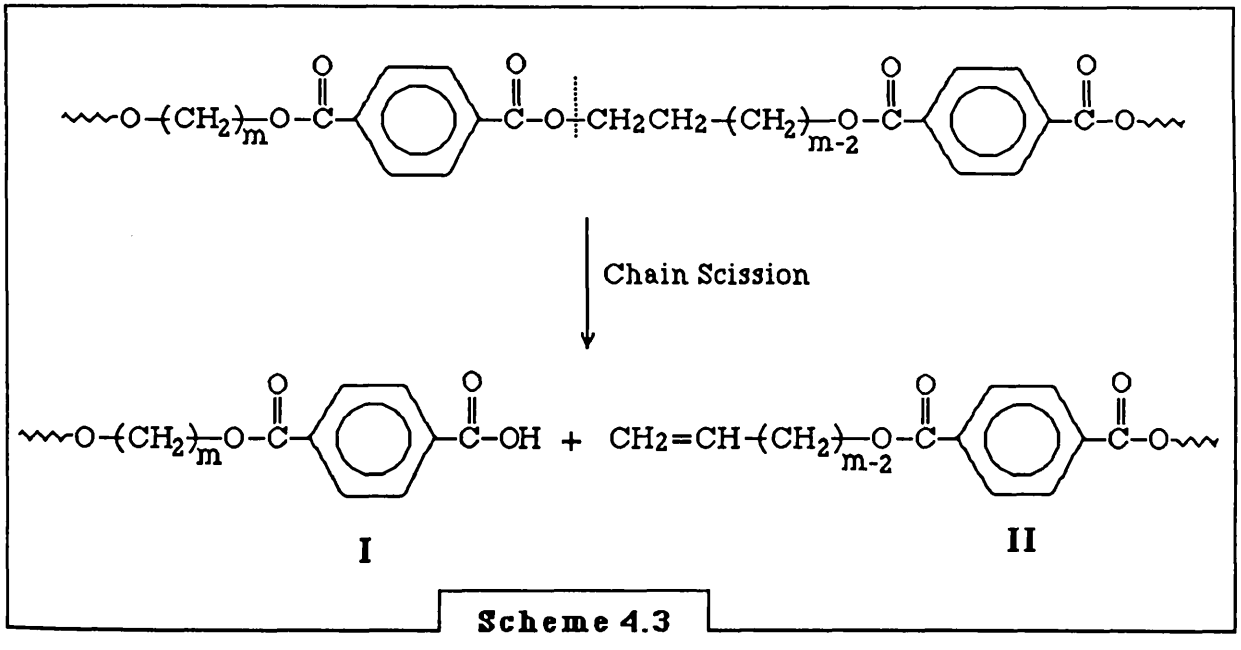

Scheme 4.3

Fragment II can produce the further short chain fragment III by homolytic cleavage at an (O–alkyl) bond followed by disproportionation, Scheme 4.4.

In the case of m,n = 4,1 and 2,2; the fragment III converted to a cyclic dimer and cyclic trimer, respectively. However, some of the cyclic trimer was recovered before the initial decomposition of PET, which contains cyclic trimer residue [43]

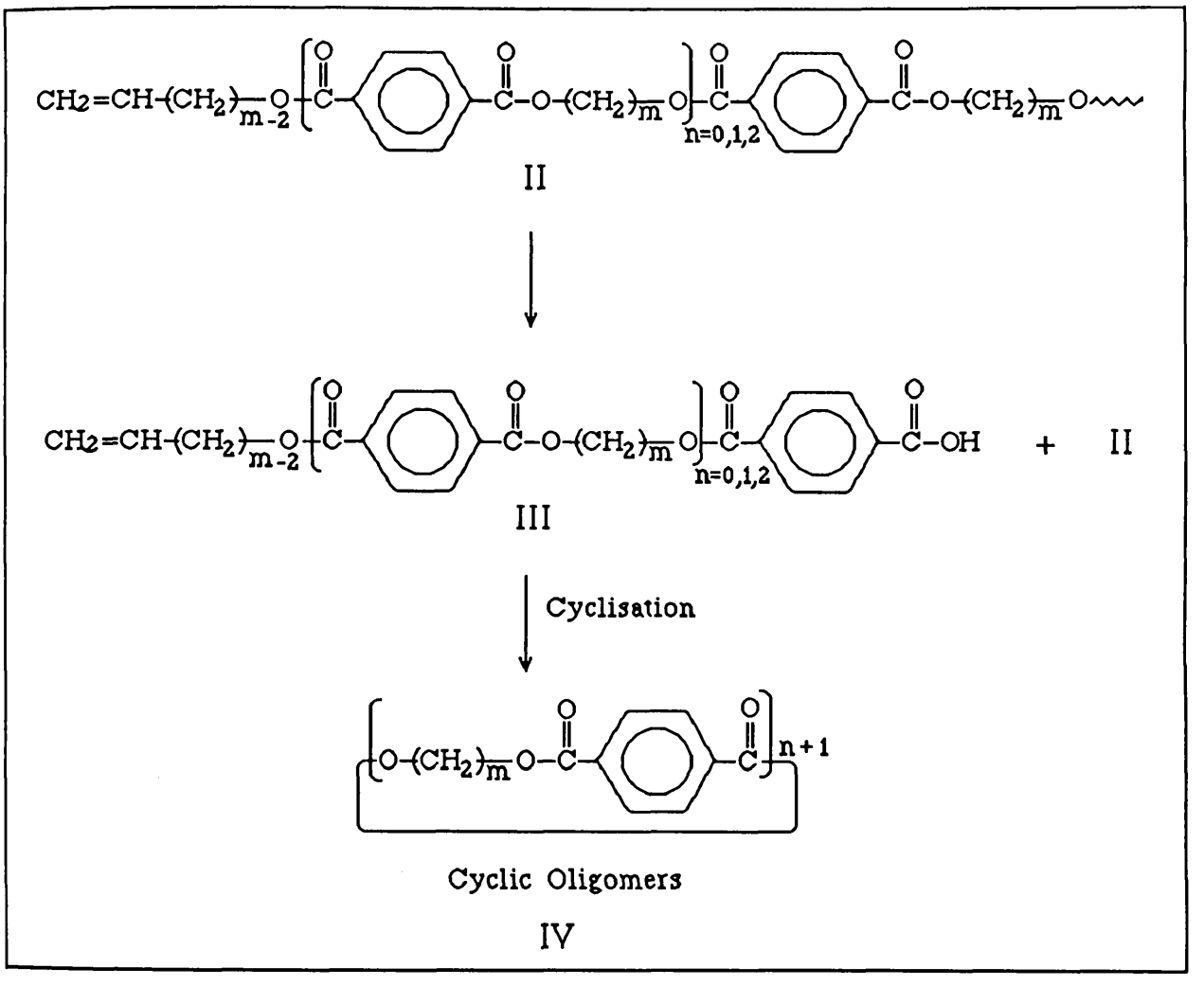

Scheme 4.4

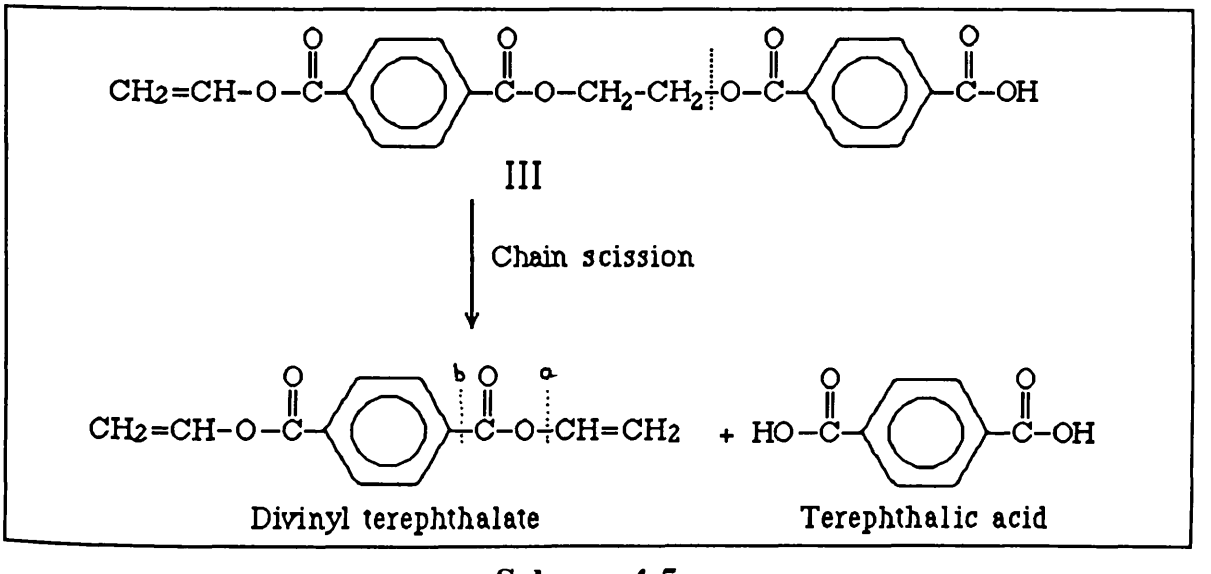

Scheme 4.5

The production of divinyl terephthalate in the degradation of PET can be accounted for by chain scission at an (O–alkyl) bond of fragment III (m,n=2,1) as shown in Scheme 4.5.

A further fragmentation of divinyl terephthalate at points (a) and (b), followed by intramolecular hydrogen abstraction leads to ethylene, carbon dioxide and vinyl benzoate.

Short chain fragments terminated by carboxylic acid end groups V, result from homolytic cleavage at an O–alkyl bond of either I or III (m,1) as shown in Scheme 4.6.

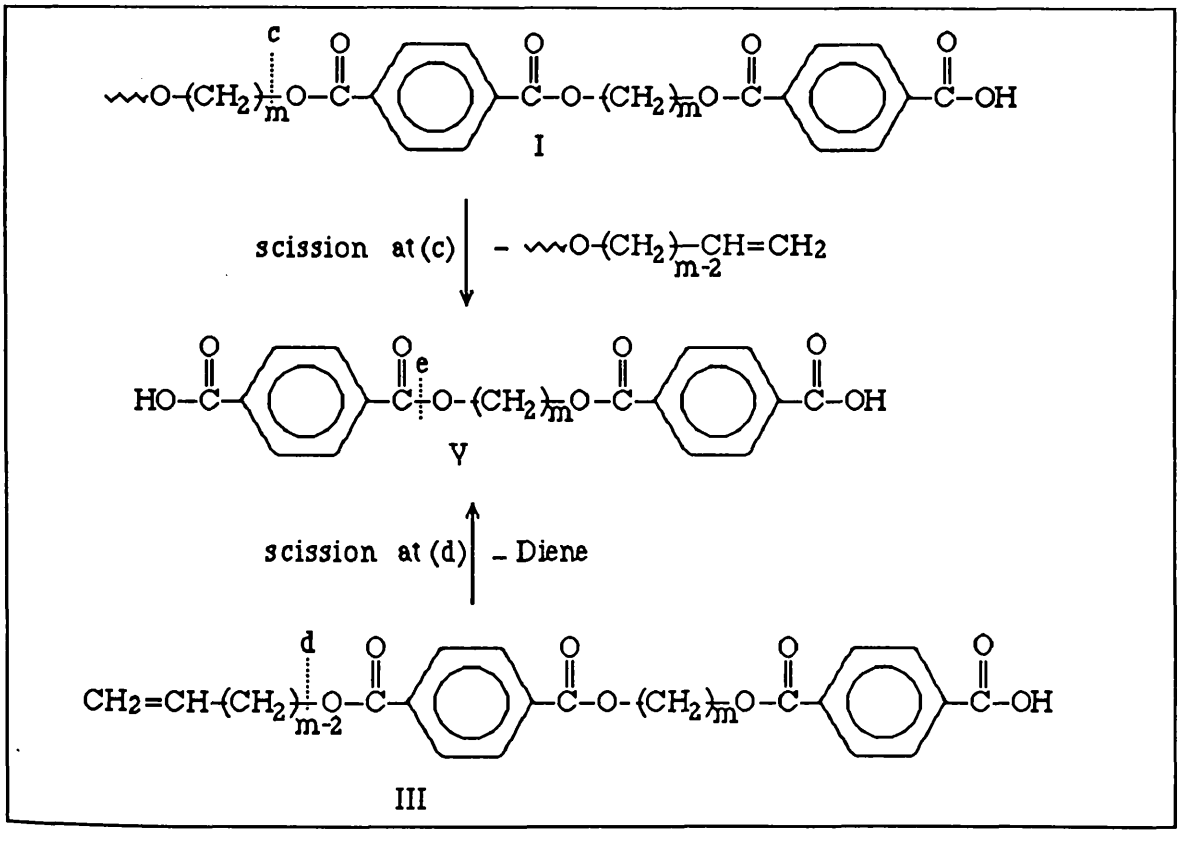

Scheme 4.6

The formation of fragment VI was accompanied by 4-carboxy benzaldehyde as a result of the fragmentation of fragment V at point (e). The polymer fragment VI might be broken at either (O–alkyl) or (O–acyl) bonds and the formation of the diol in the degradation of PBT and PDMT could be explained by a two step reaction involving scission of fragment VI at points (f) and (g), followed by hydrogen abstraction, as shown in Scheme4.7.

Unsaturated aliphatic alcohols can result from (O–alkyl) scission at point (h) of fragment VI or dehydration of the diol as shown in Scheme 4.8.

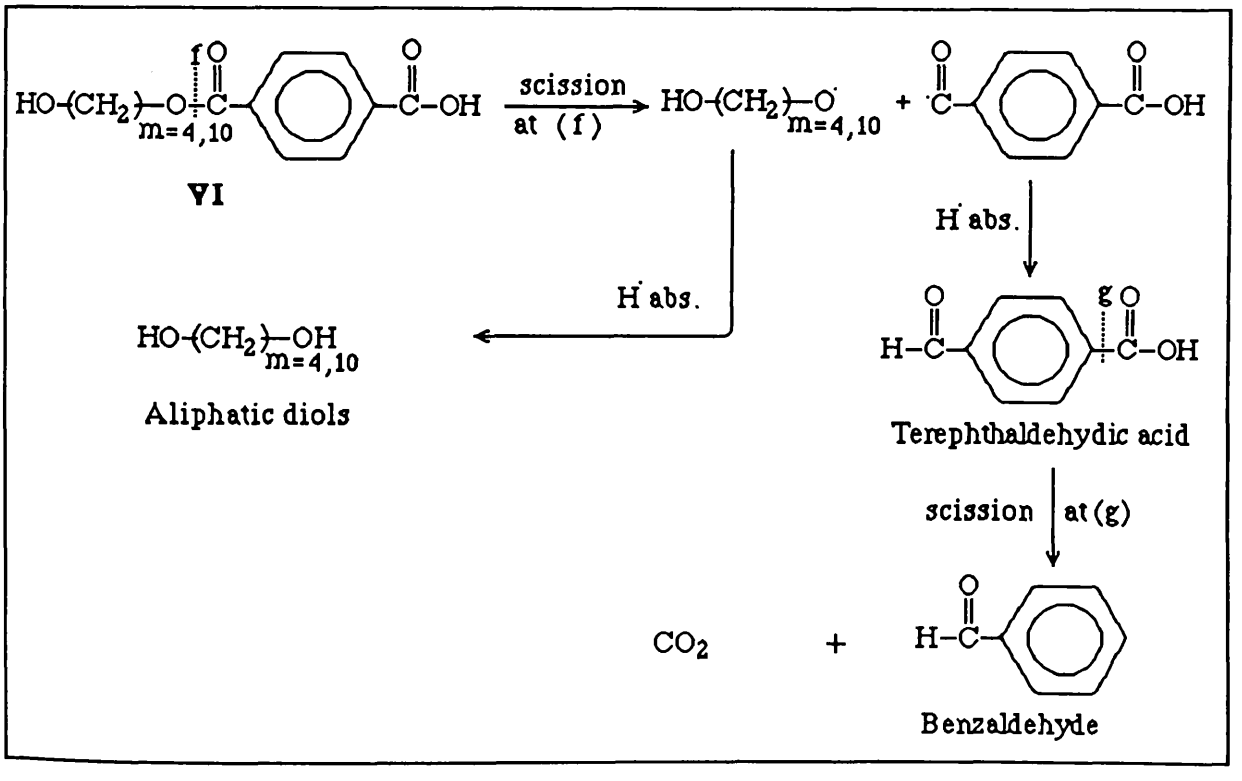

Scheme 4.7

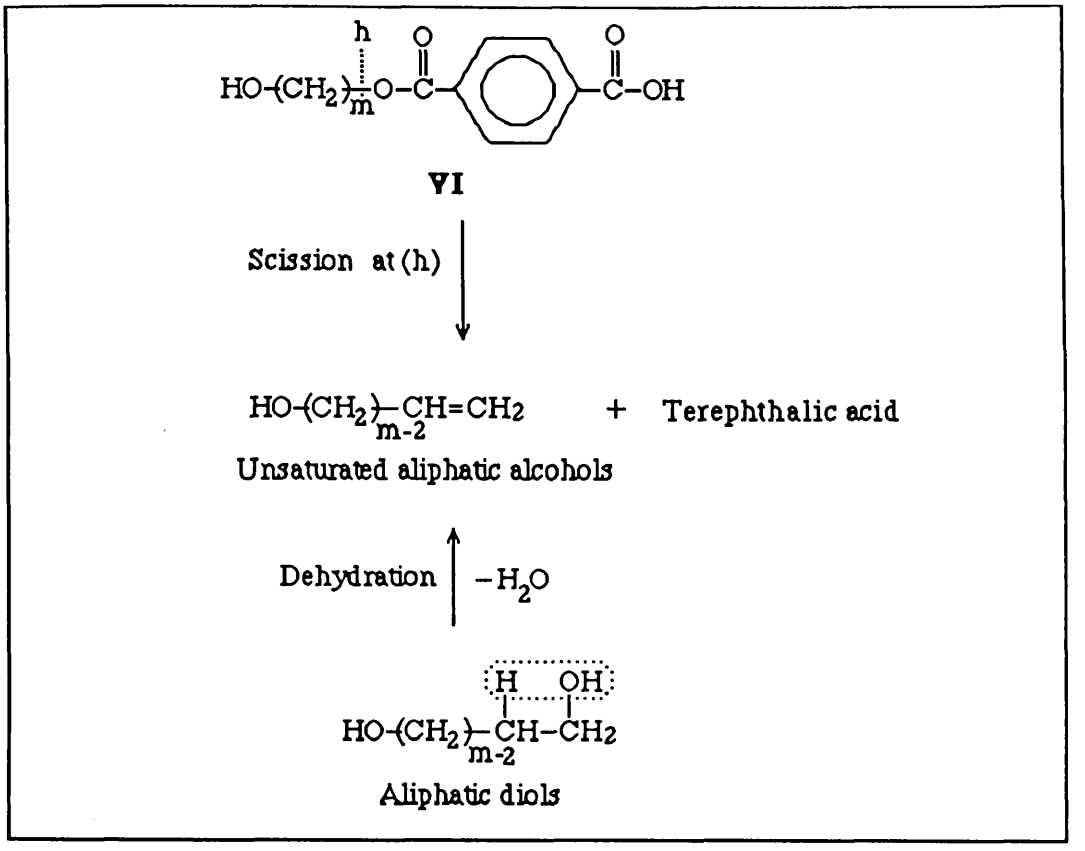

Scheme 4.8

In the case of PET, the vinyl alcohol initially formed would be detected as acetaldehyde (major product) or dioxane as illustrated in Scheme 4.9.

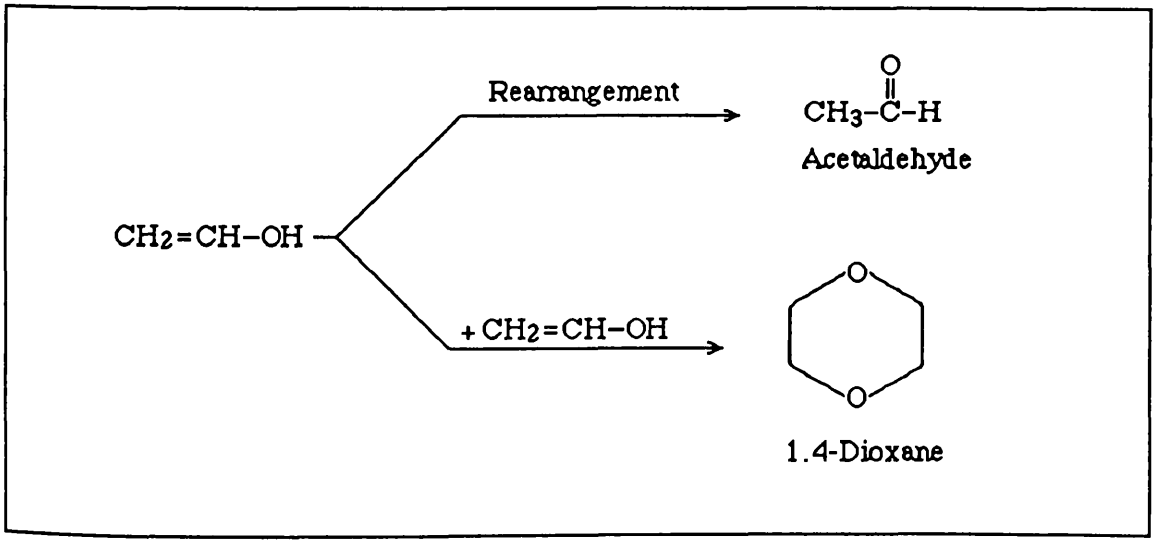

Scheme 4.9

The formation of cyclic ether (tetrahydrofuran and dihydrofuran) in PBT degradation may result from the cyclization of 3-butene-1-ol, followed by dehydrogenation as shown in Scheme 4.10.

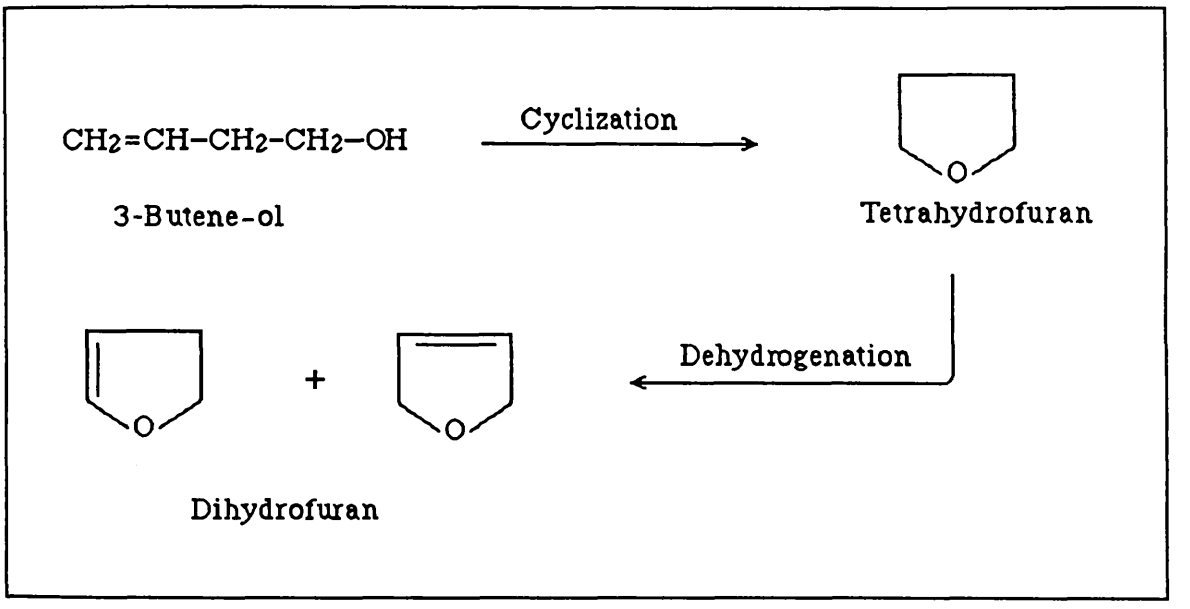

Scheme 4.10

Either homolytic cleavage at an (O–alkyl) bond of the fragment III or dehydration of unsaturated aliphatic alcohol can explain the possibility of diene production, as shown in Scheme 4.11.

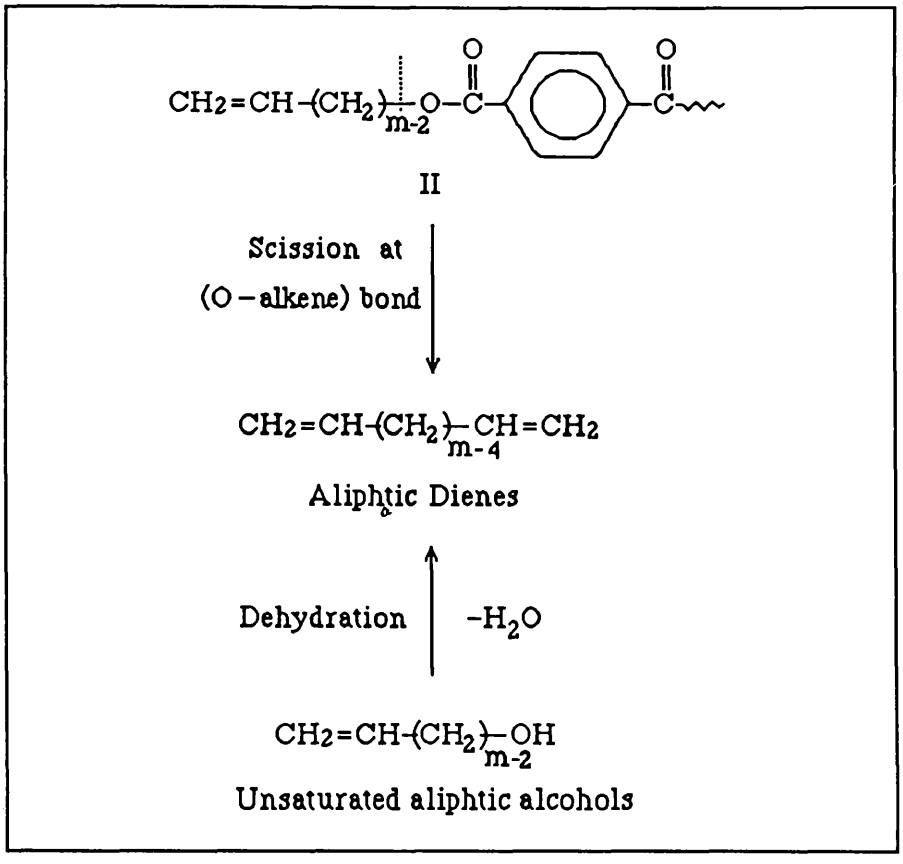

Scheme 4.11

The formation of 4-vinyl cyclohexene in PBT degradation can be explained by dimerisation of butadiene, as in Scheme 4.12.

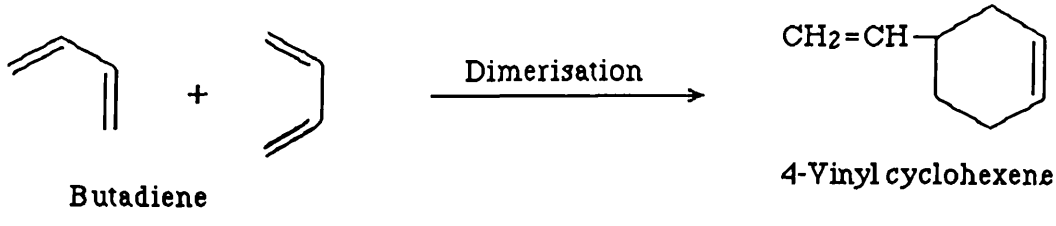

Scheme 4.12

Recombination of fragments with carboxylic acid and unsaturated ester end groups at higher temperatures will lead to a short chain fragment

containing anhydride group (CO-O-OC) and release of an unsaturated aliphatic alcohol. An alternative route is dehydration of two molecules of a short chain fragment with carboxylic acid end group (-COOH), as shown in Scheme 4.13.

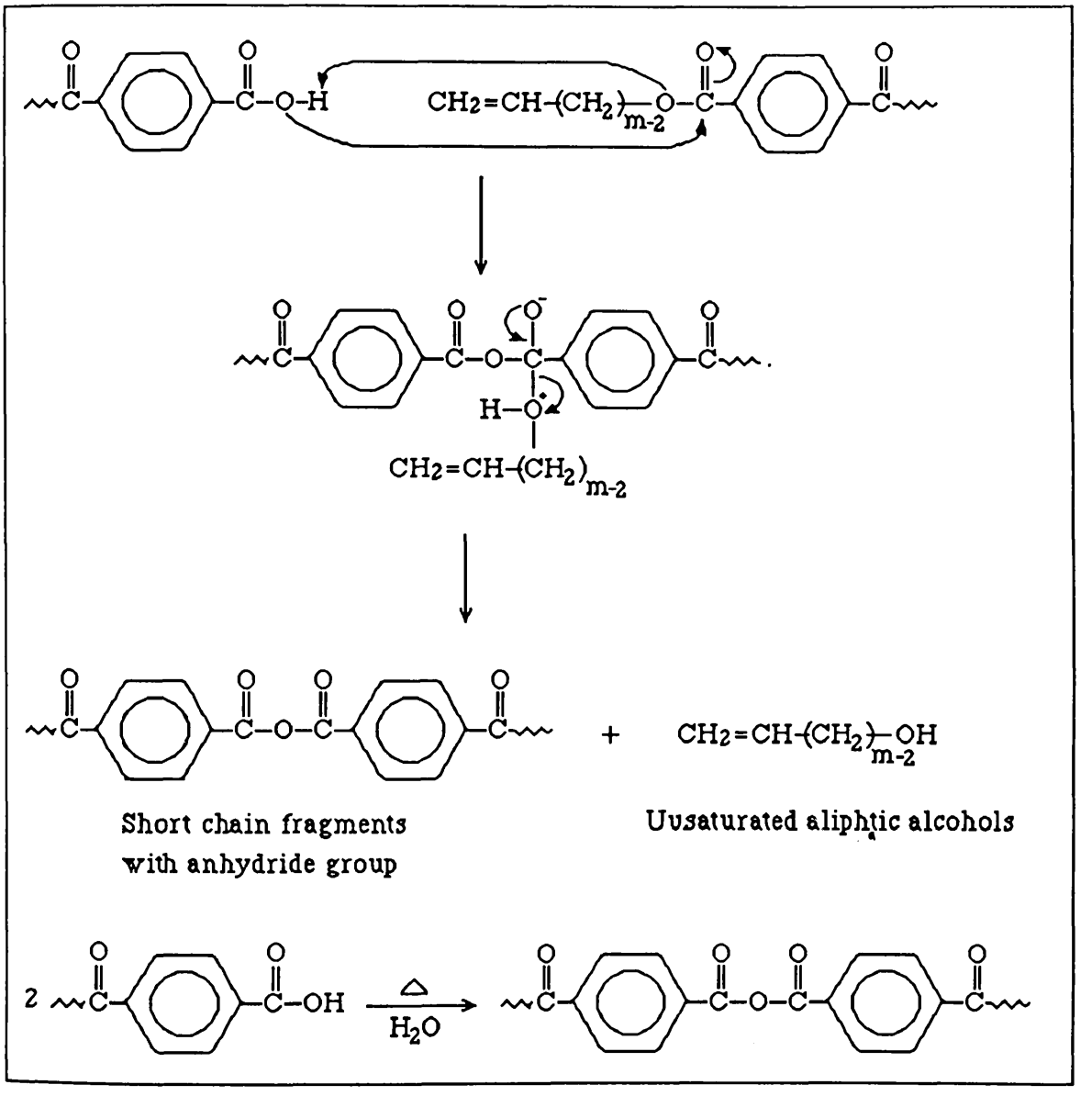

Scheme 4.13

CHAPTER FIVE

THERMAL DEGRADATION OF POLY(ETHER–ESTER)

5.1 INTRODUCTION

In our continuing study of the relationship polymer structure and thermal behaviour, the thermal degradation of poly(ether-esters) (PPEGT1 and PPEGT2) based on terephthaloyl chloride with poly ethylene glycols (Mw 200 and 1000), respectively, has been studied.

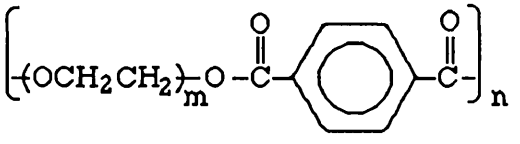

Poly(ether–ester)

where m = 4 or 22

Both polymers showed similar stages of decomposition during thermal degradation, evolving the same degradation products, although with different onset temperatures and in different relative yields of products. A general mechanism of decomposition for the two poly(ether-esters) is proposed.

Poly(ether-ester) polymers are thermoplastic elastomers which exhibit a unique combination of strength and flexibility since they are composed of two different types of segments, namely, soft and hard segments. The former are derived from poly(alkylene glycol) oligomers, having low glass transition and melting temperatures, giving flexibility to the material. The

latter are associated as crystallites to form a thermally reversible crosslinked structure, which provides the strength and dimensional stability of the material.

A number of investigations have been performed on poly(ether-esters) based on poly(tetramethylene glycol) as soft segment and poly(butylene terephthalate) as hard segment, in which the effect of such variables as molecular weight of soft segment and hard to soft segment ratio on crystallinity and morphology have been examined [54-58].

The microstructure and property changes associated with hard segment crystallisation in poly (ether-esters) have been elucidated using small angle X-ray scattering, differential scanning calorimetry (DSC) and stress-strain measurements. It has been found that an increase in phase separation between soft and hard segments occurs during crystallisation and annealing[54]. It has been shown [55,56] that as the ratio of polyether / polyester segments and the molecular weight of polyether segment increases, the stability of the copolymer decreases. The effect of chain structure on the thermal and mechanical properties of a series of poly(ether-esters), in which the crystallinity varied with the fraction and type of hard segments has been studied [57].

There have been no reports in the literature on thermal degradation and degradation products of the polymers studied in this chapter.

5.2 THERMAL ANALYSIS

5.2.1 Thermogravimetry (TG)

The TG and DTG curves for PPEGT1 and PPEGT2 (see Chapter Three), heated at 10 ^{o}C/min, under dynamic nitrogen atmosphere, are shown in

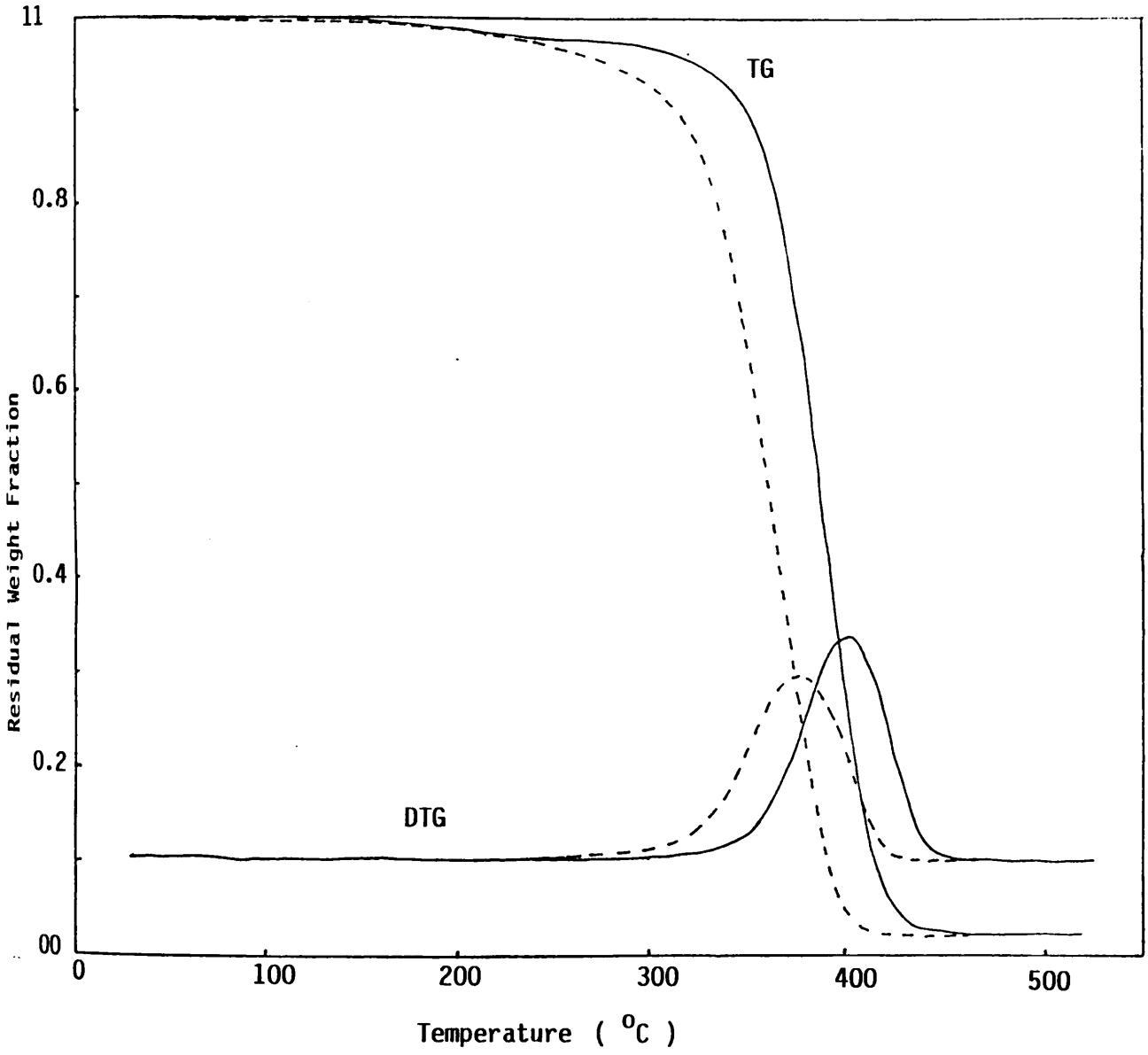

Figure 5.1: TG and DTG traces for poly(ether-ester) degradation under dynamic N_2 . Heating rate 10 ^{o}C/min . PPEGT1 (——) and PPEGT2 (– – –) , sample size 3-4 mg .

Figure 5.1. The curves show a single step decomposition, in which the weight loss from PPEGT2 begins at lower temperature than in the case of PPEGT1. The involatile material remaining at 500 °C was found to be around 3.5% of the original weight of the polymer sample.

5.2.2 Thermal volatilisation analysis (TVA)

The TVA traces from the degradation of these poly(ether-esters) are shown in Figure 5.2. The evolution of volatile products occurs in the range of 300- 440 °C, reaching maximum rate of volatilisation at 380 and 410 °C for PPEGT2 and PPEGT1, respectively.

The separation of traces corresponding to the pressure reading after 0, -45, -75, -100 and -196 °C cold traps, indicates the presence of various volatile products with different volatility including non-condensable gases.

The quantitative measurements for the main fractions of the degradation products and thermal features for the degradation of poly(ether-esters) are summarised in Table 5.1

5.3 CHARACTERISATION OF DEGRADATION PRODUCTS

The degradation products formed from the heating up to 500 °C, at heating rate of 10 °C/min under TVA conditions of poly(ether-esters) are similar, although the relative yields are different.

5.3.1 Condensable volatile products

The SATVA curves for the separation of condensable volatile products of degradation of the poly(ether-esters), shown in Figures 5.3 and 5.4,

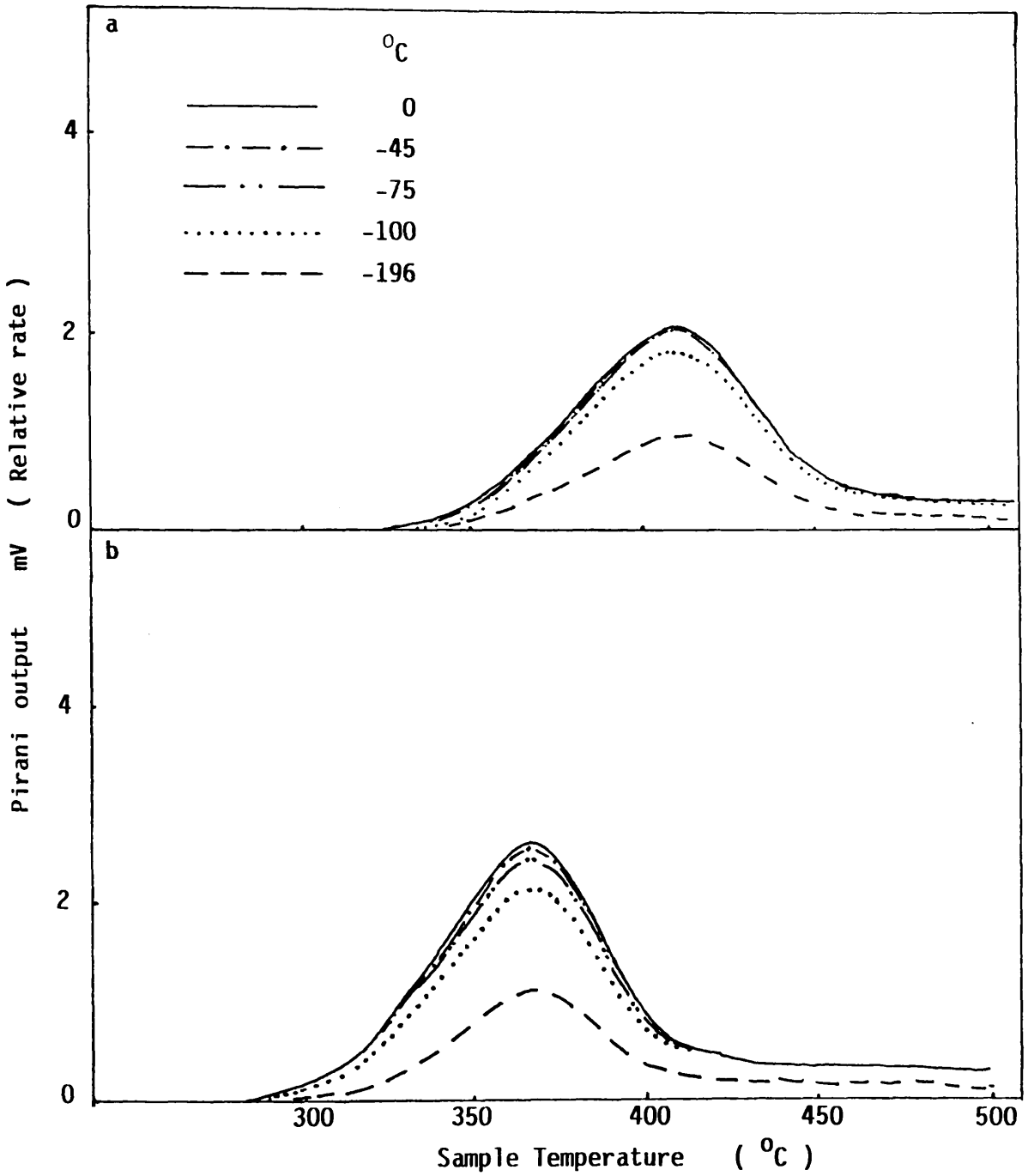

Figure 5.2: TVA traces for poly(ether-ester) degradation under vacuum . a (PPEGT1) and b (PPEGT2) . Heating rate 10 °C/min , sample size 60-70 mg .

Features		PPEGT1	PPEGT2
TVA	T onset / ^{0}C	325	280
	T max / ^{0}C	410	375
	Cold ring fraction wt %	81.4	92
	Volatile products at ambient temperature wt %	15.4	5.7
	Residual fraction wt %	3.2	2.3
TG & DTG	T onset / ^{0}C	200	300
	T max / ^{0}C	405	380
	Residual fraction wt %	2.5	2

Table 5.1: TVA, TG and DTG data for the degradation of poly(ether-esters) to 500 ^{o}C at heating rate of 10 ^{o}C/min.

exhibit many peaks. Products were collected as four main fractions. The products in fractions 1, 2 and 3 were easily identified by infrared spectroscopy as : 1, carbon dioxide and trace of ethylene; 2, formaldehyde; 3, acetaldehyde (major). The fourth fraction (liquid) was subjected to GC-MS investigation using a column consisting of BP 10 (S.G.E) containing 14 % cyanopropyl phenyl dimethyl siloxane (see Chapter Two). The gas chromatograms are shown in Figures 5.6 and 5.7 for the liquid fraction in SATVA separation of condensable volatile products from degradation of PPEGT1 and PPEGT2, respectively, and their assignments are listed in Tables 5.2 and 5.3. These indicate the presence of acetaldehyde, 1,4-dioxane, 1,3-dioxalane, methoxyacetaldehyde and ethoxyacetaldehyde, together with traces of low molecular weight carbonyl, hydroxyl, cyclic and acyclic ether compounds. In the case of PPEGT1, however, traces of methyl and ethyl benzoate are also present.

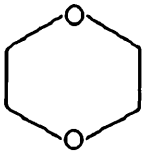

1.4-Dioxane

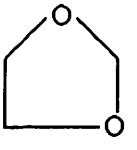

1.3-Dioxalane

5.3.2 Cold ring fraction

The cold ring fraction of products from degradation of the poly(ether-esters) was removed in each case with methylene chloride for spectroscopic analysis. The ir spectra showed the absorption bands of the original polymer, but a strong band at 3400 cm^{-1} corresponding to the hydroxyl end group of the short chain fragments was also observed.

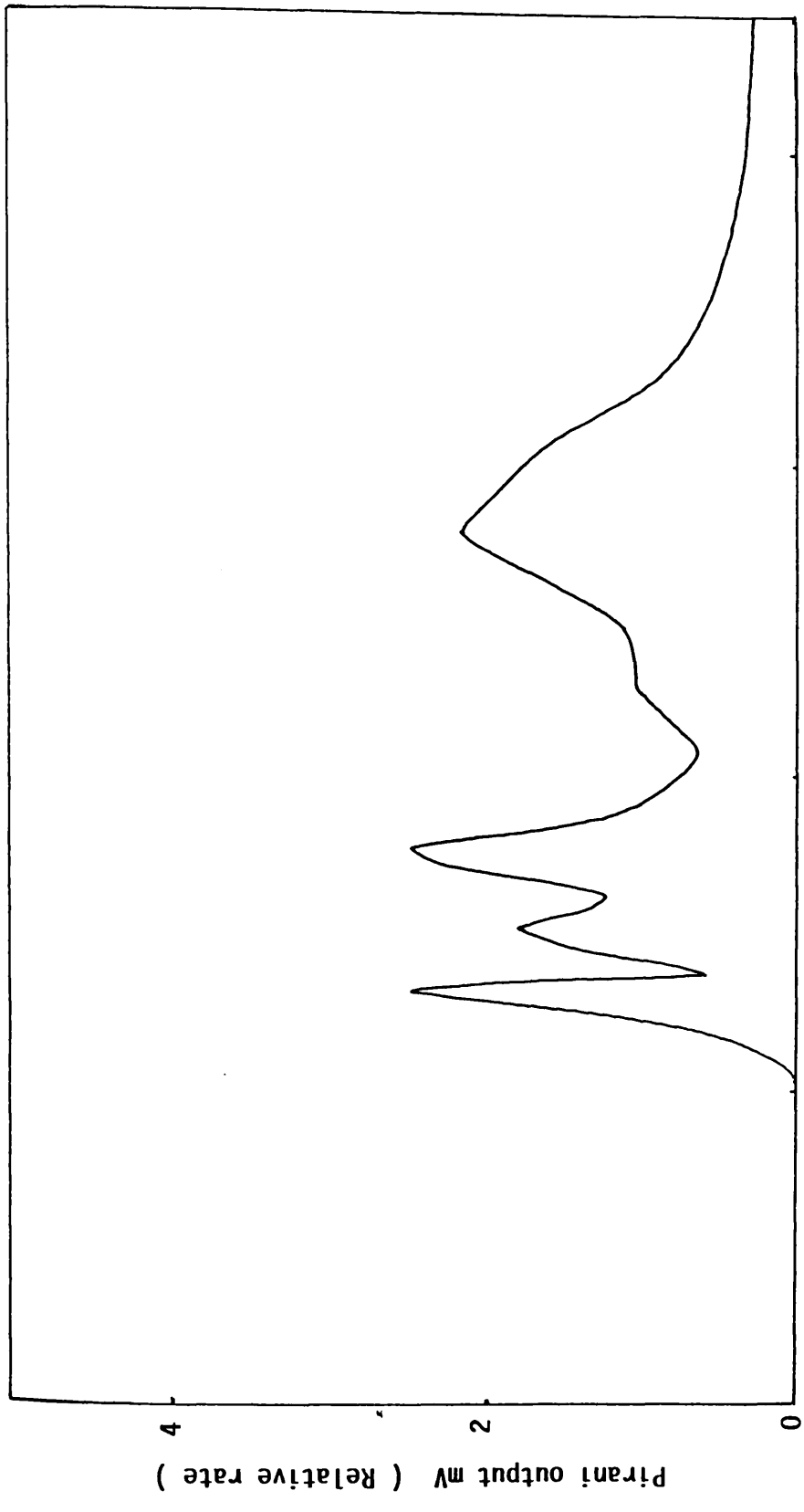

Figure5.3: Subambient TVA trace for warm up from -196 ^{o}C to ambient temperature of condensable volatile products from degradation of PPEGT1 to 500 ^{o}C .

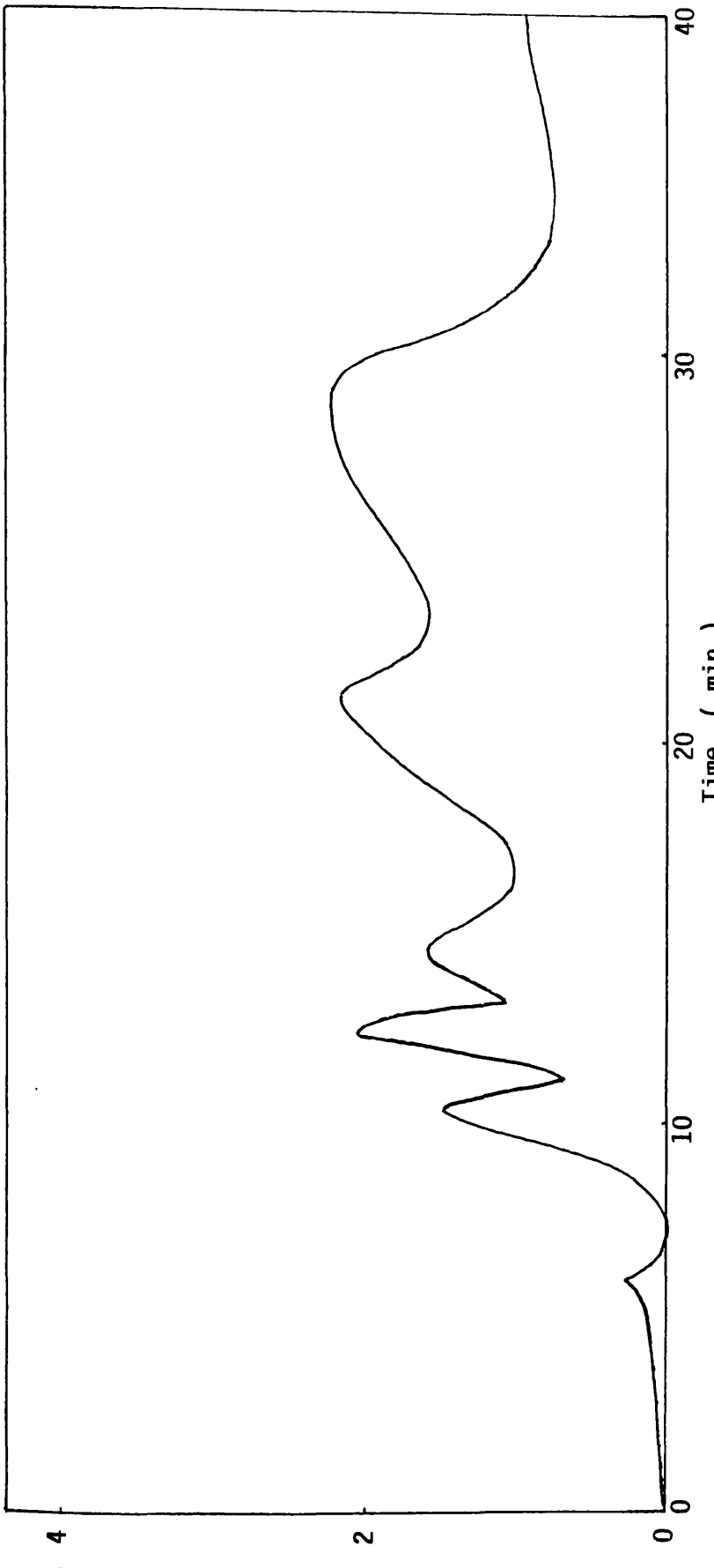

Figure 5.4: Subambient TVA trace for warm up from -196 ^{o}C to ambient temperature of condensable volatile products from degradation of PPEGT2 to 500 ^{o}C .

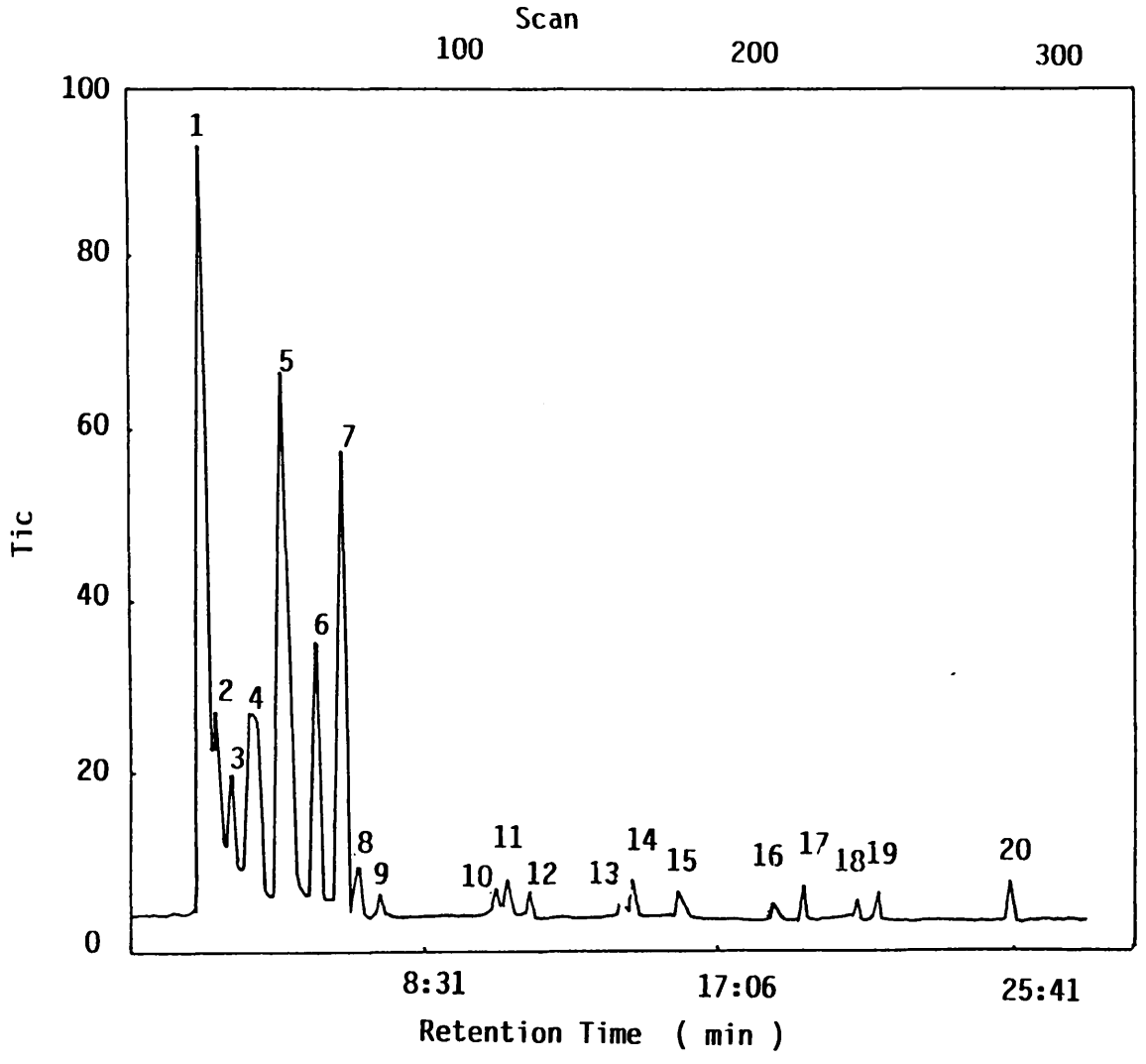

Figure 5.5: Gas chromatogram for the liquid fraction in SATVA separation of products from the degradation of PPEGT1 to 500 ^{o}C .

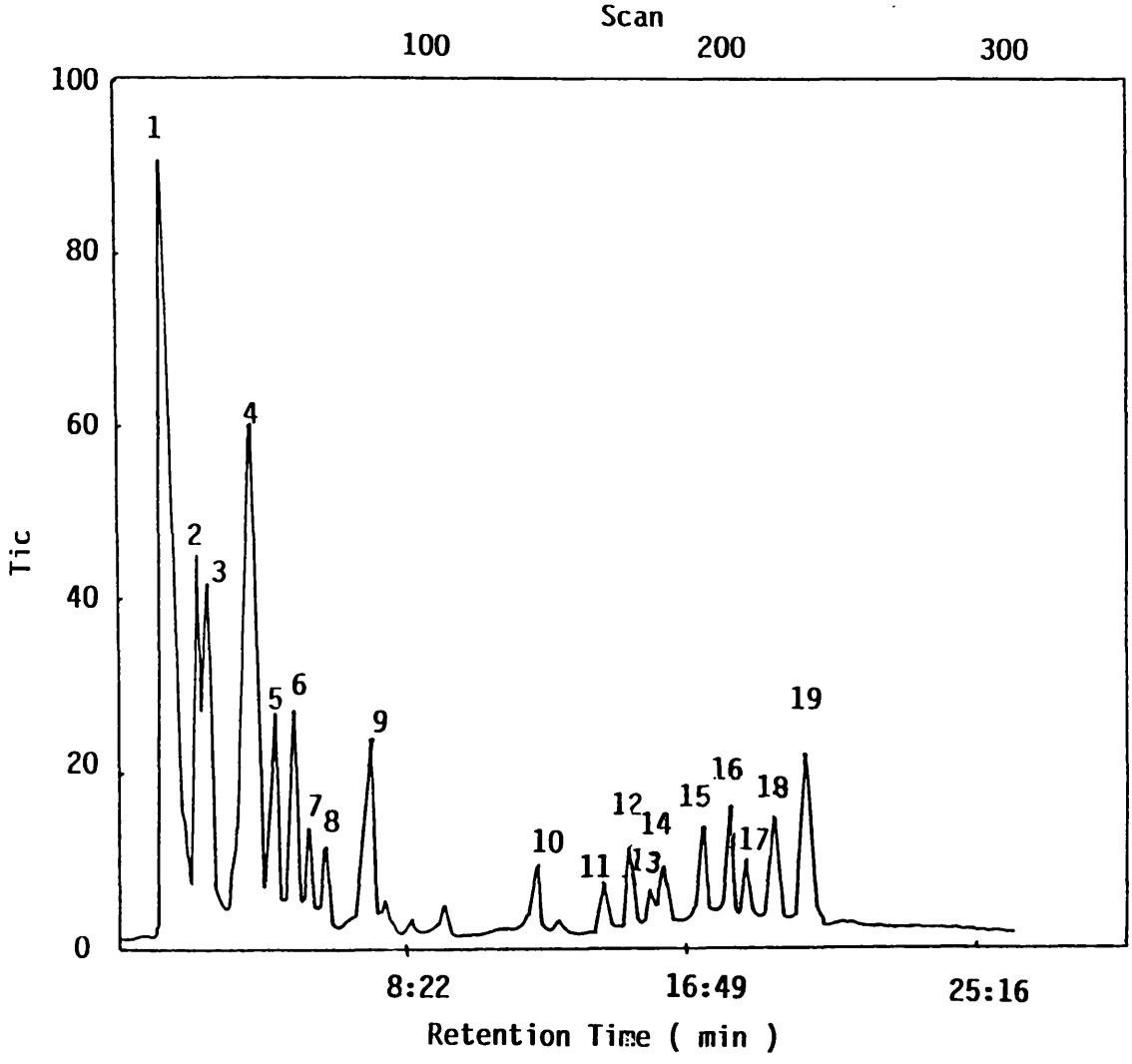

Figure 5.6: Gas chromatogram for the liquid fraction in SATVA separation of products from the degradation of PPEGT2 to 500 ^{o}C .

Peak Number	Assignment
1	Acetaldehyde
2	Methoxyacetaldehyde
3	1,4-Dioxane
4	$O{=}C\text{-}CH_2\text{-}O\text{-}CH_2CH_2$ (cyclic)
5	1,3-Dioxane
6	7-membered cyclic ring ether
7	$(CH_2CH_2\text{-}O)_n\text{-}CH_2\text{-}CO$ (cyclic)
8	$CH_2{=}CH\text{-}O\text{-}CH_2CH_2\text{-}O\text{-}CH_2\text{-}CH{=}O$
9, 10	Unidentified
11	$HO\text{-}CH_2CH_2\text{-}O\text{-}CH_2\text{-}CH{=}O$
12	Unidentified
13	1,3-Dioxalane
14	Benzaldehyde + $CH_3\text{-}O\text{-}CH_2CH_2\text{-}O\text{-}CH_2CH_3$
15	$HO\text{-}CH_2CH_2\text{-}O\text{-}CH_2CH_2\text{-}O\text{-}CH_2CH_3$
16	Unidentified
17	$CH_3CH_2O\text{-}CH_2CH_2\text{-}O\text{-}CH_2CH_2\text{-}O\text{-}CH_2CH_3$
18	Unidentified
19	Methyl benzoate
20	Ethyl benzoate

Table 5.2: Assignment of material present in the liquid fraction from SATVA separation of the products of degradation of PPEGT1 under TVA conditions to 500 ^{o}C, from the gas chromatogram as shown in Fig. 5.5.

Peak Number	Assignment
1	Acetaldehyde
2	1,3-Dioxalane
3	Ethoxyacetaldehyde
4	1,4-Dioxane
5	Unidentified
6	Glycidol
7	Unidentified
8	Diethyl ether
9	CH_3-O-CH_2CH_2-O-CH_3
10	Methyl ethyl ether
11	Unidentified
12, 13	HO-CH_2CH_2-O-CH_3
14	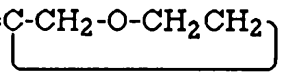
15	HO-CH_2CH_2-O-CH_2CH_3
16	HO-CH_2CH_2-O-CH_2-CH=O
17, 18	Unidentified
19	CH_3-O-CH_2CH_2-O-CH_2CH_3

Table 5.3: Assignment of materials present in the liquid fraction from SATVA separation of the products of degradation of PPEGT2 under TVA conditions to 500 ^{o}C, from the gas chromatogram as shown in Fig. 5.6.

The mass spectra obtained for the total CRF of degraded PPEGT1 sample at probe temperatures of 170, 240 and 300 °C, respectively, are shown in Figure 5.7. At 170 °C peaks corresponding to the fragment ions of terephthalic acid (m/e =166), triethylene glycol and tetraethylene glycol (m/e =149, 193, respectively) and short chain fragment A having the general formula shown below are present. The mass spectrum at 240 °C, shows peaks at m/e= 473, 429 corresponding to fragment A.

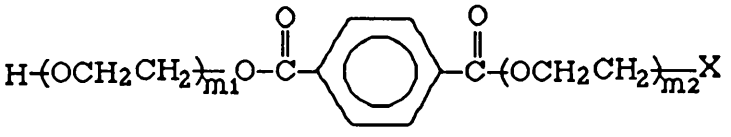

A

Where X= H, OH and $0 > m1, m2 > m = 4$ or 22

At higher temperatures (300 °C), the mass spectrum indicates the presence of short chain fragments B having the following general formula.

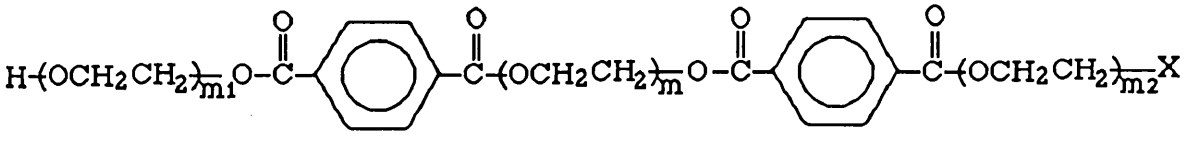

B

Where X = H, OH and $0 > m1, m2 > m = 4$ or 22

The corresponding mass spectra of CRF products from PPEGT2 degradation are reproduced in Figure 5.8. These spectra show various abundance patterns corresponding to the presence of terephthalic acid, tri- and tetraethylene glycols and short chain fragments A (m/e= 237, 325).

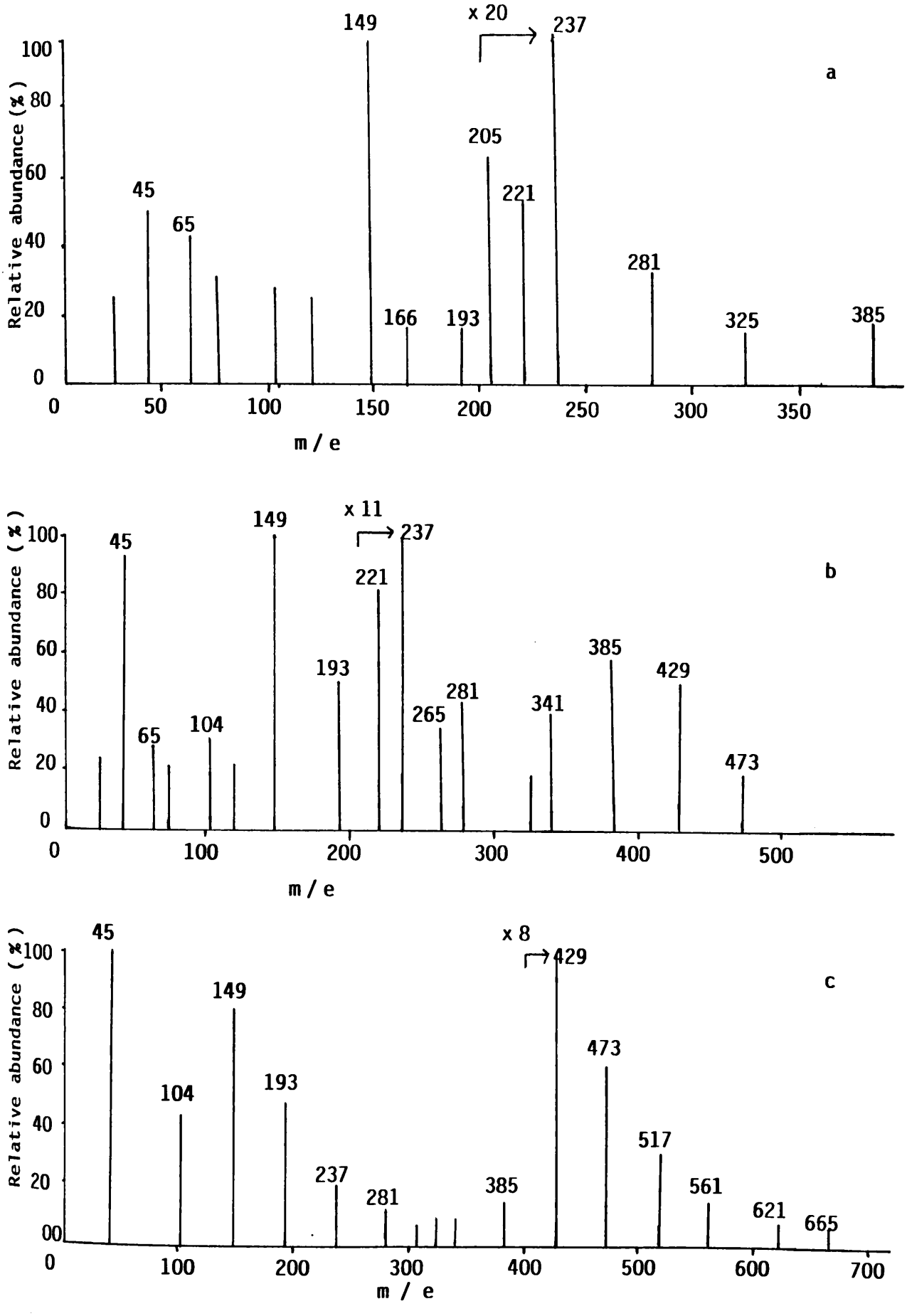

Figure 5.7: Mass spectra of the total CRF products from degradation of PPEGT1 under TVA conditions, for probe temperatures: a (170 ^{o}C), b (240 ^{o}C), c (300 ^{o}C) .

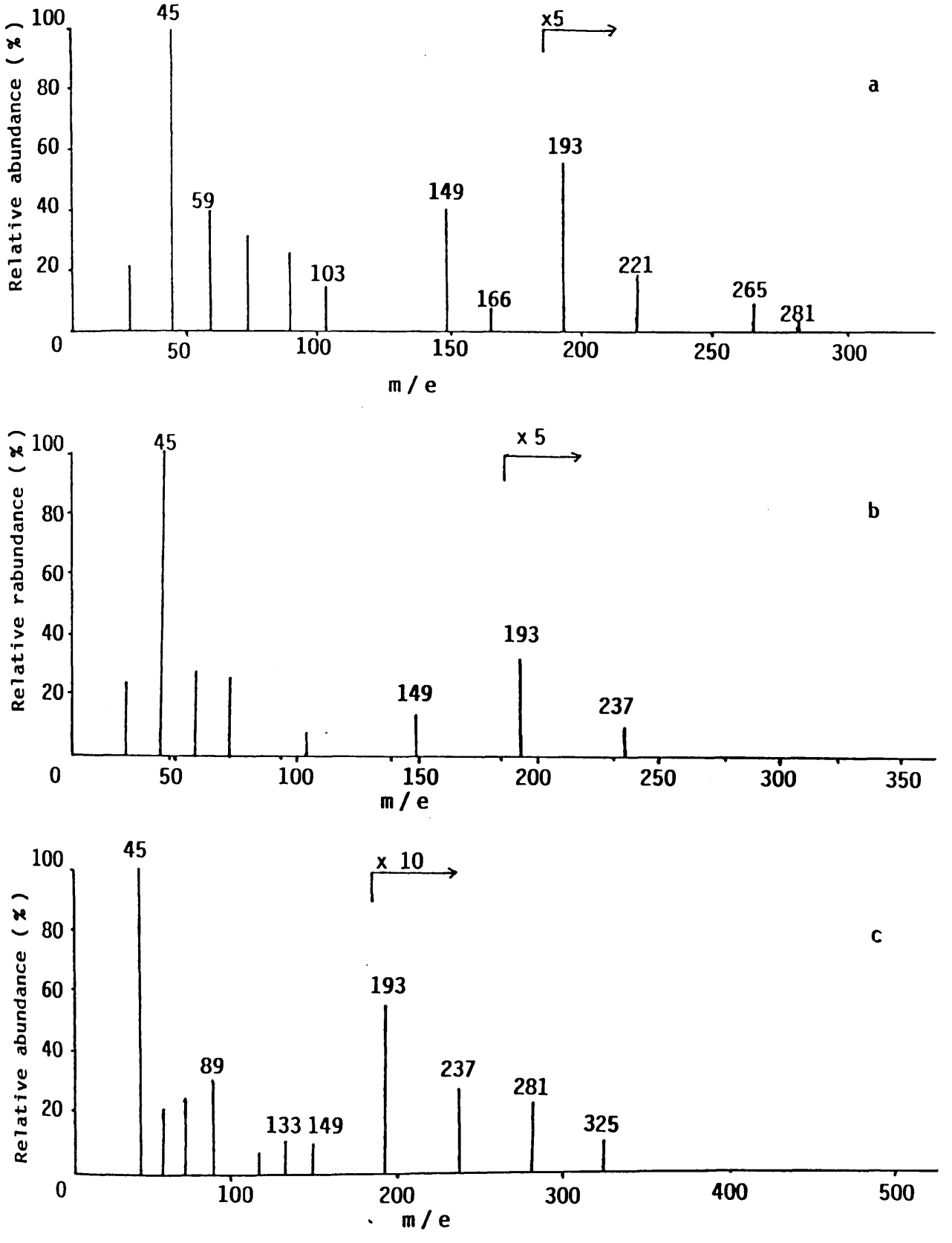

Figure 5.8: Mass spectra of the total CRF products from degradation of PPEGT2 under TVA conditions for probe temperatures: a (140 ^{o}C) , b (250 ^{o}C) and c (300 ^{o}C) .

Fragment	m/e	X	$m_1 + m_2$
A	341	OH	4
	385		5
	429		6
	473		7
	237	H	2
	281		3
	325		4
	413		6
	457		7
B	577	OH	2
	621		3
	665		4
	709		5
	517	H	1
	561		2

Table 5.4: CRF degradation products based on short chain fragments A and B.

The various degradation products identified in the CRF based on short chain fragments of the general structure A and B are summarised in Table 5.4.

5.3.3 Non-condensable gases

The gases produced from the degradation of poly(ether-esters) which are non-condensable at -196 ^{o}C, were identified using the quadrupole mass spectrometer connected directly to TVA apparatus. Carbon monoxide was found to be present as major component, together with trace of methane.

5.4 DISCUSSION

It has been reported that polyesters initially decompose by a concerted ester exchange reaction and the mechanism is generally accepted to be similar to that in poly(alkylene terephthalates).

Thermal degradation of poly(ether-ester) is a rather complex process, since the structure consists of polyether and diester segments. From the degradation products identified, it has been suggested that an ester exchange reaction mechanism occurs predominantly, accompanied by random scission along the polyether chain. The polymer chain is initially broken down at the ester linkage leading to two shorter chains I and II as shown in Scheme 5.1

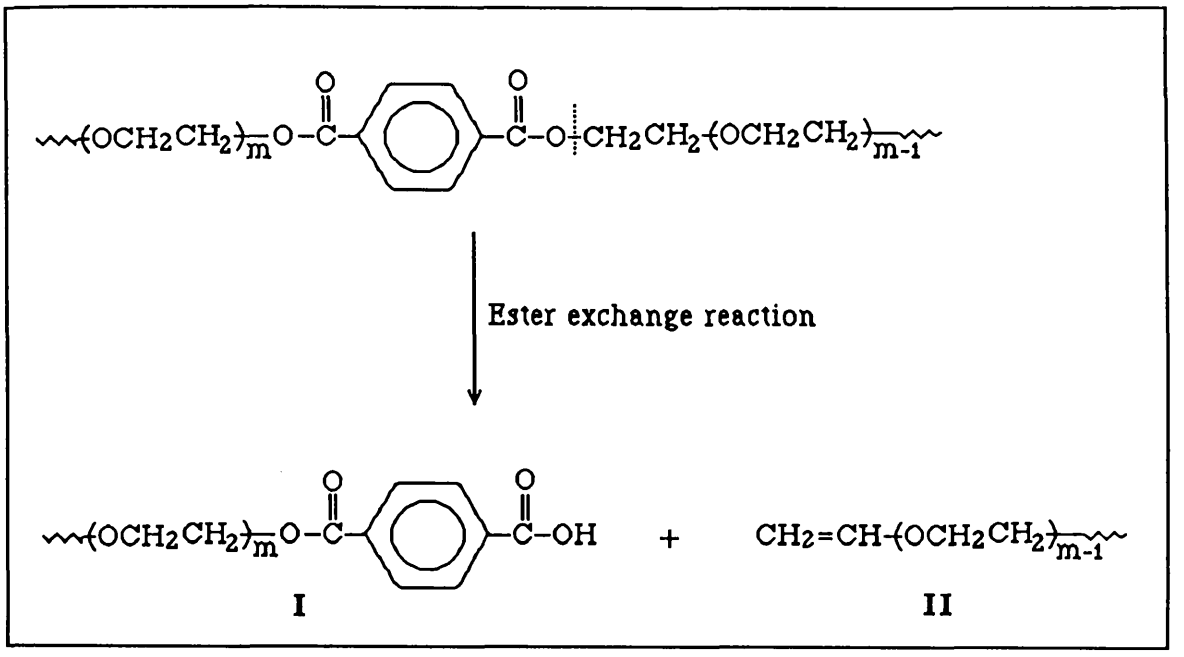

Scheme 5.1

The formation of carbon dioxide at lower temperatures is a clear indication of the interchange process as a primary stage of degradation. The vinyl ether end group II decomposes thermally into an alkene and aldehyde end, III [59]

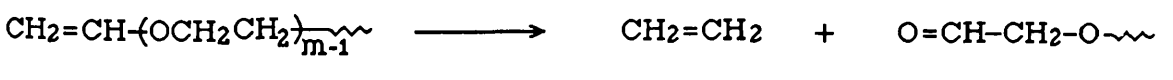

II **III**

The terminal aldehyde III may undergo further fragmentation at the backbone (C–O) and (C–C) bonds as shown in Scheme 5.2.

It is suggested that the liberation of acetaldehyde and ethoxyacetaldehyde follows (C–O) bond scissions at the respective points

(a) and (b). The fragmentation of III at the aldehyde end leads to carbon monoxide and methoxy terminal group fragment IV. This will produce methane, formaldehyde and methoxyacetaldehyde by further fragmentation at the points (c), (d) and (e), respectively. Also, it has been observed that the short chain fragment III decomposes via (C–O) bond scission at point (b) into a five membered ring ether-ketone and hydroxyl end group structure V. This is believed to give poly(ethylene glycol) oligomers with less than five units. The formation of 1,4-dioxane and 1,3-dioxalane can be imagined by chain scissions at (C–O) or (C–C) bonds of the chain fragment V, followed in each case by cyclisation, respectively.

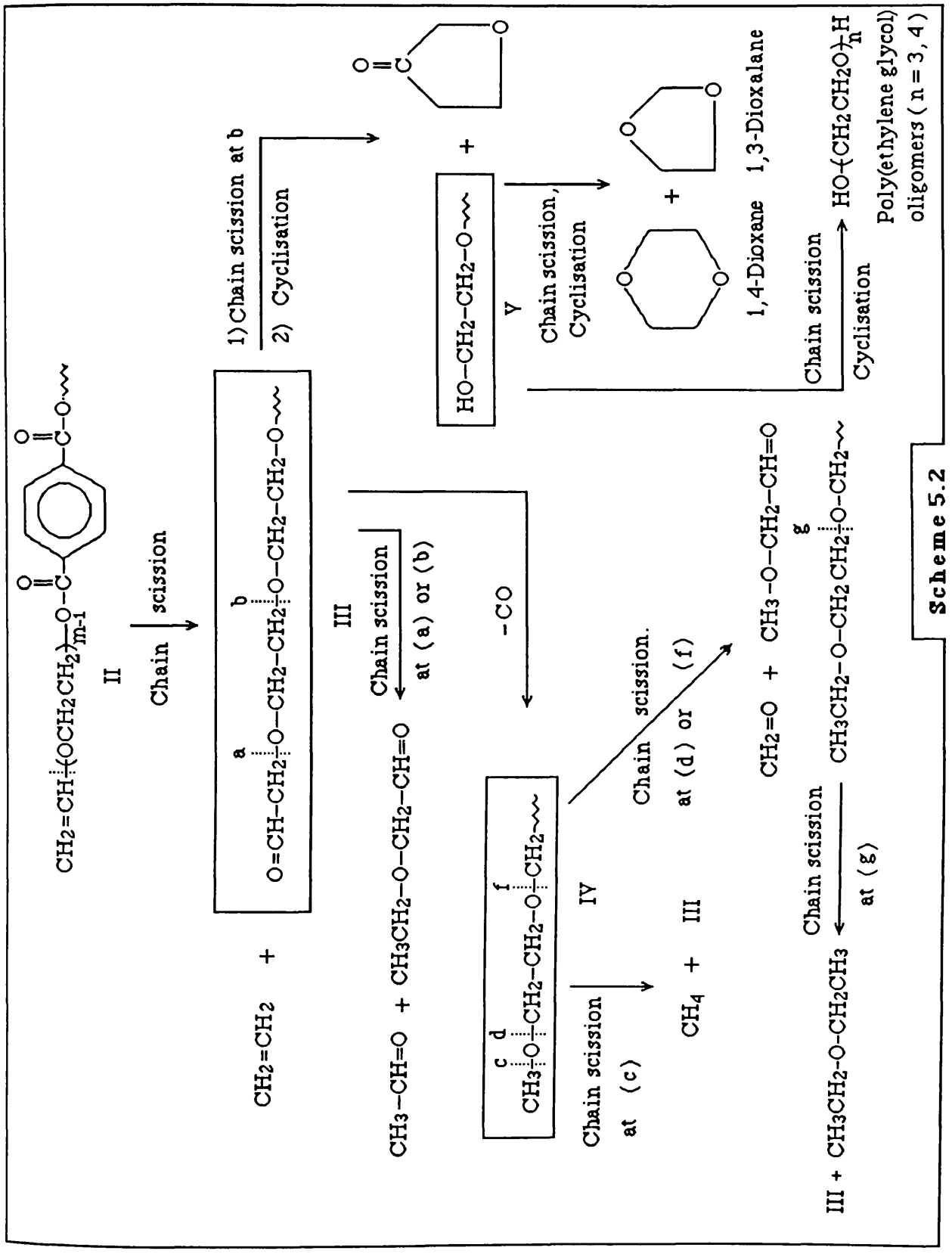
Chain scission
II
1) Chain scission at b
2) Cyclisation
III
Chain scission
at (a) or (b)
-CO
IV
Chain scission
at (c)
Chain scission.
at (d) or (f)
III
Chain scission
at (g)
V
Chain scission,
Cyclisation
1,4-Dioxane
1,3-Dioxalane
Chain scission
Cyclisation
Poly(ethylene glycol)
oligomers (n = 3, 4)

Scheme 5.2

CHAPTER SIX

THERMAL DEGRADATION OF POLYARYLATES

6.1 INTRODUCTION

Polyarylates are a special class of polyesters which exhibit excellent mechanical, good electrical and high heat resistant properties. Their thermal degradation behaviour is not well understood.

A few studies have been focused on the thermal degradation of polyarylates. Ehlers [60] analysed the degradation products in vacuum of poly(bisphenol A-isophthalate) and poly(1.4-phenylene-isophthalate) and reported that the former is appreciably less stable as a consequence of the presence of the isopropylidene group in the diol component. The major condensable volatile products of these polymers are CO, CO_2 arising from the rupture of the ester linkage, together with traces of H_2, water and benzene. Moreover methane, ethane and toluene are present in the case of poly(bisphenol A - isophthalate). In addition, the major cold ring fraction products in each degraded polymer were bisphenol A and hydroquinone, respectively. Salvatore et. al.[61] studied the thermal degradation by direct pyrolysis-mass spectrometry and reported that fully aromatic polyesters based on dihydroxybenzene and dicarboxylic acid benzene isomers (meta and para), decompose predominantly in the primary thermal degradation processes via ester exchange reactions, yielding cyclic oligomers which will lead to open chain fragments.

It has been reported [62] that fluorine substituents in fully aromatic polyarylates and aramides decrease the thermal stability but that crystallinity is higher for aramides whilst it is lower for the polyarylates. Polyarylates fluorinated in the benzene ring of the dicarboxylic acid showed higher stability than those fluorinated in the dihydric phenol component. These phenomena can be explained by the reason that fluorine substitution on the dicarboxylic acid ring causes a drop in resonance energy between the benzene ring and the ester group. The effect of halogen substitution and unit linkage on the thermal degradation and flammmability of aromatic polyamides has been studied [63] and it has been found that the thermal stability of polymers containing the para linkage is higher than that of those with meta linkages. On the other hand, the stability of halogen substituted polyamides decreased in the order Br < Cl < F < H. However, the oxygen index was higher for the halogenated polymer and increased in the order Br > Cl > F. Heitz et. al.[64] characterised the solubility, thermal and liquid crystalline properties of substituted aromatic polyesters. They showed that the incorporation of the substituent (Cl, Br, CF_3 and phenyl) into the backbone of the polymer reduces the glass transition temperature and increases the solubility of the corresponding aromatic polyesters in 4-chlorophenol, 1,1,2,2-tetrachloroethane and chloroform.

In this investigation, the preparation of polyarylates was carried out by interfacial polycondensation and by melt polymerisation (see Chapter Three). These polyarylates are based on nine different but structurally related aromatic diols reacted in each one with terephthaloyl chloride. Scheme 6.1 illustrates the specific diol monomer structures and the abbreviation codes for the corresponding polymer.

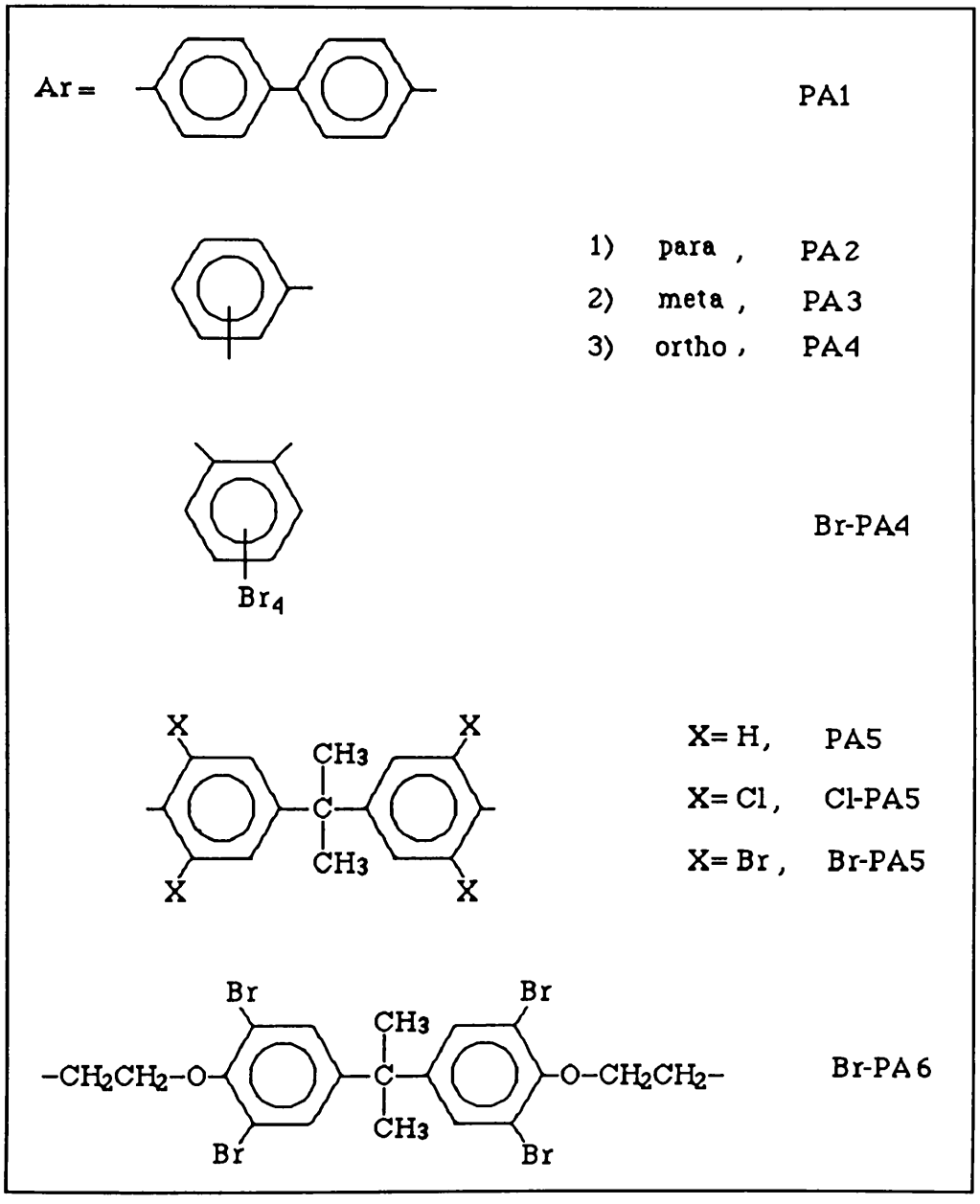
Ar =
PA1
1) para , PA2
2) meta , PA3
3) ortho , PA4
Br4
Br-PA4
X
CH3
C
X= H, PA5
X= Cl, Cl-PA5
X= Br , Br-PA5
Br
-CH2CH2-O-
O-CH2CH2-
Br-PA6

Scheme 6.1

Most of polyarylates obtained decompose in the temperature range 450-560 °C. Consequently these materials combine good thermal stability with resistance to fire. It is important to understand how the stability is affected by changing the diol structure in the backbone. Polyarylates prepared from dihydric phenols and terephthaloyl chloride have been divided for discussion into polyarylates and halogenated polyarylates (fire retardant), which consist of fully aromatic and aliphatic / aromatic polyarylates.

Each of those polymers was degraded thermally using programmed heating under TVA conditions. The degradation products were mostly identified spectroscopically, by means of IR, MS and GC-MS techniques. Thermal stability and the mechanism of decomposition induced by heat under vacuum have been studied.

6.2 POLYARYLATES

6.2.1 THERMAL ANALYSIS

6.2.1.1 Thermogravimetry (TG)

The TG and DTG curves for polyarylates recorded under dynamic nitrogen atmosphere, with a heating rate of 10 °C/min, are shown in Figure5.1. The TG curves have similar profiles in the sense that weight loss occurs in a single step, beginning above 320 °C and reaching maximum rate of weight loss (T_{max}) in the range 465-575 °C, which varied with the diol structure in the back-bone of the polymer. The material remaining as residue amounted to between 16 and 87 % of weight loss at 600 °C .

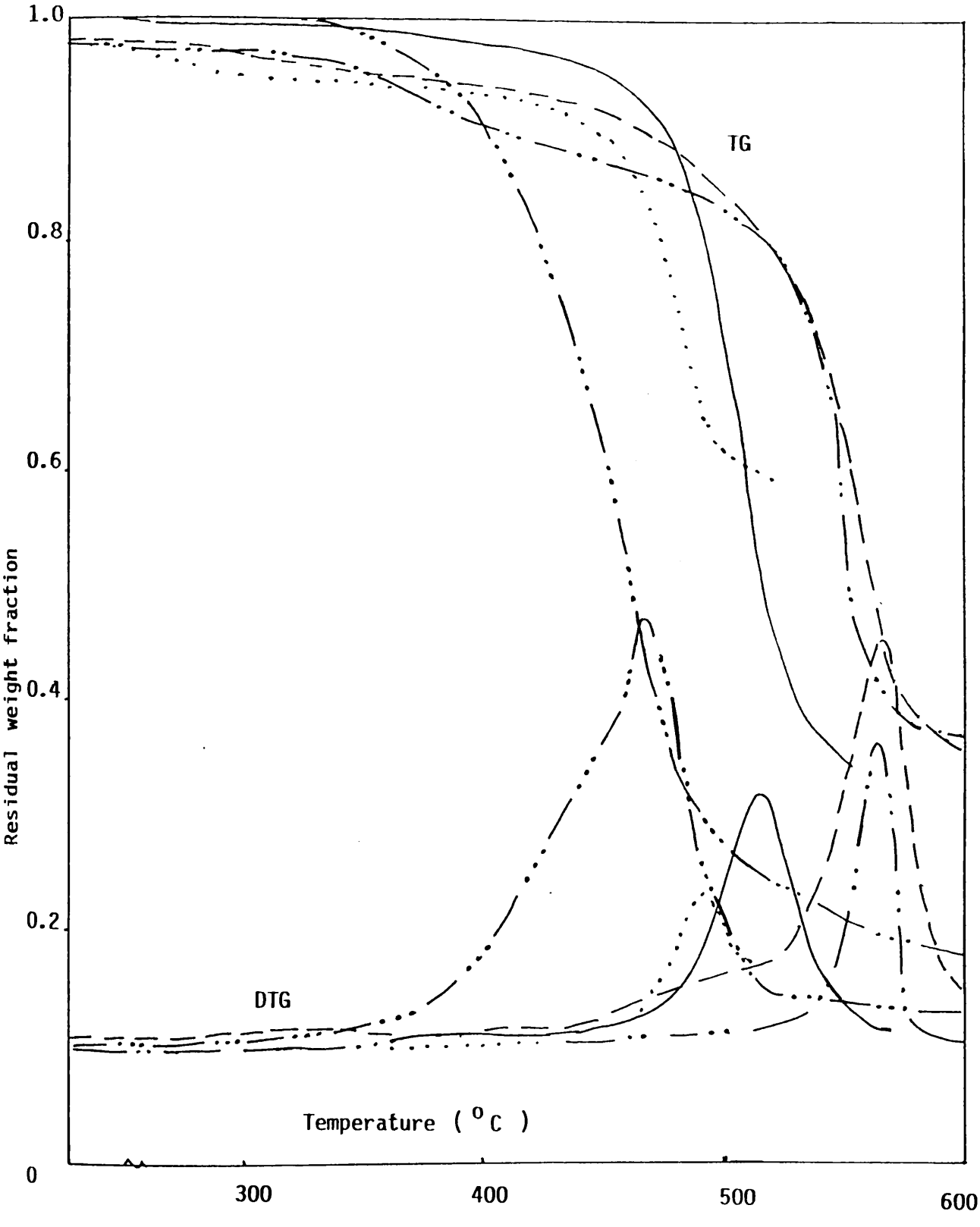

Figure 6.1 ; Thermogravimetric traces of PA1 ( ), PA2 (—), PA3 (...), PA4 (-···-), and PA5 (——) . Heating rate

6.2.1.2 Thermal volatilisation analysis (TVA)

The TVA traces for the five polyarylates (PA1– PA5) are shown in Figures 6.2-6.6. The evolution of volatile products occurs in a single stage decomposition in which the onset is around 360 °C, reaching maximum rate of volatilisation at 479-532 °C. The separation of traces corresponding to the initial temperatures 0, -45, -75, -100 and -196 °C cold traps suggests the presence of various products, with a large range of volatility including non-condensable gases.

Quantitative measurements of the main degradation product fractions are listed in Table 6.1. The effect of polymer structure on the thermal stability of polyarylates is shown in Figure 6.1 and Table 6.1, by comparison of T_{max} values of the DTG traces for PA1– PA5, where the thermal stability of these polyarylates increased in the sequence

PA4 < PA3 < PA5 < PA1 < PA2

6.2.2 CHARACTERISATION OF DEGRADATION PRODUCTS

Most of the degradation products in each of the four main fractions, obtained by degradation in the TVA apparatus to 600 °C at 10 °C/min , were identified by means of IR, MS and GC-MS techniques. The condensable volatile products were first separated by subambient TVA. The non-condensable gases, obtained from the degradation of polyarylates in a closed system, were analysed spectroscopically. Carbon monoxide was identified in all cases. In addition, methane was detected in the case of PA5, as a result of the presence of methyl groups in the diol component. The involatile material at degradation temperatures was found as black char. The results are summarised in Table 6.2 and 6.8.

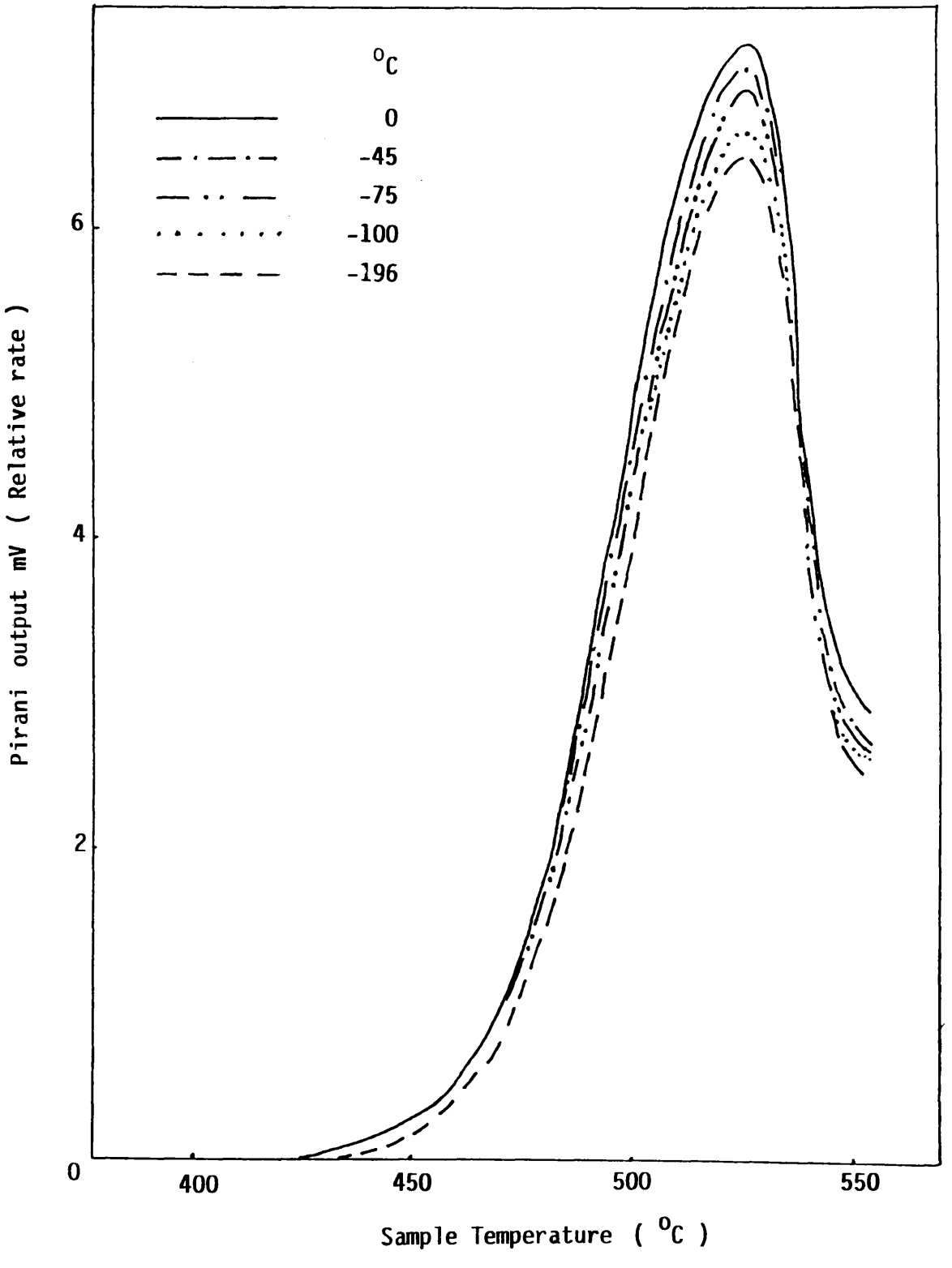

Figure 6.2 : TVA traces for PA1 . Heating rate 10 °C/min .

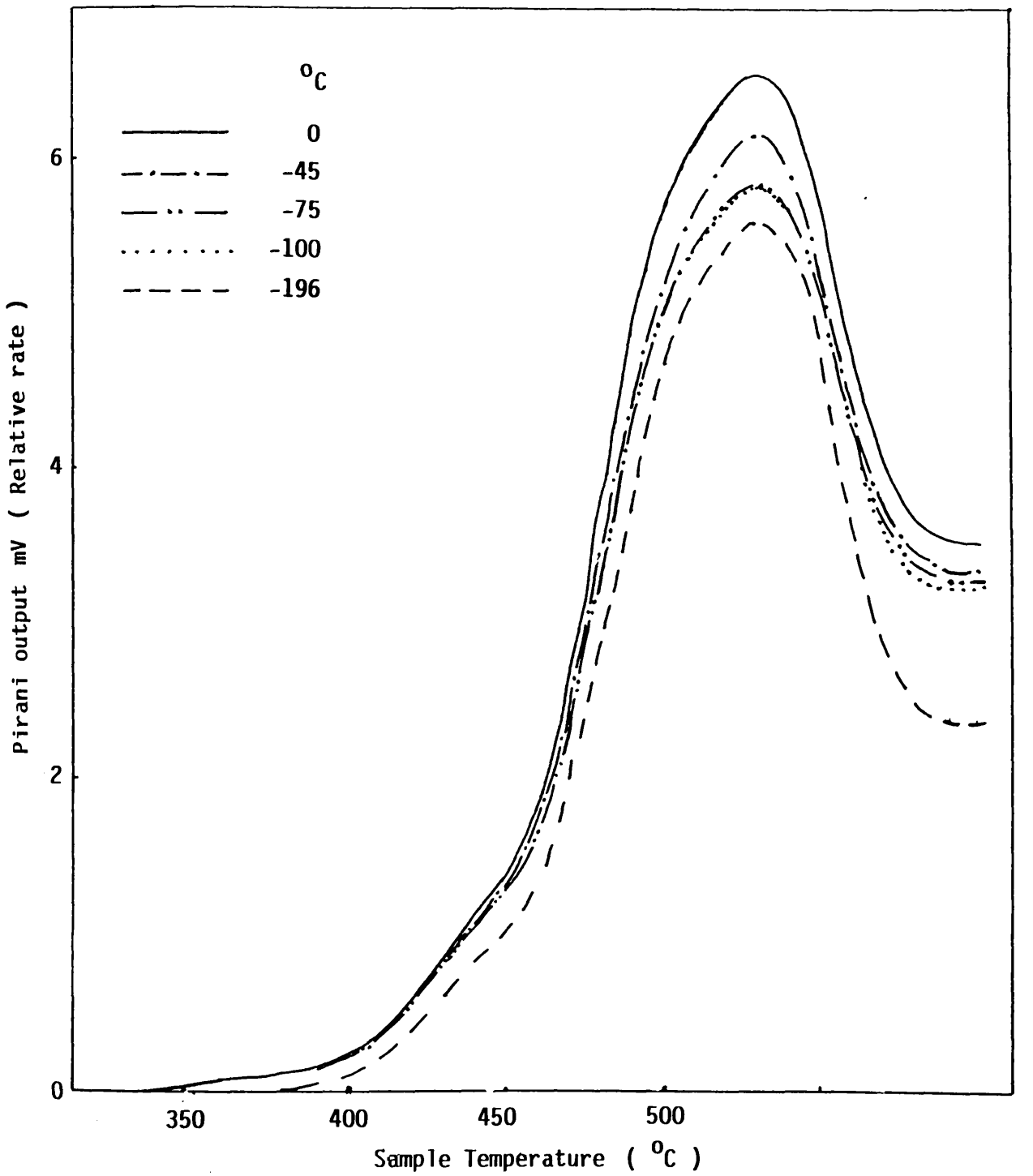

Figure 6.3 : TVA traces for PA2 . Heating rate , 10 °C/min.

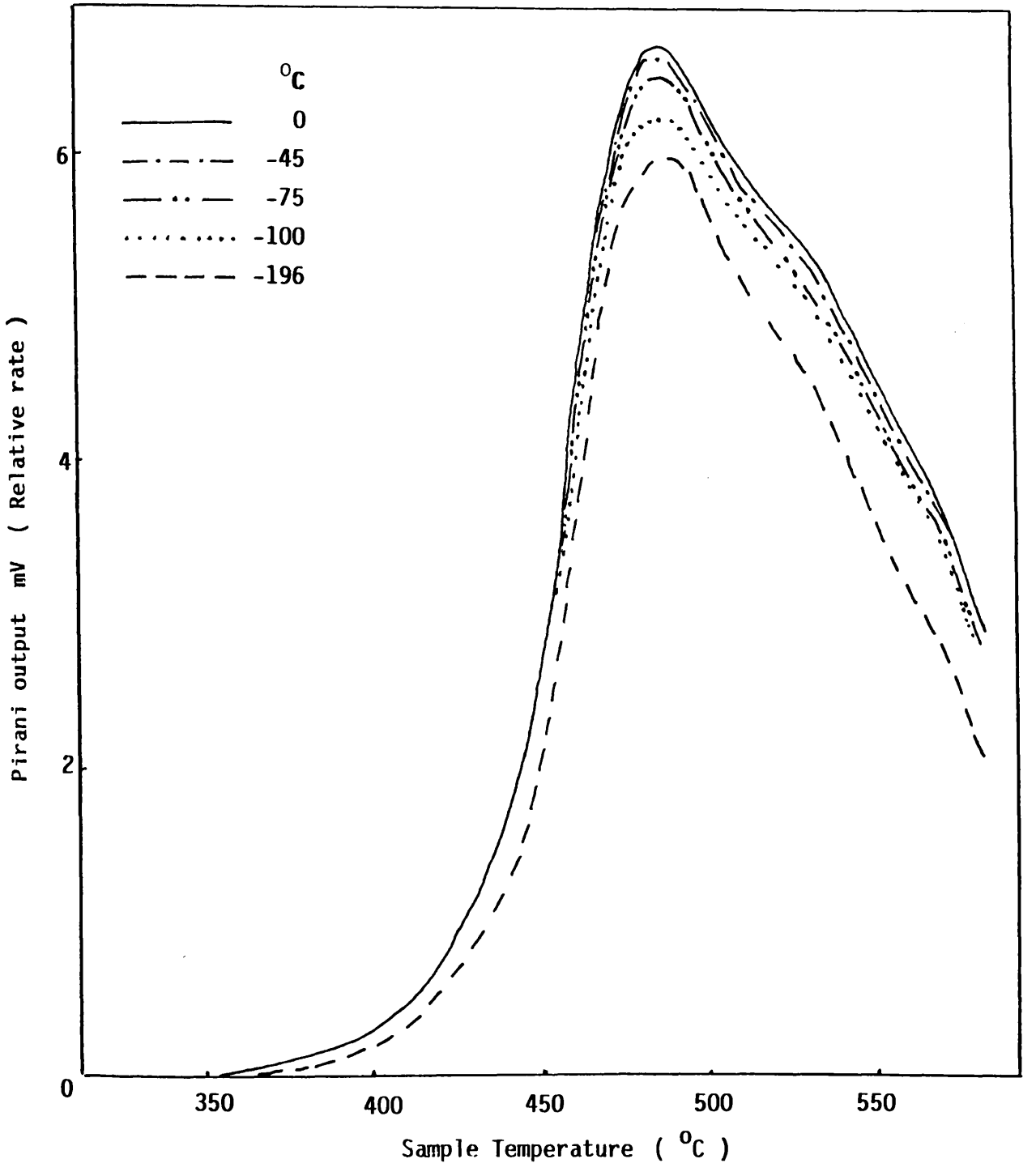

Figure 6.4: : TVA traces for PA3 . Heating rate , 10 °C/min .

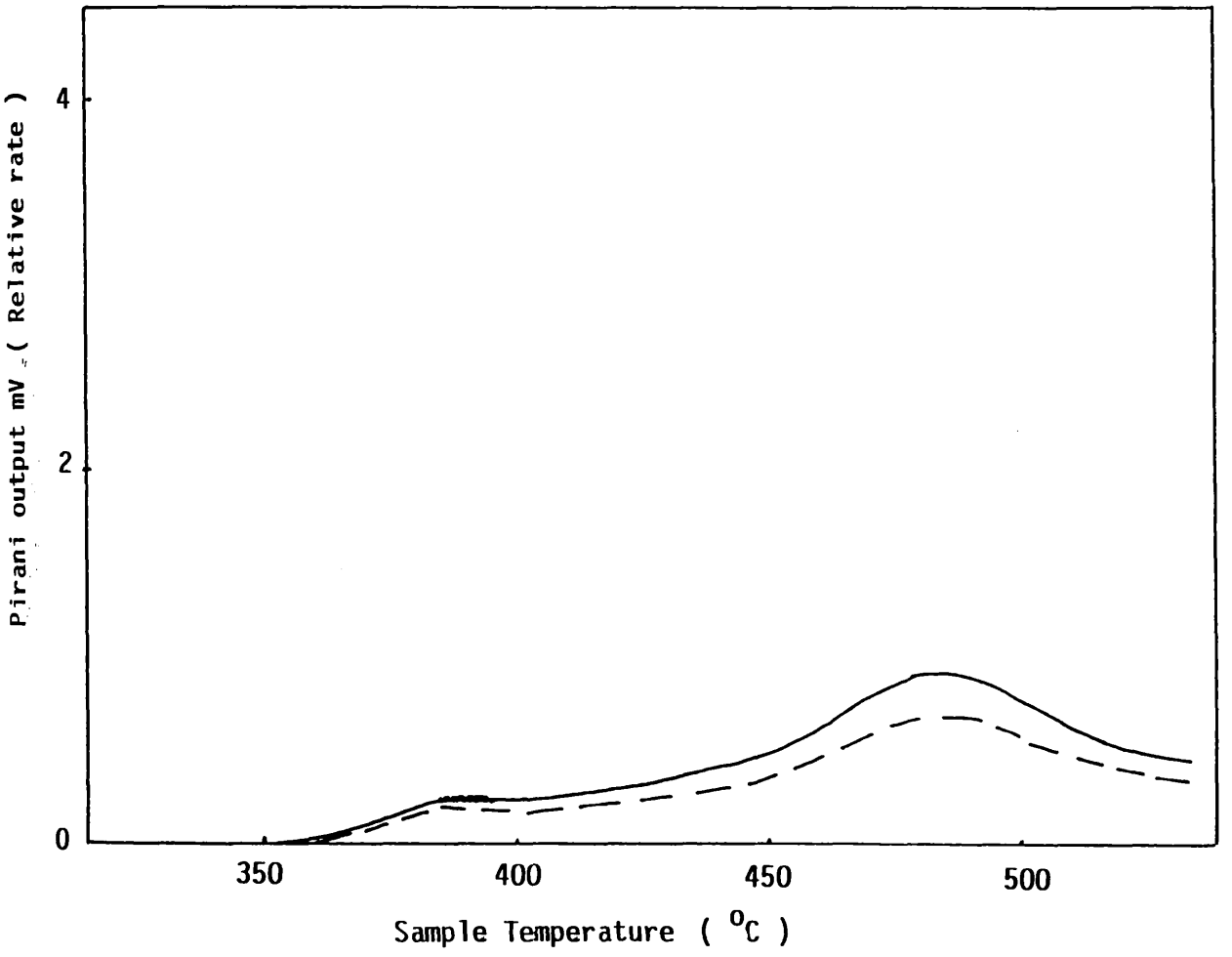

Figure 6.5 : TVA traces for PA4. Heating rate 10 °C/min .

0,-45,-75 and -100 °C (——) ; -196 °C (- - -) .

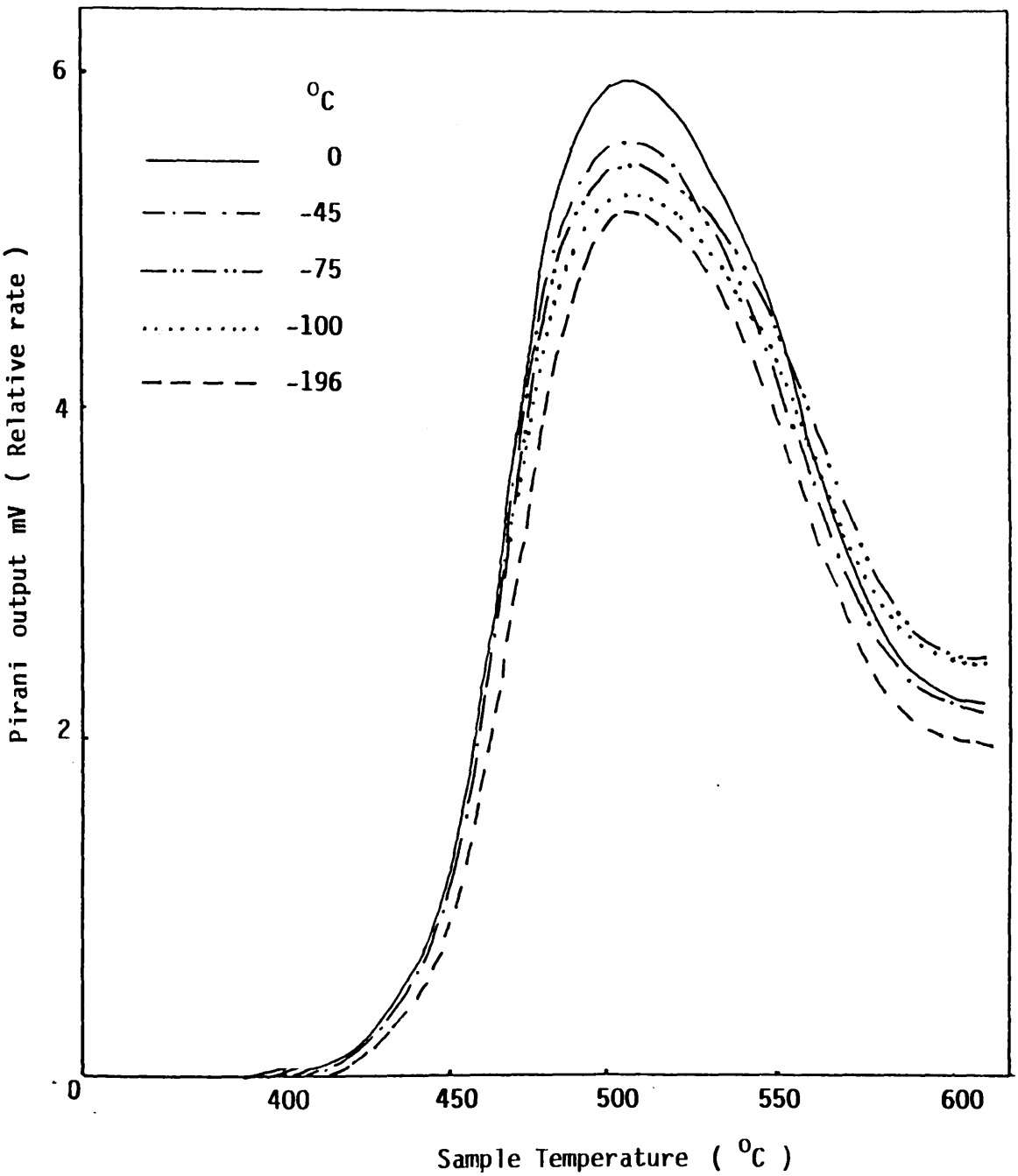

Figure 6.6 : TVA traces for PA5 . Heating rate 10 °C/min .

	Type of Polyarylates	PA1	PA2	PA3	PA4	PA5
TVA	T_{onset} / °C	426	391	355	355	485
	T_{max} / °C	526	532	492	479	512
	Residual Fraction / wt %	38.46	33.82	44.77	2.1	43
	Cold Ring Fraction / wt %	26.37	38.78	16.41	85.4	33
	Volatile Fraction at room temperature / wt %	35.17	27.4	38.82	12.5	24
TG & DTG	T (initial wt loss) / °C	300	100	200	325	200
	T_{max} / °C	565	575	492	465	515
	* Residual Fraction / wt %	41[a]	35[a]	62[b]	27.5[b]	35[c]

* Residual Fraction at : (a) 600 , (b) 500 and (c) 550 °C

Table 6.1: TVA , TG and DTG data for polyarylates.

	Cold Ring Fraction	Condensable Volatile Products	Non-condensable Gases
PA1	4.4'-Biphenol, terephthalic acid, terephthaldehydic acid, benzoic acid, 4.4'-hydroxy biphenyl benzoate and di 4.4'-hydroxybiphenyl terephthalate.	Carbon dioxide, benzene, phenol, 4-phenyl phenol, biphenyl and benzaldehyde.	Carbon monoxide
PA2	Hydroquinone, terephthalic acid, mono 4-hydroxyphenyl terephthalate and di 4-hydroxyphenyl terephthalate.	Carbon dioxide, benzene, phenol, benzoquinone, benzaldehyde and biphenyl.	Carbon monoxide
PA3	Resorcinol,terephthalic acid, benzoic acid, terephthaldehydic acid, mono 3-hydroxyphenyl terephthalate and di 3-hydroxyphenyl terephthalate.	Carbon dioxide, benzene, phenol, benzaldehyde, 3-hydroxyphenyl benzoate and biphenyl.	Carbon monoxide
PA4	Cyclic dimer	Carbon dioxide, benzene, phenol, benzaldehyde and catechol.	Carbon monoxide
Method of analysis	IR and MS	IR, MS and GC-MS	IR

Table 6.2: Products of (PA1-PA4) degradation to 600 °C in the TVA system under vacuum, using programmed heating at 10 °C / min.

6.2.2.1 Poly(4.4'-biphenylene terephthalate) (PA1)

i) Condensable volatile products

The subambient TVA curve in figure 6.7, shows three distinct peaks. The products were collected separately for further analysis. Carbon dioxide and benzene were found to be the only substances responsible for peaks 1 and 2, respectively. The products in peak 3, collected as a liquid fraction, were separated and identified by means of GC-MS using a DB5 column 1m film 15m I.D 0.25 mm containing 5 % phenyl silicone, in the range 60-325 ^{o}C, under a programmed heating rate of 5 ^{o}C/min. The gas chromatogram of the total liquid fraction is shown in Figure 6.8, which indicates the presence of benzene (due to overlap with the previous fraction) and phenol as major products, together with traces of biphenyl, 4-phenyl phenol and benzaldehyde. Table 6.3 lists the assignments for the peaks and the corresponding chemical structures.

ii) Cold ring fraction

Two different bands were observed on the inner wall upper part of the TVA tube as CRF, which were removed separately for spectroscopic analysis. The ir spectrum of the upper CRF shows strong bands at 3400, 820 and 1610 cm-1, which are characteristic frequencies of p.p'-biphenol. However, the ir spectrum of the lower part of the CRF is similar to that of the original polymer.

The mass spectra of the total CRF of degraded PA1 were obtained at probe temperatures of 200, 260, 280 and 320 ^{o}C to identify the main components as shown in Figure 6.9. Thus at 200 ^{o}C, ions at m/e = 290,

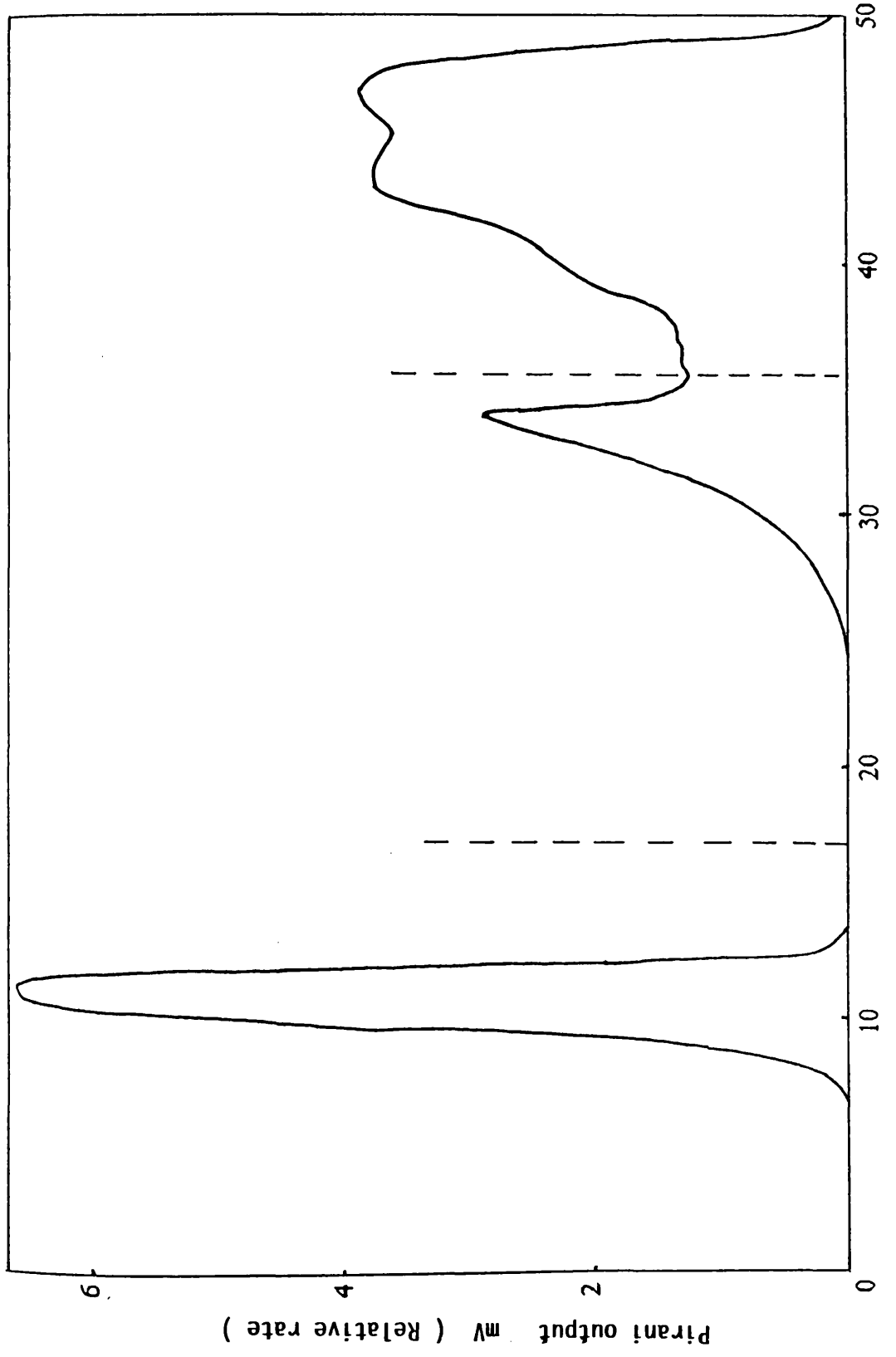

Figure 6.7: Subambient TVA trace for warm up from -196 ^{o}C to ambient temperature of condensable volatile products from degradation of PA1.

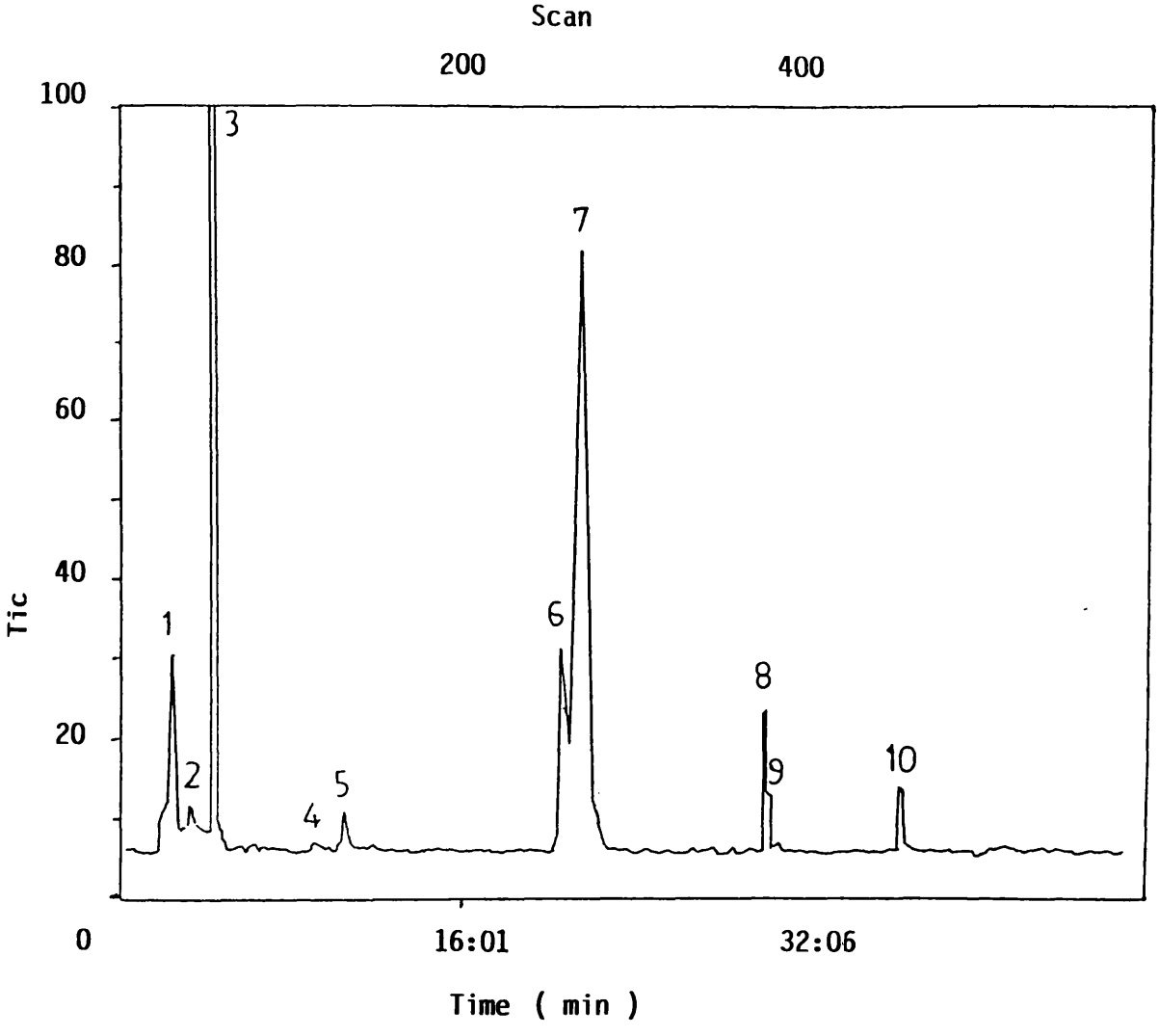

Figure 6.8 : Gas chromatogram for the liquid fraction in SATVA separation of products from the degradation of PA1.

Peak N°	Assignment	m / e
1	Acetone	43 , 58
2	Benzene	78, 51, 52
3	Unidentified	82, 55, 9
4	—	207
5	Benzaldehyde	105, 106, 77
6	Phenol	94, 65, 66
7	Unidentified	84, 55, 77, 111
8	"	55, 69, 70, 168
9	Biphenyl	154, 153

Table 6.3: The assignment of the products of the liquid fraction in SATVA separation of PA1 degradation products from the gas chromatogram in fig. 6.8.

105, 77 and 186 are due to the molecular ion and fragment ions of 4-hydroxy biphenyl benzoate as shown below

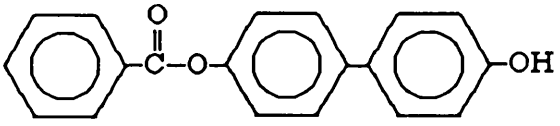

4-Hydroxybiphenyl benzoate

p.p'-Biphenol was detected in the mass spectrum obtained at probe temperature of 260 °C.

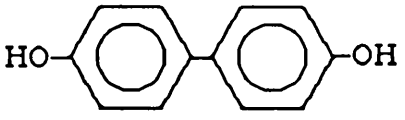

p.p'-Biphenol

The mass spectra for probe temperatures of 280 and 320 °C exhibit fragment ion peaks corresponding to the molecular ion m/e = 502 of the di 4-hydroxybiphenyl terephthalate illustrated below.

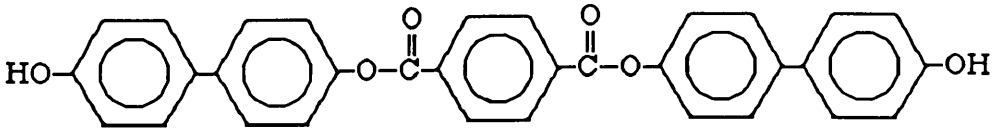

Di-4-hydroxybiphenyl terephthalate

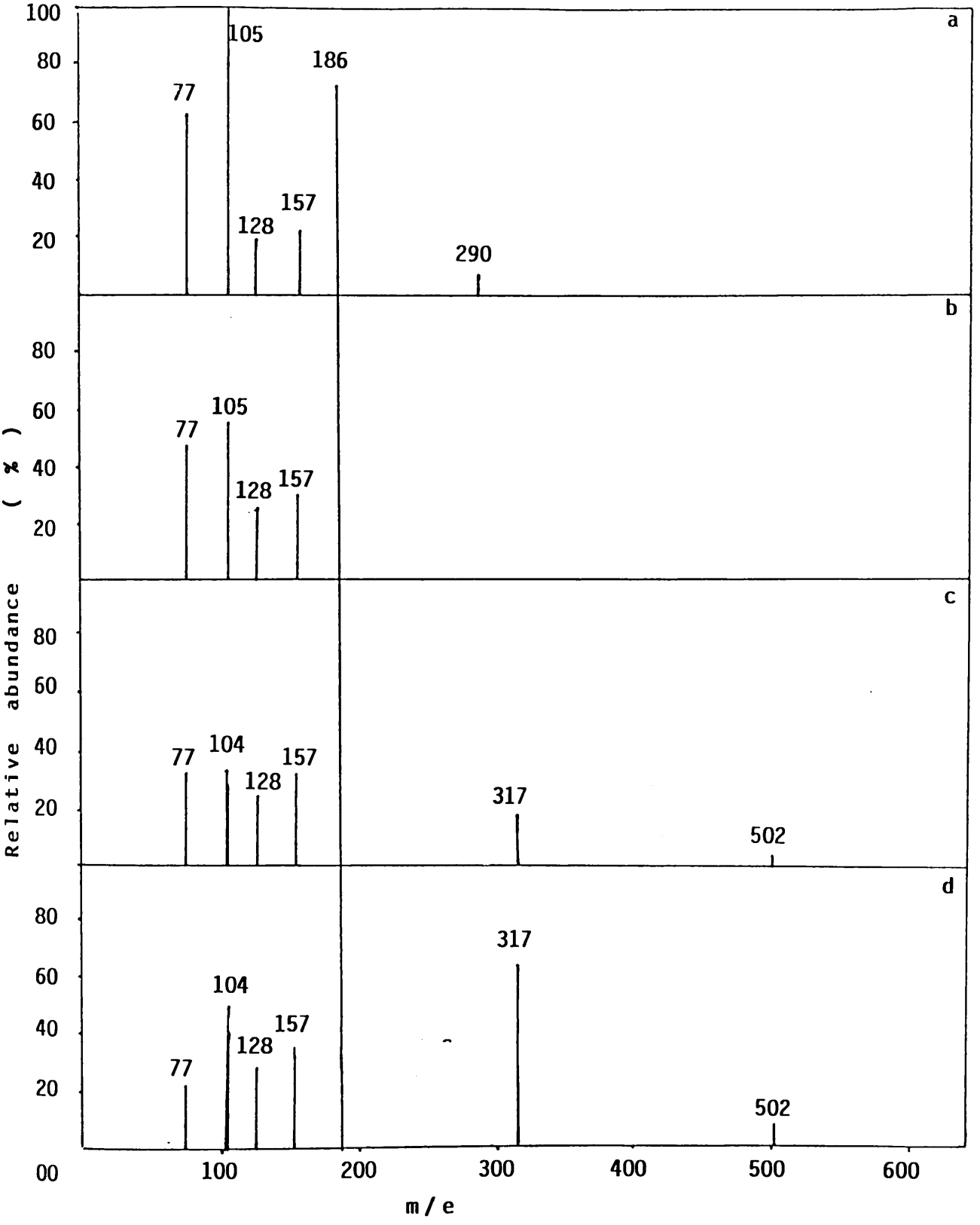

Figure 6.9: Mass spectra of the total CRF products from degradation of PA1 under TVA conditions to 600 ^{o}C for probe temperatures **a** (200 ^{o}C) , **b** (260 ^{o}C), **c** (280 ^{o}C) and **d** (320 ^{o}C).

6.2.2.2 Poly(1.4-phenylene terephthalate) (PA2)

i) Condensable volatile products

The SATVA trace in Figure 6.10 exhibits four distinct fractions. The first two were shown by means of infrared spectroscopy to be due to carbon dioxide and benzene, respectively. The last fractions were subjected to GC-MS examination. The gas chromatogram in Figure 6.11 and the assignment of each peak in Table 6.4 indicate that phenol and benzoquinone are the main components, with traces of benzaldehyde and benzene (from the last fraction).

ii) Cold ring fraction (CRF)

The CRF consisted of three bands, which were characterised separately. The upper CRF was found by ir and mass spectroscopy to consist of hydroquinone together with traces of 4-hydroxyphenyl benzoate (m/e = 214). The ir spectrum of the middle CRF shows characteristic absorptions of hydroquinone, and other bands at 1720-1690, 3450, 2640 and 2520 cm^{-1}, corresponding to the stretching vibrations of carboxylic acid and hydroxyl end groups. In addition, the mass spectrum exhibits peaks attributed to the molecular ions of terephthalic acid (m/e =166), terephthaldehydic acid (m/e = 150), benzoic acid (m/e = 122), mono and di-4-hydroxy phenyl terephthalates (m/e = 258, 350), respectively.

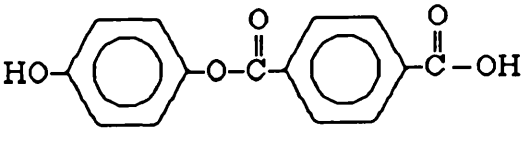

Mono-4-hydroxyphenyl terephthalate

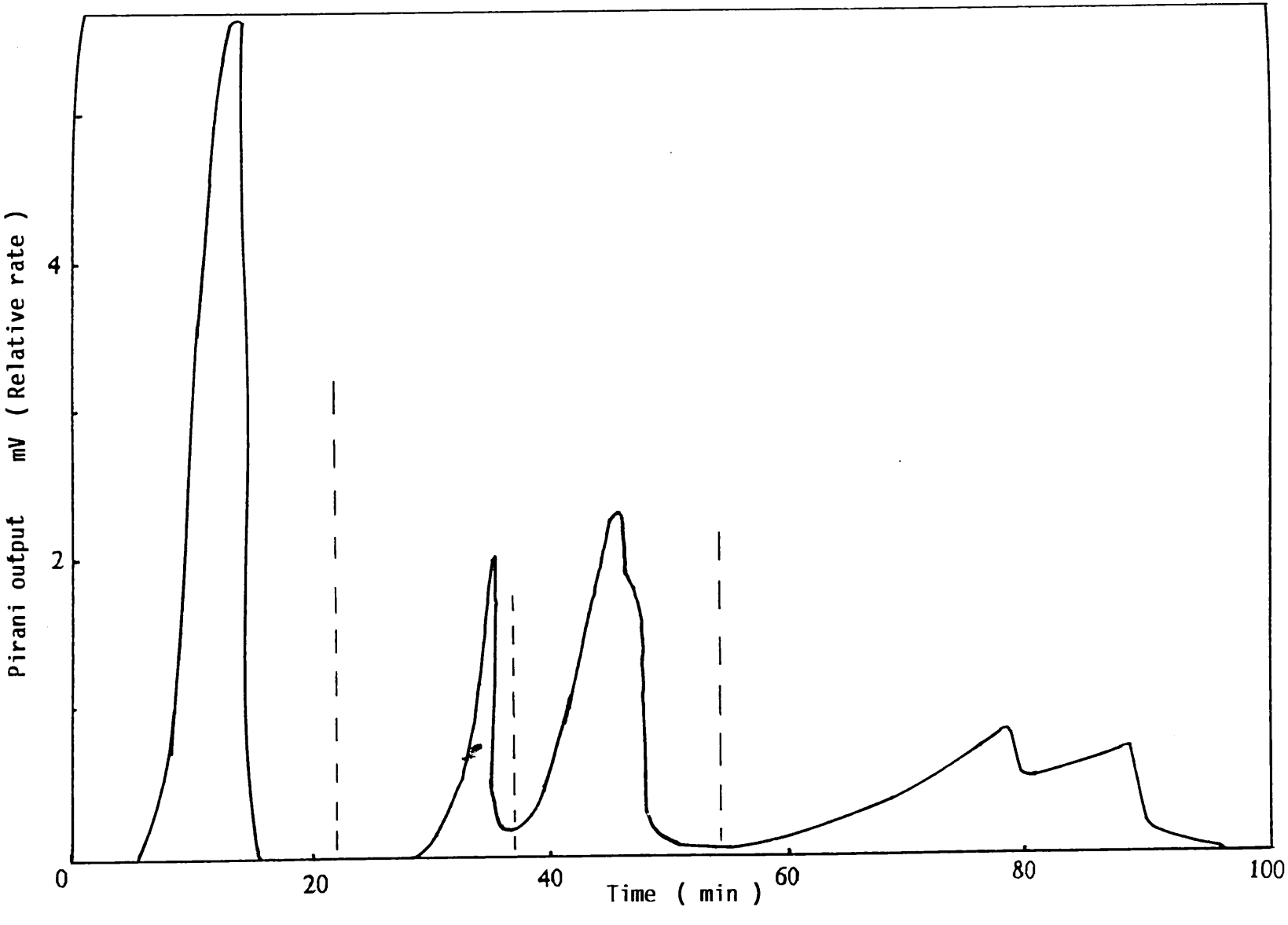

Figure 6.10: Subambient TVA trace for warm up from -196 ^{o}C to ambient temperature of condensable volatile products from degradation of PA2.

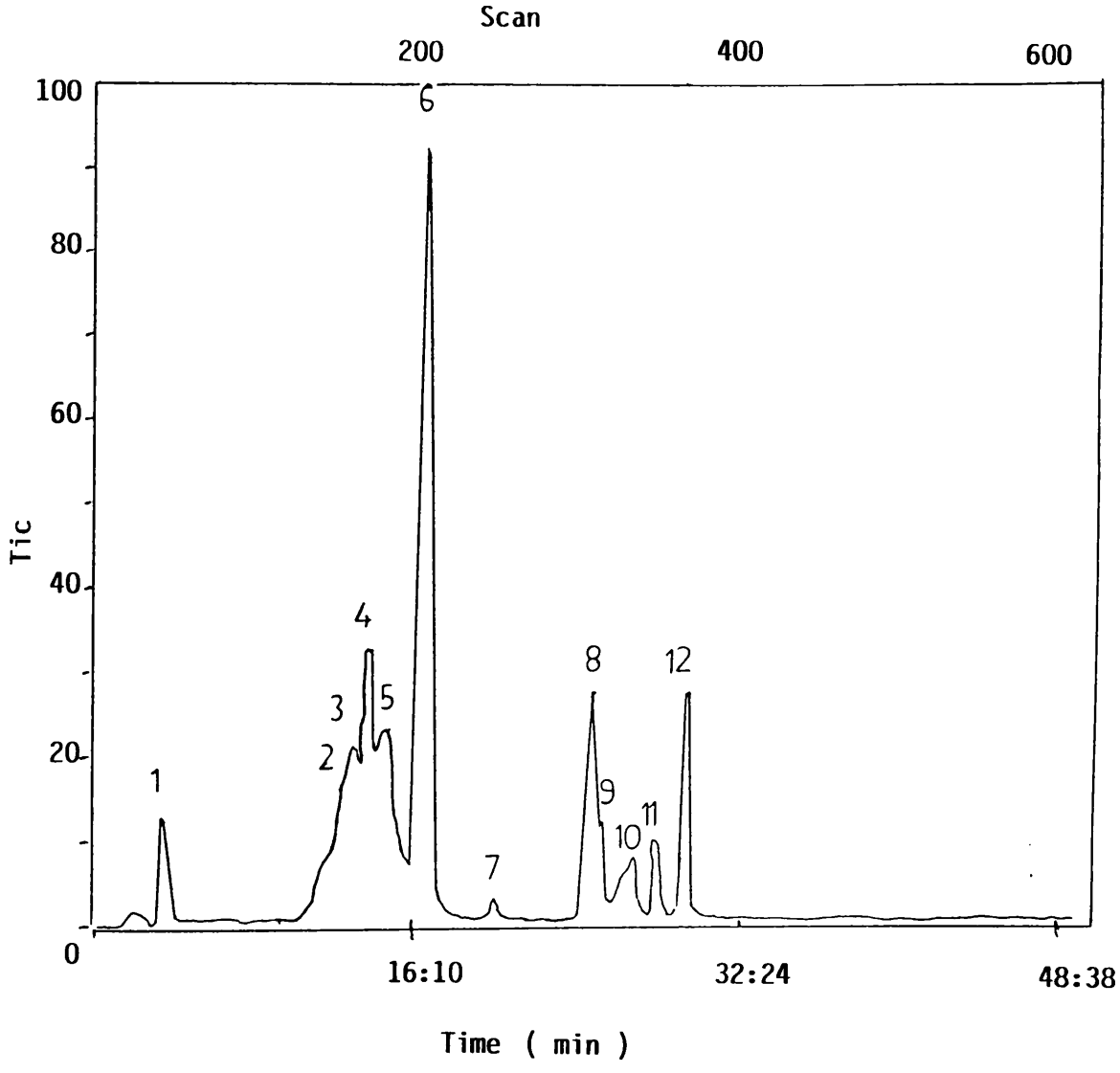

Figure 6.11 : Gas chromatogram for the liquid fraction in SATVA separation of products from the degradation of PA2.

Peak N^{o}	Assignment	m / e
1	Benzene	78 51
2,3,4,10	Benzoquinone	108 54 82
5	Benzaldehyde	105 77 106
6	Phenol	94 65
7	Unidentified	142 114
8	"	109 124
9	"	143 158
11	"	142 54 82 144
12	Biphenyl	154 153

Table 6.4: The assignment of the peaks in the gas chromatogram, shown in Fig.6.11, for the liquid fraction from SATVA separation of products of degradation to 600 ^{o}C under TVA conditions of PA2.

CRF	Component	m / e			Relative Intensity %		
Upper	4-Hydroxyphenyl benzoate	214	105		3	22	
	Hydroquinone	110	81	54	100	27	18
Middle	Benzoic acid	122	105	121	3	15	19
	Terephthaldehydic acid	150	149		10	100	
	Terephthalic acid	166	149		20	100	
	Mono 4-hydroxy phenyl terephthalate	258	241	213	5	10	1
Lower	Short chain fragment II	455	241	105	1	55	100
	" " " I	390	346	241	4	13	55
	Di 4-hydroxy phenyl terephthalate	351	241		4	55	

Table 6.5: Products identified in the CRF from the degradation of PA2 under TVA conditions to 600 ^{o}C.

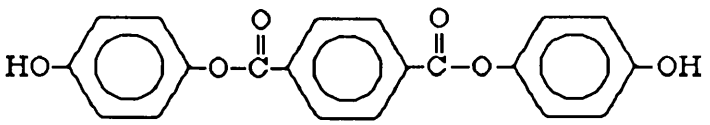

Di-4-hydroxyphenyl terephthalate

The lower CRF was identified as a mixture of dihydroxy phenyl terephthalate due to overlap with the middle fraction and short chain fragments I and II.

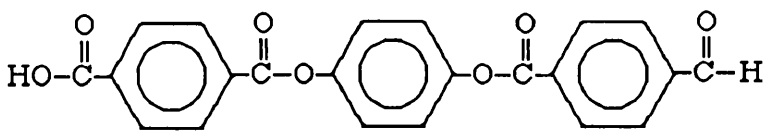

I

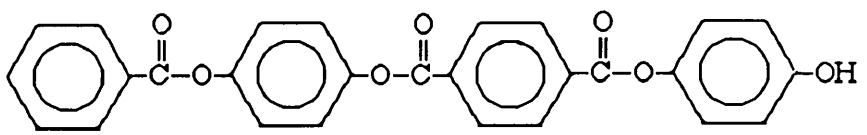

II

6.2.2.3 Poly(1.3-phenylene terephthalate) (PA3)

i) Condensable volatile products

The condensable products from the degradation of PA3 were subjected to SATVA and the curve obtained (Figure 6.12) shows three main fractions. Fractions 1 and 2 were examined as gases, their ir spectra indicate the presence of carbon dioxide and benzene, respectively. The products

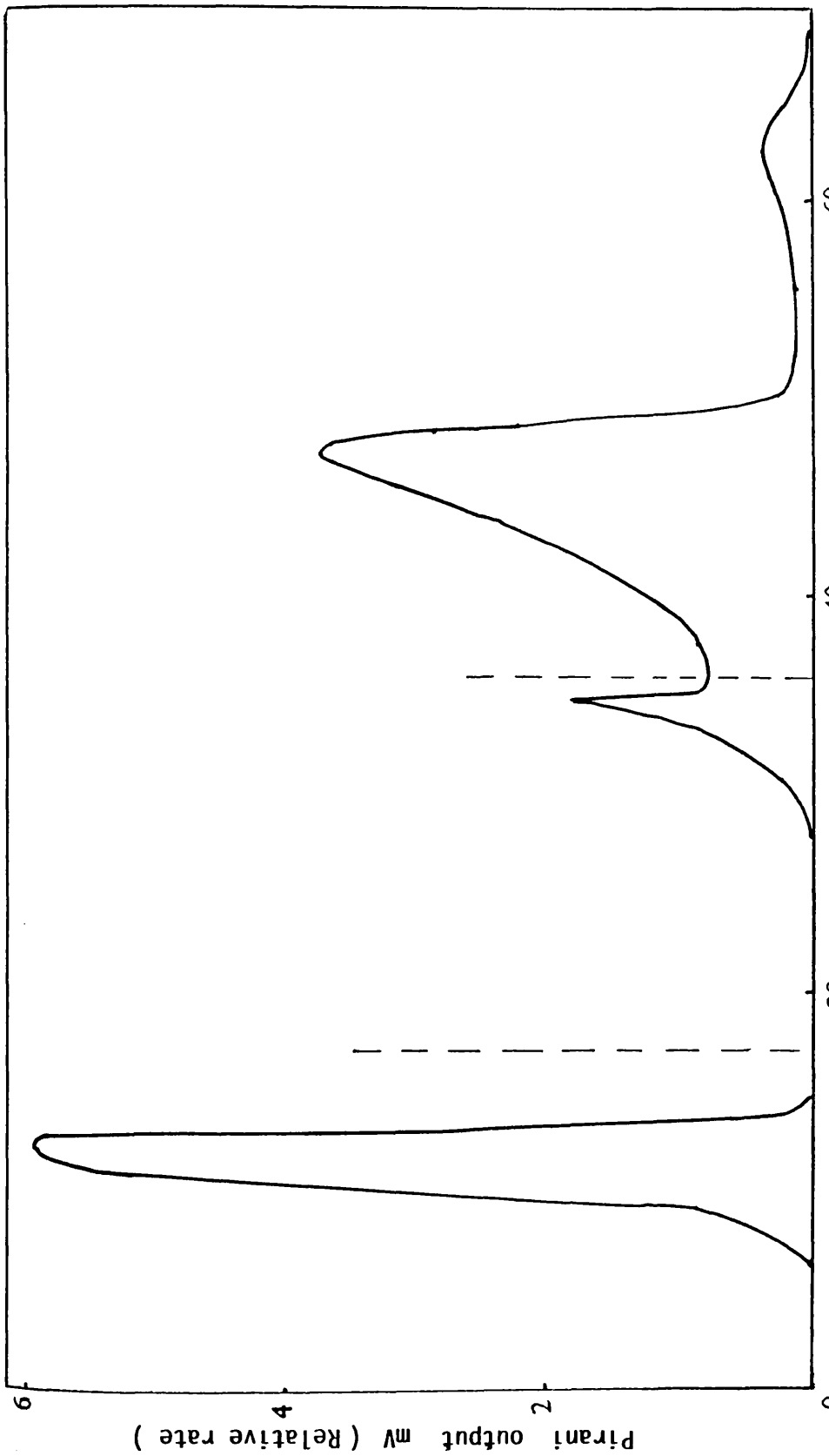

Figure 6.12: Subambient TVA trace **for warm** up from 196 ^{o}C to ambient temperature of condensable volatile products from degradation of PA3.

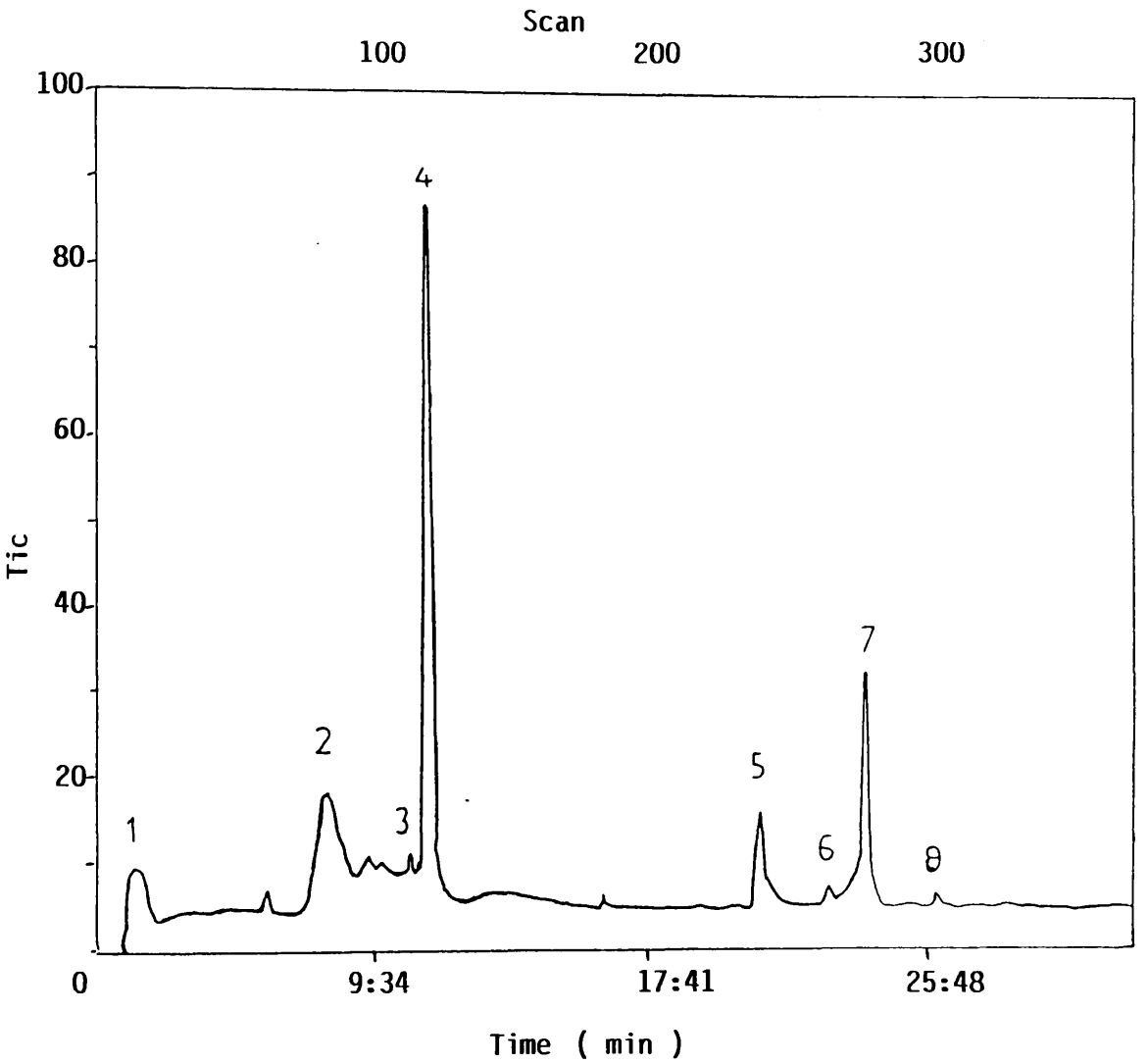

Figure 6.13 : Gas chromatogram for the liquid fraction in SATVA separation of products from the degradation of PA3.

responsible for the third fraction were subjected to GC-MS investigation. The gas chromatogram in Figure 6.13 and the assignments in Table 6.6 indicate that phenol and biphenyl are the major products, together with traces of benzaldehyde and 3-hydroxyphenyl benzoate.

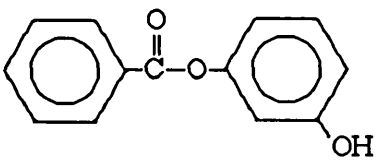

3-Hydroxyphenyl benzoate

ii) Cold ring fraction (CRF)

Some of the volatile products condensed on the cooled area upper part of TVA tube as CRF. Two bands were observed and collected separately for spectroscopic analysis. The former was found to be due to the presence of the diol resorcinol (1.3-dihydroxybenzene). The latter was further separated into fractions. The ir spectrum of the first of these showed new bands at 3200-2500 and 1685 cm^{-1}, which are characteristic the -COOH group of terephthalic acid. However, the absorption bands of the original polymer were also observed as weak bands. Furthermore, a strong sharp band at 3430 cm^{-1} is due to hydroxyl end group of the aromatic diol.

The mass spectra indicate abundant peaks corresponding to the molecular ions of five main components: benzoic acid (m/e= 122), terephthaldehydic acid (m/e = 150), terephthalic acid (m/e = 166), mono-3-hydroxyphenyl terephthalate (m/e = 258) and di-3-hydroxyphenyl terephthalate (m/e = 350).

The ir spectrum of the second fraction consisted of bands which are mainly characteristic of the original polymer. In addition, a new band at

Peak N^{o}	Assignment	m / e
1	Tetrahydrofuran (solvent)	72 42 41
2, 4	Phenol	94 65 66
3	Benzaldehyde	105 106 77
5	Unidentified	57 71 85
6	"	216 183 154
7	Biphenyl	154 153
8	Unidentified	91 55 70

Table 6.6: The assignment of the peaks in the gas chromatogram, shown in Fig.6.13, for the liquid fraction from SATVA separation of products of degradation to 600 ^{o}C under TVA conditions of PA3

		Component	m / e	Relative Intensity %
Upper CRF		Resorcinol	110 82 81	100 21 17
Lower CRF	1st	Benzoic acid	122 105	5.1 64.5
		Terephthaldehydic acid	150 149	10.4 100
		Terephthalic acid	166 149 121	23 100 21.6
	2nd	Di 3-hydroxyphenyl terephthalate	350	5.8
		Mono 3-hydroxyphenyl terephthalate	258 242 241 213	5.5 18 100 22.7

Table 6.7 Materials present in the CRF from the degradation of PA3 under TVA conditions to 500 °C.

3430 cm^{-1} corresponds to -OH stretching vibration. The mass spectrum showed many peaks corresponding to the molecular and fragment ions of mono-3-hydroxyphenyl terephthalate as major product with trace of di-3-hydroxyphenyl terephthalate due to overlap with the previous fraction. Table 6.7 summarises the products identified in the CRF fractions of PA3 degradation.

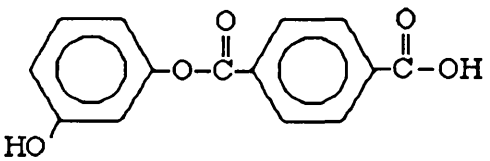

Mono-3-hydroxyphenyl terephthalate

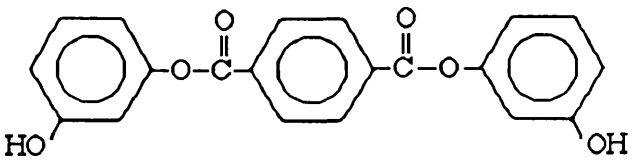

Di-3-hydroxyphenyl terephthalate

6.2.2.4 Poly(1.2-phenylene terephthalate) (PA4)

i) Condensable volatile products

The SATVA curve for the condensable volatile products from the degradation of a PA4 (Figure 6.14) shows two peaks. Carbon dioxide was identified as the product at the first peak. Materials present at the second peak were identified by a combination of IR, MS and GC-MS analysis as catechol, phenol and benzene. The gas chromatogram of the second fraction is shown in Figure 6.15.

ii) Cold ring fraction (CRF)

A white solid material which sublimed on the inner wall of the TVA tube as CRF was removed for spectroscopic analysis. Its IR and MS spectra, shown in Figures 6.16 and 6.17, respectively, indicate the presence of a cyclic dimer.

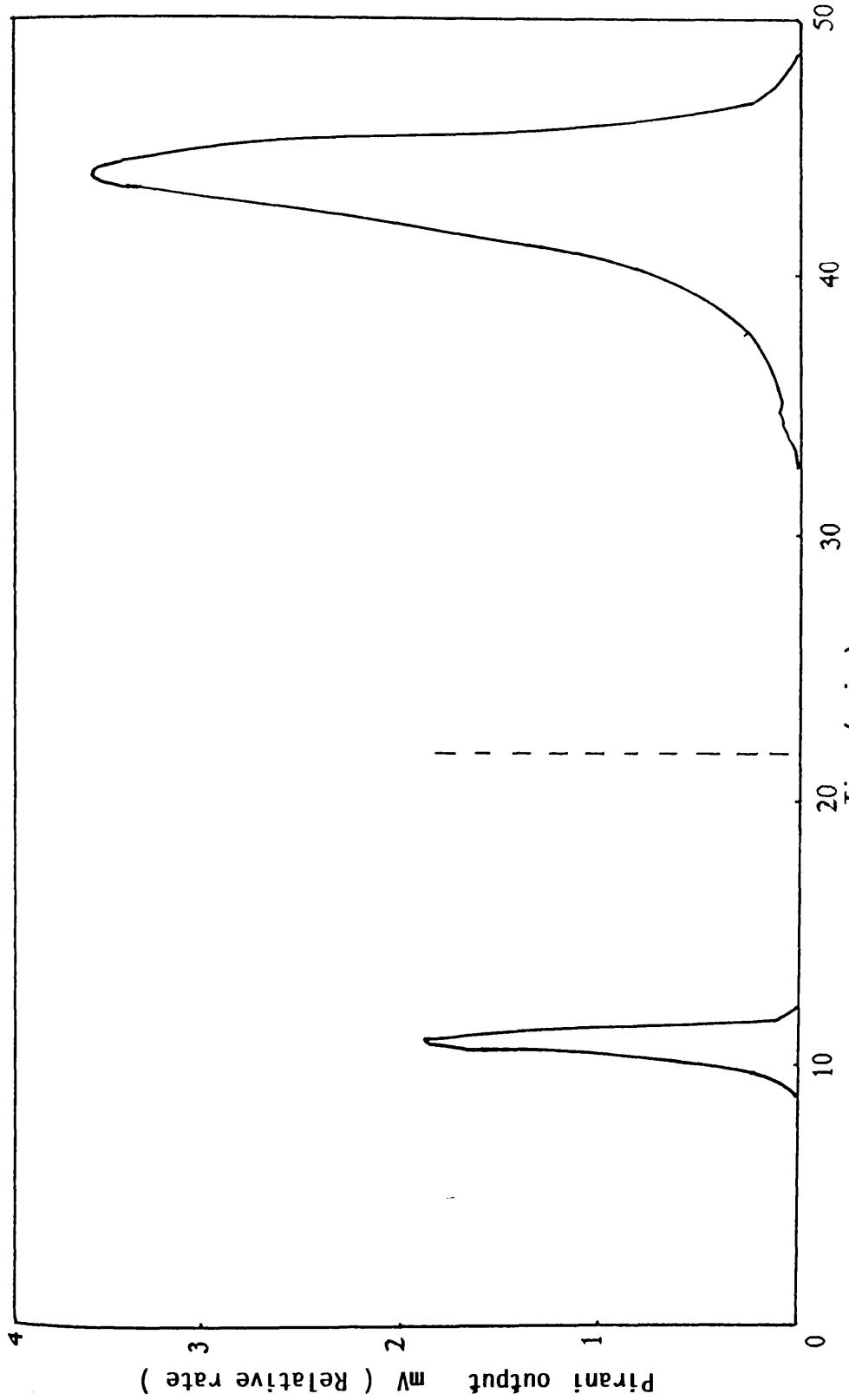

Figure 6.14: Subambient TVA trace for warm up from -196 ^{o}C to ambient temperature of condensable volatile products from degradation of PA4.

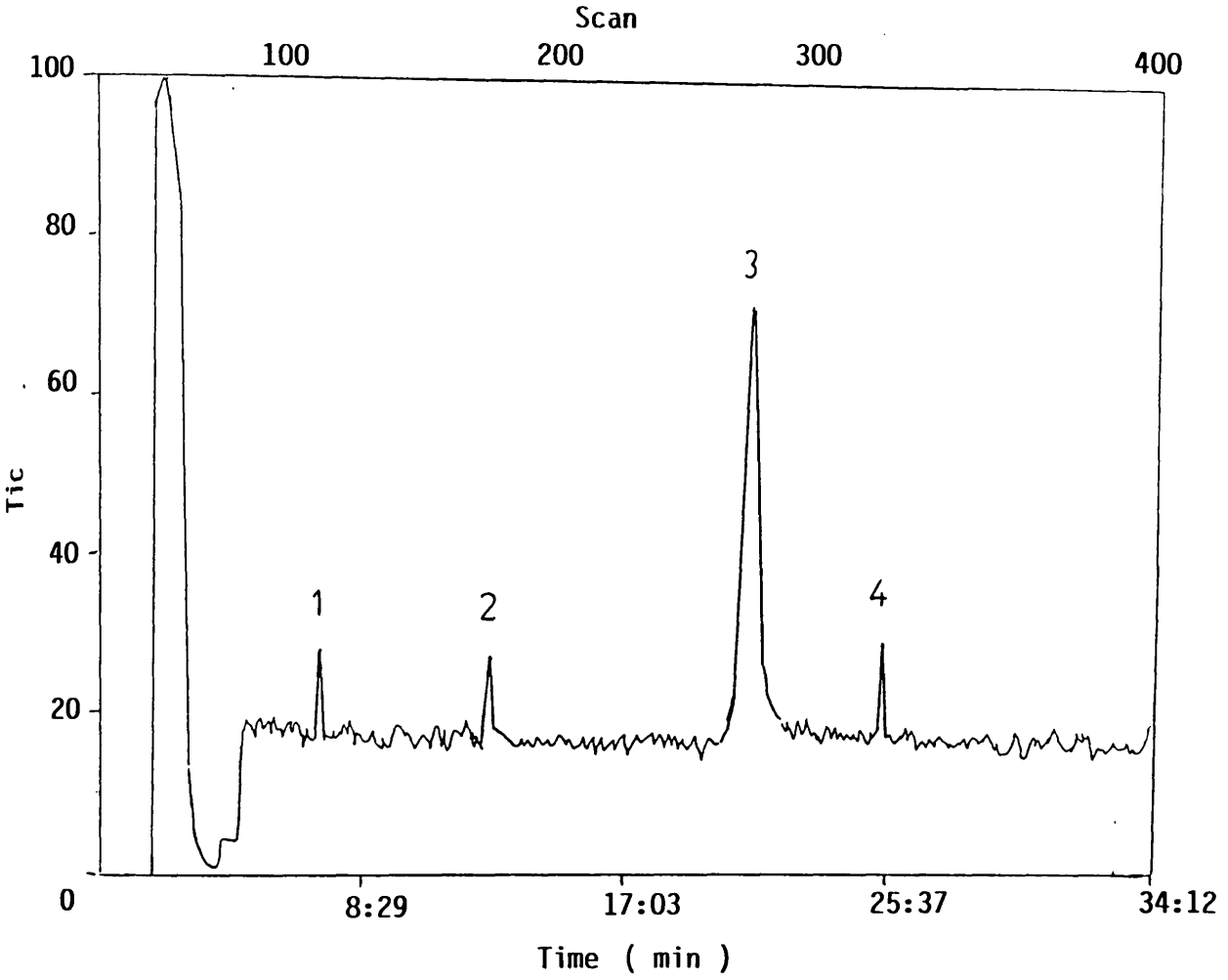

Figure 6.15 : Gas chromatogram for the liquid fraction in SATVA separation of products from the degradation of PA4 .

Assignments **1,** benzene; **2,**benzaldehyde; **3,** phenol and **4,** catechol .

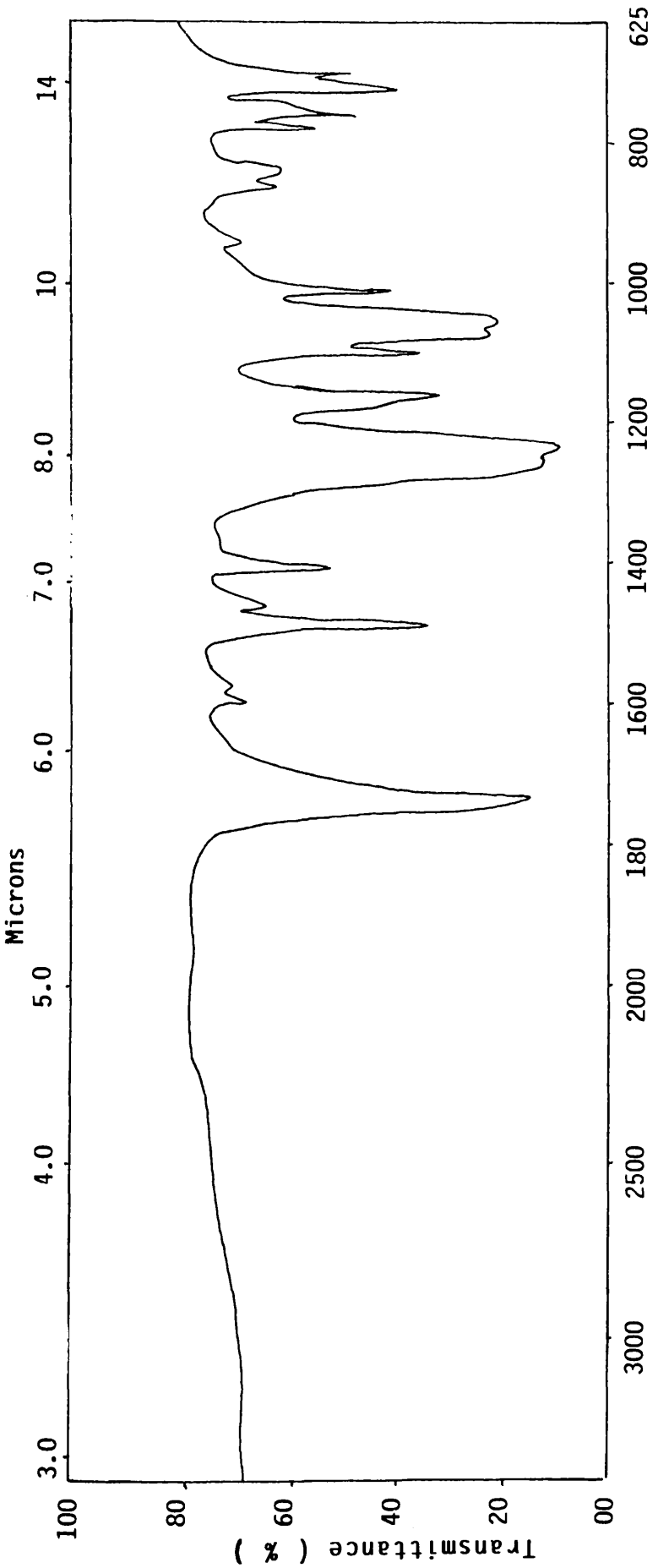

Figure 6.16: Infrared spectrum of CRF from PA4 degradation under TVA conditions.

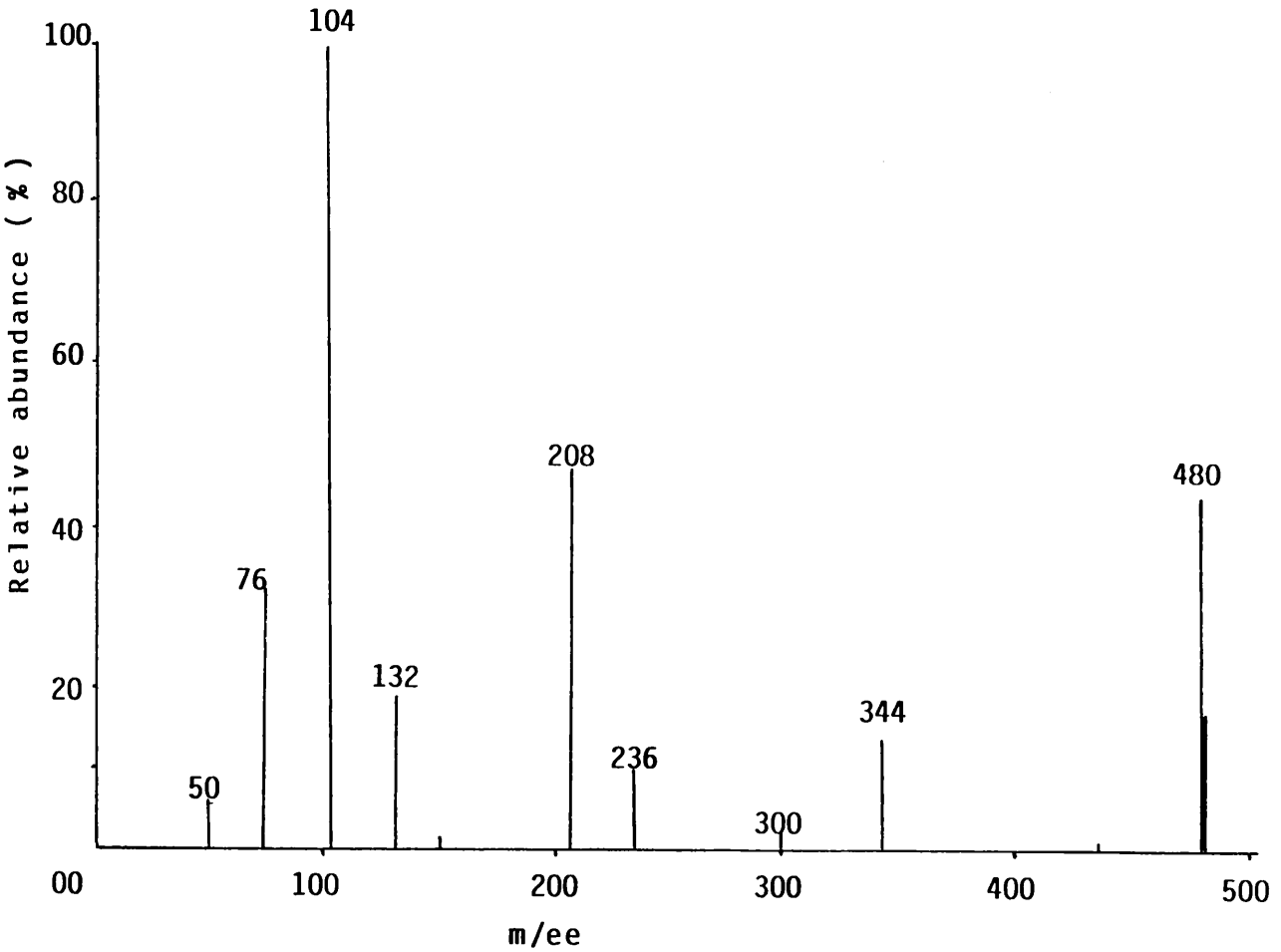

Figure 6.17: Mass spectrum of CRF from the degradation of PA4 to 500 ^{o}C under TVA conditions .

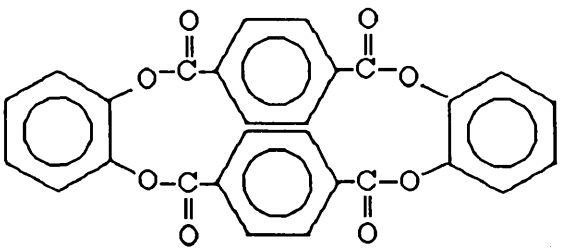

Cyclic dimer

6.2.2.5 Poly(bisphenol A terephthalate) (PA5)

6.2.2.5a Programmed Degradation

i) Condensable volatile products

The SATVA trace for the condensable volatile products from the degradation of PA5 in the TVA apparatus, shown in Figure 6.18, exhibits four fractions. Carbon dioxide and traces of ethylene were found by means of IR and MS spectroscopy to be the products of fraction 1. Benzene and toluene were identified in fractions 2 and 3, respectively. The low volatility material (fraction 4) was subjected to GC-MS examination. The gas chromatogram of the separated products shown in Figure 6.19 indicates 14 peaks and the assignment of the products is listed in Table 6.8, in which phenol, p-cresol, 4-ethyl phenol, 4-isopropyl phenol and biphenyl were identified as the main components, together with traces of ethyl benzene, isopropyl benzene and biphenyl methane.

The sublimed material on the cooled area upper part of TVA tube consisted of two solid bands, which were removed separately for further spectroscopic analysis. The ir spectrum of the former shows characteristic bands of terephthalic acid. The latter material was a mixture, the ir spectrum

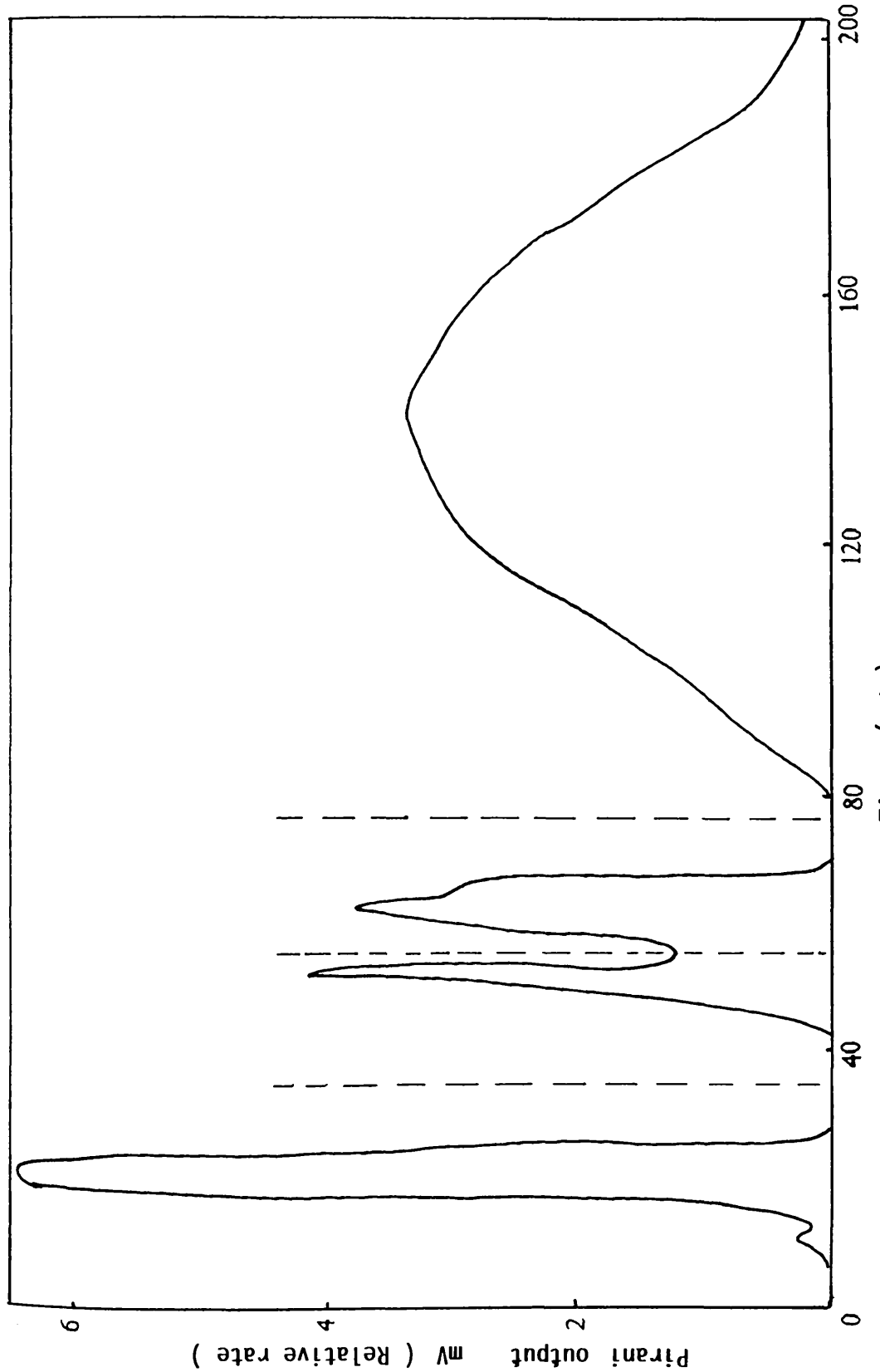

Figure 6.18 : Subambient TVA tarce for warm up from -196 ^{o}C to ambient temperature of condensable volatile products from degradation of PA5.

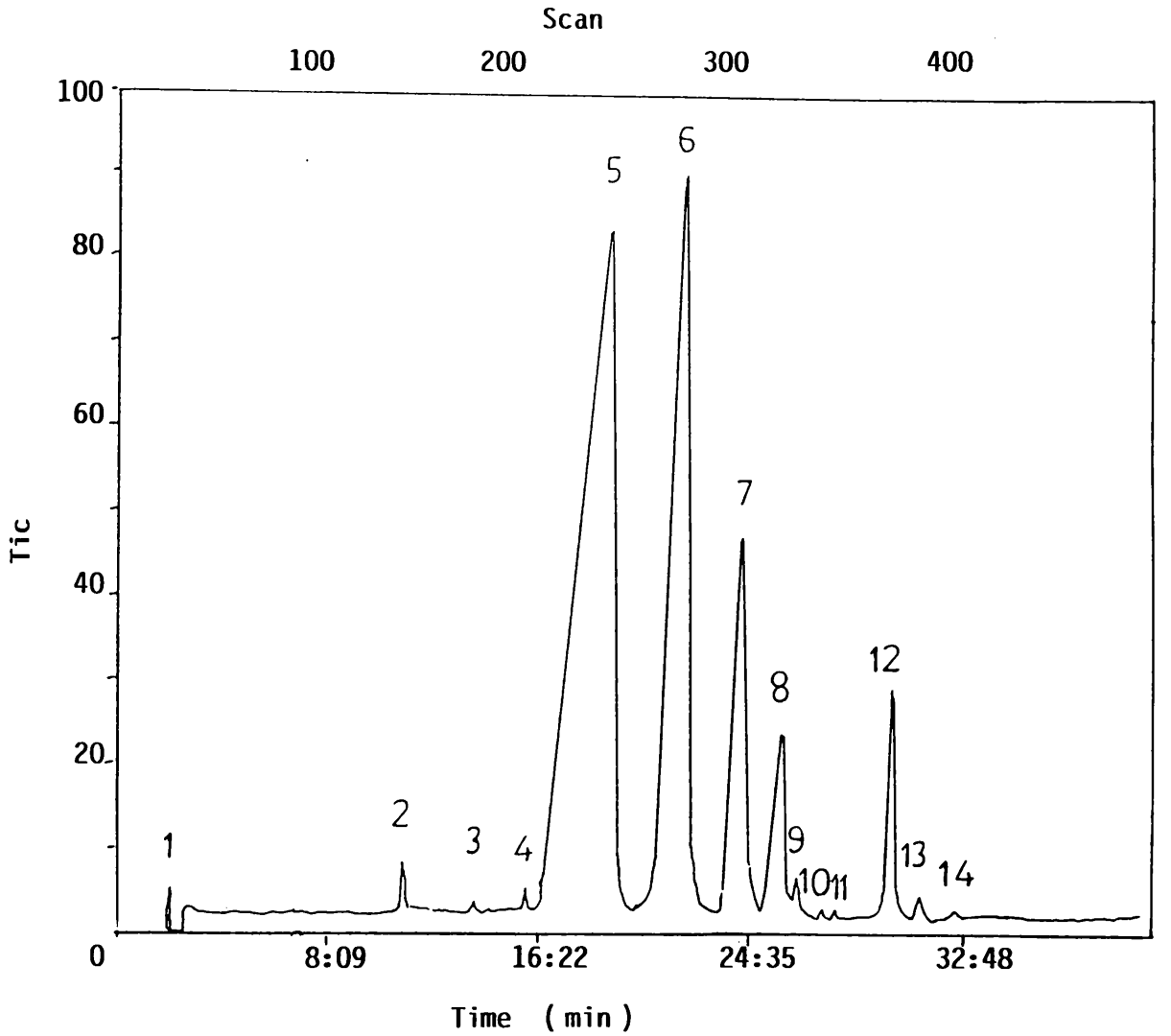

Figure 6.19: Gas chromatogram for the liquid fraction in SATVA separation of products from the degradation of PA5.

Peak N°	Assignment	m / e
1	Diethyl ether (solvent)	59 74
2	Ethyl benzene	106 91
3, 4	Isopropyl benzene	105 120
5	Phenol	94 65 66
6	4-Hydroxy toluene	107 108
7	4-Hydroxyethyl benzene	107 122
8, 9, 10	4-Hydroxyisopropyl benzene	121 107 136
11	Unidentified	107 121 142 94
12	Biphenyl	154 153
13, 14	Diphenyl methane	168 167 91

Table 6.8: The assignment of the peaks in the gas chromatogram, shown in Fig.6.19, for the liquid fraction from SATVA separation of products of degradation of PA5 to 600 °C under TVA conditions.

of which showed absorption of free (-OH) and carbonyl group linkage at 3440 and 1735 cm^{-1}, respectively. It was subjected to MS examination at 180, 250 and 320 °C. The mass spectra shown in Figure 6.20, exhibit different pattern peaks corresponding to the molecular ions of short chain fragments III, IV and bisphenol A.

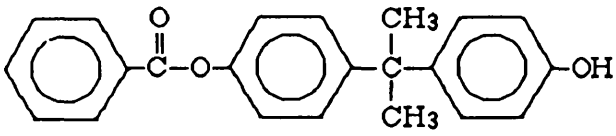

III

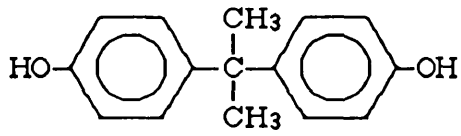

Bisphenol A

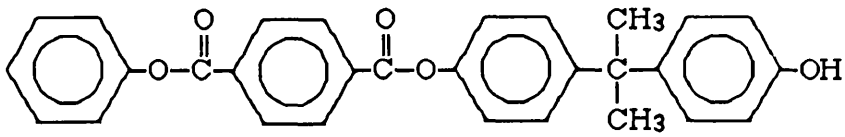

IV

Short chain fragment III has a parent ion peak at m/e = 331 which can be accounted for by loss of methyl group.

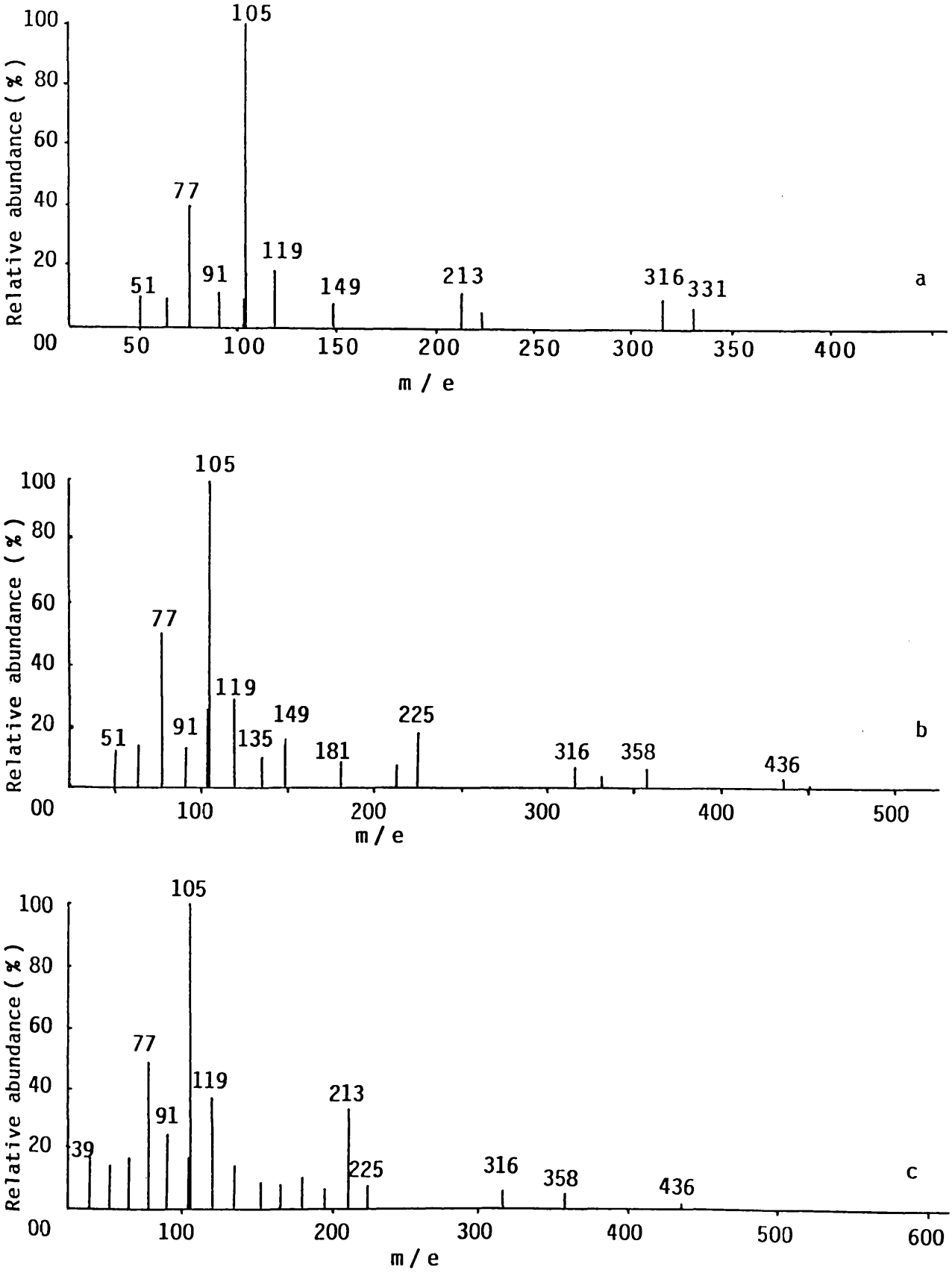

Figure 6.20: Mass spectra of the total CRF products from degradation of PA5 under TVA conditions to 600 ^{o}C for probe temperatures **a** (180 ^{o}C), **b** (250 ^{o}C) and **c** (320 ^{o}C) .

	Prducts		Methods of Analysis
Noncondensable	Carbon monoxide and methane		IR
Condensable Volatile	Major	Carbon dioxide, benzene, phenol, toluene, 4-methylphenol, 4-ethyl phenol, 4-isopropyl phenol and biphenyl.	IR & MS & GC-MS
	Minor	Ethyl benzene, isopropyl benzene, diphenylmethane, bisphenol A, 1.1-di(4-hydroxybenzene) ethane and benzaldehyde.	
Cold Ring Fraction	Terephthalic acid (major), terephthaldehydic acid , benzoic acid , bisphenol A and short chain fragments III and IV .		IR & MS

Table 6.9: Products of PA5 degradation to 600 ^{o}C under TVA conditions.

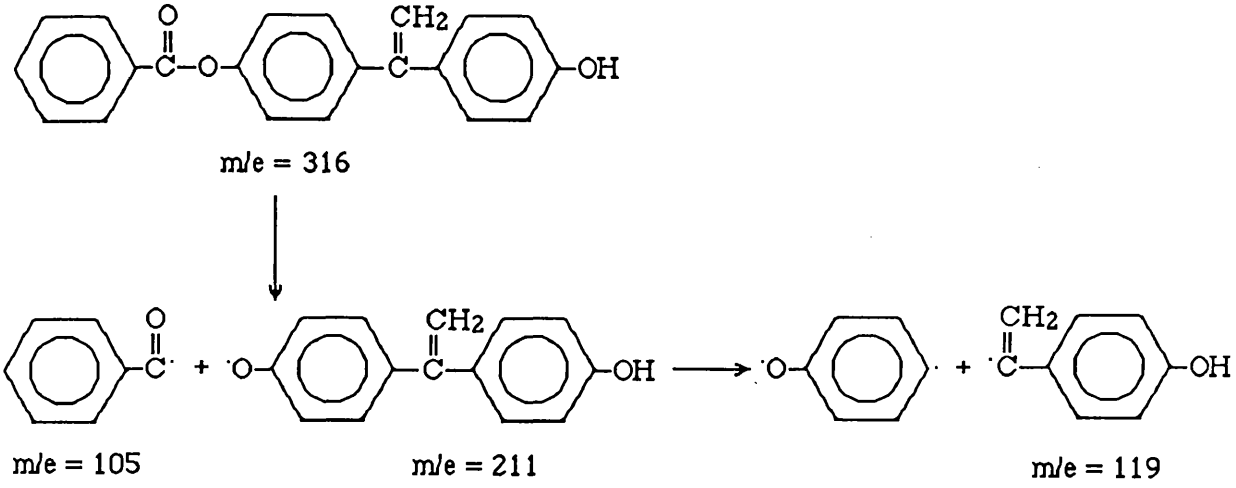

The ion peaks at m/e = 228, 213, 135 and 119 could have resulted from the fragmentation of bisphenol A.

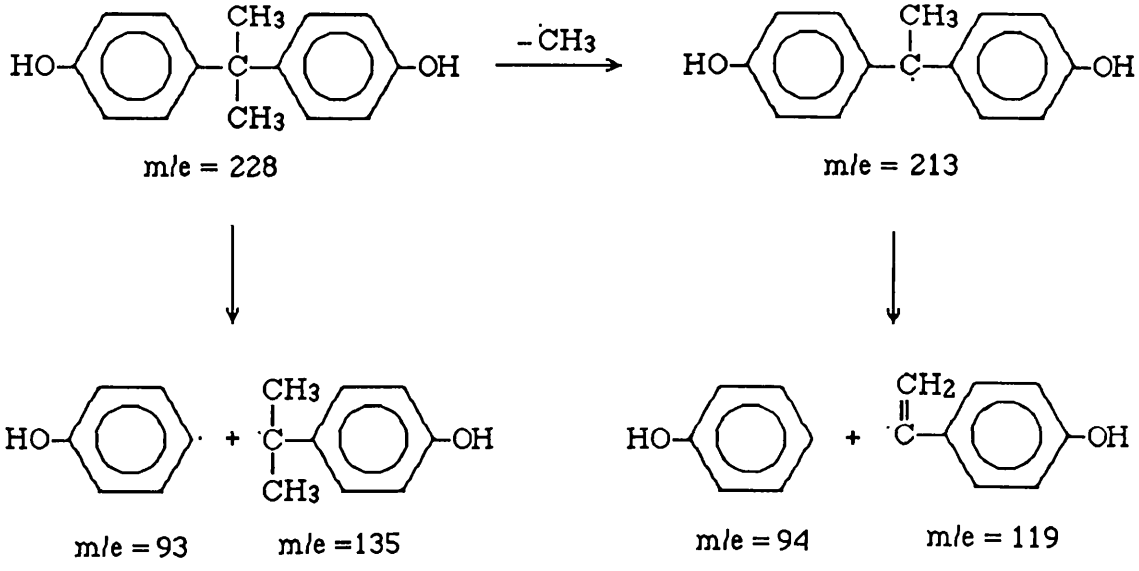

The molecular ion peaks at m/e = 451, 436 and 358 could have arisen from the short chain fragment IV.

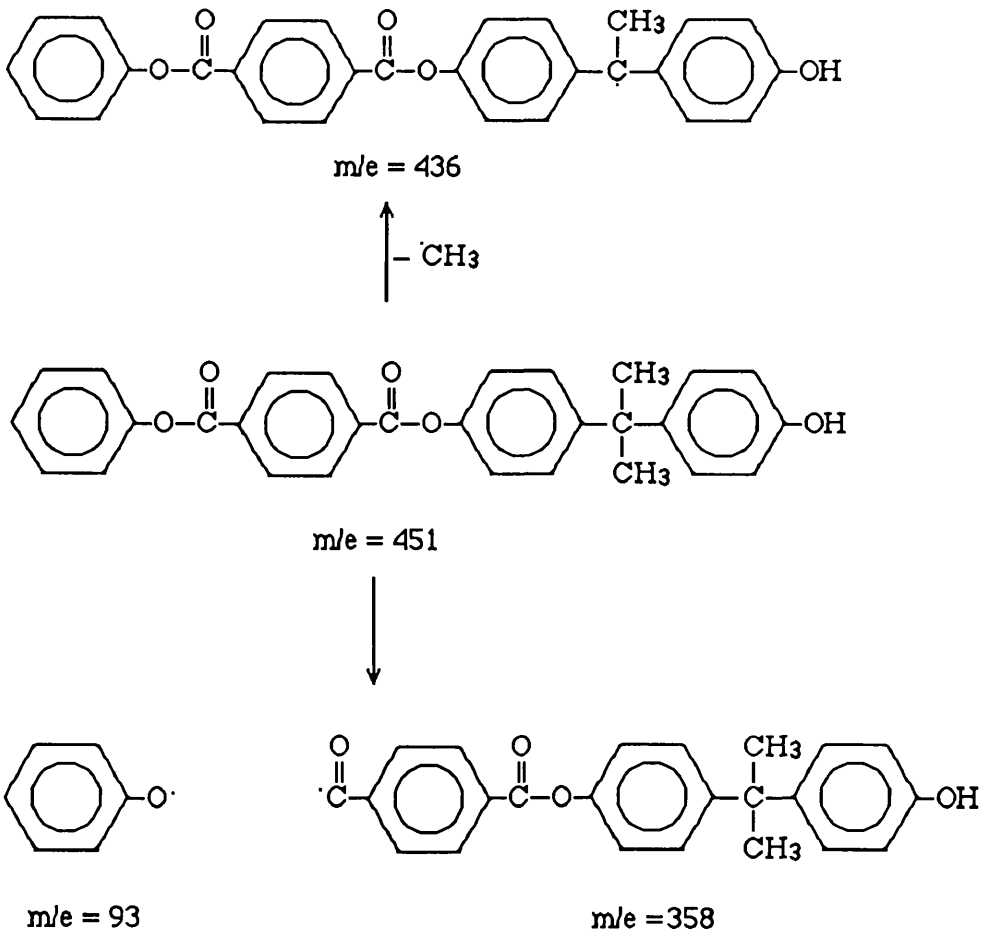

6.2.2.5b Isothermal Degradation of PA5

Sample of PA5 (200 mg) was partially degraded under vacuum at 331, 375, 425, 473 and 493 ^{o}C, each for 100 min, successively. The volatile products at each degradation temperature were collected for spectroscopic analysis.

Condensable volatile products

The SATVA curves were obtained for the condensable volatile products from the partial degradation of PA5 at the above temperatures. Traces of hydrogen chloride were detected in the partial degradation at 331 °C, furthermore bisphenol A and 1,1-di(4-hydroxyphenyl) ethane were recovered among the liquid fraction products above 375 °C. Some of the products are formed only at high temperatures i.e p-cresol, 4-isopropyl phenol, biphenyl and biphenyl methane.

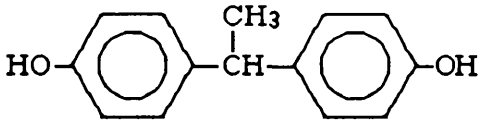

1,1-Di(4-hydroxyphenyl) ethane

Table 6.10 summarises qualitative data for the condensable volatile products at 375, 425 and 473 °C.

6.3 HALOGENATED POLYARYLATES (FIRE RETARDANT)

6.3.1 THERMAL ANALYSIS

6.3.1.1 Thermogravimetry (TG)

The TG traces for fire retardant polyarylates obtained in dynamic nitrogen atmosphere at a heating rate of 10 °C/min are shown in Figure6.21.

Product	Temperature of Condensable Volatile Products Formation			m / e
	375 °C	425 °C	473 °C	
Carbon dioxide	+	+	+	44 28
Benzene	+	+	+	78 51
Toluene	+	+	+	92 91
Ethyl benzene	+	+	+	106 91
4-Methyl phenol	-	+	+	108 107
4-Ethyl phenol	+	+	+	122 107
Isopropyl benzene	+	+	+	120 105
4-Isopropyl phenol	-	-	+	136 121 107
Phenol	+	+	+	94 65
Biphenyl	-	-	+	154 153
Diphenyl methane	-	-	+	168 167
Bisphenol A	-	+	-	228 213
1.1-Di(4-hydroxy phenyl) ethane	+	+	+	214 199

N.B (+) present , (-) absent

Table 6.10: Substances identified in the condensable volatile products from the isothermal degradation of PA5 under TVA conditions at the temperatures shown for 100 min.

Each trace exhibits a single stage decomposition during thermal degradation up to 500-600 °C. Weight loss commences above 320 °C, achieving maximum rate in the range of 437-490 °C, except for Br-PA6 (375 °C). This much lower stability is accounted for by the presence of the aliphatic diol end group in the backbone of the brominated bisphenol A component. The involatile residue at 500 °C was above 40 %, except Br-PA6 (19%).

6.3.1.2 Thermal volatilisation analysis (TVA)

The TVA curves for the fire retardant polyarylates heated to 550 °C at 10 °C/min are reproduced in Figures 6.22-6.25. The volatilisation occurs in a single step, which begins around 311 °C, reaching maximum rate of volatilisation in the range of 378-510 °C. Moreover, the separation of the TVA traces at 0, -45, -75, 100 and -196 °C indicates the presence of various volatile products with different volatility including non-condensable gases.

The quantitative measurement of the main product fractions by TVA (i.e residue, cold ring fraction and volatile liquids and gases), and the T_{onset} and T_{max} values obtained in the TG and TVA data are listed in Table 6.11.

The onset temperature for the fire retardant polyarylates determined by TG occurs at a lower temperature than by TVA. This can be explained by the fact that weight loss of CRF is detectable only by TG. Furthermore, it can be seen from Tables 6.1 and 6.11 or Figures 6.1 and 6.21 that the temperatures of the maximum rate of decomposition are higher for unhalogenated polyarylates than for the respective chlorine and bromine substituted derivatives as given below

PA5 > Cl-PA5 > Br-PA5 and PA4 > Br-PA4

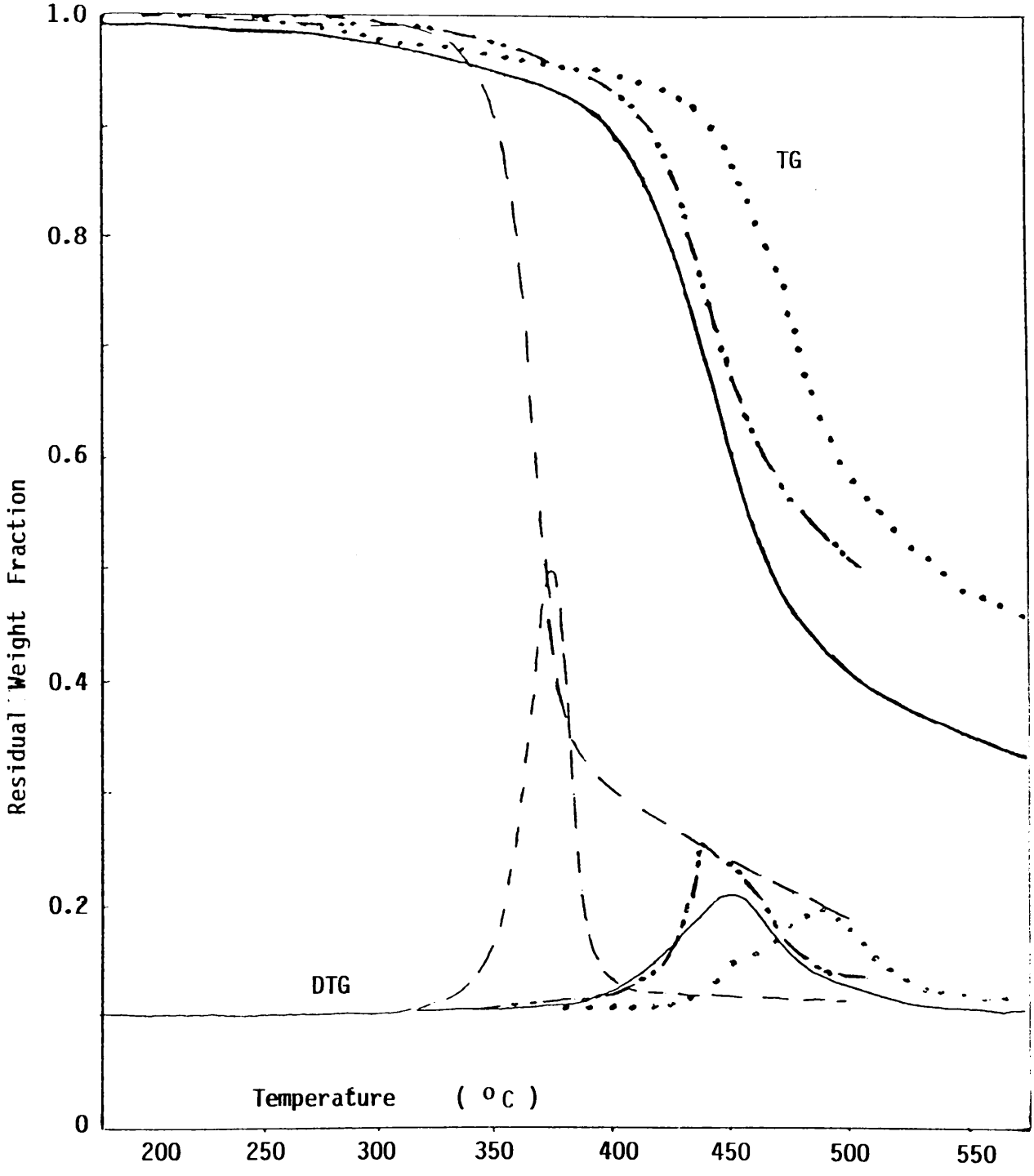

Figure 6.21 :: Thermogravametric traces of Cl-PA5 (....) , Br-PA4 (– .. –) Br-PA5(——) and Br-PA6 (---). Heating rate , 10^{o}/min; under nitrogen atmosphere.

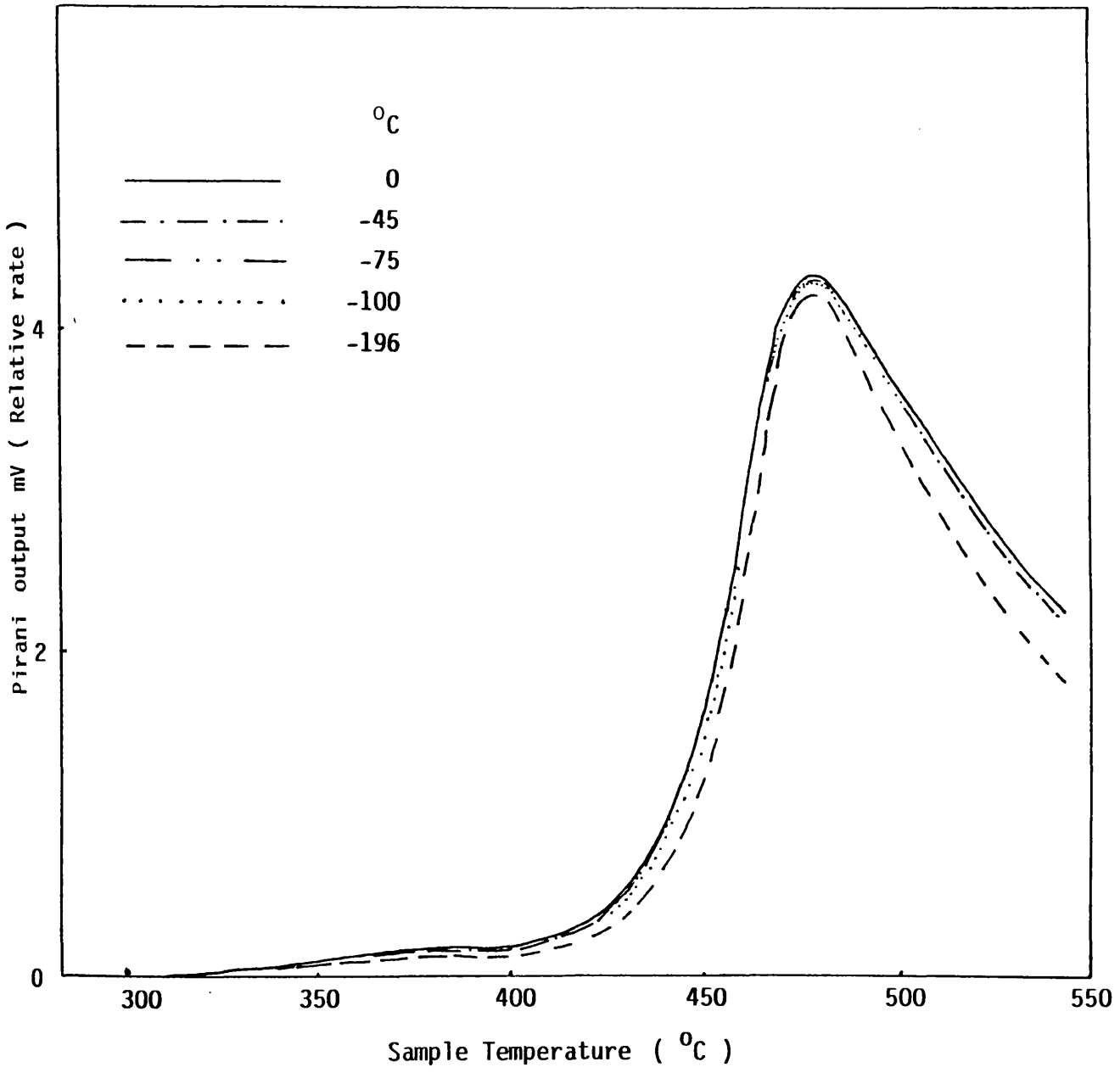

Figure 6.22 : TVA traces for Br-PA4 . Heating rate,10 °C/min .

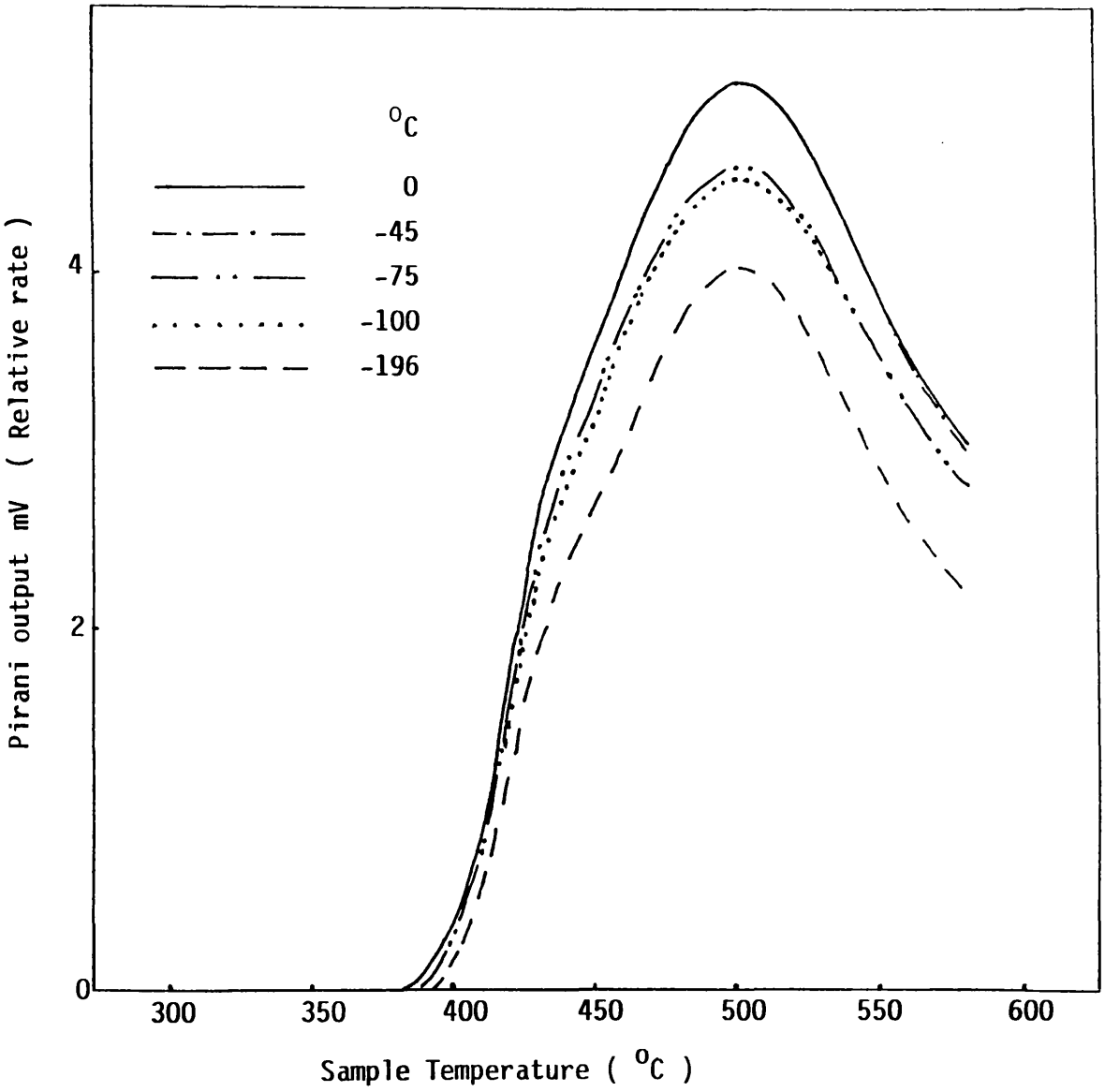

Figure 6.23: TVA traces for Cl-PA5 . Heating rate , 10 °C/min .

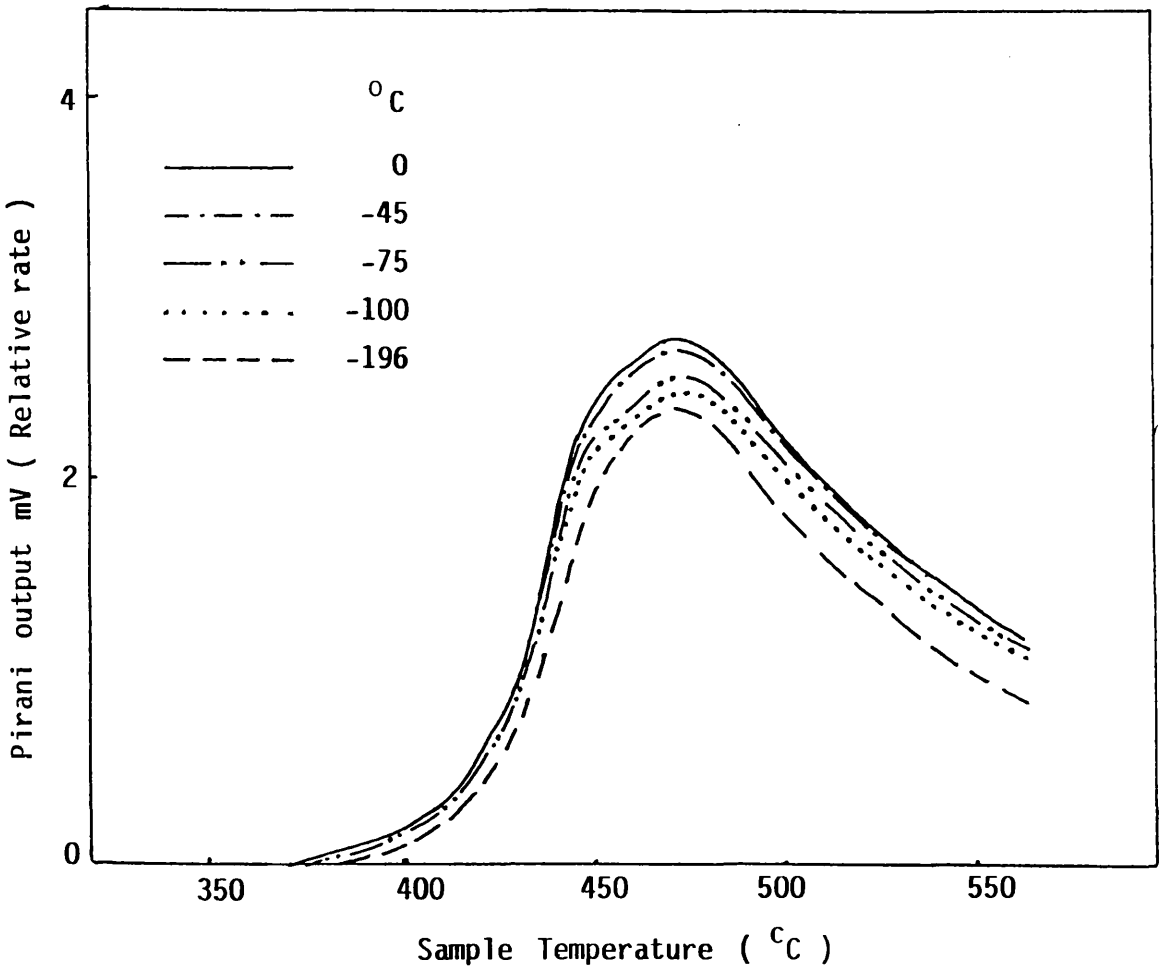

Figure 6.24 : TVA traces for Br-PA5 . Heating rate,10 °C/min .

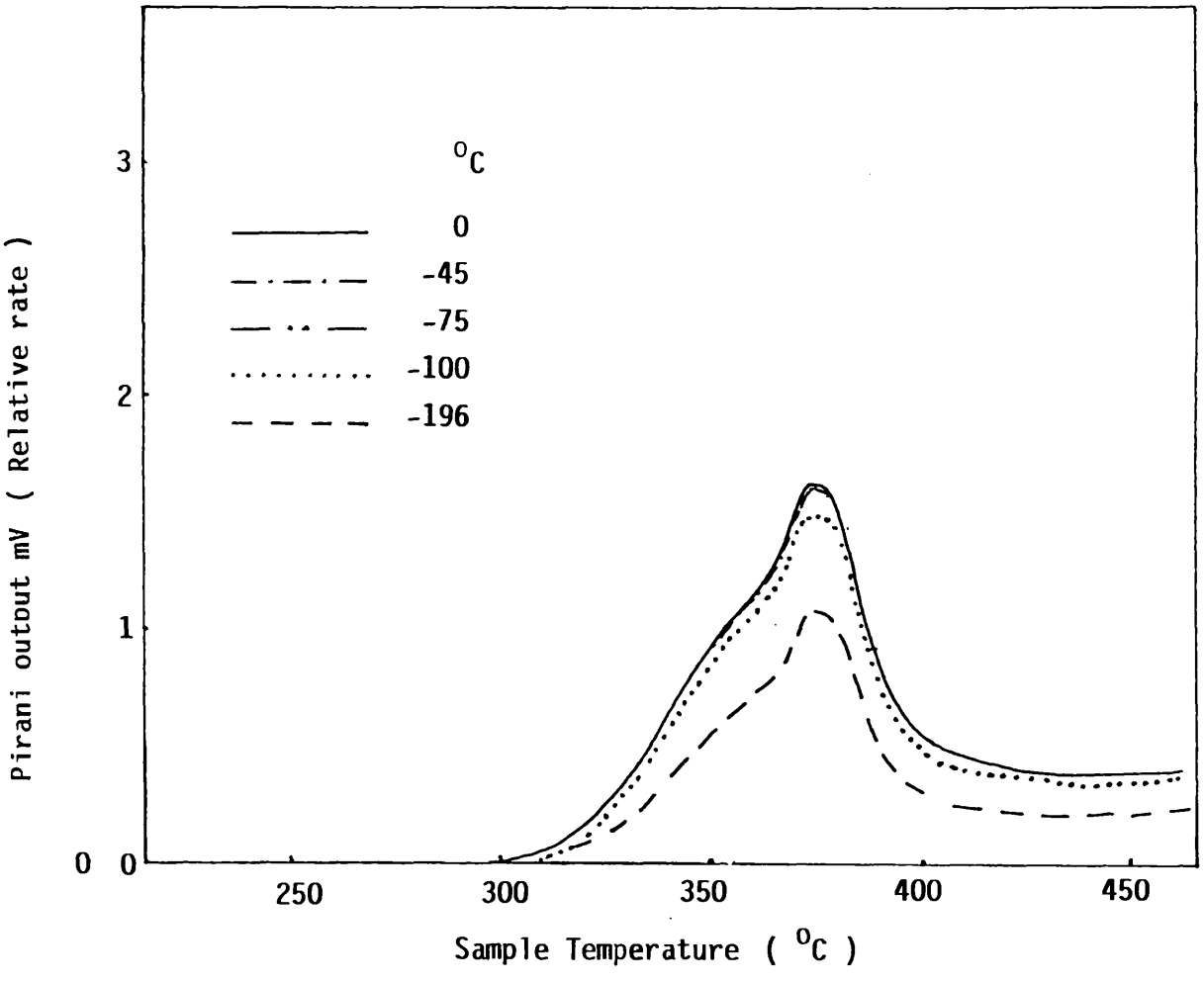

Figure 6.25 : TVA traces for Br-PA6 . Heating rate , 10 °C/min .

	Polymer code N°	Br-PA4	Cl-PA5	Br-PA5	Br-PA6
TVA	T_{onset} / °C	311	395	400	317
	T_{max} / °C	471	502	494	378
	Residual Fraction / wt %	52	42.5	43.3	11
	Cold Ring Fraction / wt %	28.5	17.5	9.3	86
	Volatile Fraction at room temperature / wt %	19.5	40	47.5	3
TG & DTG	T (initial wt loss) / °C	275	220	230	270
	T_{max} / °C	437.5	490	453	375
	Residual Fraction* / wt %	50	44	31.5	19

* Residual Fraction at 550 °C

Table 6.11 : TVA, TG and DTG data for halogenated polyarylates decomposition.

These results show that the thermal stability of these polyarylates depends on the type of the substituted halogen.

6.3.2 CHARACTERISATION OF DEGRADATION PRODUCTS

The degradation products revealed from the degraded fire retardant polyarylates were separated and identified by means of IR, MS and GC-MS techniques and results are summarised in Table 6.12.

In all the polymers studied, carbon monoxide and methane were recovered as non-condensable gases, except in the case of Br-PA4, which gives only carbon monoxide, because Br-PA4 is a fully aromatic polyarylate.

6.3.2.1 Poly(tetrabromo 1.2-phenylene terephthalate) (Br-PA4)

6.3.2.1a Programmed degradation of Br-PA4

i) Condensable volatile products

The SATVA curve obtained for this fraction from degradation of Br-PA4, shown in Figure 6.26, indicates three peaks. The first peak was found by ir spectroscopy to be due to carbon dioxide, hydrogen bromide, together with traces of hydrogen chloride. Bromine and traces of benzene were identified as the components in peak 2. The products at the third SATVA peak were characterised by means of IR, MS and GC-MS. The mass spectrum indicates the presence of benzoic acid, phenol and benzaldehyde. In addition, the GC separation in Figure 6.27 and the assignment by MS of each peak in Table 6.13 indicate 9 components, of which dibromobenzene is most important.

Polymer code N°	Noncondensable gases	Condensable gases	Liquid volatile products	Cold ring fraction
Br-PA4	Carbon monoxide	Carbon dioxide, hydrogen bromide,	Bromine, benzene, dibromobenzene and benzaldehyde.	Terephthalic acid, cyclic monomer, tetrabromocatechol, benzoic acid , and short chain fragment with (-COOH) end group.
Cl-PA5	Carbon monoxide, methane	Hydrogen chloride, carbon dioxide and ethylene	Phenols, benzene, toluene, mono- and dichlorobenzene, benzoic acid, dichlorotoluene , benzaldehyde , aromatic esters and diphenyl methane	Terephthalic acid, benzoic acid terephthaldehydic acid and tetrachlorobisphenol A .
Br-PA5	Carbon monoxide, methane.	Carbon dioxide, hydrogen bromide, ethylene and hydrogen chloride.	Phenols, bromobenzene, benzene, benzaldehyde, phenyl benzoate and aromatic diols	Terephthalic acid, benzoic acid terephthaldehydic acid tetrabromobisphenol A and short chain fragments V, VII and VIII.
Br-PA6	Carbon monoxide, methane	Carbon dioxide, hydrogen bromide, ethylene, vinyl bromide and hydrogen chloride.	Phenols, 2-bromoethanol, benzene, ethyl benzene, bromobenzene, methyl benzoate, ethyl benzoate and aromatic diol.	Terephthalic acid, benzoic acid terephthaldehydic acid tetrabromobisphenol A, short chain fragments IX and VII, mono-ethyl terephthalate and dihydroxyethyl terephthalate.

Table 6.12: Products of degradation of halogenated polyarylates to 600 °C in the TVA system under vacuum using programmed heating.

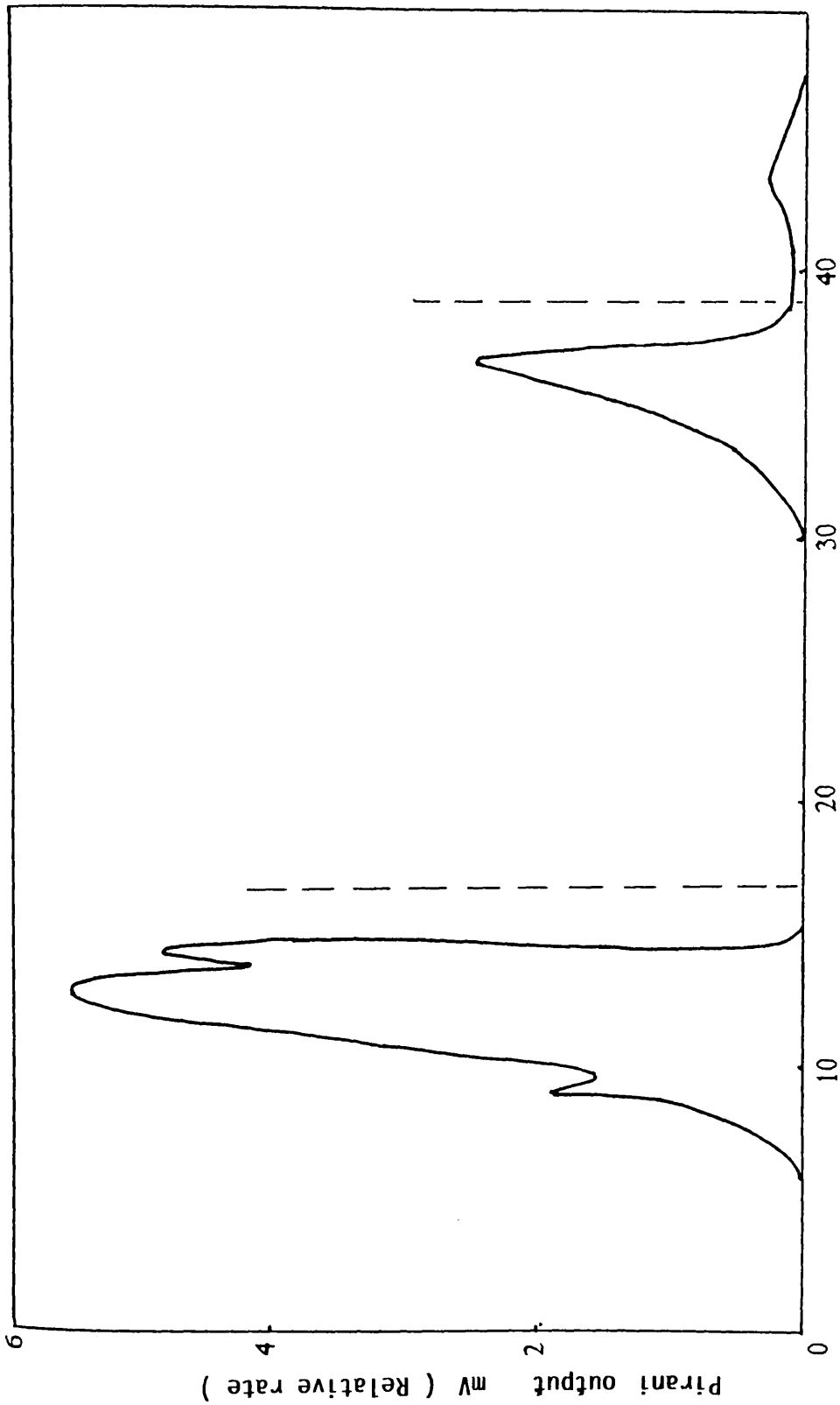

Figure 6.26 : Subambient TVA trace for warm up from -196 ^{o}C to ambient temperature of condensable volatile products from degradation of Br-PA4.

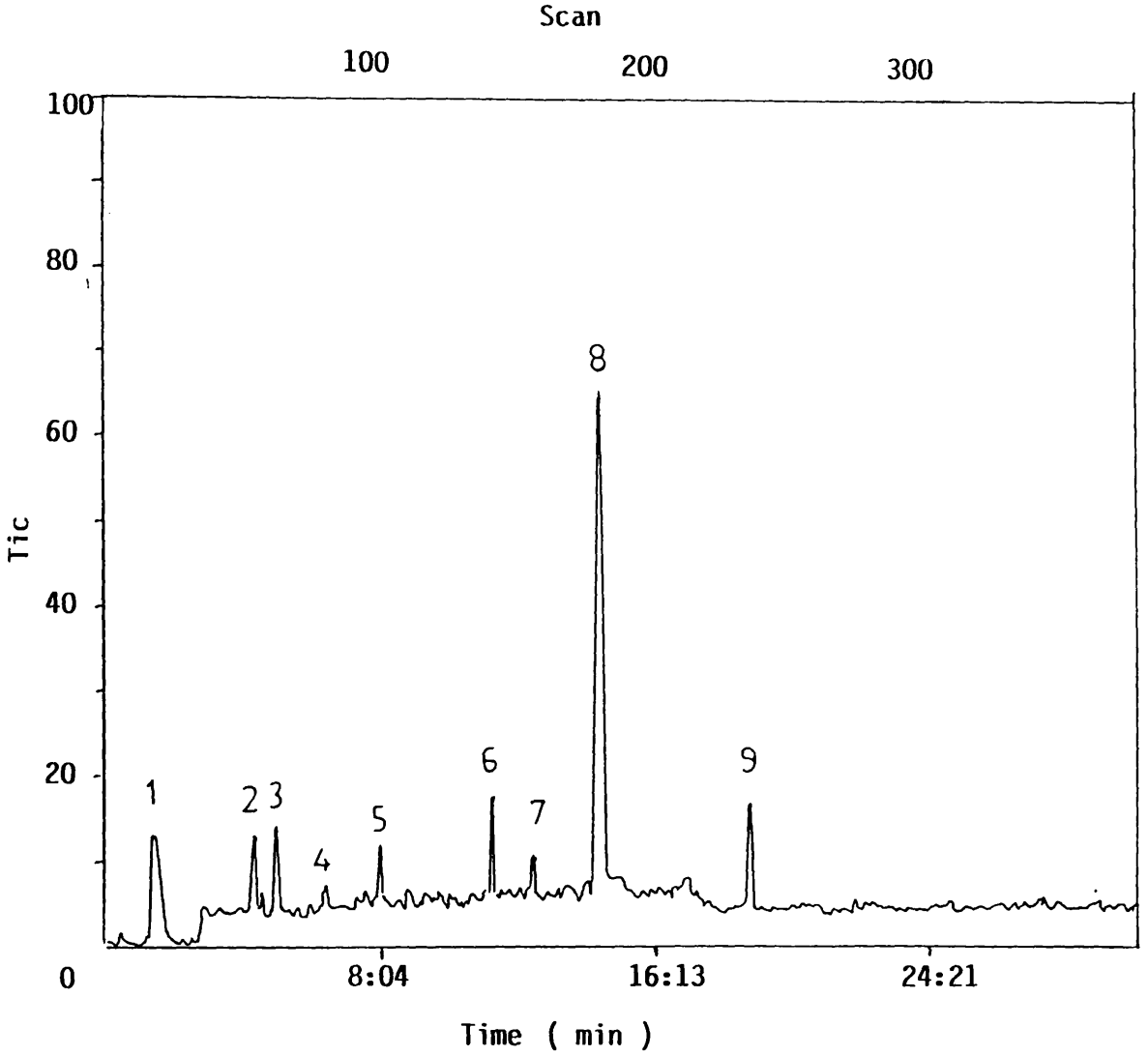

Figure 6.27 : Gas chromatogram for the liquid fraction in SATVA separation of products from the degradation of Br-PA4 .

Peak N^{o}	Assignment	m / e
1	Unidentified	94 96
2	"	207
3	Bromine	82 81 80
4	Unidentified	101 74
5	"	281 265
6	Benzaldehyde	105 77
7	Unidentified	73 85
8	Dibromobenzene	236 255
9	Unidentified	184 183

Table 6.13: The assignment of the peaks in the gas chromatogram, shown in Fig.6.27, for the liquid fraction from SATVA separation of products of degradation to 600 ^{o}C under TVA conditions of Br-PA4.

ii) Cold ring fraction (CRF)

Three solid bands were deposited on the cooled area upper part of TVA tube as CRF. Terephthalic acid was found by ir and mass spectrometry to be the main component in the upper CRF, together with traces of cyclic monomer (m/e = 556), tetrabromocatechol (m/e =426), terephthaldehydic acid and benzoic acid. The middle CRF was found to consist of short chain fragments with carboxylic acid end groups (V).

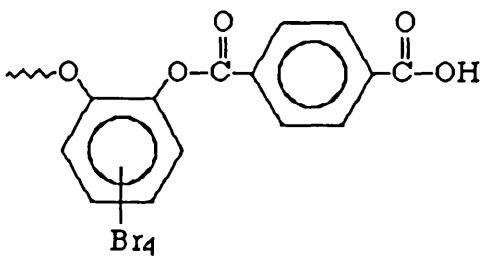

V

The ir spectrum of the lower CRF showed the characteristic absorptions of the original polymer, indicating that it consisted of shorter polymer chains.

6.3.2.1b Isothermal degradation of Br-PA4

In attempt to get better insight in the structural changes in the polymer during thermal degradation, a 200 mg sample of Br-PA4 was degraded isothermally under vacuum at 300, 350 and 370 ^{o}C each for 100 min, successively. Hydrogen chloride and terephthalic acid were detected at 300 ^{o}C. The other major condensable products begin to be evolved around

350 ^{o}C, simultaneously with short chain fragments of Br-PA4 as CRF at that temperature. At higher temperatures, the main degradation products were produced in greater amounts.

6.3.2.2 Poly(tetrachlorobisphenol A -terephthalate) (Cl-PA5)

i) Condensable volatile products

The SATVA trace from the degradation of Cl-PA5, shown in Figure 6.28, exhibits three peaks. The ir spectrum of the first peak indicated the presence of hydrogen chloride and carbon dioxide, together with a trace of ethylene. Benzene was the product responsible for the second peak. Due to the small amount and low volatility, standard analysis was not enough to identify the products of the last peak, therefore the total liquid fraction (peak 3) was subjected to GC-MS investigation. The gas chromatogram in Figure 6.29 and the assignments for each peak in Table 6.14 illustrate that 2.6-dichlorophenol, 2.6-dichloro-4-methyl phenol, benzene and 2.6-dichloro- 4-ethyl phenol are the major products, together with small amounts of benzaldehyde, chlorophenol and biphenol.

ii) Cold ring fraction (CRF)

The CRF condensed on cooled upper part of the TVA tube consisted of two bands, in which terephthalic acid and tetrachlorobisphenol A were identified by ir and mass spectroscopy as the main components, together with traces of benzoic acid.

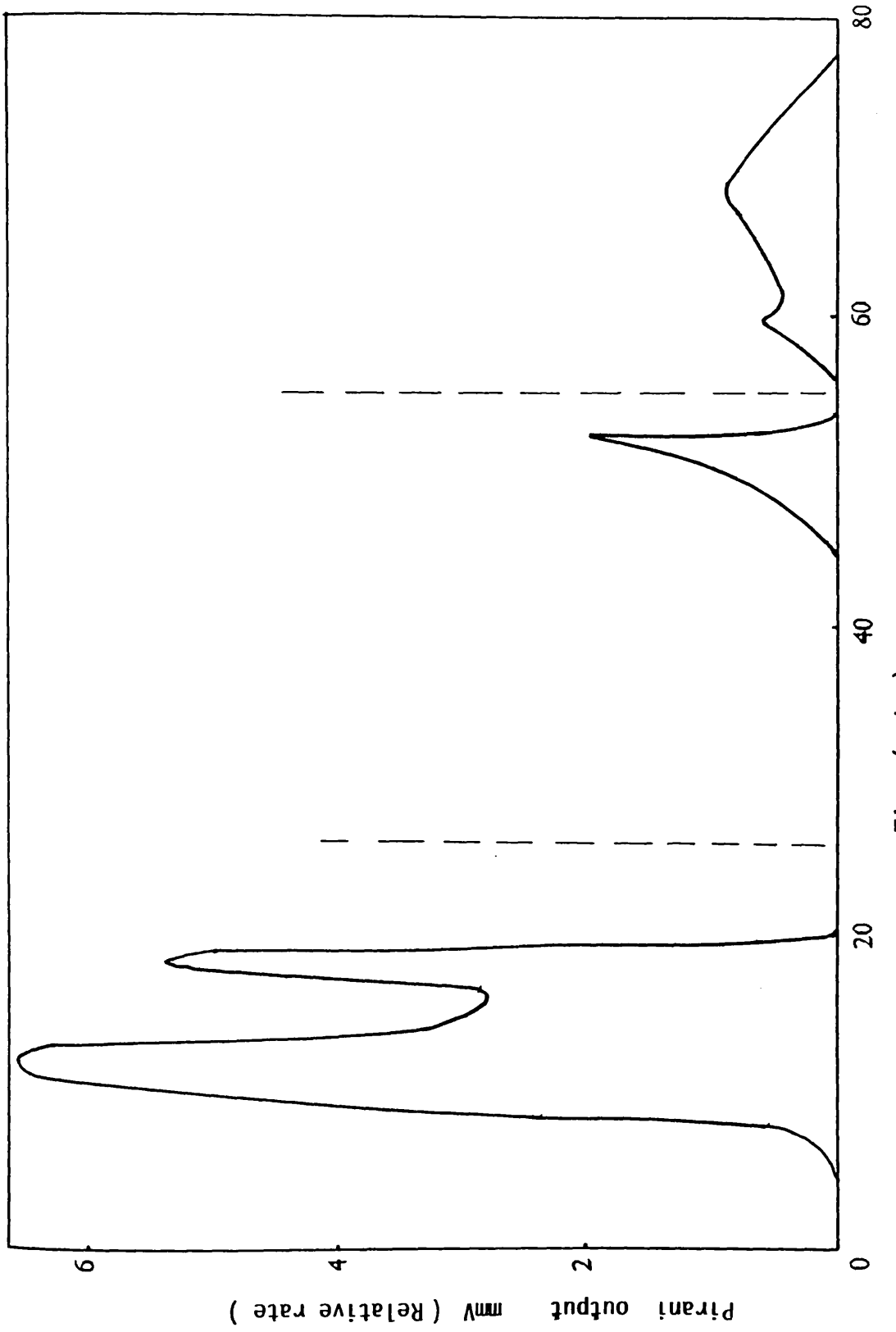

Figure 6.28 : Subambient TVA trace for warm up from 196 ^{o}C to ambient temperature of condensable volatile products from degradation of Cl-PA5 .

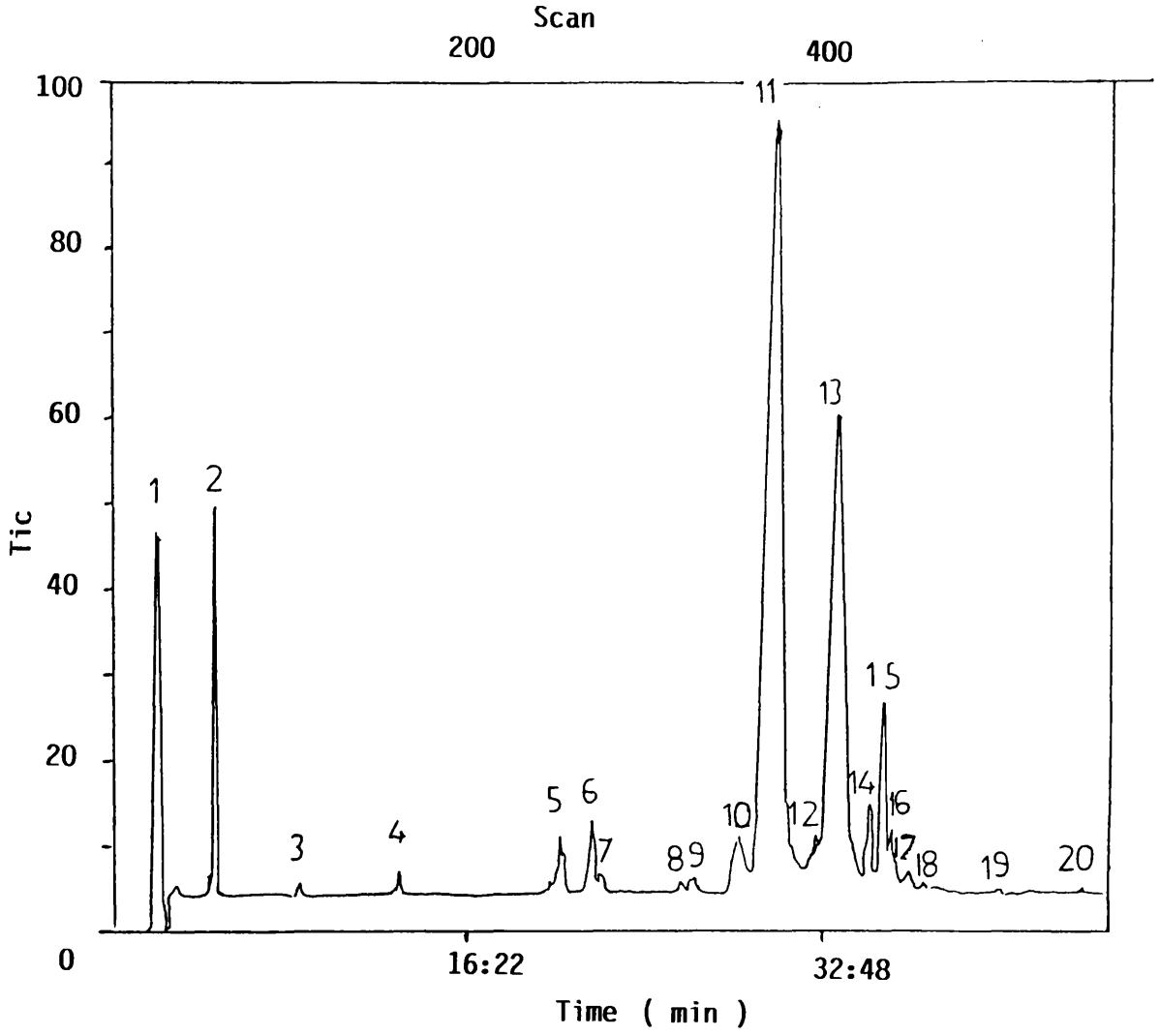

Figure 6.29 : Gas chromatogram for the liquid fraction in SATVA separation of products from the degradation of Cl-PA5 .

Peak N°	Assignment	m / e
1	Diethyl ether (solvent)	74 59
2	Benzene	78 77
3	Toluene	92 91
4	Chlorobenzene	110 112
5	Benzaldehyde	77 106 105
6	2-Chlorophenol	128 103 64
7	1.3-Dichlorobenzene	146 148 111
8	2-Chloro 4-methyl phenol	142 107
9	3.5-Dichlorotoluene	125 160 162
10, 11	2.6-Dichlorophenol	162 164 128
12	Benzoic acid	122 105 77
13	2.6-Dichloro 4-methyl phenol	176 141 178
14	Biphenyl	154 153
15	2.6-Dichloro 4-ethyl phenol	175 177 188 192
16	2.6-Dichloro 4-vinyl phenol	175 177 188 190
17	2.6-Dichloro 4-isopropyl phenol	189 191 204
18	Diphenyl methane	168 167
19	Phenyl benzoate	105 198 77
20	2-Chlorophenyl benzoate	105 128 232

Table 6.14: The assignment of the liquid fraction in SATVA separation of Cl-PA5 from the gas chromatogram as shown in Fig. 6.29.

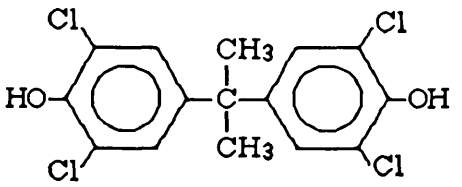

Tetrachlorobisphenol A

6.3.2.3 Poly(tetrabromobisphenol A -terephthalate) (Br-PA5)

i) Condensable volatile products

The SATVA trace in Figure 6.30 shows three peaks. The products at the first peak were identified by ir and mass spectroscopy as carbon dioxide, hydrogen bromide and ethylene, together with traces of hydrogen chloride. The second peak was due to benzene. The products at the last peak were examined by GC-MS. The gas chromatogram is shown in Figure 6.31 and the assignments for each peak are given in Table 6.15. These results indicate the presence of 4.4'-methylene bis(2-bromophenol), o-bromophenol and 2.6-dibromophenol as the major products, with traces of 4-methyl 2-bromophenol, bromobenzene and phenyl benzoate.

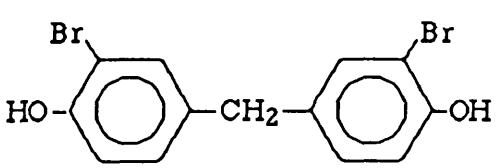

4.4'-Methylene bis(2-bromophenol)

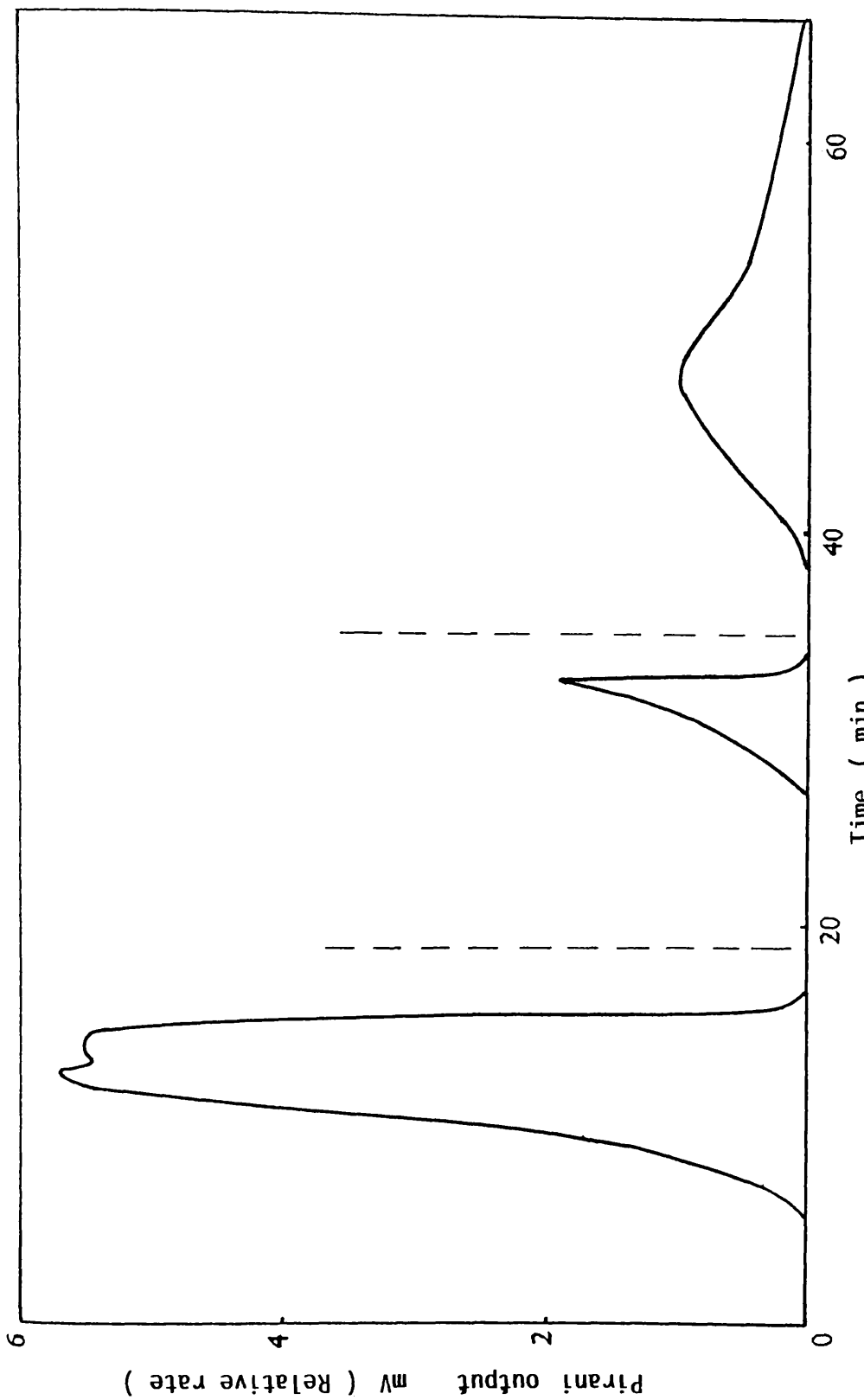

Figure 6.30 : Subambient TVA trace for warm up from 196 ^{o}C to ambient temperature of condensable volatile products from degradation of Br-PA5.

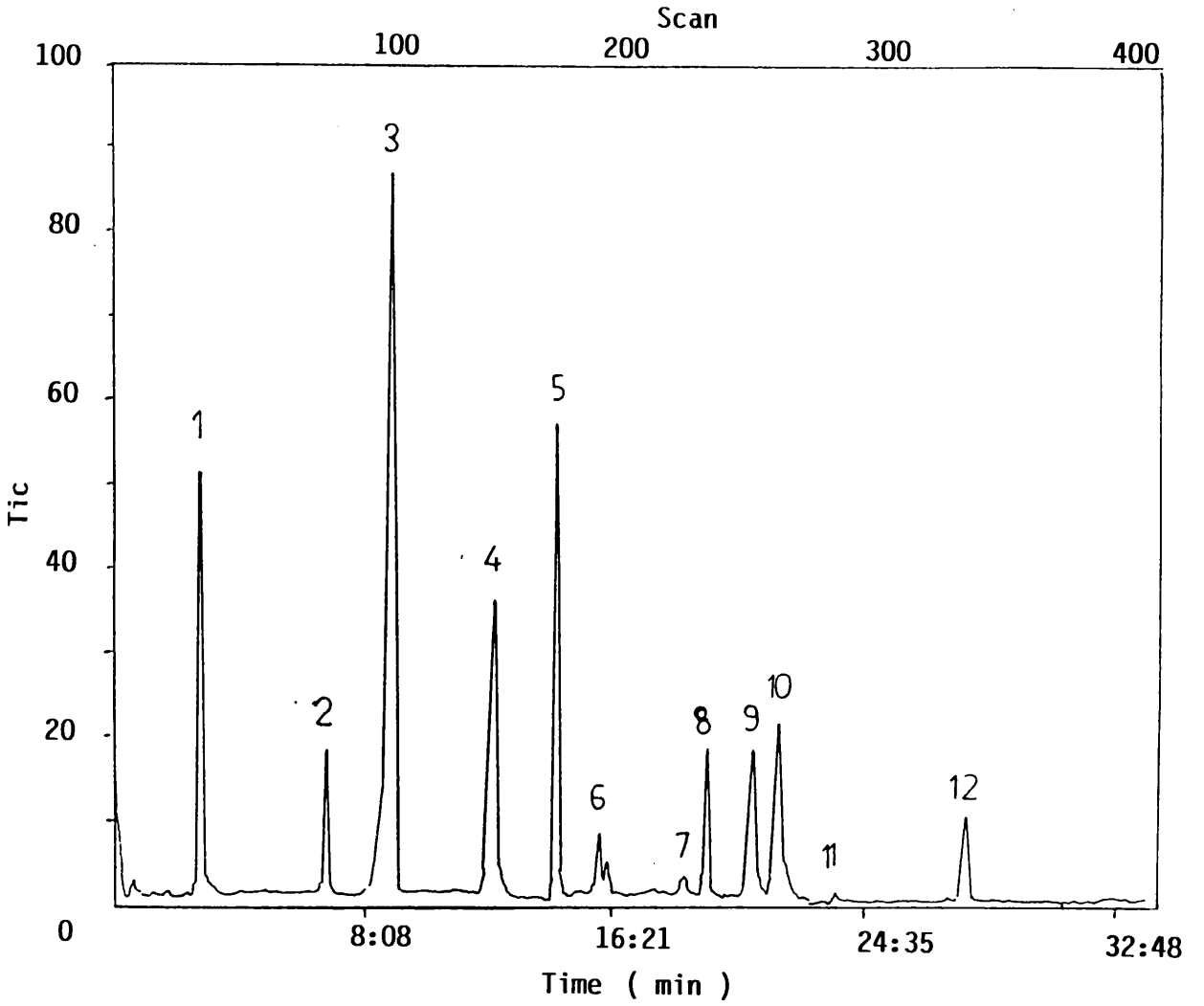

Figure 6.31 : Gas chromatogram for the liquid fraction in SATVA separation of products from the degradation of Br-PA5 .

Peak N°	Assignment	m / e
1	Unidentified	207
2	Bromobenzene	156 157 77
3	4-Ethyl 2.6- dibromophenol	281 133
4, 7	2-Bromophenol	172 173
5	4.4'-Methylene bis(2- bromophenol)	355 267
6	4-Methyl 2-bromophenol	186 107 187
8	Unidentified	429 341
9, 10	2.6-Dibromophenol	252 251
11	Unidentified	415 281 147
12	Phenyl benzoate	198 105 77

Table 6.15: The assignment of the peaks in the gas chromatogram, shown in Fig.6.31, for the liquid fraction from SATVA separation of products of degradation of Br-PA5 to 600 °C under TVA conditions.

ii) Cold Ring Fraction (CRF)

The total of CRF deposited on the cooled upper part of the TVA tube was examined by means of ir and mass spectroscopy. The ir spectrum of the CRF shows the absorption bands characteristic of terephthalic acid. In addition there is a band at 1740 cm^{-1} which is attributed to (-CO-) stretching vibration of an ester group. Mass spectra of the CRF from the degradation of Br-PA5 were obtained at probe temperatures of 200, 250, 300 and 330 ^{o}C, respectively. These spectra exhibit abundant peaks corresponding to the molecular and fragment ions of tetrabromobisphenol A (m/e = 544, 529), terephthalic acid (m/e = 166, 149) terephthaldehydic acid (m/e = 150), benzoic acid (m/e = 122) and short chain fragments VI (m/e = 676), VII (m/e = 648) and VIII (m/e = 530) as shown in Table 6.16

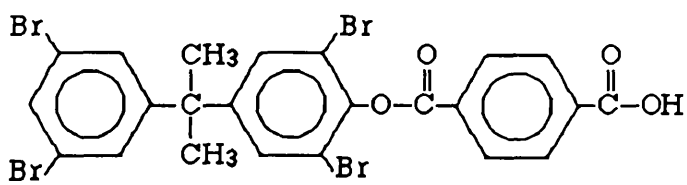

VI

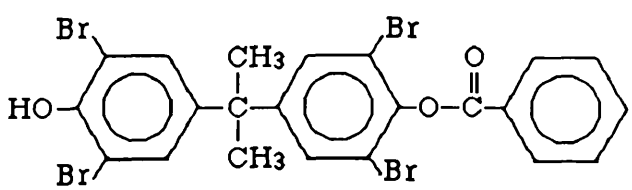

VII

Component	m / e	Abundance %			
		200 °C	250 °C	300 °C	330 °C
Tetrabromobisphenol A	545	12.4	14.2	5.2	7.5
	530	53.8	52.4	25.6	36.6
	528	38.5	35.9	17.8	25.6
Terephthalic acid	166	—	3.4	2.3	4.6
	149	—	77	21	55.5
Terephthaldehydic acid	151	22.7	10.4	8	15.3
	150	15.3	13	6.5	14.5
	149	53.4	77	21	55.5
Benzoic acid	122	—	2.6	4.4	5.7
	105	—	100	100	100
VI	676	—	0.7	—	—
	675	—	2.1	—	—
	527	—	4.3	—	—
VII	648	—	1.4	0.3	0.5
	647	—	13.2	3.3	4.7
	100	—	100	100	100
VIII	532	—	34.4	16.5	23.4
	531	—	10.4	4.9	7.2
	514	—	4	2.9	3.4

Table 6.16: Material present in the CRF from degradation of Br-PA5 under TVA conditions to 500 °C, at the probe temperatures shown.

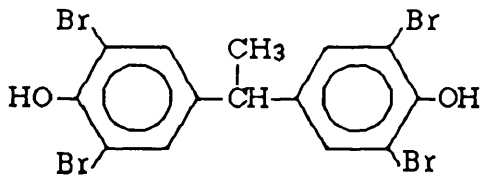

VIII

6.3.2.4 Poly(4.4'-diethoxy tetrabromobisphenol A-terephthalate) (Br-PA6)

i) Condensable volatile products

The condensable volatile products were separated into three fractions using the SATVA technique, as shown in Figure 6.32. The products in the first fraction were easily identified by ir spectroscopy as carbon dioxide and hydrogen bromide as main components, together with traces of ethylene and hydrogen chloride. The latter is produced from the acid chloride end groups. The second fraction was due to vinyl bromide. The products at the third peak were collected as liquid fraction and separated using GC-MS. A typical gas chromatogram, in which seventeen peaks are observed, is shown in Figure 6.33 and the assignments are given in Table 6.17. The principal product is 2-bromo-4-methyl phenol together with much smaller amounts of bromobenzene, methyl and ethyl benzoates and 2-bromoethanol.

ii) Cold ring fraction (CRF)

The material which collected on the cooled upper part of the TVA tube was in two distinct bands. The upper CRF was shown by ir and mass spectroscopy to consist mainly of terephthalic acid with a short chain

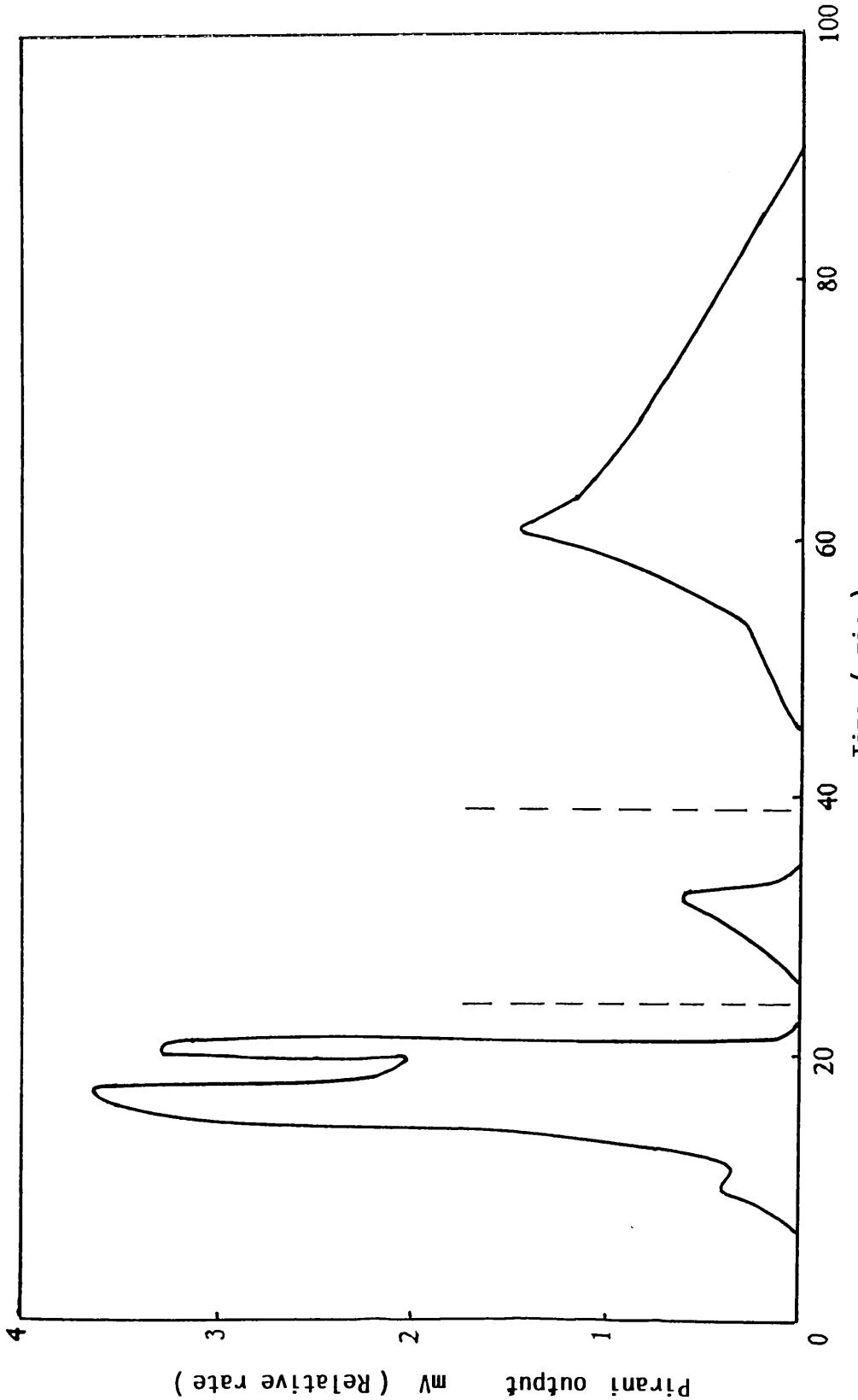

Figure 6.32 : Subambient TVA trace for warm up from 196 ^{o}C to ambient temperature of condensable volatile products from degradation of Br-PA6.

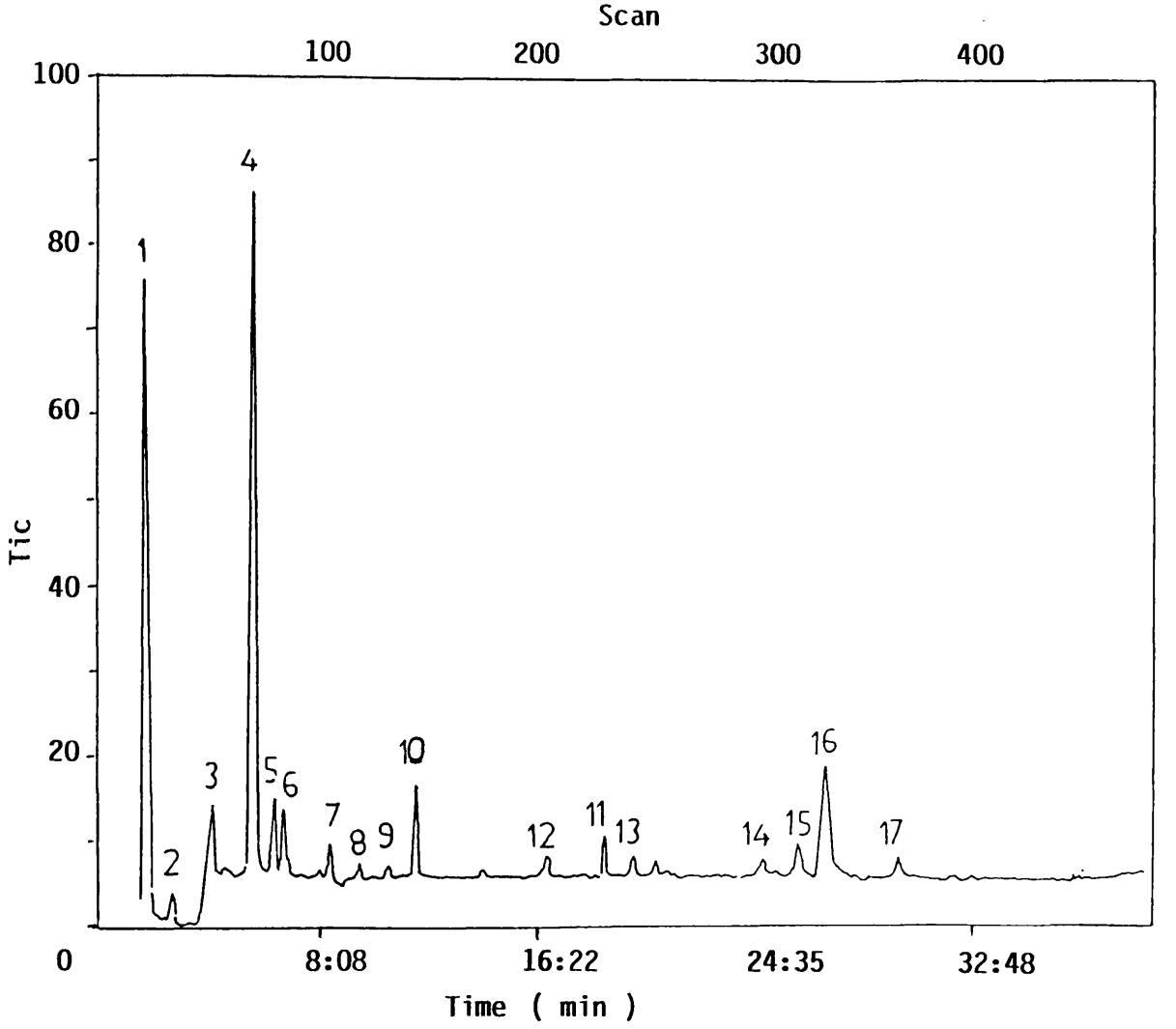

Figure 6.33 : Gas chromatogram for the liquid fraction in SATVA separation of products from the degradation of Br-PA6 .

Peak N°	Assignment	m / e
1	Diethyl ether (solvent)	74 59
2	Unidentified	70 69
3	2-Bromoethanol	124 126 45
4	4-Methyl 2-bromophenol	
5	Unidentified	96 67 53
6	"	70 69
7	Ethyl benzene	106 91
8	Bromobenzene	156 157 77
9	Unidentified	314 235 148
10	4-Ethyl 2.6-dibromophenol	281 261
11	Methyl benzoate	105 136 77
12	4.4'-Methylene bis(2-bromophenol)	355 456 267
13	Ethyl benzoate	105 77 122 150
14	Unidentified	429 341 250
15, 16	2.6-Dibromophenol	252
17	Benzoic acid	105 122 77

Table 6.17: The assignment of peaks in the gas chromatogram, shown in Fig.6.33, for the liquid fraction from SATVA separation of degradation products to 500 °C under TVA conditions of Br-PA6.

fragment, benzoic acid and terephthaldehydic acid as minor products. The ir spectrum of the lower part of CRF showed the characteristic frequencies of the original polymer. In addition, the mass spectra of the total CRF, recorded at the probe temperatures of 200, 250 and 300 ^{o}C, show peaks corresponding to the molecular and fragment ions of tetrabromobisphenol A (m/e = 544), terephthalic acid (m/e = 166), terephthaldehydic acid (m/e = 150), benzoic acid (m/e = 122), mono-ethyl terephthalate (m/e = 193), di-hydroxyethyl terephthalate (m/e = 255) and short chain fragments IX (m/e = 299, 301) and VIII (m/e = 530) as listed in Table6.18.

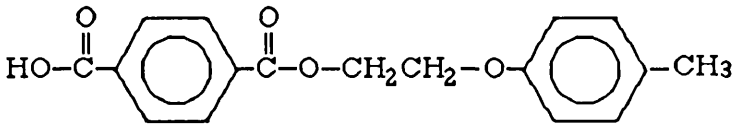

IX

6.4 MECHANISM OF DECOMPOSITION

There have been only a few studies of the thermal behaviour of polyarylates, in which attention has been focused on the formation of cyclic oligomers [61] and the effect of halogen substituents on the stability [62].

The variety of degradation products formed suggests that the general mechanism of decomposition of polyarylates may be explained on the basis of two main processes, namely, random scission and decarboxylation. The overall proposed reactions are presented by the general mechanism shown in Scheme 6.2.

Component	m / e	Abundance %		
		200 °C	250 °C	300 °C
Tetrabromobisphenol A	544	2.4	1.4	—
	529	6.1	8.1	—
Terephthalic acid	166	8.3	16.8	21.7
	149	46.3	99.9	100
Terephthaldehydic acid	150	10	12	12.8
	149	46.3	99.9	100
Benzoic acid	122	3.2	4.4	3.3
	105	28.6	33	28.9
IX	301	18.7	100	29.7
	299	21.5	99.9	29.7
Monoethyl terephthalate	194	2.5	5.9	5.2
	193	7.4	40.3	31.9
	177	4.7	11.2	8.3
VIII	532	30.4	0.4	3.6
	530	47.9	1.5	5.6
Di-hydroxyethyl terephthalate	514	27.4	57.8	35.8

Table 6.18: Materials present in the CRF from degradation of Br-PA6 under TVA conditions to 500 °C, at probe temperatures shown.

The formation of hydrogen chloride during the early stage of degradation, suggests that the predominant initial step in the decomposition is invariably acyl-chlorine bond scission, which leads to macroradical (A). There are many possible pathways for subsequent scissions of the macroradical (A) to yield various products. The formation of the cyclic monomer and dimer in the case of Br-PA4 and PA4 can be accounted for by homolytic cleavage of the macroradical (A) at the positions (e) and (h), respectively, followed in each case by cyclisation (pathway 1). The formation of dihydroxyaryl terephthalates can result from chain scissions at the positions (c) + (h), followed by hydrogen abstraction (pathway 2). Chain scission of the macroradical (A) at the position (c) + (e) can yield a diradical (B) which is most likely to produce aromatic diols. In addition, the formation of hydroquinone (from PA2) is possible by the rearrangement of the diradical (B) as stated below.

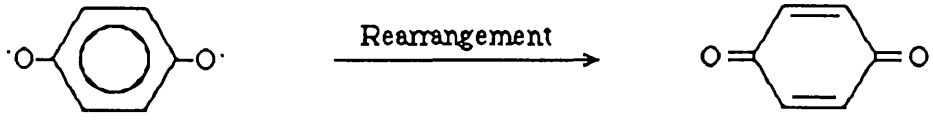

B Benzoquinone

The formation of phenols, which are among the major degradation products, can be accounted for by chain scission at (f) + (d), followed by intermolecular hydrogen abstraction to form various structure of phenols (pathway 4). By a similar mechanism, other aromatic components are formed (pathway 7). In the case of aliphatic / aromatic polyarylates, phenols and aromatic components are formed as a result of chain scissions of the phenoxy

macroradical at the points (a'), (b'), (c') and (e), followed in each case by hydrogen abstraction as shown in Scheme 6.3.

McNeill and Rincon [65] studied the thermal degradation of bisphenol A polycarbonate and suggest that the main decomposition process involves homolysis reaction rather than ester interchange reaction. Also they reported the presence of various degradation products which are almost similar to those of polyarylates based on bisphenol A. In this study, however, the initial thermal degradation of the polyarylates occurs at the ester group.

The formation of monohydroxyaryl terephthalates can be explained by chain scissions of the macroradical (A) at the positions (g) +(c) or (e) + (h), followed by hydrogen abstraction (pathway 3). In the case of all polyarylates studied, except for PA4, terephthalic acid is the major product in the cold ring fraction. The possible route is chain scissions at (g) + (e), followed by hydrogen abstraction (pathway 6).

Benzaldehyde, benzoic acid and terephthaldehydic acid may be produced by chain scissions at (a) + (c), (a) + (d) and (d) respectively, followed in each case by hydrogen abstraction of the macroradical (A).

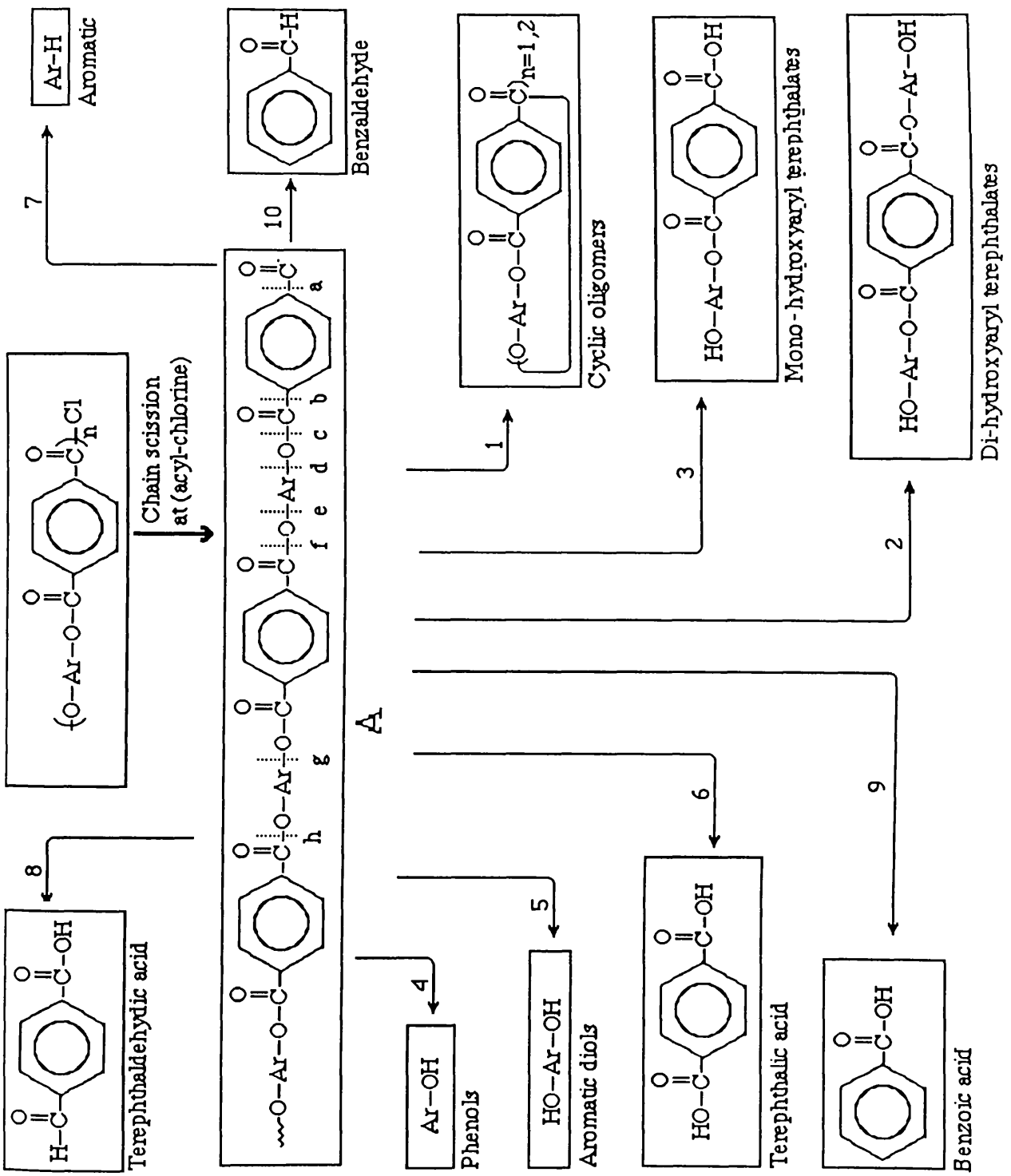
Ar-H
Aromatic
7
Benzaldehyde
10
Chain scission
at (acyl-chlorine)
Cyclic oligomers
Mono-hydroxyaryl terephthalates
Di-hydroxyaryl terephthalates
Terephthaldehydic acid
8
A
1
3
2
4
Ar-OH
Phenols
5
HO-Ar-OH
Aromatic diols
6
Terephthalic acid
9
Benzoic acid

Scheme 6.2

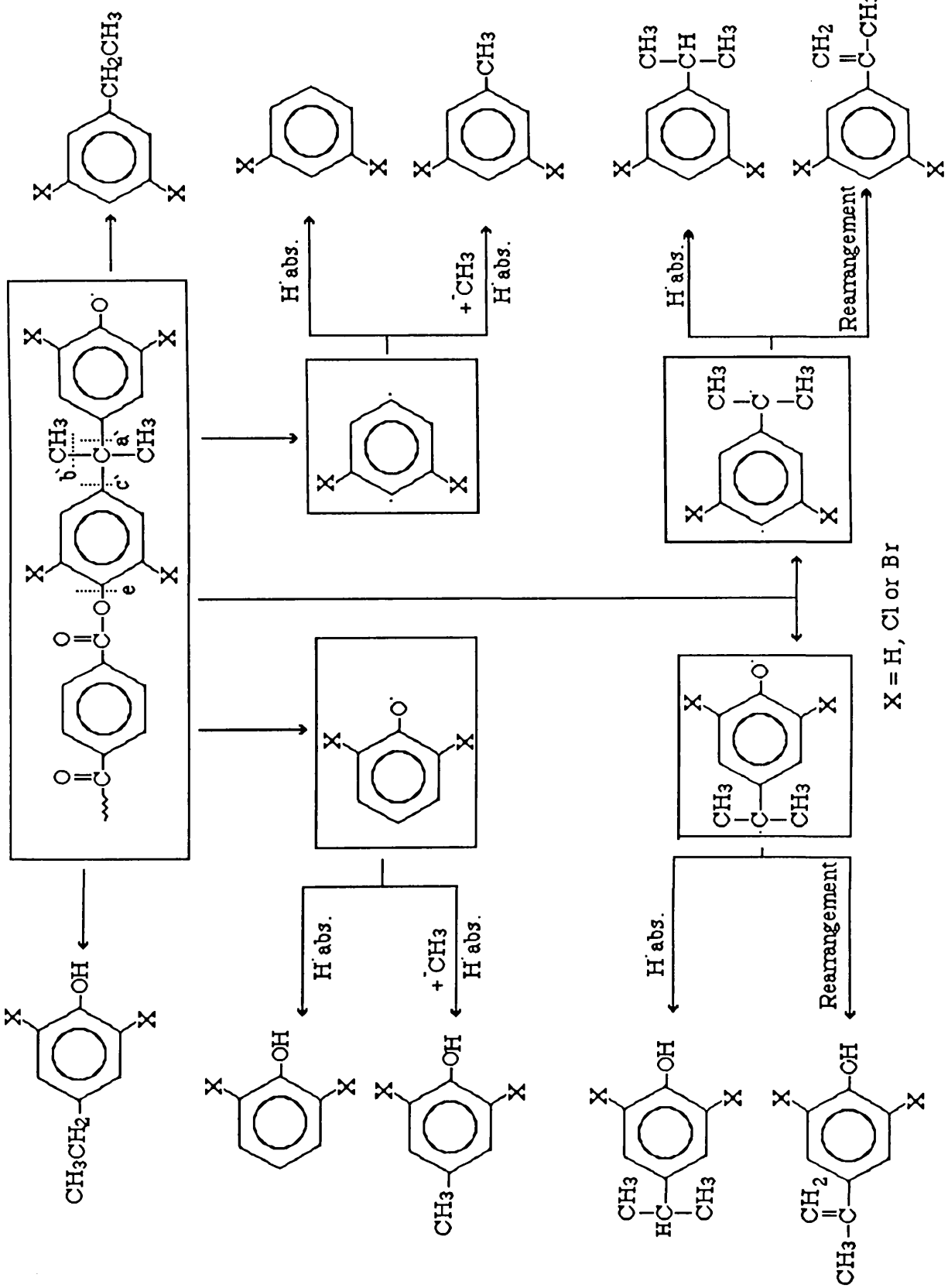

Scheme 6.3 : General mechanism for the formation of aromatics and phenols from the degradation of aromatic / aliphtic polyarylates.

CHAPTER SEVEN

THERMAL DEGRADATION OF TELECHELIC PMMA

7.1 INTRODUCTION

Thermal degradation of poly(methyl methacrylate) (PMMA) has been studied extensively by several investigators during the last 40 years. Grassie and Melville [66] reported that radically prepared PMMA degrades by chain homolysis, followed by unzipping to give quantitative yield of the monomer. The chain scission reactions may initially occur at random points along the polymer chain or specifically at "weak links".

When a vinyl monomer is polymerised by free radical addition polymerisation, termination could occur through either disproportionation or combination reactions of the two radicals as shown in Scheme 7.1 for the methyl methacrylate polymerisation. The disproportionation reaction produces polymer with equal numbers of saturated and unsaturated end groups. Hatada [67] reported that route 1 is the favoured disproportionation reaction leading to the formation of unsaturated chain ends. The combination reaction yields polymer with one head to head linkage within each chain. These abnormal linkages might influence the thermal stability of the polymer structure [68]. Bevington et. al.[69] studied the termination reaction in radical polymerisation of PMMA at 0 and 60 ^{o}C using 2,2'-azo-bis-

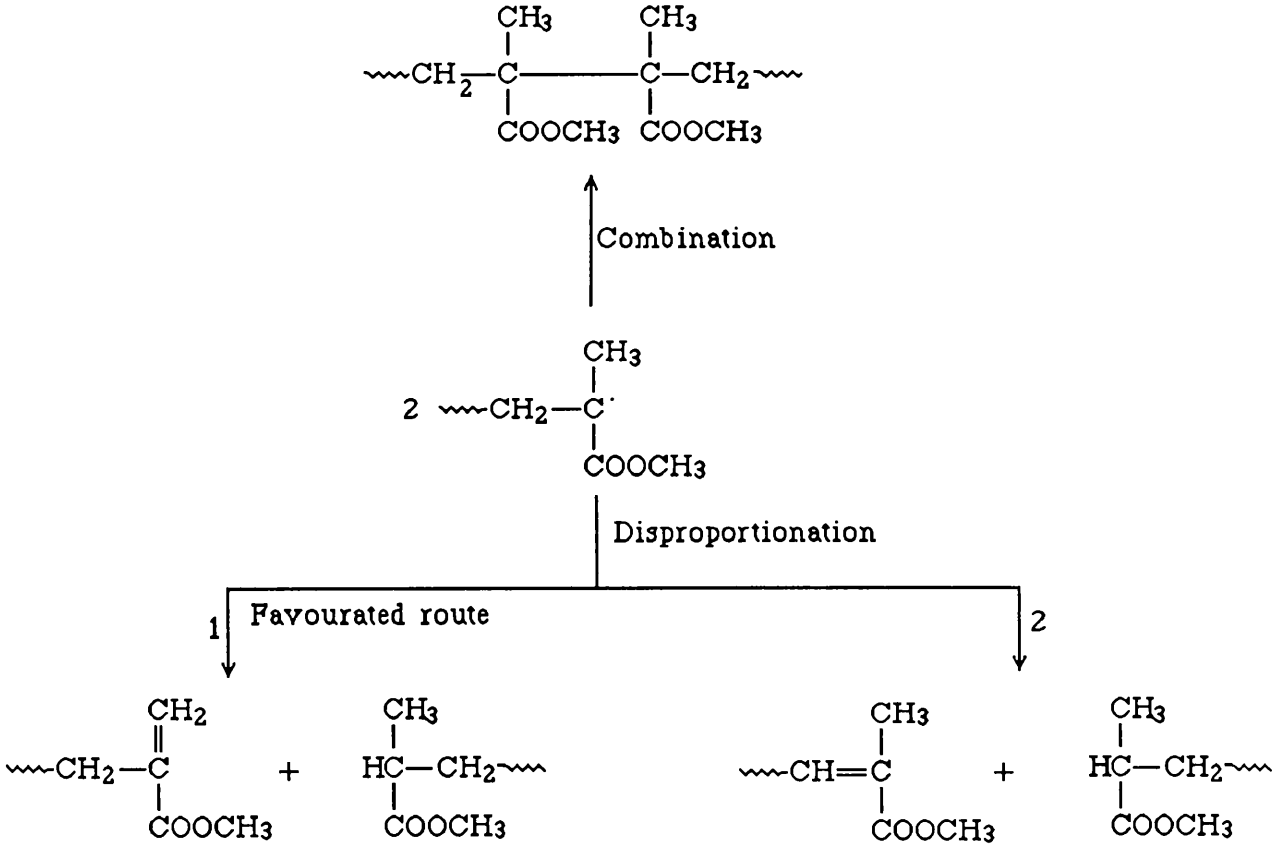
CH3
CH3
CH2—C—C—CH2
COOCH3
COOCH3
Combination
2
CH2—C
CH3
COOCH3
Disproportionation
1
Favourated route
2
CH2
CH2—C
COOCH3
+
CH3
HC—CH2
COOCH3
CH3
CH=C
COOCH3
+
CH3
HC—CH2
COOCH3

Scheme 7.1

isobutyronitrile labeled with ^{14}C as initiator. They found that PMMA radicals undergo disproportionation 6 times as frequently as combination at 60 ^{o}C and 1.5 times as frequently at 0 ^{o}C.

It has been reported that both head to head and unsaturated linkages are weak bonds in the PMMA structure [66,68,70-75]. Grassie and Melville[66] suggested that the unsaturated end groups formed as a result of termination by disproportionation during the polymerisation process are weak links, at which the degradation was first initiated. At higher temperatures the degradation occurs at random points along the polymer chain yielding monomer.

McNeill found that the thermal stability of PMMA is dependent on the method of preparation (whether radical or anionic) and on the molecular weight. In radical PMMA, two stages of decomposition were observed, the first being due to unsaturated chain ends and the second to the random chain scissions. In the case of anionic PMMA, however, the absence of the first peak indicates the influence of double bonds present in the free radical PMMA.Also he observed that as the initial molecular weight increases the T_{max} is higher for the first peak and is lower for the second. In high molecular weight PMMA, the zip length is shorter than the chain length, so in the weak link initiated fragmentation (first peak) the chains do not disappear completely. For Mn = zip length (ca. 200) or less, the chain length is less than the zip length and the chains unzip completely from the unsaturated chain ends [70].

Kashiwagi et.al.[71] found that the thermal degradation of (radically polymerised) PMMA occurs in three distinct stages, and suggested that the first two correspond to initiation at weak links due to head to head and unsaturated end groups, at 165 and 270 ^{o}C, respectively. No direct evidence

was presented, however, for the explanation of the first peak, which is also possibly due to the release of trapped volatile material such as solvent used during the isolation of the polymer since the polymer softens in this temperature region. However, others have reported that the unsaturated end group in PMMA is less stable than the head to head linkage [72].

Manring et. al.[73], showed that the thermal stability of saturated PMMA,which contains no inherent weak link, and head to head PMMA with a degree of polymerisation (DP > 200) are identical. However, when DP<100, head to head PMMA is less stable, indicating that as the molecular weight of the polymer increases, the effective rate of head to head bond scission decreases.

Kashiwagi et.al.[71] studied the degradation of PMMA using thermogravimety (TG), and claimed that the thermal oxidative degradation of PMMA (prepared by radical or anionic route), occurs in one stage with a maximum rate of weight loss at 300 ^{o}C, indicating the effectiveness of gas phase oxygen on the chain scission at head to head linkages.

The preparation of normal and telechelic PMMA has been fully described in chapter three. These polymers have the general structural formula shown below

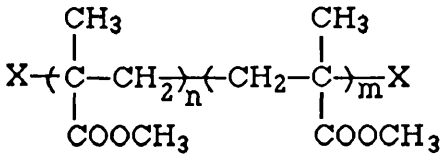

Where X= -H, -COONa, -COOH, -CH_2CH_2ONa and -CH_2CH_2OH

Presumably all these polymer samples have Mn < zip length (i.e. Mn < 20000) and once the radical end forms, the macroradical will unzip completely.

In this chapter, the thermal degradation of telechelic PMMA with terminal -COONa, -COOH, -CH_2CH_2ONa and -CH_2CH_2OH groups has been studied extensively using programmed heating in vacuum or nitrogen atmosphere. The degradation products were fully characterised by means of IR, MS and GC-MS techniques. The general mechanism of decomposition has been proposed.

7.2 THERMAL ANALYSIS

7.2.1 Thermogravimetry (TG)

The TG curves for the normal and α,ω– bifunctional PMMA samples, obtained under dynamic nitrogen atmosphere (50 ml/min) and at a heating rate of 10 ^{o}C/min, are shown in Figure 7.1. The earliest weight loss is attributed to the evolution of petroleum ether, from which the polymer was precipitated. The first step of degradation begins above 210 ^{o}C prior to the main degradation in the range of 325-410 ^{o}C.

The involatile material remaining as a residue at 500 ^{o}C was less than 10% of the original weight of the bifunctional polymer samples and negligible in the case of normal PMMA.

7.2.2 Differential Thermal Analysis (DTA)

The DTA traces for the normal and α,ω–bifunctional PMMA samples are shown in Figure 7.2. The initial weak endothermic peak at 120-150 ^{o}C is due to release of trapped volatile material (petroleum ether). The later endothermic peak is attributed to the main degradation process as illustrated in Table 7.1. Unfortunately, the evolution of precipitant petroleum

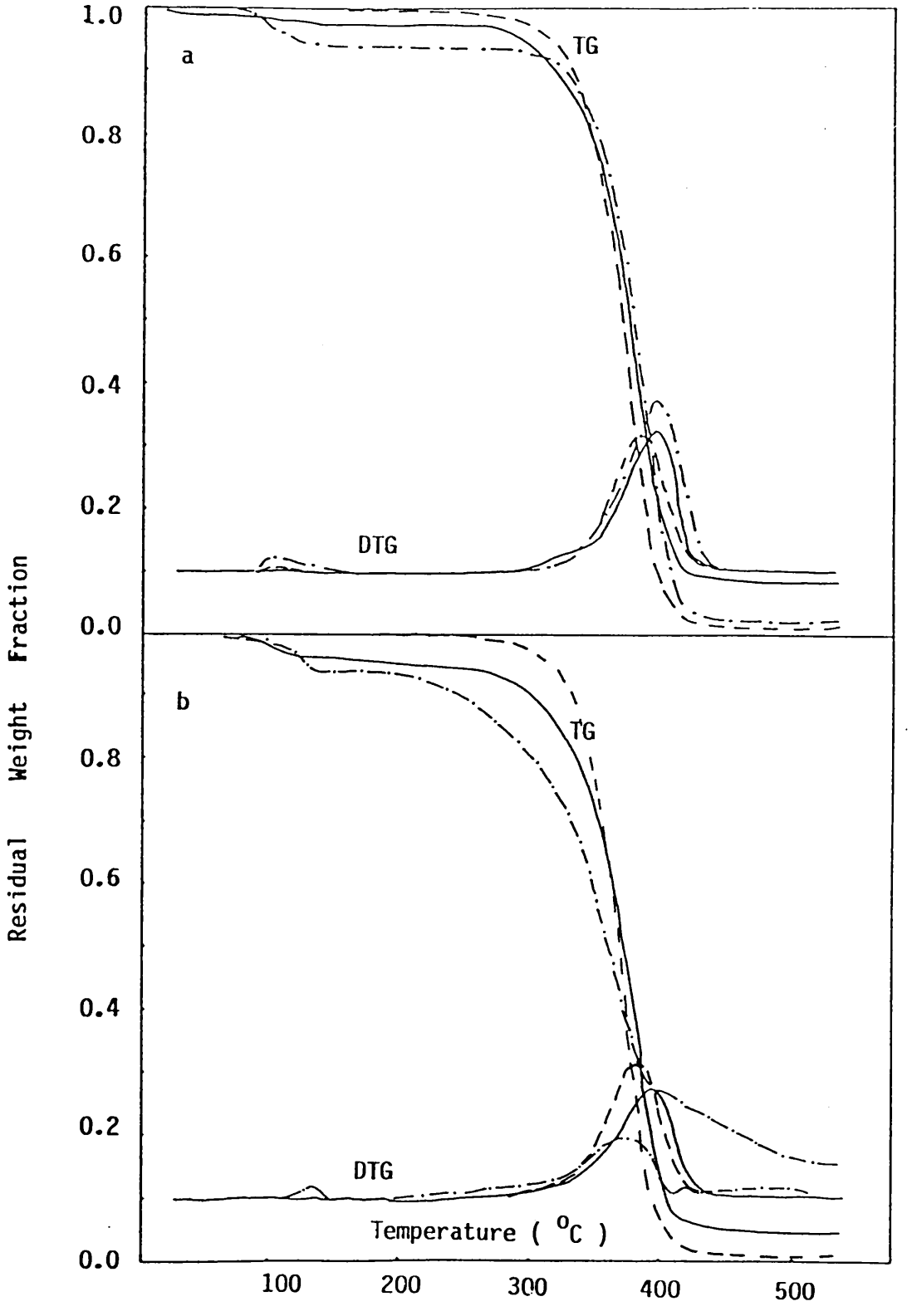

Figure 7.1: TG and DTG traces for degradation of normal and telechelic PMMA under dynamic N_2. Heating rate of 10 °C/min.

a) PMMA-CH_2CH_2ONa (——), PMMA-CH_2CH_2OH (— · —) and PMMA-H (– – –).

b) PMMA-COOH (——), PMMA-COONa (—·—·—) and PMMA-H (– – –).

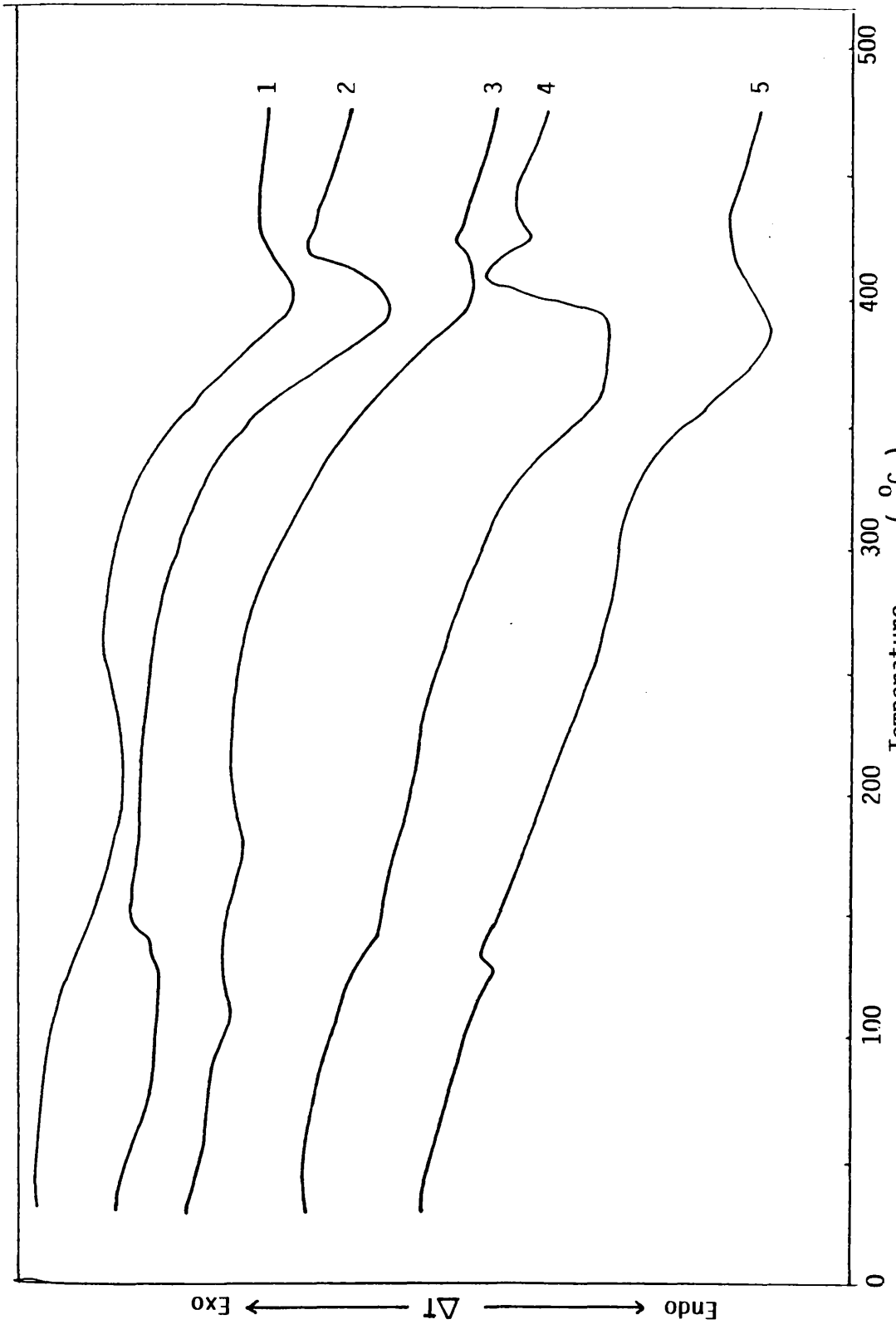

Figure 7.2: DTA curves for 1) PMMA-CH_2CH_2OH , 2) PMMA-CH_2CH_2ONa , 3) PMMA-COOH 4) PMMA-COONa and 5) PMMA-H under dynamic N_2 (50 ml/min) .

	DTG		TG		DTA	
End group in PMMA	T_{max} / °C	Range of wt loss / °C	% wt loss for each stage	% wt of residue at 500 °C	T_{max} / °C	Thermal effect
-H	–	25 – 325	7		125	endothermic[a]
	385	325 – 500	91.5	1.5	385	endothermic[b]
-COONa	132	25 – 150	6			
	–	150 – 325	20.5			
	385	325 – 410	48.5		390	endothermic[b]
	–	410 – 500	10	15	425	endothermic
-COOH	100	25 – 150	3.5			
	–	150 – 325	11.5			
	395	325 – 500	80.5	4.5	400	endothermic[b]
-CH2CH2ONa	132	25 – 150	2.5			
	–	150 – 325	12.5			
	395	325 – 500	76.5	8.5	395	endothermic[b]
-CH2CH2OH	105	25 – 150	6			
	–	150 – 350	14			
	390	350 – 500	77.5	2	395	endothermic[b]

a) glass transition temperature , b) decomposition process

Table 7.1: TG, DTG and DTA data for normal and telechelic PMMA under dynamic N_2 (50 ml / min, 10 °C/min)

ether limits the usefulness of DTA in determining the second order glass transition temperature for the polymers.

7.2.3 Thermal volatilisation analysis (TVA)

The TVA traces for the normal and α,ω–bifunctional PMMA are reproduced in Figures 7.3-7.7. For all of the polymers except PMMA-COONa, the evolution of volatile degradation products begins above 250 °C, leading to the main stage of decomposition which occurs in the range of 325-420 °C, reaching maximum rate of volatilisation around 375-400 °C. In the case of PMMA-COONa, however, onset of degradation is at 210 °C and in addition, a third stage decomposition was observed above 400 °C.

In each of the α,ω- bifunctional PMMA samples, there is an increase in response in the -75, -100 and -196 °C traces at the end of the main stage of decomposition, compared with the TVA behaviour of normal PMMA. This phenomenon is due to the fact that a side chain reaction process, releasing low boiling point volatile products.

Cold ring fraction and residue were also present in all casès, except for normal PMMA. The formation of non-condensable gases was detected during the main stage of decomposition process.

The main features of the TVA data are summarised in Table 7.2. Although the initial decomposition of PMMA-COONa begins 50 °C earlier than for the remaining polymers, telechelic PMMA with the terminal carboxylic acid or sodium carboxylate groups shows higher stability as measured by T_{max} . The residue left from the degradation of telechelic PMMA samples was greater in polymers containing sodium ion . Evidently the involatile material remaining as residue consists mainly of sodium carbonate.

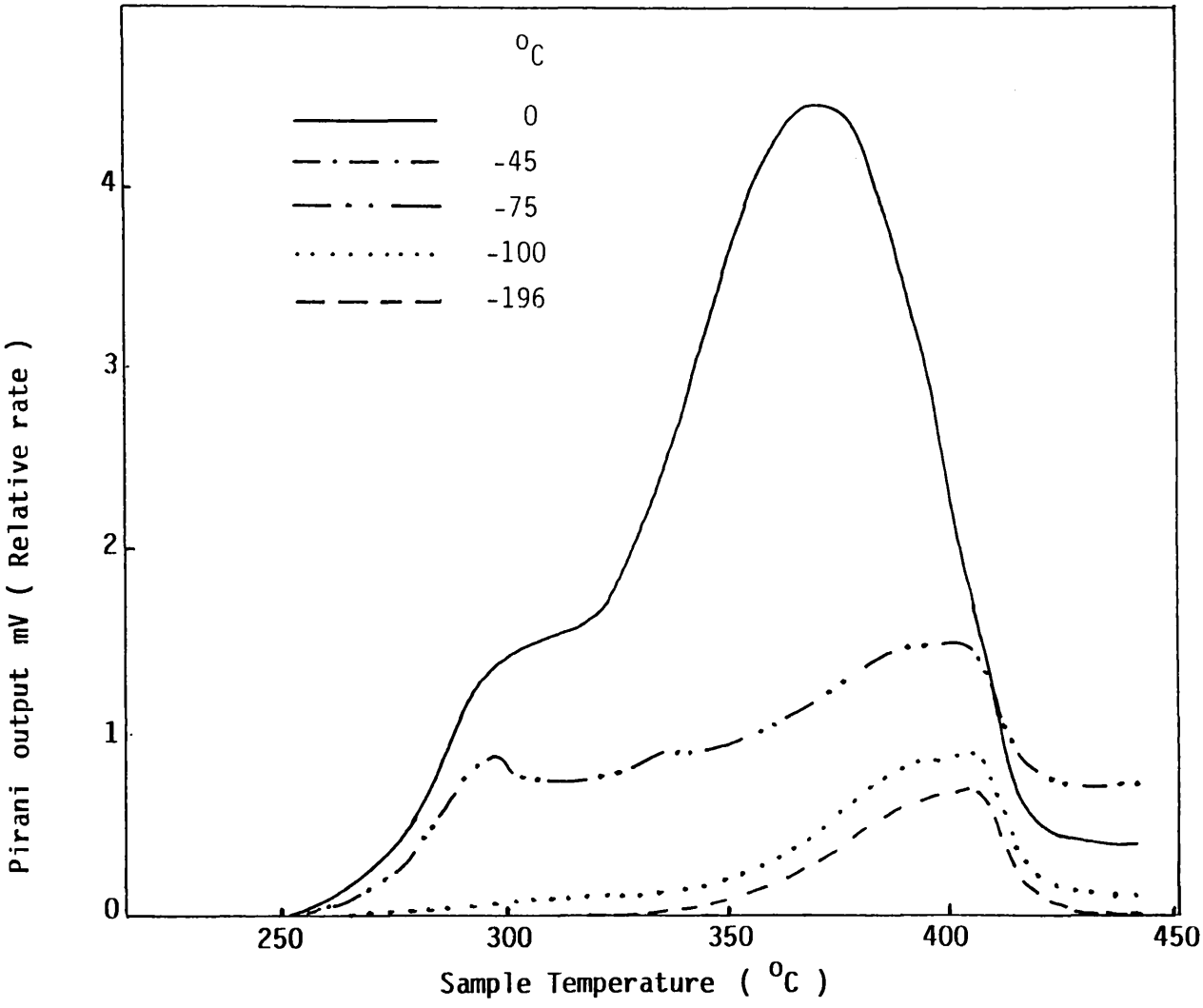

Figure 7.3: TVA traces for PMMA-H heated to 500 °C. Heating rate of 10 °C/min .

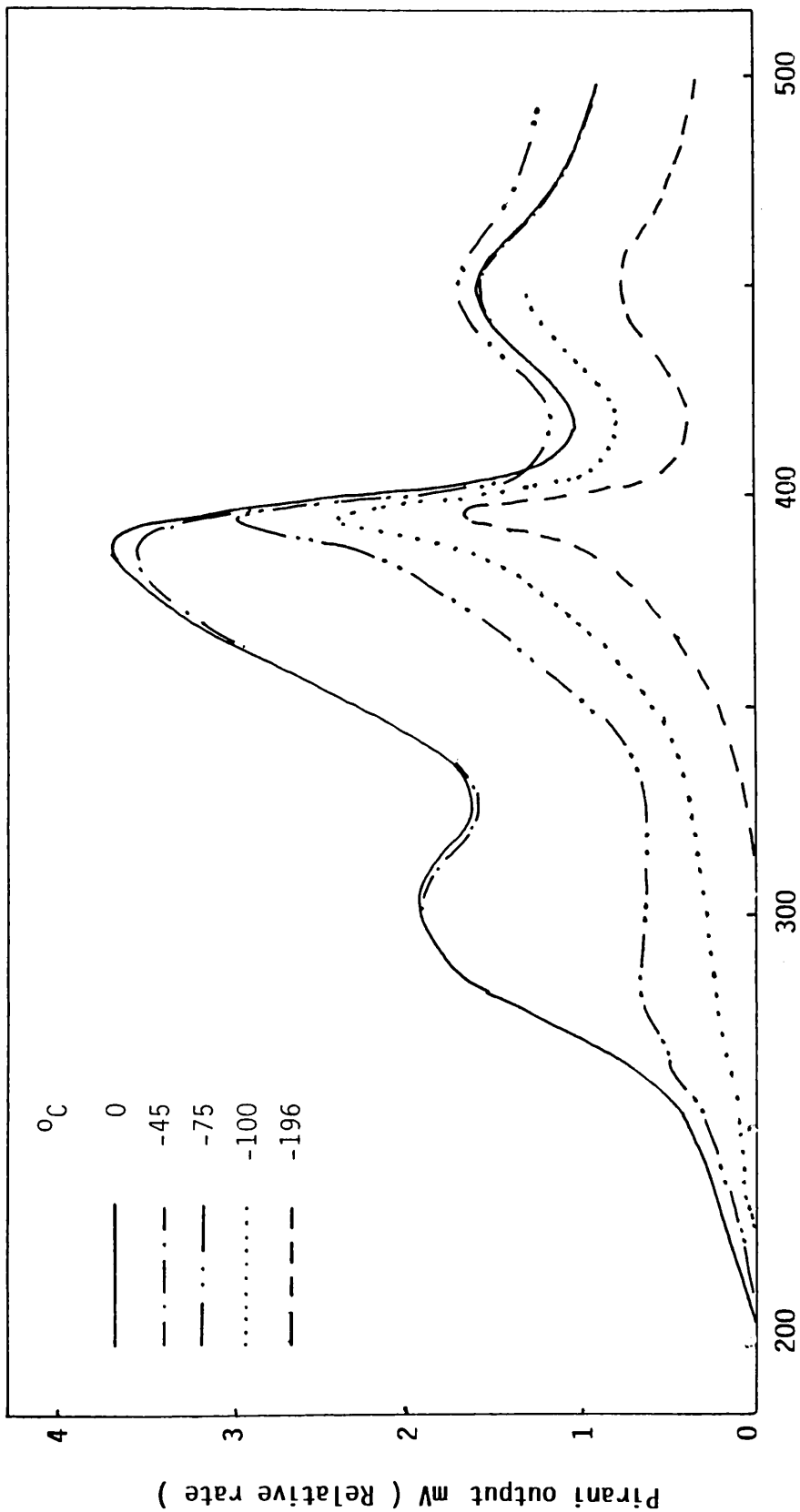

Figure 7.4: TVA traces for PMMA-COONa heated to 500 ^{o}C . Heating rate 10 ^{o}C/min .

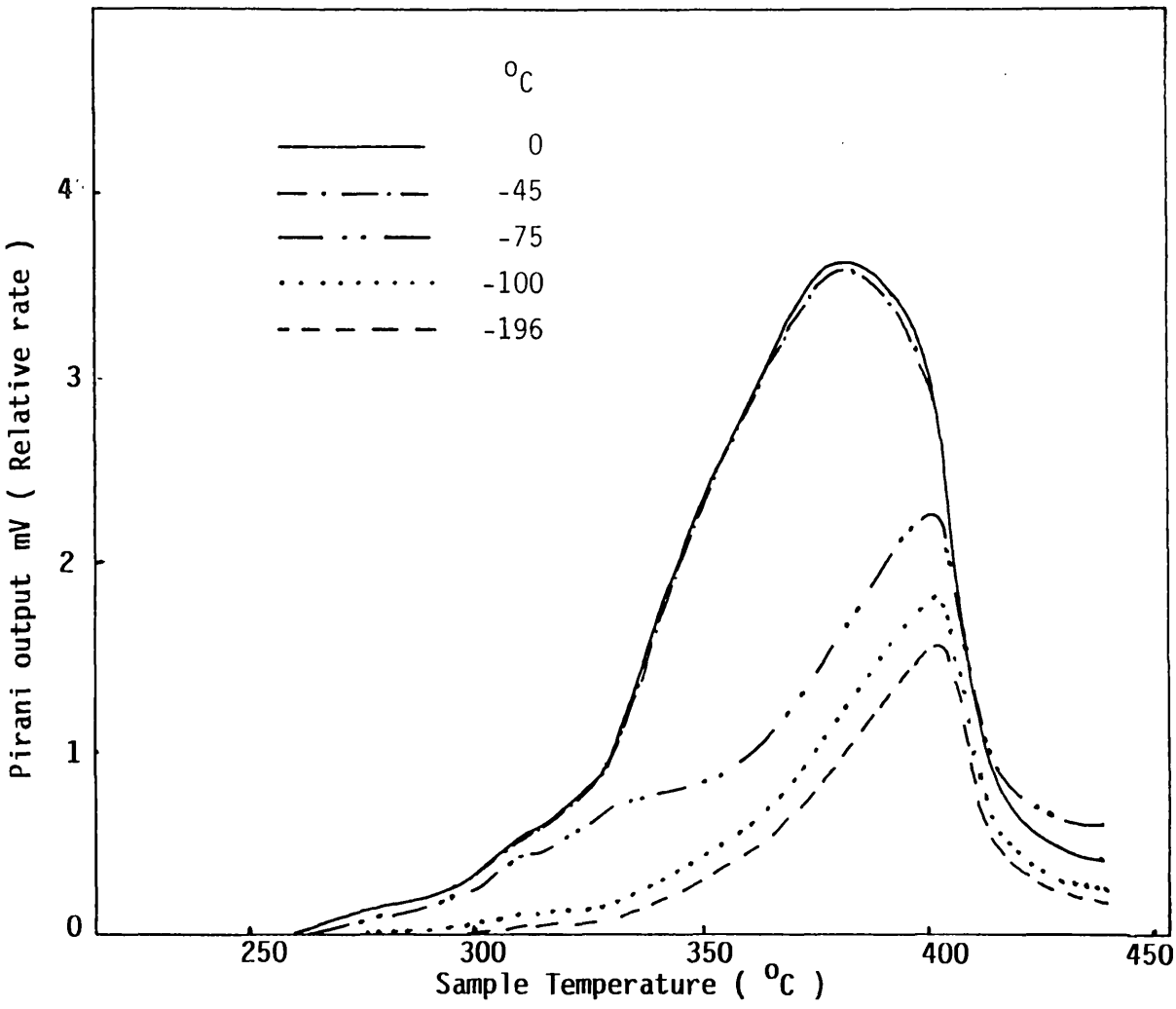

Figure 7.5: TVA traces for PMMA-COOH heated to 500 °C . Heating rate rate of 10 °C/min .

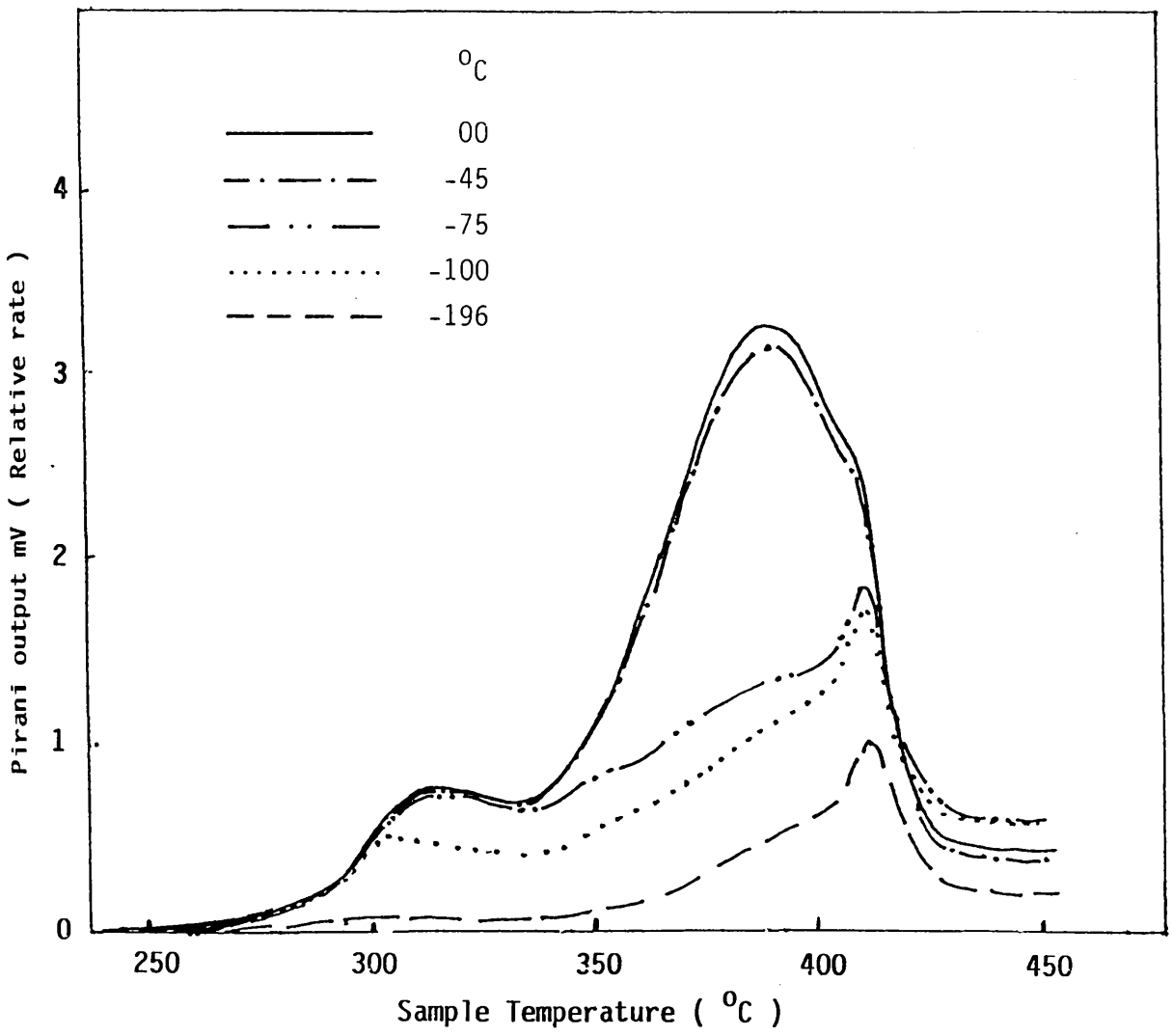

Figure 7.6: TVA traces for PMMA-CH_2CH_2ONa heated to 500 °C . Heating rate of 10 °C/min .

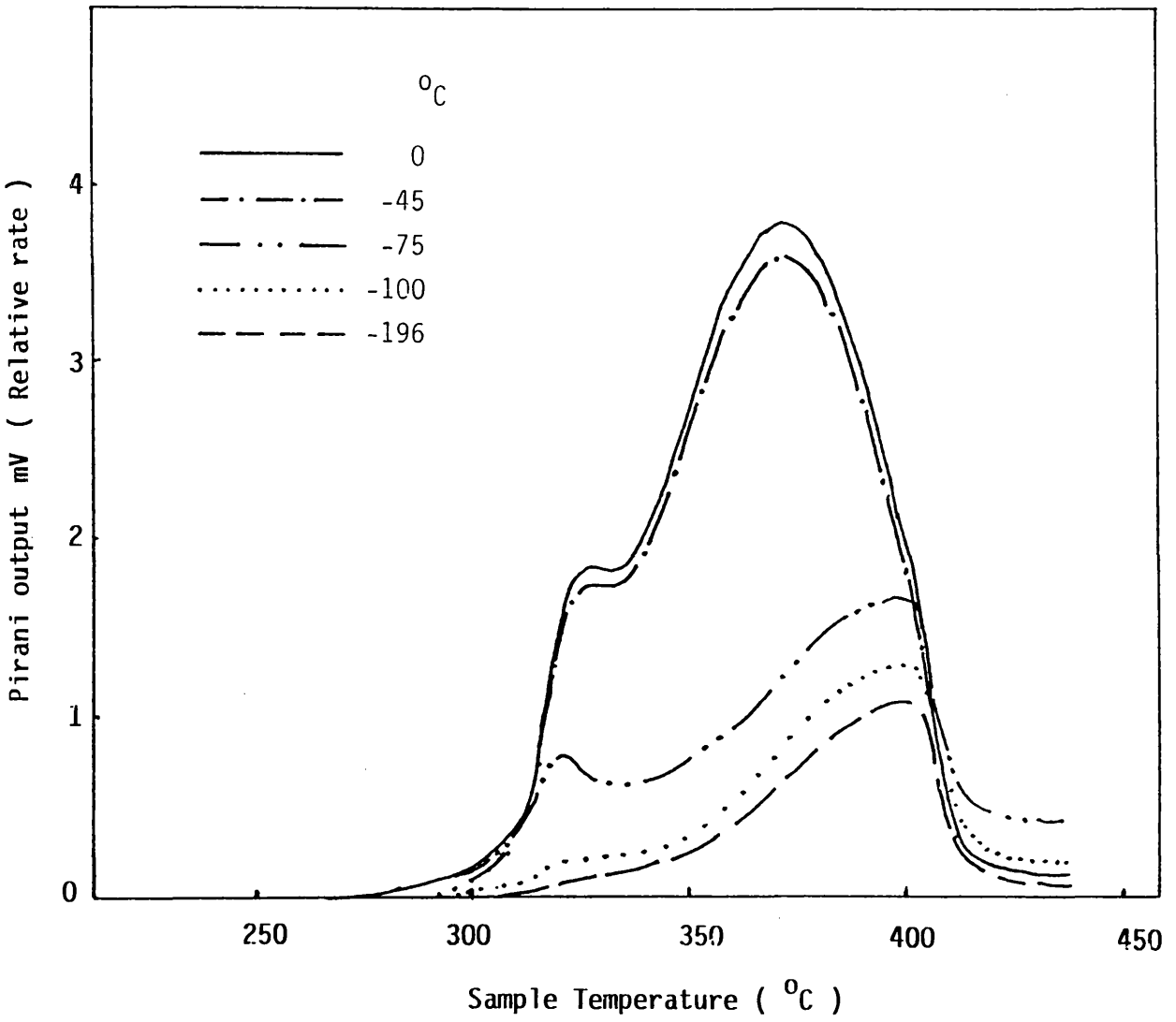

Figure 7.7: TVA traces for PMMA-CH_2CH_2OH heated to 500 °C . Heating rate of 10 °C/min .

PMMA	Functional end group				
	-H	-COONa	-COOH	$-CH_2CH_2ONa$	$-CH_2CH_2OH$
T_{onset} / °C	270	205	265	252	270
$T_{max\,1}$ / °C	–	305	–	310	328
$T_{max\,2}$ / °C					
a)	370	390	385	382	375
b)	–	395	400	410	400
$T_{max\,3}$ / °C	–	445	–	–	–
Volatile products at room temperature wt %	100	76.6	84.2	83.6	87.9
Cold ring fraction wt %	–	12.9	12.5	11.5	10.2
Residual fraction at 500 °C wt %	–	10.5	3.3	4.9	1.9

Table 7.2: TVA data for the degradation of normal and telechelic PMMA samples heated to 500 °C

Quantitative measurement indicated that the residue from the degradation of PMMA-COONa is about twice that from PMMA-CH_2CH_2ONa. This might be due, however, to the higher molecular weight of PMMA-CH_2CH_2ONa.

7.3 CHARATERISATION OF DEGRADATION PRODUCTS

The products released from the heating to 500 °C of normal and α,ω–bifunctional poly(methyl methacrylate) under TVA conditions were fractionated into four main types in accordance with their volatility. The condensable volatile products at -196 °C, were further divided into gases and liquids, which were analysed by means of IR, MS and GC-MS techniques. The cold ring fraction formed on upper part of the inner wall of the TVA tube was dissolved in low boiling point solvent (methylene chloride) for quantitative and spectroscopic analysis. The residual fraction was found to consist of sodium carbonate in polymers containing sodium metal and char for the remaining α,ω–bifunctional PMMA samples.

7.3.1 Condensable Volatile Products

The SATVA traces for the condensable volatile products from the degradation of normal and α,ω–bifunctional PMMA samples, shown in Figures 7.8-7.12, exhibit two main fractions in general. The first fraction products were found to consist mainly of carbon dioxide (major) and dimethyl ether, together with traces of butene-1, isobutene and dimethyl ketene (PMMA-COONa only). In contrast, only a trace of carbon dioxide was detected from normal PMMA.

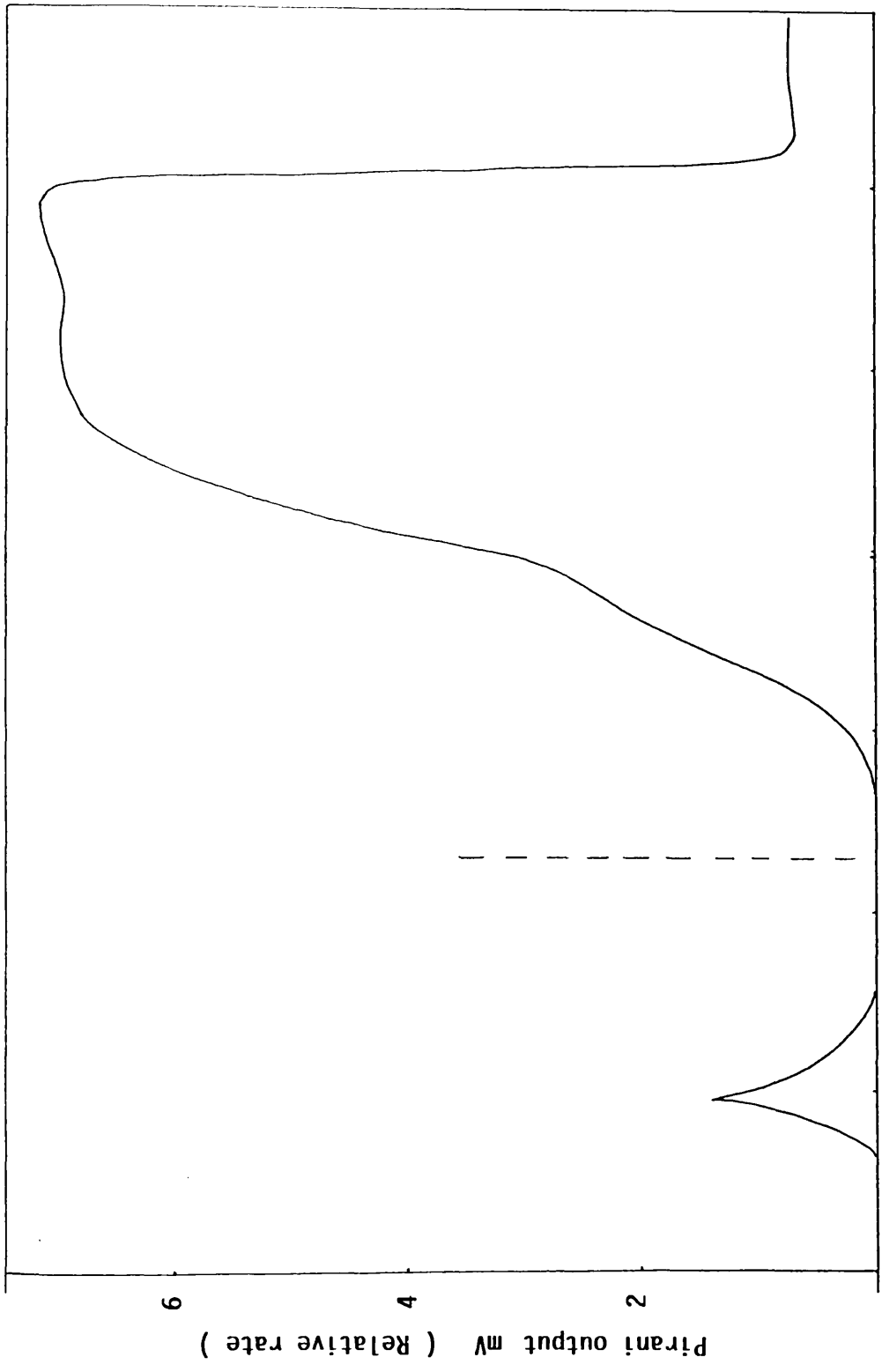

Figure 7.8: Subambient TVA trace for warm up from -196 ^{o}C to ambient temperature of condensable volatile products from degradation of PMMA to 500 ^{o}C .

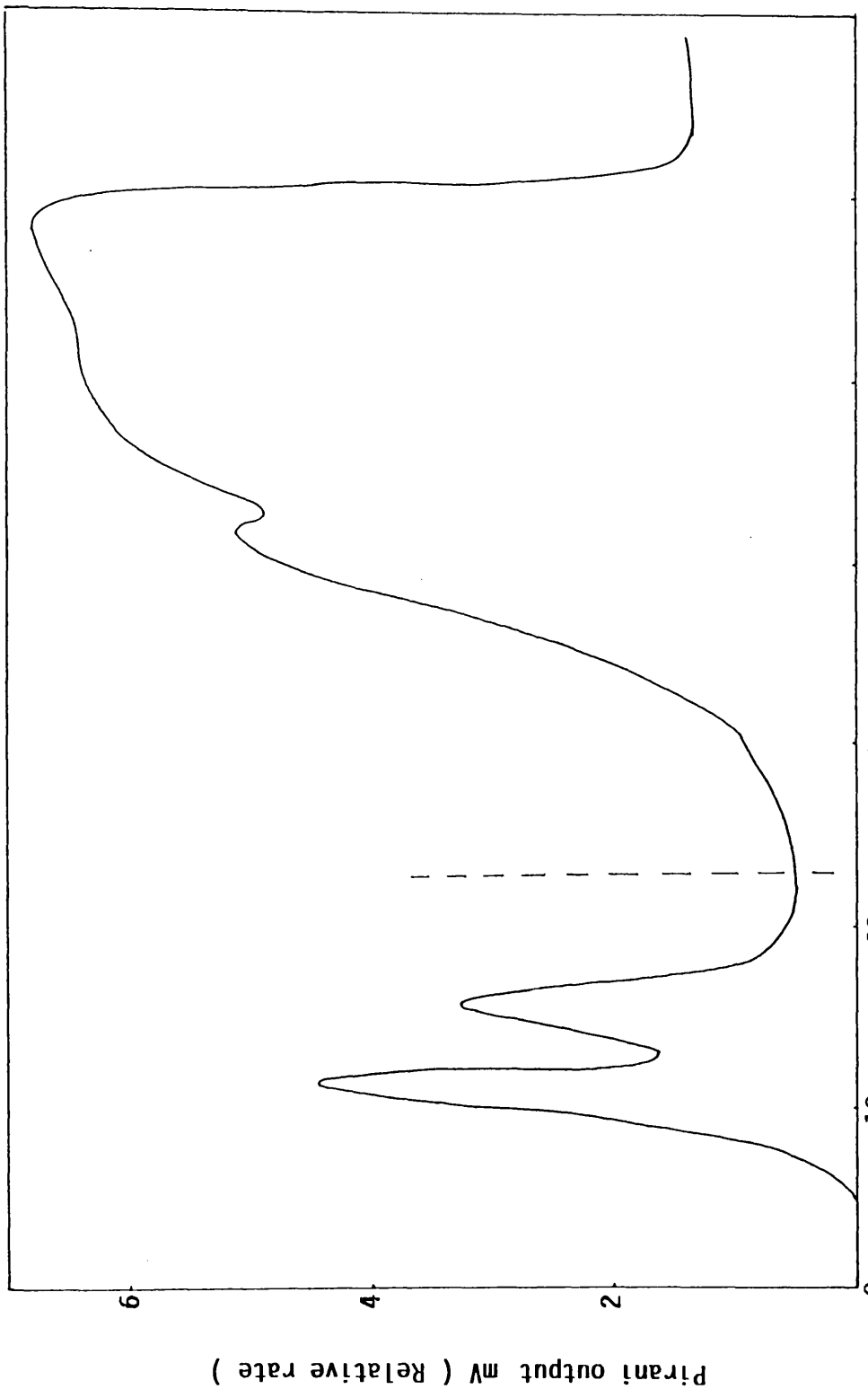

Figure 7.9: Subambient TVA trace for warm up from -196 ^{o}C to ambient temperature of condensable volatile products from degradation of PMMA-COONa to 500 ^{o}C .

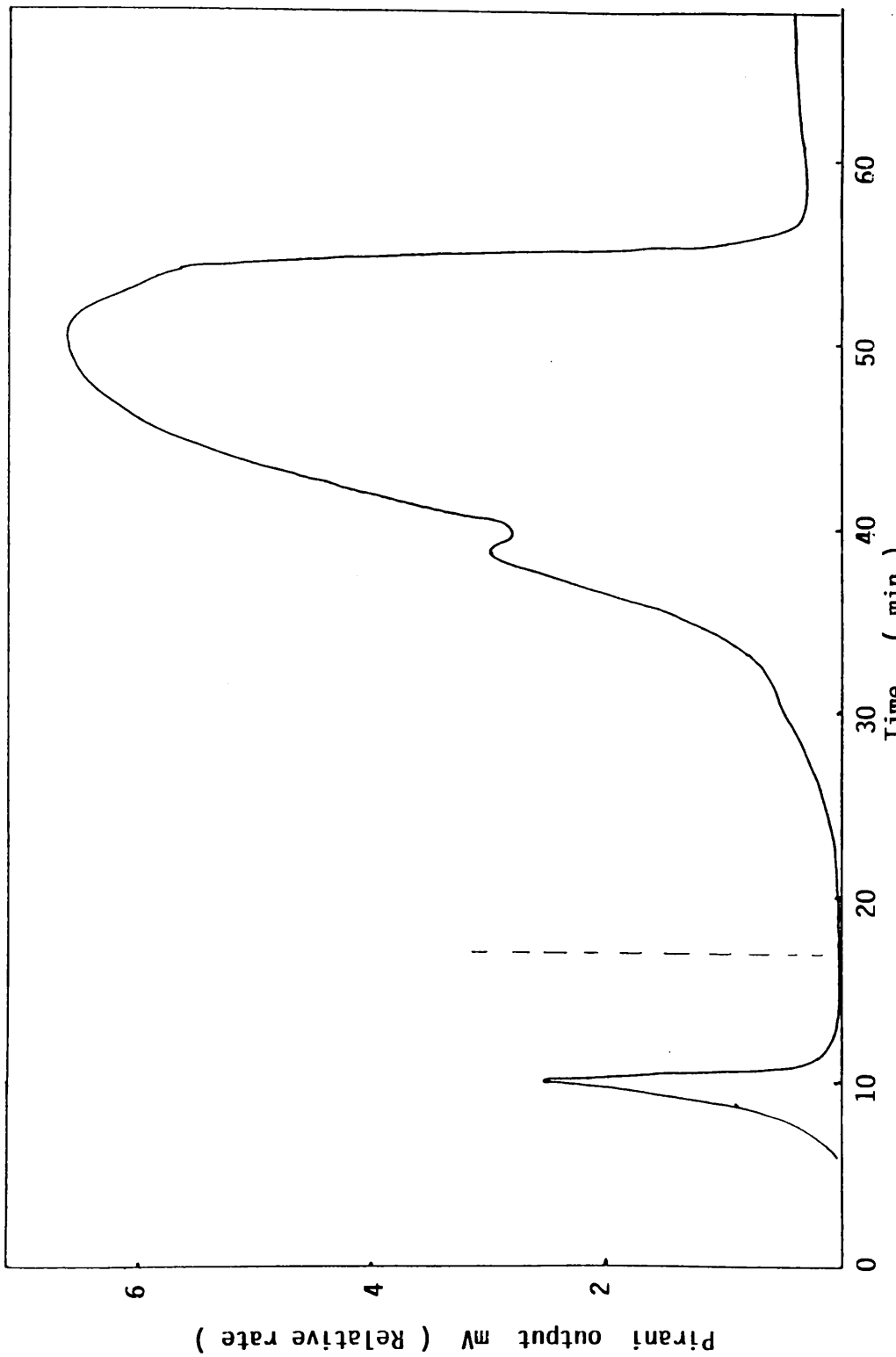

Figure 7.10: Subambient TVA trace for warm up from -196 ^{o}C to ambient temperature of condensable volatile products from degradation of PMMA-COOH to 500 ^{o}C.

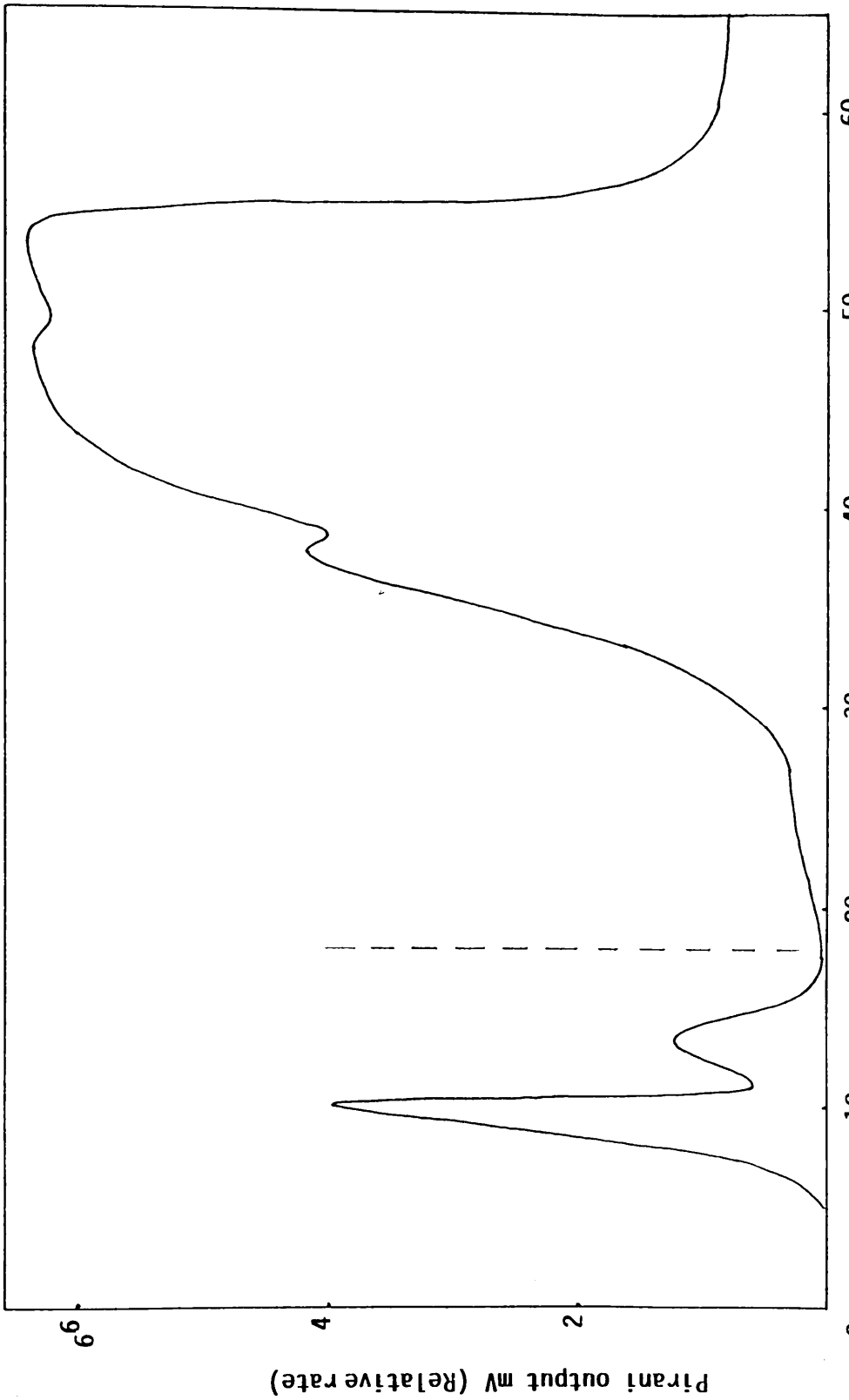

Figure 7.11: Subambient TVA trace for warm up from -196 ^{o}C to ambient temperature of condensable volatile products from degradation of PMMA-CH_2CH_2ONa to 500 ^{o}C .

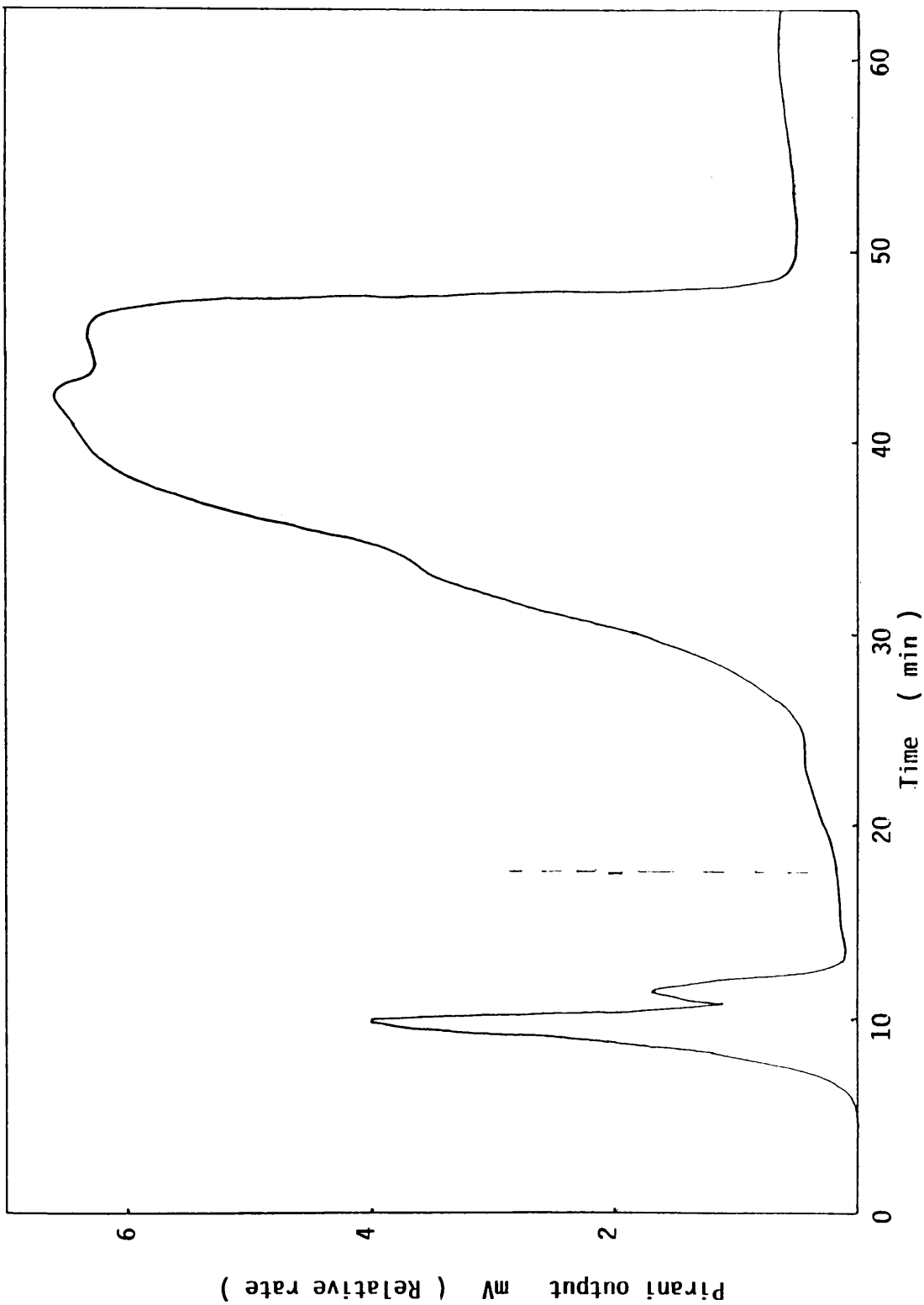

Figure 7.12: Subambient TVA trace for warm up from -196 ^{o}C to ambient temperature of condensable volatile products from degradation of PMMA-CH_2CH_2OH to 500 ^{o}C .

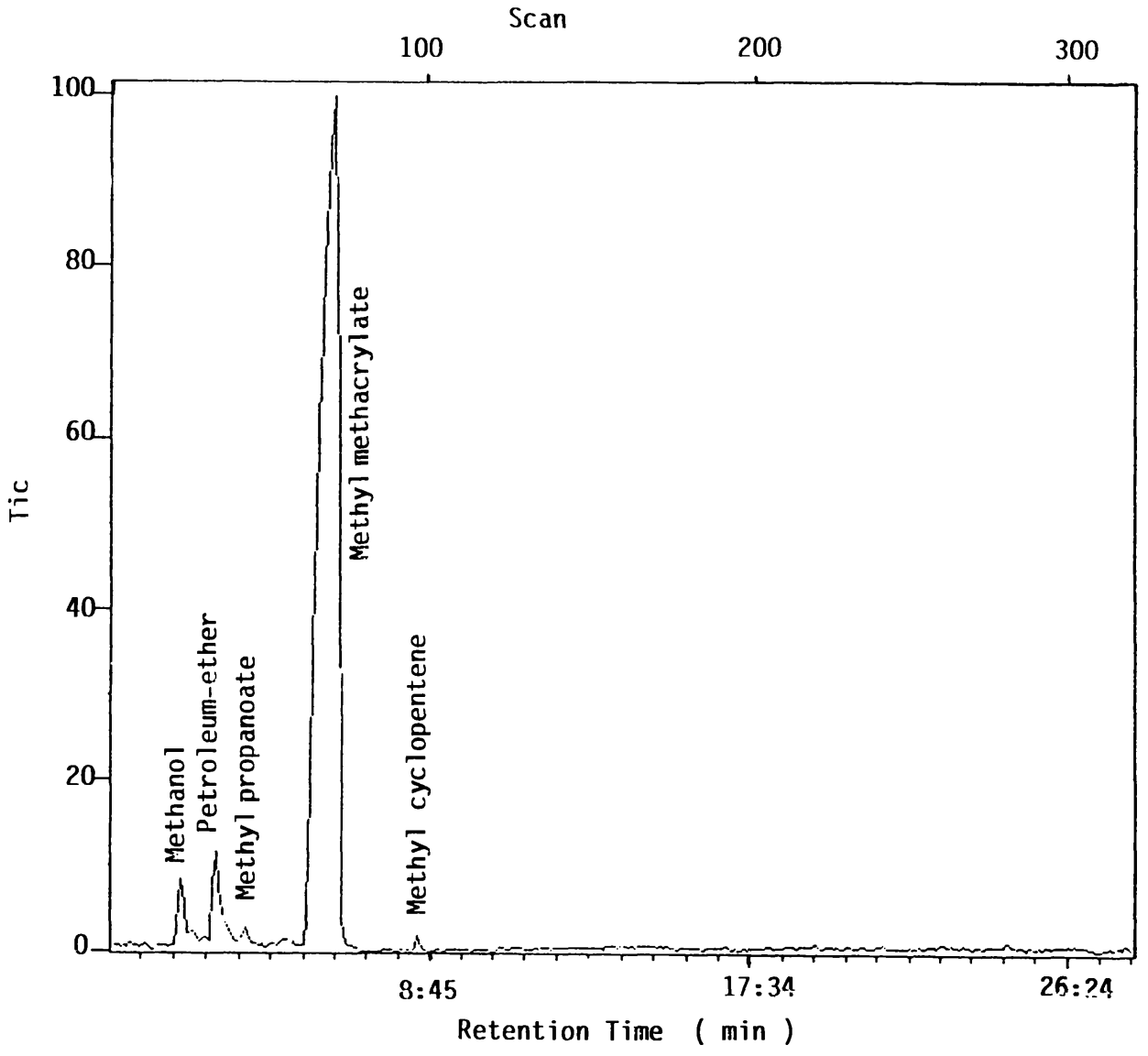

Figure 7.13: Gas chromatogram for the liquid fraction in SATVA separation of products from the degradation of PMMA-COONa to 500 ^{o}C.

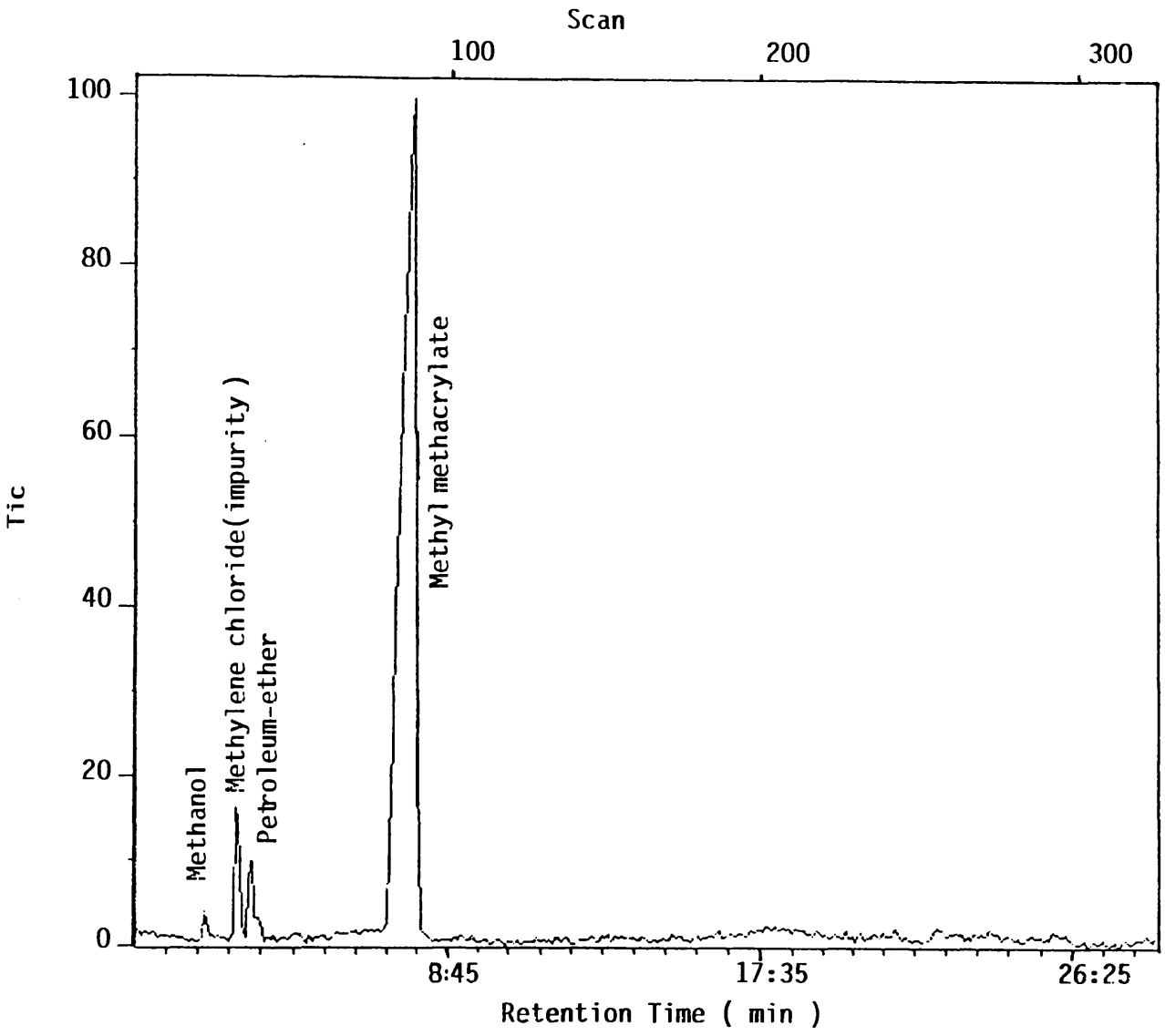

Figure 7.14: Gas chromatogram for the liquid fraction in SATVA separation of products from the degradation of PMMA-COOH to 500 ^{o}C.

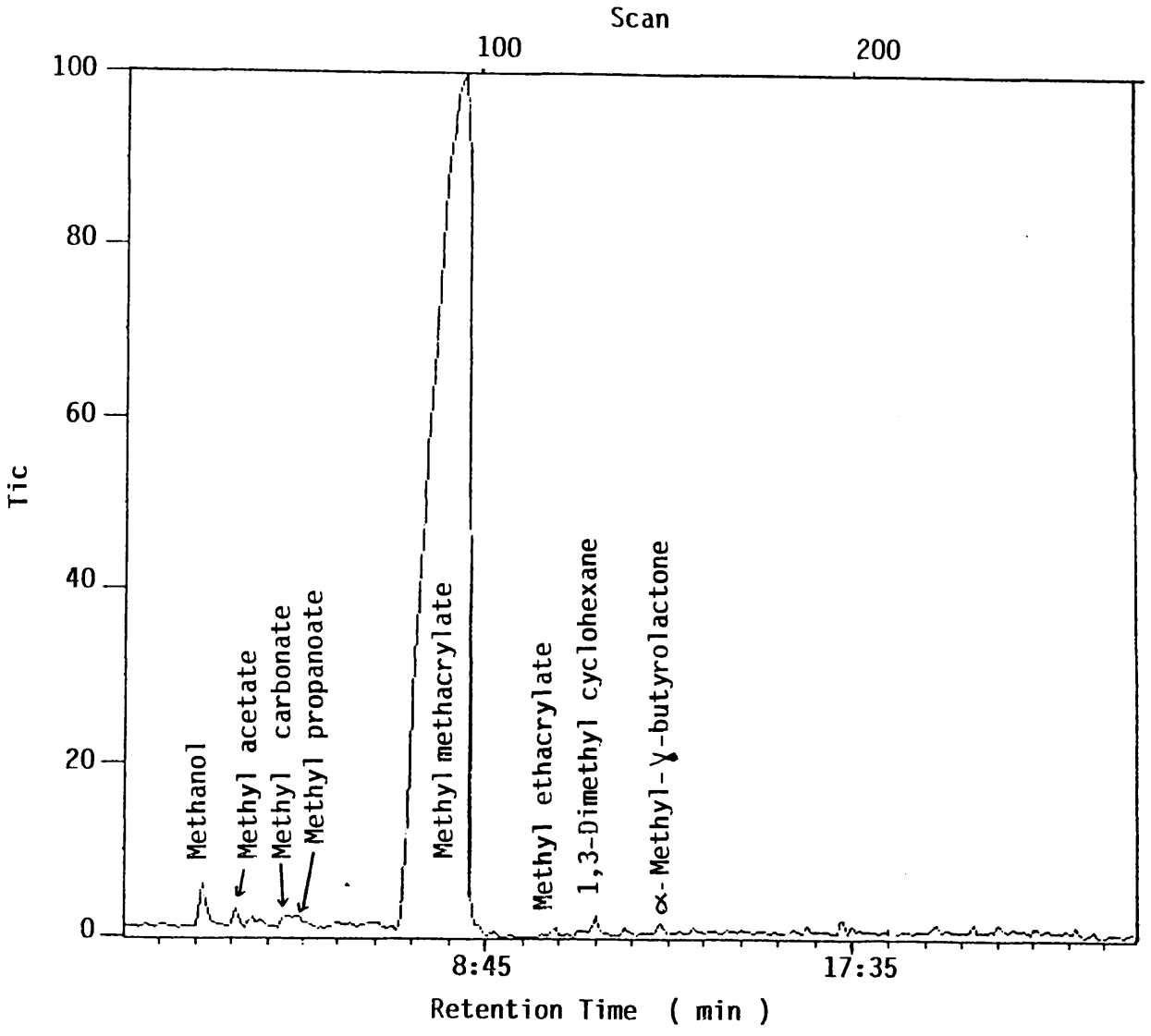

Figure 7.15: Gas chromatogram for the liquid fraction in SATVA separation of products from the degradation of PMMA-CH_2CH_2ONa to 500 ^oC .

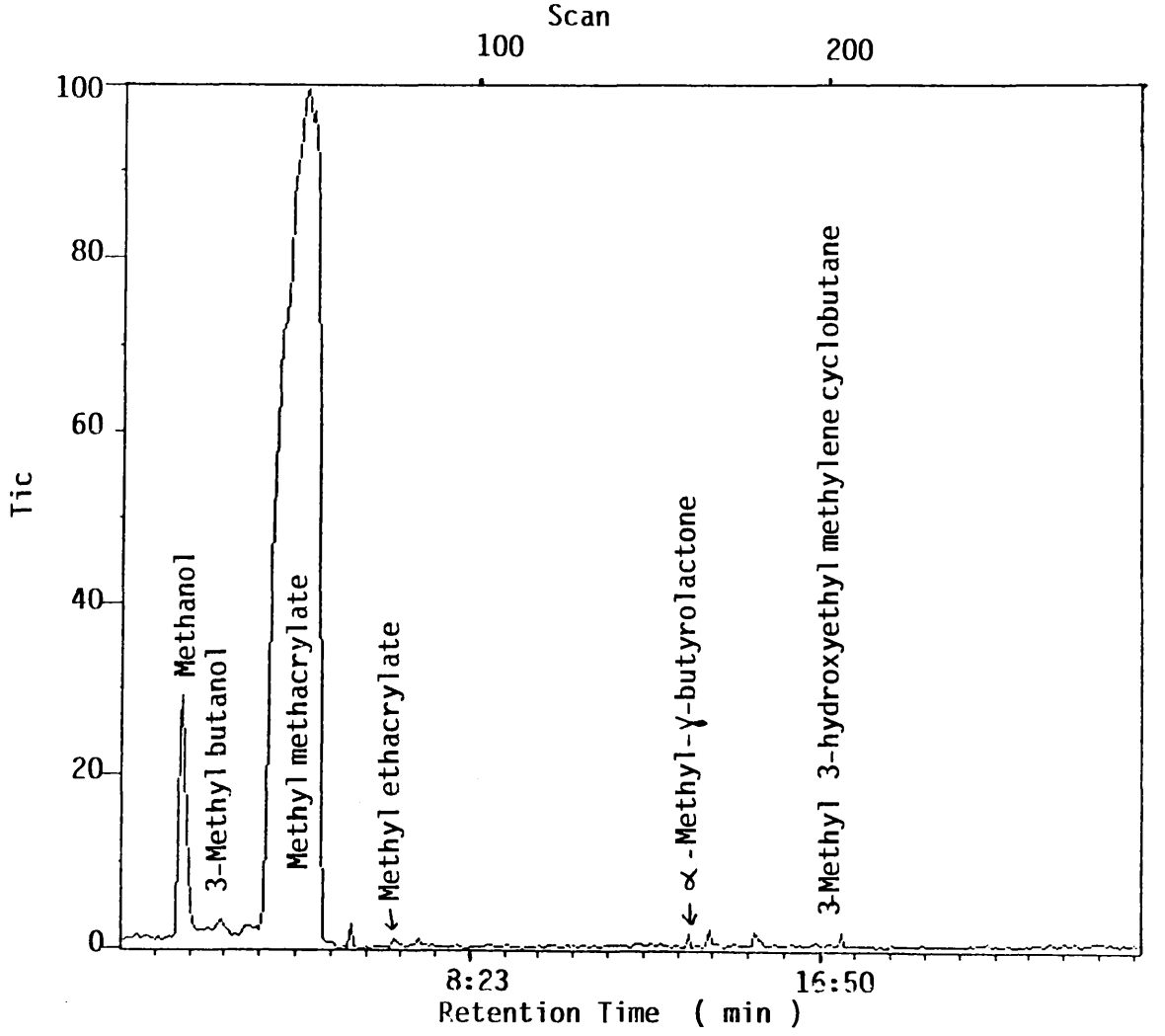

Figure 7.16: Gas chromatogram for the liquid fraction in SATVA separation of products from the degradation of PMMA-CH_2CH_2OH to 500 ^oC.

The second fraction was collected as liquid and consisted mainly of methyl methacrylate with small amounts of methanol and petroleum ether. In addition, the total liquid fraction from each polymer, was subjected to GC-MS examination using a column BP 10 containing 14 % cyanopropyl dimethyl siloxane. The gas chromatograms for the liquid fraction products in SATVA separation from the degradation of each of the α,ω-bifunctional PMMA samples are shown in Figures 7.13-7.16. The major peak in all of the gas chromatograms is entirely due to methyl methacrylate, together with less amount of methanol and precipitant petroleum-ether. In addition a variety of volatile products are present in the case of PMMA with $-CH_2CH_2ONa$ and $-CH_2CH_2OH$ ends. Their gas chromatograms exhibit the presence of methyl methacrylate, methanol, methyl ethacrylate, α-methyl- γ-butyrolactone , methyl propanoate, and methyl acetate, cyclohexane , 4-methyl-4-pentene-2-one, 1,3-dimethyl cyclohexane [PMMA-CH_2CH_2ONa only], 3-methyl 1-butanol and 3-methyl-3-hydroxyethyl methylene cyclobutane [PMMA-CH_2CH_2OH], as listed in Tables 7.3 and 7.4.

7.3.2 Cold ring fraction (CRF)

There is no CRF produced in the degradation of normal PMMA.

The ir spectra of the total CRF from degradation of each of the telechelic PMMA samples, reproduced in Figure 7.17, are identical in most respects to that of normal PMMA.

The ir spectra of the CRF from PMMA-COOH and PMMA-COONa degradation show a shoulder at 1695 cm^{-1} corresponding to the stretching vibration of the carboxylic acid absorption. This indicates that the CRF consists of short chain fragments with terminal -COOH groups. The mass

		Products		Methods of Analysis
		PMMA – COONa	PMMA – COOH	
Non-condensable			Carbon monoxide, methane	IR
Condensable volatile	Gases	Dimethyl ketene	Carbon dioxide , butene-1, isobutene and dimethyl ether	IR, MS
	Liquids	Methyl cyclopentene and methyl propanoate	methyl mathacrylate, methanol and petroleum ether	IR , MS, GC–MS
Cold ring fraction			Saturated and unsaturated short chain fragments (dimer-pentamer) with –COOH end group	IR , MS
Residue		Sodium carbonate	Char	IR

Table 7.3: Products identified from the degradation of PMMA – COONa and PMMA – COOH under TVA conditions.

Products					Methods of Analysis
		PMMA – CH_2CH_2ONa	PMMA – CH_2CH_2OH		
Non-condensable			Carbon monoxide, methane		IR
Condensable volatile	Gases		Carbon dioxide , butene-1, isobutene and dimethyl ether		IR, MS
	Liquids	Methyl acetate, cyclohexane, 4-methyl 4-penten-2-one and 1,3-dimethyl cyclohexane.	Methyl mathacrylate, methanol, α-methyl γ-butyrolactone, methyl ethacrylate and methyl propanoate	3-Methyl 3-hydroxyethyl methylene cyclobutene, 3-methyl 1-butanol	IR, MS, GC–MS
Cold ring fraction			Saturated and unsaturated (dimer–pentamer), short chain fragments with five ring lactone or hydroxyethyl end groups.		IR, MS
Residue		Sodium carbonate	Char		IR

Table 7.4: Products identified from the degradation of PMMA–CH_2CH_2ONa and PMMA–CH_2CH_2OH under TVA conditions.

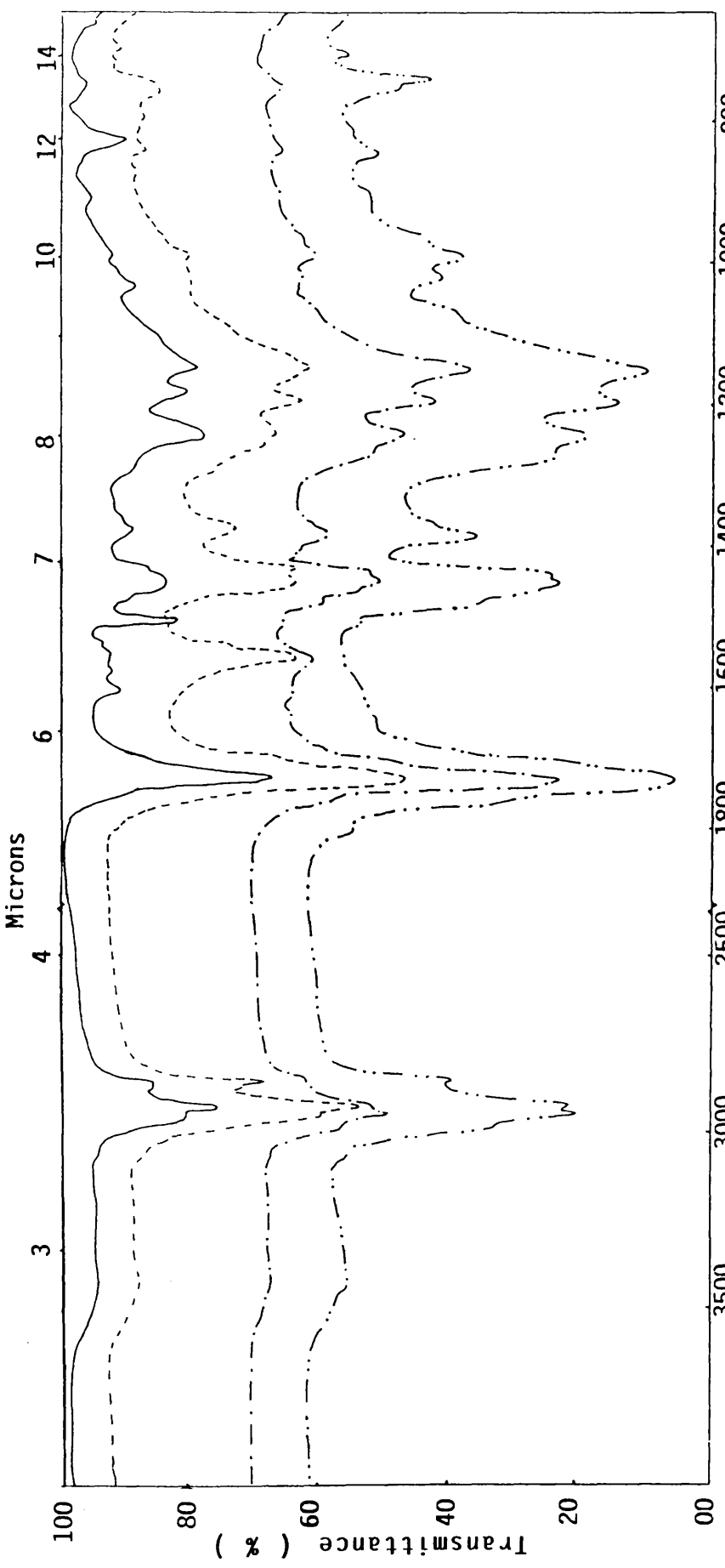

Figure 7.17: Infrared spectra of total CRF from telechelic PMMA samples under TVA conditions to 500 °C. PMMA-CH_2CH_2OH (——) , PMMA-COOH (- - -) , PMMA-COONa (—·—) and PMMA-CH_2CH_2ONa (—··—) .

Products	m/e		Functional end group of PMMA			
			-COONa	-COOH	$-CH_2CH_2ONa$	$-CH_2CH_2OH$
Saturated / Unsaturated dimer	202	200	present	present	present	present
" " trimer	302	300	"	"	"	"
" " tetramer	402	400	"	"	"	"
" " pentamer	502	500	"	"	"	"
Saturated oligomers with -COOH end group						
dimer trimer	229	329	"	"	absent	absent
tetramer	429		"	absent	"	"
pentamer	529		"	present	"	"
Saturated oligomers with $-CH_2CH_2OH$ end group						
dimer trimer	246	346	absent	absent	present	present
tetramer pentamer	446	546	"	"	"	"
Short chain fragments with five ring lactone end group	-		"	"	"	"

Table 7.5: Degradation products identified in CRF of telechelic PMMA degradation by means of MS and IR spectroscopy.

spectra obtained for the total CRF at different probe temperatures indicated saturated and unsaturated oligomers with less than six units.

The ir spectra for the CRF from PMMA-CH_2CH_2ONa and PMMA-CH_2CH_2OH degradation exhibit a new weak band at 1800 cm^{-1}, which is due to the stretching vibration of a five membered ring lactone. This indicates the interaction of the functional end group with the neighbouring ester group to form the cyclic structure. The mass spectra showed fragment ions corresponding to the hydroxyl terminated dimer (m/e 246), trimer (m/e 346), tetramer (m/e 446) and pentamer (m/e 546), all together with saturated and unsaturated oligomers with less than six units.

Table 7.5 summarises the CRF products identified by means of IR and MS spectroscopy.

7.4 MECHANISM OF DECOMPOSITION

From the information obtained on stability and by the identification of products of degradation, it is evident that the mechanism of the thermal degradation of α,ω-bifunctional PMMA is influenced by the functional end groups. Nevertheless, the main reaction decomposition is that from which methyl methacrylate is produced by chain scission reactions at random points along the polymer chain, followed by unzipping as illustrated in Scheme 7.2.

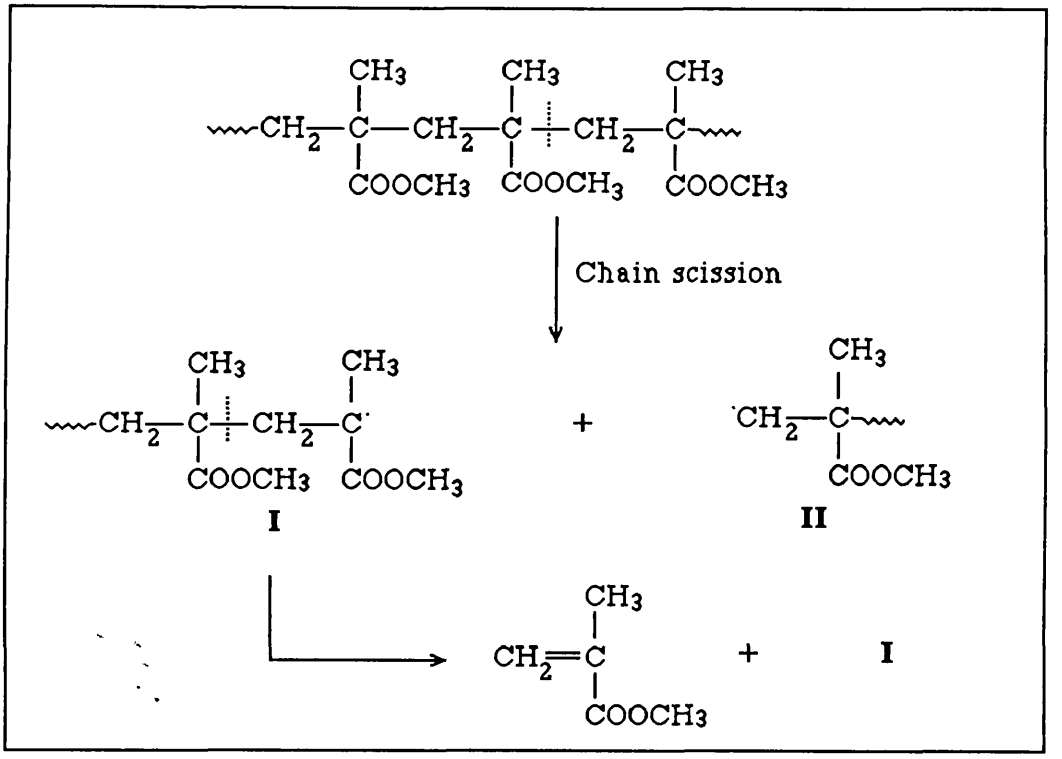

Scheme 7.2

A higher temperatures, side group reactions occur in all four α,ω-bifunctional PMMA samples and the variety of degradation products obtained suggests the elimination of part or all of the side groups. These reaction account for the formation of isobutene, butene-1, carbon dioxide, methanol, methane and dimethyl ether and is believed to involve the radical II as shown in Scheme 7.3. The intermediate species (III) may undergo rearrangement and abstracts hydrogen to form butene-1.

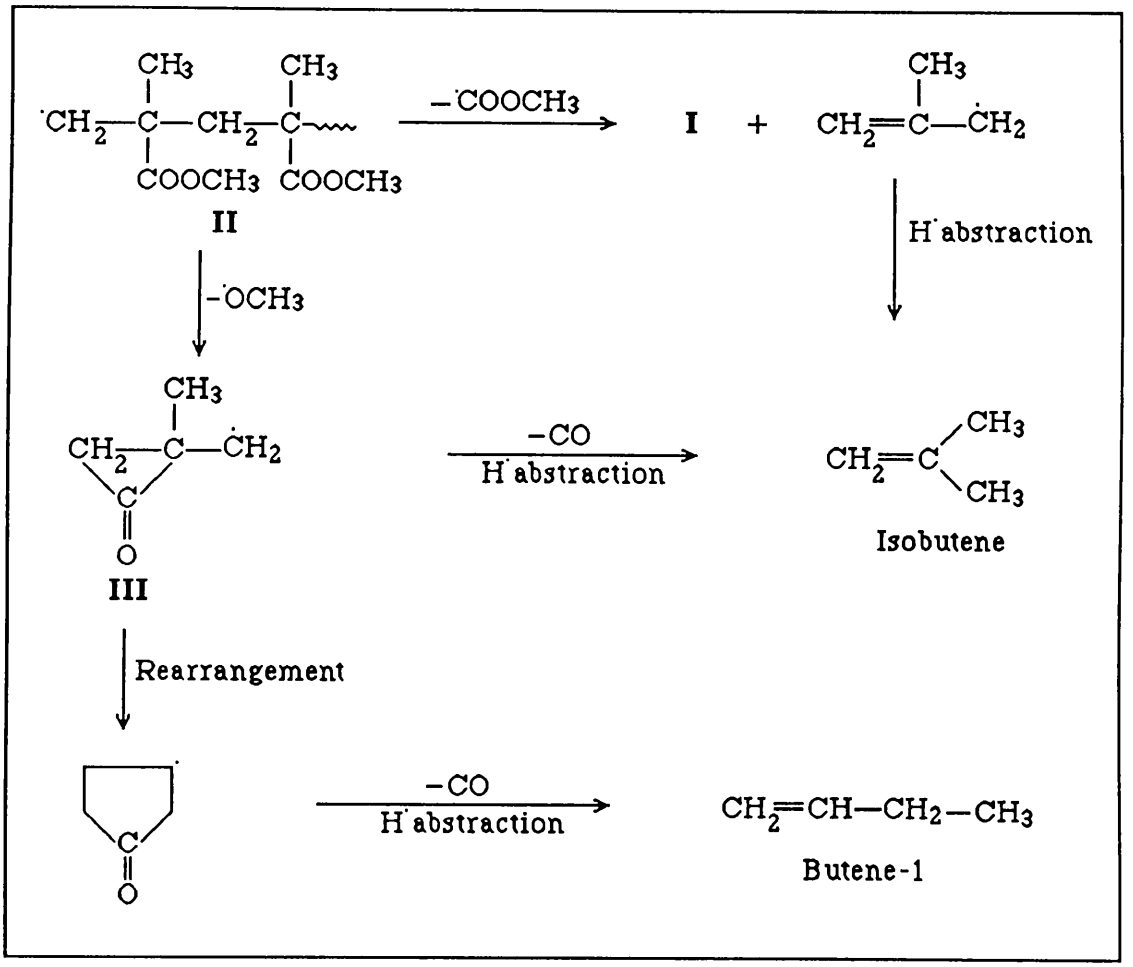

Scheme 7.3

Reactions of ·OCH3 and ·COOCH3 radicals can lead to yield carbon dioxide, dimethyl ether and methanol.

$$\cdot OCH_3 + \cdot COOCH_3 \longrightarrow CO_2 + CH_3OCH_3$$

$$\cdot OCH_3 \xrightarrow{H\cdot\ abstraction} CH_3OH$$

In the case of PMMA with the terminal $-CH_2CH_2ONa$ and $-CH_2CH_2OH$ groups, various degradation products are present. A reaction mechanism supported by the identification of these products is shown in Scheme 7.4.

The interaction of the functional end group with the neighbouring side ester group is believed to result in chains with five membered ring lactone ends prior to formation of α-methyl-γ-butyrolactone. CRF products must result from chain scissions within a few units of these ends.

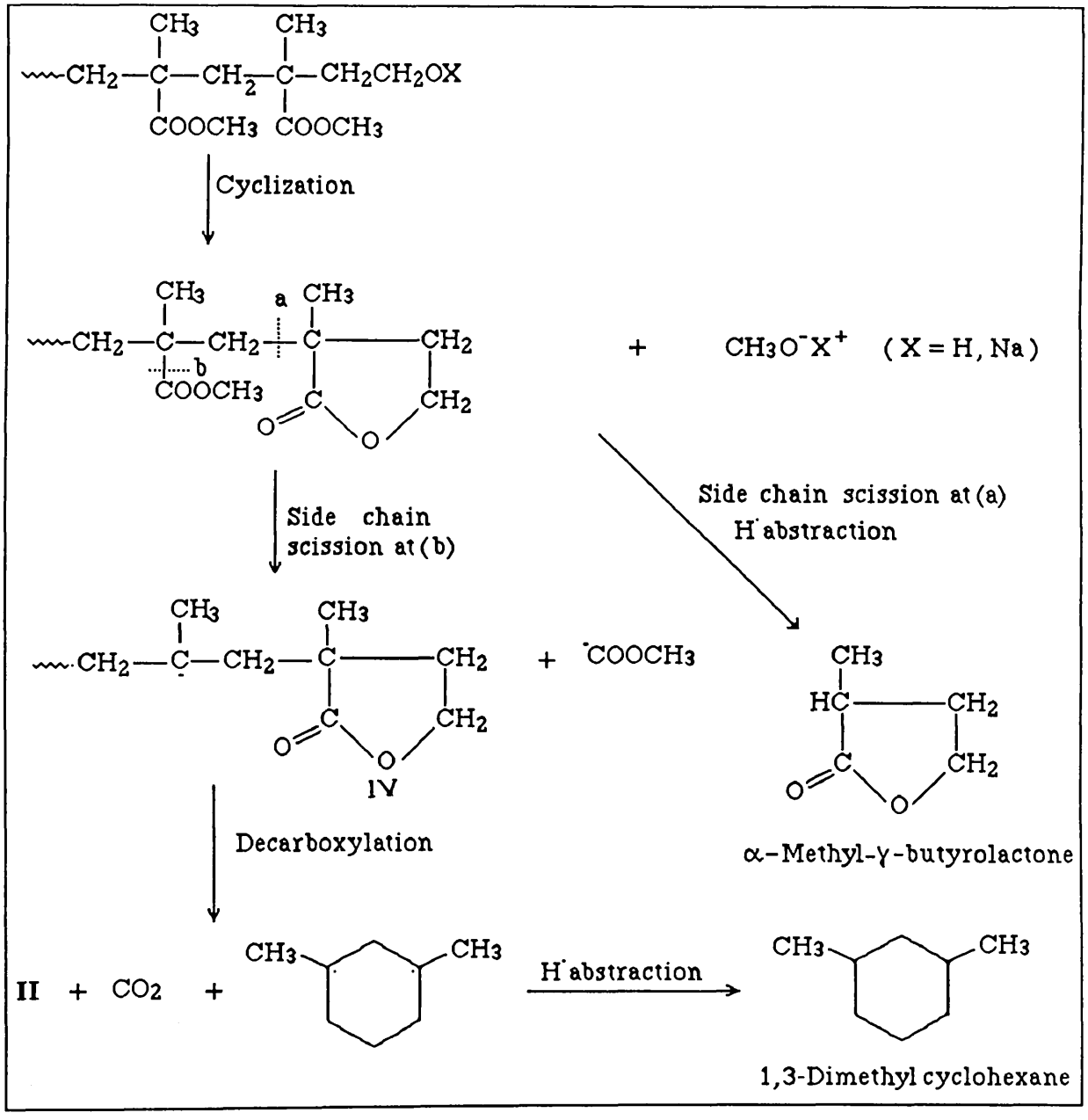

Scheme 7.4

In the case of PMMA-CH_2CH_2ONa, 1,3 dimethyl cyclohexane may be produced by the decarboxylation of the short chain fragment IV, followed by intramolecular hydrogen abstraction.

The formation of methyl ethacrylate is accounted for by chain scission at (a) and (c) as illustrated in Scheme 7.5.

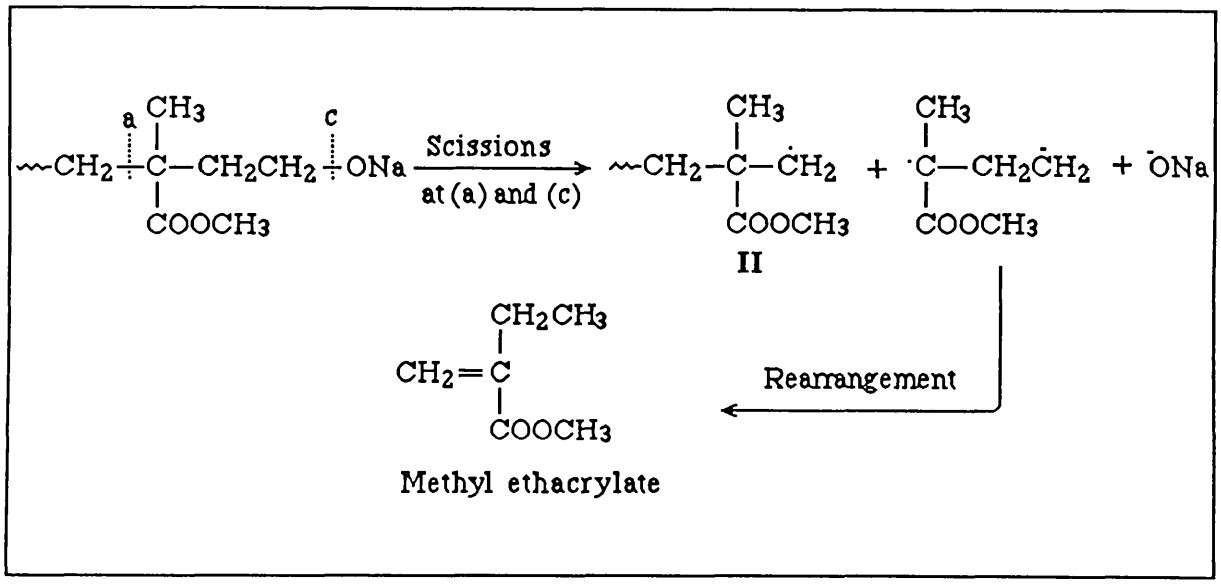

Scheme 7.5

The formation of traces of 3-methyl-3-hydroxyethyl methylene cyclobutane in the degradation of PMMA-CH_2CH_2OH is accounted for by side chain scission of the two neighbouring ester groups to the functional end group forming intermediate species IV followed by rearrangement as illustrated in Scheme 7.6.

The possible routes for the formation of sodium carbonate from the degradation of PMMA-COONa and PMMA-CH_2CH_2ONa are shown in Scheme 7.7. The absence of sodium oxide as residue, particularly for the degraded PMMA-CH_2CH_2ONa, can be explained by the presence of carbon dioxide in the atmosphere which instantly converts it to sodium carbonate.

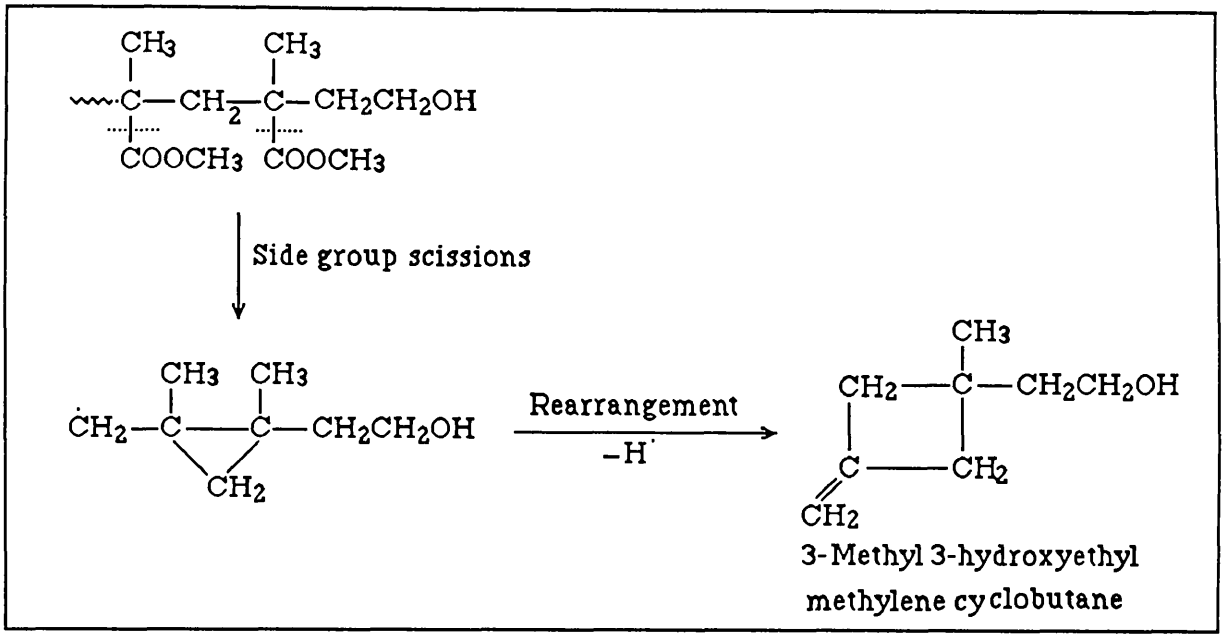

Scheme 7.6

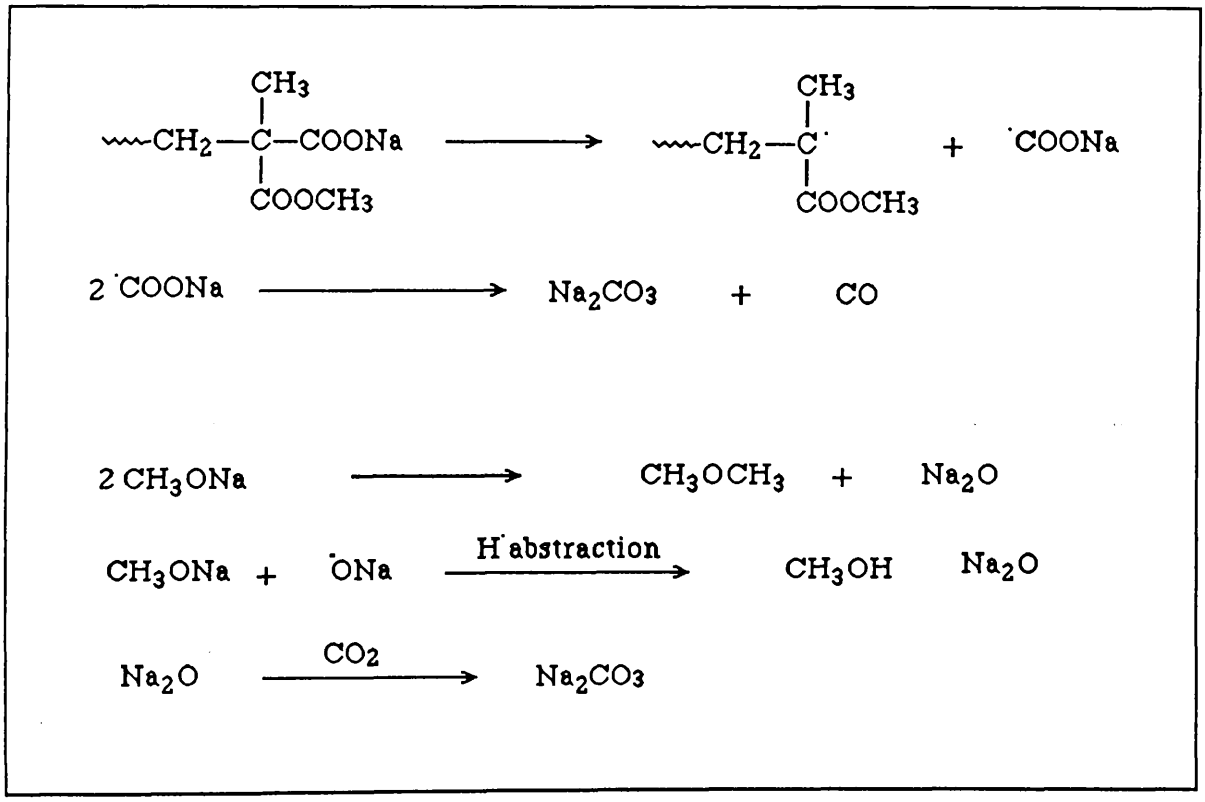

Scheme 7.7

CHAPTER EIGHT

8.1 GENERAL CONCLUSIONS

The thermal degradation studies of polyesters reported in this thesis, indicate that the favoured mechanisms for different polyesters under high vacuum conditions, can be summarised as follows.

Poly(alkylene terephthalates) and poly(ether-esters) (Chapter 4 and 5) follow the same mechanism of degradation, in which the initial decomposition by ester interchange reaction occurs in preference to homolytic cleavage of bonds into radicals. This is followed by other reactions involving the fragmentation of the diol units and ester bond in the backbone of polymer. It is important to notice that these homolytic processes in the degradation of poly(alkylene terephthalates) and poly(ether-esters) take place at temperatures well above the initial decomposition temperature of the ester link.

In the case of aromatic polyesters (polyarylates), studied in Chapter 6, the degradation is initiated by homolytic scission at an acyl-chlorine end group leading to a macroradical which undergoes random chain scissions releasing a large range of degradation products. When fire retardant structures (Cl, Br -contain ing) are introduced into these polyarylates as reactives, some changes are observed in their thermal stability. It is interesting to note that the derivative TG traces (DTG) (Chapter 6) show that the T_{max} is affected by both halogen substitution and the position linkage. In addition, the thermal stability of these polyarylates appears to increase in the following order

PA4 (ortho-para) < PA3 (meta-para) < PA2 (para-para)

Br-PA5 < Cl-PA5 < PA5.

These observations, together with the fact that there is an increase in the amount of residue, supports the suggestion of crosslinking processes in the degradation of polyarylates containing halogen in the aromatic ring. This showed the effectiveness of halogen in polymer fire retardancy as a result of vapour phase and condensed phase reactions.

The study of the thermal degradation of telechelic poly(methyl methacrylates) showed that methyl methacrylate remains the predominant degradation product ,although the functional end groups play a part in the formation of some CRF products. At higher temperatures, side group reactions occurred in the degradation of all α,ω-bifunctional PMMA as shown by the presence of CO_2, methanol and dimethyl ether.

8.2 SUGGESTIONS FOR FURTHER WORK

1) Investigation of the effect of some fire retardant additives such as APP (ammonium polyphosphate) on stability and mechanism of degradation of the poly(ether-esters) studied in Chapter 5.

2) A more detailed examination on the behaviour of polyarylates and halogenated polyarylates using Oxygen Index (OI) measurement to estimate the resistance of flame.

3) Study of the thermal degradation of (PMMA- polyester) copolymers based on α,ω-bifunctional PMMA oligomers and terephthaloyl chloride, polyarylates or other molecule of related structure.

****

REFERENCES

1- W. H. Carothers et. al., *J. Am. Chem. Soc.* , a) **51**, 2560 (1929) b) **52**, 3292 (1930) and c) **55**, 5031 (1933).

2- J. R. Whinfield and J. T. Dickson, *Chem. Abst.*, **41**, 1495f (1947).

3- J. R. Whinfield and J. T. Dickson, *Chem. Abst.*, **43**, 4896g (1949).

4- J. I. Kroschwitz, "*Encyclopedia of Polymer Science and Engineering*",Vol.12, John Wiley and Sons,Inc., New York, 1988, p.88.

5- M. Levine and S. C. Temin, *J. Polym. Sci.*, **28**, 179 (1958).

6- W. M. Eareckson, *J. Polym. Sci.* , **40**, 399 (1959).

7- V. Percec, C. Pugh and S. D. Pask, in "*Comprehensive Polymer Science*" Vol.6,eds. G. C. Eastmond, A. Ledwith, S. Russo, and P. Sigwalt, Pergamon Press, Oxford, 1989, p.281.

8- O. Byer, *Angew. Chem.* , **59**, 257 (1947).

9- C. H. Bamford, A. D. Jenkins and R. P. Wayne, *Trans. Faraday Soc.*, **56**, 932 (1960).

10- M. Morton, " *Anionic Polymerisation Principles and Practice* ", Academic Press Inc., London, 1983.

11- W. Schnabel, " *Polymer Degradation Principles and Practical Application*", Hanser International, München, 1981.

12- N. Grassie and G. Scott, " *Polymer Degradation and Stabilisation* ", Cambridge, University Press, Cambridge, 1985.

13- W. L. Hawkins, "*Polymer Degradation and Stabilization*", Spring-Verrlag, Berlin Heidelberg, 1984.

14- D. H. Grant and N. Grassie, *Polymer* , **1**, 445 (1960).

15- K. Mitani, T. Ogata, H. Awaya and Y. Tomari, *J. Polym. Sci. Polym. Chem. Ed.*, **13**, 2813 (1975).

16- R. R. Stromberg, S. Straus and B. G. Achhamer, *J. Polym. Sci.*, **35**, 355 (1959).

17- N. Grassie in " *Developments in Polymer Degradation -1* ", ed. N. Grassie, Applied Science, London, 1977, p.137.

18- F. X. Roux, R. Audebert and C. Quivoron, *Eur. Polym. J.*, **9**, 815 (1973).

19- S. L. Kwolek, P. W. Morgan , J. R. Schaefgen and L. W. Gulrich, *Macromolecules*, **10**, 1390 (1977).

20- E. Buta and S. Petris, V. Frosini and M. Pasquini, *Eur. Polym. J.*, **7**, 387, (1971).

21- H. H. Jellinek and H. Fujiwara, *J. Polym. Sci. A-1*, **10**, 1719 (1972).

22- N. Grassie and M. Zulfiqar in " *Developments in Polymer Stabilisation-1*", ed. G. Scott, Applied Science Publishers, London, 1979, p. 197.

23- I. C. McNeill, *J. Polym. Sci. A-1*, **4**, 2479, (1966).

24- I. C. McNeill, *Eur. Polym. J.*, **3**, 409, (1967).

25- I. C. McNeill and D. Neil in " *Thermal Analysis* ", eds. R. F. Schwenker and P. D. Garn, Academic Press, New York, 1969 p. 353.

26- I. C. McNeill in " *Thermal Analysis*", eds. R. F. Schwenker and P. D. Garn, Academic Press, New York, 1969, p. 417.

27- I. C. McNeill, *Eur. Polym. J.*, **6**, 373 (1970).

28- I. C. McNeill in "*Developments in Polymer Degradation-1*", ed. N. Grassie, Applied Science Publishers , London, p.43, 1977.

29- I. C. Mc Neill, L. Ackerman, S. N. Gupta, M. Zulfiqar and S. Zulfiqar, *J. Polym. Sci. Polym. Chem. Ed.*, **15**, 2381 (1977).

30- L. Ackerman and W. J. McGill, *J. S. Afr. Chem. Inst.*, **26**, 82 (1973).

31- W. J. McGill, L. Payne and J. Fourie, *J. Appl. Polym. Sci.*, **22**, 2669, (1978).

32- W. J. McGill in "*Developments in Polymer Degradation-5*", ed. N. Grassie, Applied Science Publishers, London, 1984, p.1.

33- R. H. Pierson, A. N. Fletcher and E. St. C. Gantz, *Anal. Chem.*, **28**, 1218 (1956).

34- "*The Aldrich Libreray of Infrared Spectra*", ed. C. J. Pouchert, Aldrich Chemical Co., Milwaukee, 1981.

35- "*The Sadtler Handbook of Infrared Spectra*" ed. W. W. Simons, Sadtler-Heyden, London, 1978.

36- P. J. Flory and F. S. Leutner, U. S. Pat. 2 623, 034 (December 23, 1952)

37- E. M. E. Mansour, A. I Khalifa and L. Rateb, J. Macromol. Sci. Chem., A16(3), 651 (1981).

38- E. Breitmaier, W. Voelter, " Carbon-13 Spectroscopy ", VCH Verlagsgesellschaft mbH, D 6940 Weinhein (West Germany), 1987.

39- R. M. Lum, *J. Polym. Sci. Polym. Chem. Ed.*, 17, 203 (1979).

40- V. Passalacqua, F. Pilati, V. Zamboni, and P. Manaresi, *Polymer* , **17**, 1044 (1976).

41- E. P. Goodings, *Soc. Chem. Ind.*, (London), Monograph, **13**, 211 (1961).

42- H. Zimmermann, in " *Developments in Polymer Degradation -5*", ed. N. Grassie, Applied Science Publishers, London, 1979, p.79.

43- J. G. Smith, C. J. Kibler, and B. J. Sublett, *J. Polym. Sci. A -1*, **4**, 1851 (1966).

44- J. C. Gilland, Jr. , J. S. Lewis, *Angew. Makromol. Chem.*, **54**, 49 (1976).

45- K. Burzin and P. J. Frenzel, *Angew. Makromol. Chem.*, **71**, 61, (1978).

46- G. C. East and A. M. Girshab, *Polymer*, **23**, 323 (1982).

47- S. Shiono, *J. Polym. Sci. Polym. Chem. Ed.*, **17**, 4123 (1979).

48- S. Foti, M. Giuffrida, P. Maravi, and G. Montaudo, *J. Polym. Sci. Polym. Chem. Ed.*, **22**, 1217 (1984).

49- I. Lüderwald, in "*Developments in Polymer Degradation -2*", ed. N. Grassie, Applied Scince Publishers, London, 1977, p.77.

50- R. E. Adams, *J. Polym. Sci. Polym. Chem. Ed.*, **20**, 119 (1982).

51- I. Lüderwald and H. Urrutia, *Makromol. Chem.*, **177 (3)**, 2079 (1976).

52- T. Uzawa, M. Kanassashi, R. Sakamoto and M. Ohama, "*Preprints for the 18th Conference on Polymer* ", Japan,1969, p. 321.

53- K. Yoda, A. Tsuboi, M. Wada, and R. Yamadera, *J. Appl. Polym. Sci.*, **14**, 2357, (1970).

54- J. C. Stevenson and S. L. Cooper, *Macromolecules*, **21**, 1309 (1988).

55- C. M. Boussias, R. H. Peters and R. H. Still, *J. Appl. Polym. Sci.*, **25**, 855 (1980).

56- M. A. Vallance and S. L. Cooper, *Macromolecules*, **17**, 1208 (1984).

57- J. L. Castles, M. A Vallance, J. M. McKenna and S. L. Cooper, *J. Polym. Sci. Polym. Phys. Ed.*, **23**, 2119 (1985).

58- L. Zhu and G. Wegner, *Makromol. Chem.*, **182**, 3625 (1981).

59- T. Blades, *Can. J. Chem.*, **31**, 418 (1953).

60- G. F. L. Ehlers, K. R. Fisch, and W. R. Powell, *J. Polym. Sci. A-1*, **7**, 2969 (1969).

61- S. Foti, M. Giuffrida, P. Maravigna, and G. Montaudo, *J. Polym. Sci. Polym. Chem. Ed.*, **22**, 1201 (1984).

62- T. Kiyotsukuri, N. Tsutsumi, K. Okada, and K. Asai, *J. Polym. Sci. Part A*, **26**, 2225 (1988).

63- M. Kapuscinska, E. M. Pearce,H. F. M. Chung, C. C. Ching, and Q. X. Zhou, *J. Polym. Sci. Polym. Chem. Ed.*, **22**, 3999 (1984).

64- W. Heitz and Niebner, *Makromol. Chem.*, **191**, 3625 (1990).

65- I. C. McNeill and A. Rincon, *Poly. Deg. and Stab.*, in Press.

66- N. Grassie and H. W. Melville, *Proc. Roy. Soc.*, **A 199**, 1, 14, 24 (1949).

67- K. Hatada, T. Kitayama and E. Masuda, *Polym. J*, **18**, 395 (1986).

68- D. H. Solomon, *J. Macromol. Sci. Chem.*, **A 17(2)**, 337 (1982).

69- J. C. Bevington, H. W. Melville and R. P. Taylor, *J. Polym. Sci.*, **14**, 463 (1954).

70- I. C McNeill, *Eur. Polym. J.*, **4**, 21 (1968).

71- T. Kashiwagi, A. Inaba, J. E. Brown, K. Hatada, T. Kitayama and E. Masuda, *Macromolecules*, **19**, 2160 (1986)

72- A. Meisters, G. Moad, E. Rizzardo and D. H. Solomon, P*olym. Bull.*, **20**, 499 (1988).

73- L. E. Manring, D. Y. Sogah and G. M. Cohen, *Macromolecules*, **22**, 4652 (1989).

74- J. R. MacCallum, *Makromol. Chem.*, **83**, 137 (1965).

75- E. Giannetti, R. Mazzocchi, *J. Polym. Sci. Polym. Chem. Ed.*, **24**, 2517 (1986).

****